

University Of Strathclyde
Department of Naval Architecture, Ocean and Marine
Engineering
Faculty of Engineering

“Probabilistic modelling of the process of evacuation for ship
crises management”

Yasmine Hifi

MPhil Thesis

2017

Copyright statement

This thesis is the result of the author's original research. It has been composed by the author and has not been previously submitted for examination which has led to the award of a degree.

The copyright of this thesis belongs to the author under the terms of the United Kingdom Copyright Acts as qualified by University of Strathclyde Regulation 3.50. Due acknowledgement must always be made of the use of any material contained in, or derived from, this thesis.

Signed: Yasmine Hifi

Date: June 2017

Acknowledgements

Special thanks go to my supervisor Professor Dracos Vassalos.

I would also like to thank, Mr Alexandros Ginnis from the National Technical University of Athens, for his review and comments and Professor Panagiotis Kaklis, for his constructive comments and suggestions.

My warmest thanks to my husband Nabile for his patience, suggestions and help during the preparation of this thesis and my two boys Amine and Iliane, who kept asking if I still needed to do work on my thesis every time I was on the computer.

ABSTRACT

Evacuation analysis of passenger ships is mandatory since June 2016 for all passenger ships as prescribed by the International Maritime Organisation (IMO) in the revised guidelines for evacuation analysis (MSC.Circ.1533).

The advanced evacuation analysis defined in the IMO guidelines, relies on the usage of computer models to simulate the movement of people and their interactions with the environment and the other evacuees. These models are powerful tools which allow for a detailed representation of the environment and the people specific characteristics and behaviour.

Setting up and running simulations is a very time consuming process and the bigger and more complex the ship or building is, the longer it takes.

In situations when time is critical such as during emergencies and when a fast assessment of the evacuation time is needed, then relying on evacuation simulation tools might not be an option.

Having a simplified model that can capture the different factors influencing the evacuation process and predict the total evacuation time would be a real advantage.

In the research presented here, an attempt to develop such a simplified model has been made.

The work undertaken during this research focused on investigating the possibility to derive a parametric model that could be simple enough to produce fast estimates of evacuation times but also capture the different elements of the evacuation process to satisfactory accuracy

Different parametric models were investigated. The nature of the problem led to investigate arrival processes, which were a good candidate for the underlying model explaining the evacuation of passengers. A close analysis showed that a Batch Non-Homogeneous Poisson Process (Batch NHPP) was needed to model the problem at hand.

The batch arrivals and the NHPP are independent of each other so they were modelled and studied separately.

The data used in this research came from a number of simulations (8 000 individual runs) performed with the Evacuation simulation software Evi as well as from the validation dataset produced by the EU-funded project SAFEGUARD and its associated Evi simulation runs (about 200 runs).

The work was split between the fitting of the batch sizes of the arrivals and the NHPP. A complete analysis of the data was performed.

The fitting of the batch sizes as well as the arrivals with the selected models produced very good results.

Then, using the fitted models, new data was generated and analysed. The results were compared to the original data for both the batch sizes and the NHPP.

Table of Contents

Acknowledgements.....	iii
ABSTRACT	iv
1 INTRODUCTION AND STRUCTURE OF THE THESIS	15
1.1 Introduction.....	15
1.2 Structure of the thesis	16
2 SCOPE AND OBJECTIVES	18
2.1 General Remarks	18
2.2 Aim and objectives.....	18
2.3 Contribution	18
3 CRITICAL REVIEW.....	20
3.1 General Remarks	20
3.2 Evacuation analysis software	20
3.3 Non-Homogeneous Poisson Process (NHPP)	21
4 THE EVACUABILITY INDEX (EVI) SOFTWARE	23
4.1 General Remarks	23
4.2 IMO Guidelines for Evacuation Analysis	23
4.3 Evacuability Index Software: Evi.....	25
4.3.1 Evi- Evacuation Simulation Tool.....	25
4.3.2 Evacuability Index	34
4.3.3 Additional Features of Evi.....	35
5 FIRST APPROACH AND THE PROPOSED PARAMETRIC MODEL	36
5.1 General Remarks	36
5.2 First parametric model.....	36
5.3 Proposed parametric model.....	39
5.3.1 Batch arrivals	42
5.3.2 Non-Homogenous Poisson Process.....	42
6 EVACUATION DATA	47
6.1 General Remarks	47
6.2 Data quality	47
6.3 Ship model.....	48
6.4 Simulation setting.....	51

6.4.1	IMO Scenarios.....	51
6.4.2	Parameters of the simulated scenarios.....	52
6.5	Analysis of the simulated data	53
6.5.1	Analysis of the batch sizes and events count for the Day cases.....	53
6.5.2	Analysis of the simulated data for the Night cases.....	60
6.5.3	Discussion	67
6.6	Real data	67
6.6.1	SGDVS1.....	68
6.6.2	SGDVS2.....	73
6.6.3	Analysis of the real data: SGDVS1 dataset	76
6.6.4	Analysis of the real data: SGDVS2 dataset	82
6.6.5	Discussion	84
6.7	Concluding remarks	84
7	BATCH FITTING.....	86
7.1	General Remarks	86
7.2	Batch fitting.....	86
7.2.1	Batch fitting: Simulated data	86
7.3	Simulating the batch sizes: simulated data.....	92
7.3.1	Day cases results	93
7.3.2	Night cases results	99
7.3.3	Discussion	103
7.3.4	Conclusion	107
7.4	Batch fitting: Real data.....	108
7.4.1	Discussion	109
7.4.2	Simulating the batch sizes: Real data.....	111
7.5	Concluding Remarks	117
8	NON-HOMOGENEOUS POISSON PROCESS (NHPP) FITTING.....	119
8.1	General Remarks	119
8.2	NHPP model fitting: Simulation data.....	119
8.2.1	Day cases	120
8.2.2	Night cases.....	124
8.2.3	Sensitivity of the fitting to the chosen input data	129
8.2.4	Discussion	130

8.3	NHPP model fitting: Real data	131
8.3.1	Actual data.....	131
8.3.2	Discussion	131
8.3.3	Corresponding simulated data	137
8.3.4	Discussion	138
8.4	Simulating NHPP	148
8.5	Concluding Remarks	152
9	CONCLUSIONS AND FUTURE WORK	153
9.1	General Remarks	153
9.2	Summary of the research.....	153
9.3	Conclusions.....	154
9.4	Future work	156
	REFERENCES.....	158
	Appendix I - Summary values for the parameter of the geometric distribution, the event counts and the Max batch size.	160
	Appendix II - Results of batch simulations for a hundred and a thousand runs: Percentage changes for Max batch size statistics.....	164
	Appendix III - Coefficient values of the polynomial rate function of the NHPP.....	180

List of Figures

Figure 4-1: Agent model.....	26
Figure 4-2: Searching directions. Agents are represented by the blue circles	29
Figure 5-1: Sigmoid function.....	37
Figure 5-2: Example of fitting results for the sigmoid curve	38
Figure 5-3: Plot of residual for fitting evacuation curve with a sigmoid function	39
Figure 5-4: Example of arrival rates for different interval lengths (10s, 20s and 30s) for the same evacuation data	41
Figure 5-5: Example of fit using sum of exponential for rate function	43
Figure 6-1: Evi model of the ROPAX ship used for the study.....	50
Figure 6-2: Location of the muster stations on-board the ship.....	50
Figure 6-3: Variation of max and min values of the maximum batch size for the day case per passengers load.	54
Figure 6-4: Variation of number of events in the simulation runs for the day case per passengers load.	55
Figure 6-5: Variation of max and min values of the maximum batch size for the day case with fixed reaction per passengers load.	56
Figure 6-6: Variation of number of events in the simulation runs for the day with fixed reaction case per passengers load.....	56
Figure 6-7: Variation of max and min values of the maximum batch size for the day case with fixed speed per passengers load.....	57
Figure 6-8: Variation of number of events in the simulation runs for the day with fixed speed case per passengers load	57
Figure 6-9: Variation of max and min values of the maximum batch size for the day case with fixed speed and reaction per passengers load.	58
Figure 6-10: Variation of number of events in the simulation runs for the day with fixed speed and reaction case per passengers load.....	58
Figure 6-11: Variation of the min and max values of the maximum batch size per passengers load for the night case.....	60
Figure 6-12: Variation of the min and max values of the number of events per passengers load for the Night case.	61
Figure 6-13: Variation of the min and max values of the maximum batch size per passengers load for the night fixed reaction case	62
Figure 6-14: Variation of the min and max values of the number of events per passengers load for the Night fixed reaction case.....	62
Figure 6-15: Variation of the min and max values of the maximum batch size per passengers load for the night fixed speed case.....	63
Figure 6-16: Variation of the min and max values of the number of events per passengers load for the Night fixed speed case	64
Figure 6-17: Variation of the min and max values of the maximum batch size per passengers load for the night fixed speed and reaction case	65

Figure 6-18: Variation of the min and max values of the number of events per passengers load for the Night fixed speed and reaction case	65
Figure 6-19: RoPax layout- taken from [27]	69
Figure 6-20: Location of RoPax Muster Stations - taken from [27]	69
Figure 6-21: Stating locations of the passengers during the drill on-board the RoPax Ferry - taken from [27]	70
Figure 6-22: Cruise ship layout- taken from [28]	74
Figure 6-23: Location of Cruise ship Muster Stations - taken from [28]	74
Figure 6-24: Comparison of the events count from simulation results with the trial data per muster station for scenario A	78
Figure 6-25: Comparison of the events count from simulation results with the trial data per muster station for scenario B	79
Figure 6-26: Comparison of the events count from simulation results with the trial data per muster station for scenario C	79
Figure 6-27: Comparison of the max batch size values from simulation results with the trial data per muster station for scenario A	80
Figure 6-28: Comparison of the max batch size values from simulation results with the trial data per muster station for scenario B	80
Figure 6-29: Comparison of the max batch size values from simulation results with the trial data per muster station for scenario C	81
Figure 6-30: Comparison of the events count from simulation results with the trial data per muster station for SGDVS2	83
Figure 6-31: Comparison of the max batch size values from simulation results with the trial data per muster station for SGVDS2	83
Figure 7-1: Percentage change (from min to max) in the value of the geometric distribution parameters with varying population loads for the day scenarios.	88
Figure 7-2: Changes of probability values for batch sizes for a day scenario for a 20% passengers load.	89
Figure 7-3: Percentage change (from min to max) in the value of the geometric distribution parameters with varying population loads for the night scenarios.	90
Figure 7-4: Changes of probability values for batch sizes for a night scenario for a 20% passengers load.	91
Figure 7-5: Events counts: simulated vs original for Day case Random.....	94
Figure 7-6: Events counts: simulated vs original for Day fixed reaction	95
Figure 7-7: Events counts: simulated vs original for Day fixed speed.....	95
Figure 7-8: Events counts: simulated vs original for Day fixed speed and reaction case.....	96
Figure 7-9: Max batch size statistics: simulated vs original for the Day random case.....	97
Figure 7-10: Max batch size statistics: simulated vs original for the Day fixed reaction case.....	97
Figure 7-11: Max batch size statistics: simulated vs original for the Day fixed speed case	98
Figure 7-12: Max batch size statistics: simulated vs original for the Day fixed speed and reaction case.....	98
Figure 7-13: Events counts: simulated vs original for Night case	99
Figure 7-14: Events counts: simulated vs original for Night fixed reaction.....	100

Figure 7-15: Events counts: simulated vs original for Night fixed speed	100
Figure 7-16: Events counts: simulated vs original for night fixed speed and reaction	101
Figure 7-17: Max batch size statistics: simulated vs original for the Night random case	102
Figure 7-18: Max batch size statistics: simulated vs original for the Night fixed reaction case	102
Figure 7-19: Max batch size statistics: simulated vs original for the Night fixed speed case	103
Figure 7-20: Max batch size statistics: simulated vs original for the Night fixed speed and reaction case.....	103
Figure 7-21: Percentage change in values of the parameter of the geometric distribution derived from the different simulation runs scenarios when compared to trial data for SGVDS1	110
Figure 7-22: Percentage change in values of the parameter of the geometric distribution derived from the simulation runs when compared to trial data for SGVDS2.	111
Figure 7-23: Max batch size average values from simulation compared to trial data max batch size. SGVDS1.....	112
Figure 7-24: Max batch size average values from simulation compared to trial data max batch size. SGVDS2.....	113
Figure 7-25: Max batch size average values from simulation compared to Evi runs of the trial data max batch size. SGVDS1- Scenario A.....	114
Figure 7-26: Max batch size average values from simulation compared to Evi runs of the trial data max batch size. SGVDS1- Scenario B.	115
Figure 7-27: Max batch size average values from simulation compared to Evi runs of the trial data max batch size. SGVDS1- Scenario C	115
Figure 7-28: Max batch size average values from simulation compared to Evi runs of the trial data max batch size. SGVDS2.	116
Figure 7-29: Percentage change in average value of max batch size for real and simulated data for SGVDS2.....	117
Figure 8-1: variation of number of coefficient of the rate function per scenario and passenger load for the day cases.	120
Figure 8-2: Fitted and original arrival process for the day cases for (a) 10% passenger load, (b) 20% passenger load, (c) 30% passenger load, (d) 40% passenger load, (e) 50% passenger load, (f) 60% passenger load, (g) 70% passenger load, (h) 80% passenger load, (i) 90% passenger load, (j) 100% passenger load	123
Figure 8-3: variation of number of coefficient of the rate function per scenario and passenger load for the night cases.	124
Figure 8-4: variation of number of coefficient of the rate function per scenario and passenger load for the night cases after selecting different runs.	125
Figure 8-5: Fitted and original arrival process for the night cases for (a) 10% passenger load, (b) 20% passenger load, (c) 30% passenger load, (d) 40% passenger load, (e) 50% passenger load, (f) 60% passenger load, (g) 70% passenger load, (h) 80% passenger load, (i) 90% passenger load, (j) 100% passenger load	128

Figure 8-6: Variation of R^2 value over fitting of 10 different runs of Day scenario for 10% passenger load.....	129
Figure 8-7: Fitted and original arrival process for SGVDS1 (a) Muster Station A, (b) Muster Station B, (c) Muster Station C, (d) Muster Station D, (e) Overall.	134
Figure 8-8: Fitted and original arrival process for SGVDS2 (a) Muster Station A, (b) Muster Station B, (c) Muster Station C, (d) Muster Station D, (e) Overall.....	136
Figure 8-9: Fitted and original arrival process for SGVDS1 Scenario A (a) Muster Station A, (b) Muster Station B, (c) Muster Station C, (d) Muster Station D, (e) Overall.	141
Figure 8-10: Fitted and original arrival process for SGVDS1 Scenario B (a) Muster Station A, (b) Muster Station B, (c) Muster Station C, (d) Muster Station D, (e) Overall.	143
Figure 8-11: Fitted and original arrival process for SGVDS1 Scenario C (a) Muster Station A, (b) Muster Station B, (c) Muster Station C, (d) Muster Station D, (e) Overall.	145
Figure 8-12: Fitted and original arrival process for SGVDS2 (a) Muster Station A, (b) Muster Station B, (c) Muster Station C, (d) Muster Station D, (e) Overall.....	147
Figure 8-13: Generation of NHPP Algorithm	150
Figure 8-14: Generated NHPP curves (scaled).....	151

List of Tables

Table 4-1: Composition of population (age and gender)	32
Table 4-2: Min and max values of the uniform distribution for walking speed on flat terrain per population group	33
Table 4-3: Min and max values of the uniform distribution for walking up and down stairs per population group	34
Table 6-1: ship particulars	48
Table 6-2: Max and min number of events for different passengers loads and for the different day cases.	59
Table 6-3: Max and min number of events for different passengers loads and for the different night cases.....	66
Table 6-4: Number and starting location for the passengers wearing IR tags. RoPax Ferry- Adapted from [27]	71
Table 6-5: Number and starting location for the passengers not wearing IR tags. RoPax Ferry- Adapted from [27]	72
Table 6-6: Number and starting location for the passengers on-board the Cruise ship- Adapted from [28]	75
Table 6-7: Event counts and max batch size for SGVDS1 dataset	76
Table 6-8: Statistics of the events count and max batch size for the Scenario A simulations for SGVDS1	77
Table 6-9: Statistics of the events count and max batch size for the Scenario B simulations for SGVDS1	77
Table 6-10: Statistics of the events count and max batch size for the Scenario C simulations for SGVDS1	77
Table 6-11: Event counts and max batch size for SGVDS2 dataset.....	82
Table 6-12: Statistics of the events count and max batch size for simulation for SGVDS2....	82
Table 7-1: Fitting of geometric distribution parameter. Results for day case.....	87
Table 7-2: Fitting of geometric distribution parameter. Results for night case	90
Table 7-3: Average absolute percentage change for the different night cases for the events count	104
Table 7-4: Average absolute percentage change for the different Day cases for the events count	105
Table 7-5: Average absolute percentage change for the different Night cases for the max batch size.....	106
Table 7-6: Average absolute percentage change for the different Day cases for the max batch size.....	107
Table 7-7: Values of the fitted parameter for the geometric distribution for SGDVS1 dataset	108
Table 7-8: Values of the fitted parameter for the geometric distribution for SGDVS2 dataset	108
Table 7-9: Values of the fitted parameter for the geometric distribution for Evi simulations corresponding to SGDVS1 dataset	109

Table 7-10: Values of the fitted parameter for the geometric distribution for Evi simulations corresponding to SGDVS2 dataset	109
Table 8-1: Number of coefficient of the rate function of the NHPP for the day case scenarios.....	120
Table 8-2: Number of coefficient of the rate function of the NHPP for the night case scenarios.....	125
Table 8-3: Variation in number of coefficients for 10 different runs of Day scenario, 10% passenger load	129
Table 8-4: Model Coefficients for both SGDVS1 and SGVDS2	131
Table 8-5: Model Coefficients for simulated runs of SGDVS1	138
Table 8-6: Model Coefficients for simulated runs of SGVDS2	138
Table 8-7: number of events for the generated NHPP for SGDVS1.....	150

1 INTRODUCTION AND STRUCTURE OF THE THESIS

1.1 Introduction

Evacuation analysis of passenger ships is now mandatory for all passenger ships as prescribed by the International Maritime Organisation (IMO) in the revised guidelines for evacuation of passenger ships which came into force in June 2016 [2]. This came as a result of discussions at IMO, after the Costa Concordia accident [1].

Modelling the evacuation of people from any enclosed space, be it a building or a ship is a challenging and complex task. In most cases the analysis relies on computer models (simulation) of the people movements and interactions with their environment and the other evacuees.

These powerful tools allow for a detailed representation of the environment (ship, building, etc. ...) and the people specific characteristics and behaviour. A great deal can be learned by observing the simulations and their outcome such as overall evacuation time and bottle neck locations but this comes at a price: time. Setting up and running simulations is a very time consuming process and the bigger and more complex the ship or building is, the longer it takes.

In situations when time is critical such as during emergencies and when a fast assessment of the evacuation time is needed, then relying on evacuation simulation tools might not be an option.

In these situations, having a simplified model that can capture the different factors influencing the evacuation process and predict the total evacuation time would be a real advantage.

The model might not be restricted to emergency situations. Any time a quick estimation of the overall evacuation time is needed, the model could be used.

In the research presented here, an attempt to develop such a simplified model has been made. The process and methodology adopted as well as the obtained results are presented and explained throughout the chapters of this thesis.

The next section will outline the structure of the thesis and gives a brief description of each chapter.

1.2 Structure of the thesis

This thesis is organised in 9 chapters as follows:

- Chapter 1: **Introduction and Structure of the thesis**

This chapter outlines the overall structure of the thesis

- Chapter 2: **Scope and objectives**

The scope and objectives of the research are described in this chapter.

- Chapter 3: **Critical review**

This chapter provides an overview of the way evacuation simulation is modelled and the leading software tools available. It also discusses agent arrival processes.

- Chapter 4: **Evacuation software**

This chapter describes in more detail the evacuation software tool used to generate the data for this work.

- Chapter 5: **First approach and the proposed parametric model**

The different approaches considered during the development of the parametric model and the model adopted are explained in this chapter.

- Chapter 6: **Evacuation Data**

The data used in this research, how it was obtained and the requisite analysis are presented in this chapter.

- Chapter 7: **Batch fitting**

This chapter describes the fitting of the agent arrival batches for the available datasets. It also describes the generation of batches based on the results of the fitting.

- Chapter 8: **Non-Homogeneous Poisson Process (NHPP) fitting**

Explaining the fitting of the NHPP and discussing its generation based on the results of the fitting is the subject of this chapter.

- Chapter 9: **Conclusion and future work**

Finally, this chapter concludes the thesis and discusses future work.

2 SCOPE AND OBJECTIVES

2.1 General Remarks

Evacuation simulation tools are very useful tools to assess ships in terms of the evacuation time. They are also used to identify areas of congestions and bottlenecks on-board. They can be used at the concept design stage to evaluate different options for example or help address potential problems. During operations, these can help with crew training for example but one area where evacuation simulation might not be of too much help is during an emergency situation on-board where the total evacuation time needs to be estimated and known in a matter of seconds. Although computers are more and more powerful these days, for ships the size of the “Oasis of the seas”, for example, with more than 8000 people on-board, performing an evacuation simulation during a crisis when every second counts, would not be the way forward.

2.2 Aim and objectives

The aim of this thesis is to propose a newly developed parametric model for prediction of passengers evacuation time based on input from a large number of simulations as well as real data.

In order to achieve this aim the following objectives are defined:

- Propose a model that describes the evacuation process
- Identify the parameters of the model based on data produced by the simulation software
- Compare the result to a set of real data.

2.3 Contribution

The work presented here will contribute to improve the evacuation assessment by providing a fast evaluation of the evacuation time of a vessel in time of crises.

It is hoped that this research will open the door to a more in-depth analysis of simplified models of evacuation to be used in emergencies, for example as part of a decision support system on-board.

3 CRITICAL REVIEW

3.1 General Remarks

In this chapter some of the available evacuation simulation tools will be reviewed as well as the agent arrival processes and the methods to model these.

3.2 Evacuation analysis software

Following the introduction of the IMO guidelines for evacuation analysis [2] the use of advance evacuation analysis tools (computer based) in the maritime industry started being consistently used mainly for rule compliance but also for design and operation.

There exists a number of different software for ship evacuation. These can be categorised as: flow models and agent-based models.

The flow models address the problem at macroscopic level. People movements are modelled as flow through “pipes” in a graphical representation of the geometry. The second type of models, the agent-based models, considers the interaction between people and with the environment at a microscopic level. For this kind of models, the geometry is represented in detail.

The first type of models is quite easy to implement and make use of network flow algorithms and methods, but fails to capture important aspects such as the interaction between agents like avoidance, group effect (where people tend to move as a group at the pace of the slowest member) or the counter-flow effect when people move in opposite directions. These aspects are accommodated by the second type of models.

Another category of model, which combines both micro and macro level of planning is the mesoscopic models. At the micro-level, rules are in place to govern agents’ movements from way finding to avoidance strategies while at a macro-level there is the path planning process.

Models can further be distinguished by their modelling of the environment (geometry) where some models are grid based and others model the environment as a continuum.

There exists a number of simulation software available on the market specific to the maritime field. Some of the agent-based models are briefly reviewed here.

Maritime Exodus [5] was developed at the Fire Safety Engineering Group of the University of Greenwich and is part of the Exodus suite of software. The ship geometry is modelled as a grid and is specified automatically using a DXF file or manually using the interactive tools provided with the software. The software comprises five core interacting sub-models: the Passenger, Movement, Behaviour, Toxicity and Hazard sub-models. The motion and behaviour of each individual is determined by a set of heuristics or rules which are mostly stochastic.

ANEAS [3] jointly developed by TraffGo-HT and GL (now DNV GL), is also a grid-based model. The software is based on PedGo [6] with additional functionalities for the use within the marine industry. PedGo has three components: an editor to construct the model, the simulation core and a viewer to visualise the simulation.

Odigo [4], developed by Principia, models the ship as a continuum. It is an integrated tool including a pre-processor, a simulation engine, and a post-processor. The simulation engine uses a multi-agent method of a cognitive/reactive hybrid type. The agent definition (features and starting position) are stochastically defined. The agents act upon objectives (join cabin, move to craft), which can be chained (succession of events).

Finally, Evi which was developed by the Ship Stability Research Centre at the University of Strathclyde and Safety At Sea Ltd (now part of the Brookes Bell Group), which is used in this study and is presented in detail in a dedicated chapter of the thesis (Chapter 4).

3.3 Non-Homogeneous Poisson Process (NHPP)

This part of the chapter will focus on the arrival processes in general and on the Non-Homogeneous Poisson Process (NHPP) in particular.

Traditionally, arrival processes (people at bus stops, calls at call centres, etc....) have been modelled using a Poisson distribution. When the rate of arrivals is constant, then a Poisson Process is used to model the arrivals. However, when the rate of arrivals changes over time then a non-homogeneous or sometimes referred to as non-stationary Poisson Process, is

more appropriate. The change in the arrival over time is defined by a rate or intensity function, which characterises the non-homogeneous Poisson Process.

In other words, to be able to define a NHPP its rate function needs to be properly modelled.

Modelling of the rate function can either be achieved through parametric or non-parametric estimations.

Leemis [7] proposed a non-parametric technique for estimating the cumulative intensity function of a NHPP for arrivals to queuing systems (but not limited to such arrivals) where the modeller is not required to specify any parameters or weighting functions.

For parametric models, the rate function is modelled as a piecewise linear [8-9] or piecewise polynomial [10] function. Others, such as MacLean [11] proposed an exponential rate function estimated using maximum likelihood estimator.

The work presented in this thesis uses a non-parametric method developed by Kuhl and Wilson [12]. The method is explained in detail in Chapter 5 and it is not further reviewed here.

For completeness, a brief note on methods for the generation (simulation) of Non-Homogeneous Poisson Process is provided here. The main and widely used methods to generate a NHPP are the inverse method and the thinning method [15]. The inverse method (which is considered in this study) uses the inverse of the cumulative rate function to produce the events of the NHPP. The thinning method assumes that the intensity function has an upper constant bound. Arrival times are generated using the constant bound, then events are either rejected or accepted based on the thinning criterion. The interested reader is referred to Gerhardt and Nelson [16] and Devroye [17] for more details.

4 THE EVACUABILITY INDEX (EVI) SOFTWARE

4.1 General Remarks

The objective of this chapter is to present the background of the evacuation simulation tool **Evacuability Index (Evi)** used to produce part of the data needed to deliver this work.

The advanced evacuation simulation software **Evi** is a commercial software developed at the Ship Stability Research Centre (SSRC) of the University of Strathclyde and maintained and commercialised by Brookes Bell Safety At Sea.

This chapter will briefly introduce **Evi** notions as well as the IMO Guidelines for Evacuation analysis.

4.2 IMO Guidelines for Evacuation Analysis

For a better understanding of the work presented in this thesis and before describing **Evi**, there is a need to present some background notions related to the evacuation of ships and in particular the IMO guidelines for evacuation analysis.

What follows is a very brief overview of the guidelines. The reader is referred to the IMO circular 1533 for more detail [2].

Here and throughout this thesis, evacuation refers to the mustering process of passengers at Assembly (or Muster) Stations on-board.

The IMO guidelines define the necessary information to perform an evacuation analysis of a passenger ship and explain the steps needed to perform the analysis. The Guidelines propose two methods to perform the analysis: the simplified method and the advanced evacuation analysis, which requires the use of computer tools. The advanced evacuation analysis, which is of interest in this work, is the subject of Annex 3 of the IMO circular.

In order to perform an evacuation analysis, the ship geometry, topology and related semantics should be known prior to the start of such analysis and, in particular the escape routes and the location of the assembly (muster) stations. All this information will be used to build the ship model.

The Guidelines also make a number of assumptions as follows:

- The passengers and crew are represented as unique individuals with specified individual abilities and response times;
- Passengers and crew will evacuate via the main escape routes unless otherwise stated - full availability of escape arrangements is considered;
- A safety factor having a value of 1.25 is introduced in the calculation to take account of modelling omissions and assumptions. These issues include:
 - The crew will immediately be at the evacuation duty stations ready to assist the passengers;
 - Passengers follow the signage system and crew instructions (i.e., route selection is not predicted by the analysis);
 - Smoke, heat and toxic fire products present in fire effluent are not considered to impact passenger/crew performance;
 - Family group behaviour is not considered in the analysis; and
 - Ship motion, heel, and trim are not considered.

The requisite scenarios (benchmarks) for the analysis are defined as follows:

- a night case scenario where all passengers are in their cabins,
- a day case scenario where all passengers are in public spaces and
- two other scenarios: one for day scenario and one for night scenario with reduced escape route availability.
- Two additional scenarios that may be considered as appropriate:
 - if an open deck is outfitted and used by passengers, the open deck can be considered as a public space for the day case.
 - If embarkation stations are different from assembly stations, the analysis of travel duration from assembly stations to entry point of LSA should be taken into account.

The evacuation time is calculated and then compared with the performance standards, which are:

$$1.25(R + T) + \frac{2}{3}(E + L) \leq n$$

$$(E + L) \leq 30 \text{ min}$$

Where:

R: Response duration

T: Travel duration

E: Embarkation duration for the Life Saving Appliances

L: Launching duration of the Life Saving Appliances

n: 60 minutes for Ro-Ro passenger ships and for passenger ships with less than 3 Main Vertical Zones (MVZ).

80 minutes for ships with more than 3 MVZs

4.3 Evacuability Index Software: Evi.

4.3.1 Evi- Evacuation Simulation Tool

Following the introduction of the IMO Guidelines and the background information needed to perform an evacuation analysis, this section will briefly describe Evi.

Evi is an “agent” based evacuation simulation tool specifically tailored to ship environment, which incorporates the following aspects:

- Multi-Agent modelling
- Synchronisation
- Modelling Human behaviour
- Demographics.

These are further explained below

a) Multi-Agent Modelling

An ‘agent’ is defined as an encapsulation of code and data, which is capable of executing independently the appropriate piece of code depending on its own state (the encapsulated data), the observables (the environment) and the stimuli (messages from other parts of the system or interactively provided).

- The agent’s action model is a 'sense-decide-act' loop.

- The sense step is the interface of the agent with the data structures representing the environment.
- The decision process requires access to the perceived information. It is an access interface between the environment and the agents.
- An environment is defined to be an artificial representation of the space where agents evolve and is implemented as a collection of data structures in the computer.

To address the modelling of human behaviour at the microscopic and macroscopic level, the agent model itself can be seen as being composed of a number of levels (Figure 4-1).

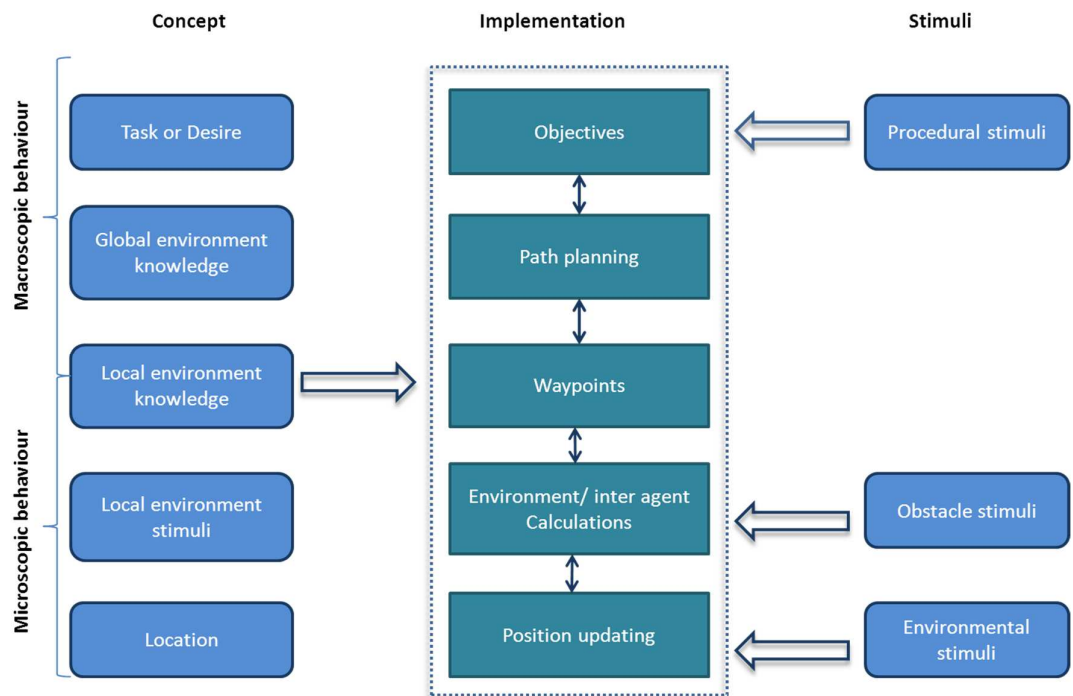


Figure 4-1: Agent model

At the highest level, an Objective defines agent task or desire. In order to fulfil this desire, the Objective requests a path plan (routing) to be calculated, which defines how an agent will advance from the current location to the destination. Once this data structure is in place, the agent will select a waypoint, an intermediate location to travel to, usually in direct line-of-sight from the agent (i.e. within a convex region). With a defined direction to travel to, defined by the waypoint, the agent will move towards that location using position

updating. In doing so, the agent will avoid the boundaries of spaces and other agents in the locality by taking account of environment and inter-agent conflicts.

The different aspects of this model are discussed hereafter:

I. The environment model

Modelling of the environment is one of the most important aspects of multi-agent modelling. This consists of three aspects: geometry, topology and domain semantics. The whole ship layout is segmented into Euclidean convex regions with a structure of a linear space, directly connected if they have a common gate. This connectivity topology, for all computation and analysis purposes can be represented by a graph.

In ship layout terms, regions correspond to spaces and gates correspond to doors. Regions can be defined as rectangular or convex polygons with attributes that control initial conditions and semantic information that agents may query when traversing through (such as initial number of persons, fire zone, destination, etc.).

Two regions are called directly connected if they have a common gate (real or artificial doors). Regions can be located at different level entities, called decks, defined by the height above a reference level or baseline. The problem of finding the path of an agent to a muster point becomes reduced to searching the topology graph.

The perception model of the agents will be able to use the information in these three abstractions at different levels of the decision processes.

A first exhaustive search over the gate graph is used in Evi to choose the optimal path (shortest path) to be used for high level planning activities.

II. Mesoscopic Modelling

When an agent travels along a route it will have to interact with other agents along the route and react to the surrounding environment. The Macroscopic modelling addresses the problem of how agents may find their way from one part of the ship environment to another (high-level planning), and the Microscopic modelling considers how individuals interact with the environment within close proximity (low-level planning). Mesoscopic modelling accounts for both.

III. Microscopic behaviour:

The microscopic model covers the behaviour of movement of agents within spaces. It dictates the way agents avoid boundaries of spaces and how to avoid other agents. Given these constraints, the objective is to steer the agent towards a local destination (waypoint) in an optimal manner without being uncooperative towards the other agents in the space.

IV. High level planning: Path planning and graph search

The path-planning algorithm computes the distance from the Assembly station to all the doors in the graph in a pre-processing phase (before the actual simulation starts) and the information about the distance is stored with each door.

When an agent is located in a region, the distance information from each door of the region can be obtained, thus allowing the agent to use the shortest path leading to the destination area. Re-planning during the evacuation is still possible if for some reason the path is blocked.

V. Low level planning: Steering of agents

Pursuit of a static target acts to steer the agent towards a specified position in global space. This behaviour adjusts the agent so that the velocity is radially aligned towards the target. The “desired velocity” is a vector in the direction from the agent to the target representing global “flow speed”, adjusted on the basis of local density.

The steering vector is the difference between the desired velocity and the agent’s current velocity. In the absence of any obstacle or other evacuees, every agent will “flow” along the evacuation route i.e. it will be passing through the gates unobstructed. Otherwise avoidance heuristics are used to avoid collision with the neighbouring agents and obstacles present along the evacuation path.

b) Synchronisation

One of the most important aspects of the microscopic behaviour algorithms is the synchronisation between agents. Considering the total number of agents in the simulation of an evacuation scenario in e.g., large passenger ships, updating each one of them at the same time would require substantial parallel processing of the information.

In Evi the update process is performed in two steps as follows:

- First Step

In the first step, the Perception–Decision Phase where all agents calculate / update their information using one environment state but do not move (they perceive the update in parallel). This is further explained hereafter.

Perception phase:

The perception algorithm checks the space (in the form of discrete directions see Figure 4-2) around the agent for boundaries and other agents.

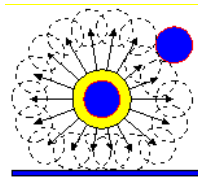


Figure 4-2: Searching directions. Agents are represented by the blue circles

The calculation stops if a direction is found where the agent can progress without breaching any walls or interfering with other agents.

Decision phase:

The decision algorithm uses a rational rule-based process to select the action to take for the current time step. The decision process makes use of information on the previous time step combined with information acquired from the Perception algorithm.

Before entering the decision process, the algorithm first gathers state information from the current environment that may affect the perception process. This includes update of the desired travel direction, consideration of the current waypoint and selection of the current maximum speed.

- Second Step:

In the second step, the action phase is where agents carry out their calculated / updated actions.

Speed of advance

Each agent is assigned a walking speed represented by a random variable according to its age and gender (this aspect is discussed in more detail in the section about demographics below). During the simulation the speed is adjusted to the density of the crowd in the region as defined in the IMO guidelines [2]. The crowd density corresponding to an evacuee in an escape route describes the number of persons divided by the available escape route area pertinent to the space where the evacuee is located. As the model geometry is reproduced to exact measurements of the actual vessel, the density calculations are deemed to be very accurate.

Additionally, when long queues form, the effect on speed of advance is calculated rigorously on the basis of the queue length.

c) Modelling human behaviour

There is a large number of parameters that are likely to affect the evolution and the outcome of an evacuation scenario. Some are related to the population profile (number, age, gender, persons of impaired mobility and so on), passenger distribution (spatial and temporal) and crew number, distribution and functionality in any given crisis. Others are related to behavioural aspects.

Within Evi, people on-board are treated as agents moving in a “command” and “decision” structure where agents representing passengers are mainly controlled with two objectives (tasks):

- The “Evacuate” objective (default objective) is used to assign an assembly station to an agent and control the route it takes to get there.
- The “Lost” objective is applied to passenger agents when they are modelled as lost, as part of the initial conditions of the scenario. Lost agents will select exit doors randomly. This behaviour continues until route information is found from the environment or a crew member.

Agents representing Crew have a wider range of objectives:

- The Control objective is used to model crew procedural activities such as Stairway Guiding. The objective has the effect that passengers near the controlling agent crew increase their speed and any lost agents are directed to an assembly station.

- The Search objective is used to model crew travelling around the environment making passenger agents aware of the evacuation. This behaviour reduces passengers' awareness (reaction) time.
- The Inspect Clear objective is similar to the Search objective except that the crew agent will wait until all passenger agents have left the space before proceeding to the next space to be searched.
- The Re Route objective is used to direct passenger agents to alternative routes.

In addition to these objectives, a messaging system exists which provides a way for agents to communicate between them.

Through messaging, crew agents can directly affect the behaviour of passenger agents.

For example, a passenger agent will receive information about the location of the muster station from crew members or about alternative routes to use.

Passenger agents can also send messages to other passenger agents informing them of the presence of a blocked door.

Two forms of messages are supported:

- Local verbal messages are broadcast at the location of the sending agent and travel for only a short distance, controlled by the range distribution for passengers and crew separately.
- System wide messages are broadcast at the centre of all spaces and have an unlimited range of travel (represents PA system for example).

d) **Demographics:**

All parameters related to human decision or action, are modelled as random variables with user-defined probability distributions. Variables such as awareness/response time, gender and walking speed are referred to as demographics.

During simulations, Monte-Carlo sampling is carried out to derive the values of response time and walking speed for each agent taking part in the simulation.

The IMO guidelines define the population demographics as follows:

Passengers groups	Percentage of passengers (%)
Females younger than 30 years	7
Females 30-50 years old	7
Females older than 50 years	16
Females older than 50 years mobility impaired 1	10
Females older than 50 years mobility impaired 2	10
Males younger than 30 years	7
Males 30-50 years old	7
Males older than 50 years	16
Males older than 50 years mobility impaired 1	10
Males older than 50 years mobility impaired 2	10
Crew groups	Percentage of crew (%)
Crew females	50
Crew males	50

Table 4-1: Composition of population (age and gender)

The reaction time is defined by the following log normal distribution.

For the Night cases:

$$y = \frac{1.01875}{\sqrt{2\pi} \cdot 0.84(x - 400)} \exp \left[-\frac{(\ln(x - 400) - 3.95)^2}{2 \times 0.84^2} \right]$$

And $400 < x < 700$

For the Day cases:

$$y = \frac{1.00808}{\sqrt{2\pi} \cdot 0.94x} \exp \left[-\frac{(\ln(x) - 3.44)^2}{2 \times 0.94^2} \right]$$

and $0 < x < 300$

Walking speeds are defined per age group for flat terrain and up and down the stairs as a uniform distribution, min and max of which are as follows:

1) For flat terrain

	Walking speed (m/s)	
	Min	Max
Passengers groups		
Females younger than 30 years	0.93	1.55
Females 30-50 years old	0.71	1.19
Females older than 50 years	0.56	0.94
Females older than 50 years mobility impaired 1	0.43	0.71
Females older than 50 years mobility impaired 2	0.37	0.61
Males younger than 30 years	1.11	1.85
Males 30-50 years old	0.97	1.62
Males older than 50 years	0.84	1.4
Males older than 50 years mobility impaired 1	0.64	1.06
Males older than 50 years mobility impaired 2	0.55	0.91
Crew groups	Min	Max
Crew females	0.93	1.55
Crew males	1.11	1.85

Table 4-2: Min and max values of the uniform distribution for walking speed on flat terrain per population group

2) For stairs

	Walking speed Down (m/s)		Walking speed Up (m/s)	
	Min	Max	Min	Max
Passengers groups				
Females younger than 30 years	0.56	0.94	0.47	0.79
Females 30-50 years old	0.49	0.81	0.44	0.74
Females older than 50 years	0.45	0.75	0.37	0.61
Females older than 50 years mobility impaired 1	0.34	0.56	0.28	0.46
Females older than 50 years mobility impaired 2	0.29	0.49	0.23	0.39
Males younger than 30 years	0.76	1.26	0.5	0.84
Males 30-50 years old	0.64	1.07	0.47	0.79
Males older than 50 years	0.5	0.84	0.38	0.64
Males older than 50 years mobility impaired 1	0.38	0.64	0.29	0.49
Males older than 50 years mobility impaired 2	0.33	0.55	0.25	0.41
Crew groups	Min	Max	Min	Max
Crew females	0.56	0.94	0.47	0.79
Crew males	0.76	1.26	0.5	0.84

Table 4-3: Min and max values of the uniform distribution for walking up and down stairs per population group

These values have been used in the simulations performed for this work.

If or when different values are used, this will be explained and defined.

4.3.2 Evacuability Index

For the purpose of undertaking evacuation analysis, a number of performance measures can be evaluated, such as time for a group of persons to clear a particular area or time for all agents to complete assembly.

Considering the above, Evacuability is defined to be the ability to complete a specific objective (for example to evacuate a ship environment) within a given time for given initial conditions as follows:

$$E = f\{\text{env, d, r}(t), s(n_i); t\}$$

where:

env: represents the ship model (geometry, topology, semantics)

d: initial distribution (spatial location) of the people on-board,

r(t): initial reaction time of people on-board (cue perception, interpretation of instructions, ...)

s(n_i): walking speed of individual people

4.3.3 Additional Features of Evi

Evi software offers the capability of assessing the impact of hazards associated with flooding and fire.

Time histories of ship motions and flood water in the ship compartmentation from time-domain flooding simulation tools can be imported into Evi. The impact of ship motions and floodwater on the agents is modelled by applying walking speed reduction coefficients that are functions of the inclination of the escape routes due to heel and/or trim of the ship, generated by the damage [20, 18].

In terms of fire hazards, Evi is capable of importing fire hazards information from fire analysis tools such as Fire Dynamics Simulator (FDS) [19]. Fire hazards are described in the form of parameters such as temperature, heat fluxes, concentration of toxic gases (such as CO, CO₂) and oxygen, smoke density, visibility, etc.

Including these two hazards was out of the scope of the work completed in this thesis. Taking into account their effects can be the subject of future work.

5 FIRST APPROACH AND THE PROPOSED PARAMETRIC MODEL

5.1 General Remarks

The evaluation of a ship evacuation process is either based on real drills or on model simulations. The research presented in this thesis attempts to develop a method to estimate the ship evacuation time, based on real data and simulated data using Evi software, to be incorporated in a decision support system to be used at the design stage and for design planning to improve the ship safety and make the evacuation more efficient.

To achieve this goal, it is important to (a) study the evacuation process as discussed in Chapter 4 and to (b) use the evacuation curves estimated from the different simulations for ship evacuation processes (that are ship types dependent).

The methodology to estimate the required time for a ship evacuation is explained in this chapter.

5.2 First parametric model

Predictions of ship evacuation time usually are obtained from running a simulation or by measurements on-board (drills). Both are time consuming. Without an effective and fast predictive capability method to estimate the evacuation time, the use of such simulation models and full-scale trials cannot be avoided.

The first approach considered to assess the ship evacuation time, using data from the simulated evacuation curves was the use of a sigmoid function

With the evacuation curves having a typical “S” shape, the sigmoid function was the obvious choice.

There exist different formulae of the sigmoid curve. The formulation that produced to best agreement with the evacuation curves produced by Evi is the function given by (Eq. 5-1) [21] the shape of which can be seen in Figure 5-1:

$$y = A_b + \frac{A_t - A_b}{1 + \exp(-(x - x_0)/w)}$$

Eq. 5-1

Where:

- A_b : Is the point of intersection of the curve and the Y axis
- A_t : Asymptotic value when $x \rightarrow \infty$
- x_0 : Is the inflexion point of the curve
- w : Is the difference between x_i and x_j

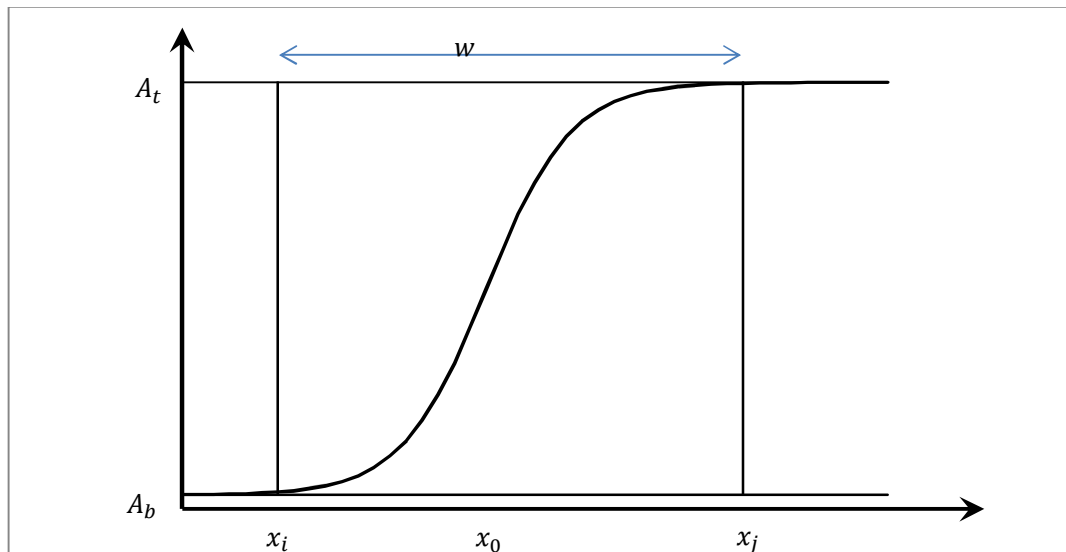


Figure 5-1: Sigmoid function

For the purpose of the work and for the set of data available, the initial parameters values were taken to be:

$$A_b = 0$$

$A_t =$ total number of passengers onboard

$x_0 =$ middle of time interval

$w =$ length of interval $[t_{1/4}, t_{3/4}]$ where $t_{1/4}$ and $t_{3/4}$ are times of the first and third quarters of the total time interval of the evacuation

With the exception of A_b , all the parameters above have been adjusted during the fitting process to obtain the best fit.

The sigmoid defined by (Eq. 5-1) produced good results ($R^2 = 0.993$) in terms of fitting the data produced by the simulations although the sigmoid tends to overestimate the number of passengers at the muster stations at the beginning of the simulation as can be seen in (Figure 5-2).

Initially, the function proposed seemed to give a good estimation of the evacuation time compared with the simulation model (Evi), but a closer look at the residual for the curve fitting (Figure 5-3) showed trends in the residuals (no random relationship) meaning that an underlying phenomenon is not captured by the proposed fitting model.

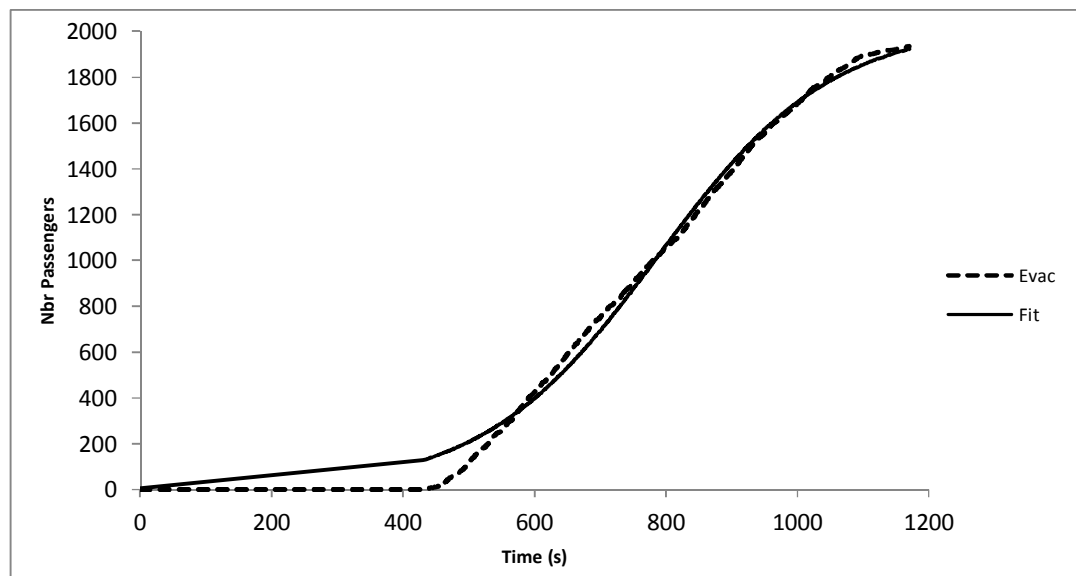


Figure 5-2: Example of fitting results for the sigmoid curve

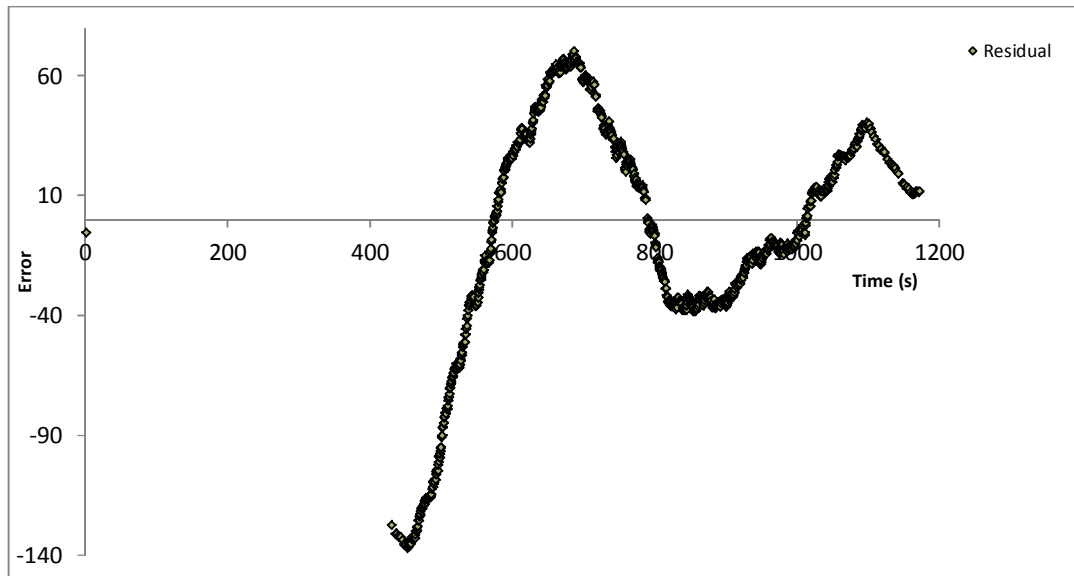


Figure 5-3: Plot of residual for fitting evacuation curve with a sigmoid function

In order to obtain a better fitting, it was then decided to extend the study and investigate other approaches that could be used to estimate the evacuation time. The approach that has been selected is discussed in the following section.

5.3 Proposed parametric model

As explained above, the first approach using a sigmoid function was not conclusive even though the fitting seemed fine at first sight. Other models were then investigated.

In a real situation, an evacuation can be seen as an arrival process to the muster station of the people on-board the ship. Mathematically speaking, an arrival process to a specific location can be modelled using Poisson Processes.

In probability theory, the Poisson process is widely used to model random points in time.

A Poisson process is defined as a counting process (counting of occurrences of events overtime) as follows [22]:

A stochastic process $\{X(t): t \geq 0\}$ is a Poisson process if:

1. $X(0) = 0$
2. For $0 = t_0 < t_1 < \dots < t_n$,
 $X(t_1) - X(t_0), X(t_2) - X(t_1), \dots, X(t_n) - X(t_{n-1})$ are independent
3. There is a function $\lambda(t)$ called **intensity function** or instantaneous arrival rate at time t , such that for a small h :

$$P(X(t+h) - X(t) = 1) = h\lambda(t) + o(h) \quad \text{Eq. 5-2}$$

$$P(X(t+h) - X(t) \geq 2) = o(h) \quad \text{Eq. 5-3}$$

Where $o(h)$ is a number whose magnitude is smaller than that of h .

$\lambda(t)$ is nonnegative integrable function and the corresponding mean value function is given by:

$$\mu(t) = E[X(t)] = \int_0^t \lambda(z) dz, \forall t \geq 0 \quad \text{Eq. 5-4}$$

If $\lambda(t)$ is a positive constant, the Poisson process is called **Homogeneous Poisson Process** with rate λ .

For processes where the arrival rate is a function of time, the Poisson process is called **Non-Homogeneous Poisson Process (NHPP)** or **Non-Stationary Poisson Process (NSPP)**. In the rest of the thesis the first terminology will be used.

When analysing the simulation data, it was clear that the arrival rate of the agents in the muster station was not constant. As such a homogeneous Poisson process could not be used as a model for the data (see Figure 5-4 for example of arrival rates).

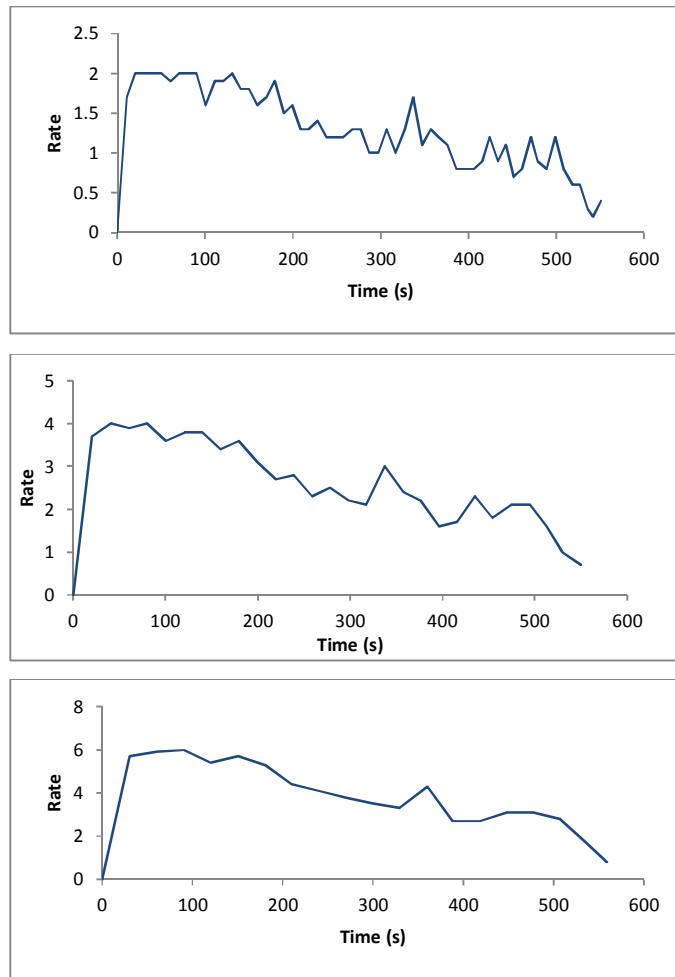


Figure 5-4: Example of arrival rates for different interval lengths (10s, 20s and 30s) for the same evacuation data

The arrivals at muster stations within a specific time interval $[t_i, t_j]$ will be independent from (not influenced by) the arrivals at the muster stations during another time interval $[t_k, t_l]$ with $i \neq j \neq k \neq l$, as arrivals will be governed by the initial positions of agents, the reaction time and walking speed which follow random probability distributions.

Another characteristic of the arrivals at the muster stations was the fact that people arrive at the muster stations in groups or batches where the size of the group varies from 1 to n (where the maximum value of n is the total number of people on-board).

To account for both these features the model selected to represent the data is a **Batch Non-Homogeneous Poisson Process (BNHPP)** arrival model.

The BNHPP arrival model can be decomposed into two distinct models: modelling the number of passengers arriving in each batch and modelling the arrival events. These two problems can be addressed independently.

5.3.1 Batch arrivals

Let $Bnum$ be a discrete random variable representing the number of passengers per batch arriving at the muster stations.

Batch sizes can be modelled by a Geometric distribution. Thus:

$$Bnum \sim Geom(p)$$

and its probability mass function is given by:

$$P(Bnum = k) = p(1 - p)^{k-1}, k \geq 1 \quad \text{Eq. 5-5}$$

The parameter of the probability function will be derived from the data during the fitting process.

5.3.2 Non-Homogenous Poisson Process

A Non-Homogenous Poisson Process (NHPP) is completely characterised by its rate or mean value function. A number of methods parametric and non-parametric exist to estimate the rate function of NHPP from arrival data.

A first model for the rate function was used; the sum of exponential functions of the form:

$$\lambda(t) = ae^{bt} + ce^{dt} \quad \text{Eq. 5-6}$$

Where a, b, c, d are parameters to be estimated.

The result of the fit was good in terms of R^2 and also visually but the residuals did not exhibit a random pattern as can be seen in the figure below.

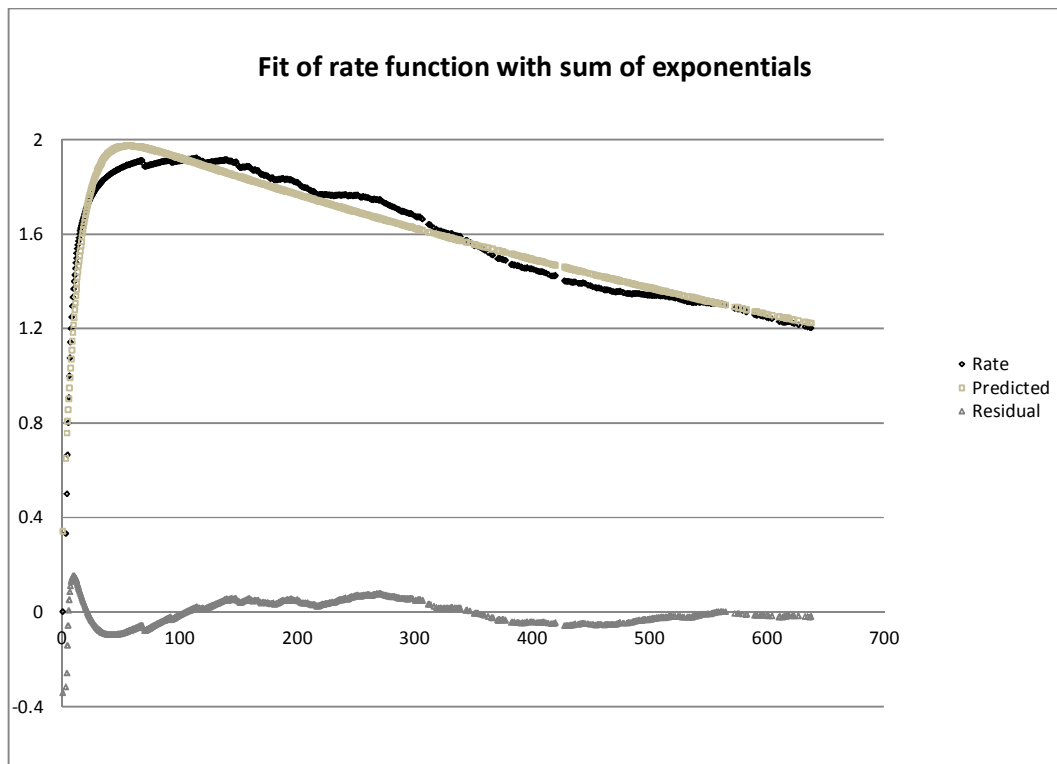


Figure 5-5: Example of fit using sum of exponential for rate function

The reason for the poor fit is that in order to use conventional regression analysis, the response needs to be independent, normally distributed with a constant variance, which is not the case for NHPP observations.

The following model developed by Kuhl and Wilson [12-14] is the model used in Chapter 8 to find a fit to the rate function. It is explained in the rest of this section. The model description is largely based on [14].

The objective is to fit the mean-value function of the NHPP to *a single realisation* of observed arrivals over the interval $(0, S]$. The following semiparametric model is proposed:

$$\mu(t) = \mu(S)R(t), \forall t \in (0, S] \quad \text{Eq. 5-7}$$

Where $R(t)$ is a non-decreasing function representing the cumulative proportion of arrivals up to time t .

A uniformly accurate approximation to the function $R(t)$ can be achieved using a polynomial of sufficiently high degree r with the special following form:

$$R(t) = \begin{cases} t/S, & r = 1 \\ \sum_{k=1}^{r-1} \beta_k (t/S)^k + \left(1 - \sum_{k=1}^{r-1} \beta_k\right) (t/S)^r, & r > 1 \end{cases} \quad \text{Eq. 5-8}$$

The coefficient vector $\mathbf{B}_r = (\beta_1, \dots, \beta_{r-1})$ is constrained so that $R'(t) \geq 0, \forall t \in (0, S]$

The form of the above equation ensures that $R(0) = 0$ and $R(S) = 1$ for all values of \mathbf{B}_r .

To estimate the function $R(t)$, the following procedure is applied:

- Transform the data using a variance-stabilising transformation;
- For the transformed data, estimate the degree r of the best-fitting polynomial using a modified likelihood ratio test; and
- Given the polynomial degree r , estimate the vector \mathbf{B}_r by applying the method of least squares to the original arrival data.

Let $W_i = i/N(S)$ be the cumulative proportional arrivals up to time $t_{(i)}$ of the i^{th} arrival for $i = 1, 2, \dots, N(S)$.

The variance stabilising transformation for $i = 1, \dots, N(S)$ is of the form:

$$Y_i = \sin^{-1}(\sqrt{W_i}) \quad \text{Eq. 5-9}$$

Arrival times are also scaled as follows:

$$Z_i = t_i/S \quad \text{Eq. 5-10}$$

For the transformed points $[Y_i, Z_i]$, the aim is to fit the statistical model $E[Y_i] = f_r(Z_i; \mathbf{C}_r)$ such that:

$$f_r(u; \mathbf{C}_r) = \begin{cases} \frac{\pi}{2}u, & r = 1 \\ \sum_{k=1}^{r-1} C_k u^k + \left(\frac{\pi}{2} - \sum_{k=1}^{r-1} C_k \right) u^r, & r > 1 \end{cases} \quad \text{Eq. 5-11}$$

For $u \in [0,1]$ and \mathbf{C}_r is the coefficient vector:

$$\mathbf{C}_r \equiv \begin{cases} \pi/2 & \text{if } r = 1 \\ [C_1, \dots, C_{r-1}]^T & \text{if } r > 1 \end{cases} \quad \text{Eq. 5-12}$$

Subject to the constraint $f'_r(u; \mathbf{C}_r) \geq 0$.

The vector \mathbf{C}_r is estimated via constrained least square for successive values of r for the transformed data set of size $m = N(S)$:

$$\tilde{\mathbf{C}}_r = \arg \min_{\tilde{\mathbf{C}}_r: f'_r(u; \tilde{\mathbf{C}}_r) \geq 0} \sum_{i=1}^m [Y_i - f_r(Z_i; \tilde{\mathbf{C}}_r)]^2 \quad \text{Eq. 5-13}$$

The error sum of squares for $r \geq 2$ is given by:

$$SSE_r = \sum_{i=1}^m [Y_i - f_r(Z_i; \tilde{\mathbf{C}}_r)]^2 \quad \text{Eq. 5-14}$$

For $r = 1$,

$$SSE_1 = \sum_{i=1}^m \left[Y_i - \frac{i\pi}{2(m+1)} \right]^2 \quad \text{Eq. 5-15}$$

Let $\tilde{\sigma}_r^2$ be the estimator of the response variance for each r , given by:

$$\tilde{\sigma}_r^2 = \frac{SSE_r}{m} \quad \text{Eq. 5-16}$$

And let

$$\bar{Y} = \frac{\sum_{i=1}^m Y_i}{m} \quad \text{Eq. 5-17}$$

then the total sum of squares is given by:

$$SST = \sum_{i=1}^m [Y_i - \bar{Y}]^2 \quad \text{Eq. 5-18}$$

The final estimate of r is given by:

$$\tilde{r} = \begin{cases} 1 & \text{if } SSE_1/SST < 0.01 \text{ or } m \leq 2 \\ \min \left\{ r: r \geq 2; -m \ln \left(\frac{\tilde{\sigma}_r^2}{\tilde{\sigma}_{r-1}^2} \right) \leq \chi_{1-\alpha}^2(1) \right\} - 1 & \text{else} \end{cases} \quad \text{Eq. 5-19}$$

For a significance level α and $\chi_{1-\alpha}^2(1)$ is the $1 - \alpha$ quantile of the chi-squared distribution with 1 degree of freedom.

Once the degree \tilde{r} is determined the vector $\mathbf{B}_{\tilde{r}}$ is estimated by solving the least squares problem with the original data:

$$\tilde{\mathbf{B}}_{\tilde{r}} = \arg \min_{\mathbf{B}_{\tilde{r}}: R'_r(u; \mathbf{B}_{\tilde{r}}) \geq 0} \sum_{i=1}^m [W_i - R_r(t; \tilde{\mathbf{B}}_{\tilde{r}})]^2 \quad \text{Eq. 5-20}$$

For $\tilde{r} \geq 2$ and if $\tilde{r} = 1$, then $\tilde{\mathbf{B}}_1 = \beta_1 = 1$.

The estimator of the mean value function is thus,

$$\tilde{\mu}(t) = N(S)R(t, \tilde{r}, \tilde{\mathbf{B}}_{\tilde{r}}) \forall t \in (0, S] \quad \text{Eq. 5-21}$$

and the estimated rate function

$$\tilde{\lambda}(t) = \tilde{\mu}'(t) \forall t \in (0, S] \quad \text{Eq. 5-22}$$

6 EVACUATION DATA

6.1 General Remarks

This chapter presents the data produced and used to derive the Non Homogenous Poisson Process (NHPP) Models. At the beginning of the study, it was planned to only use simulated data because of the lack of any other ship evacuation data. Later on, the author was involved in the EU FP7-funded project SAFEGUAD [23] and it was decided to include the datasets produced by the project in the present study.

Two different data sets were used for the analysis described in this chapter:

- evacuation simulation data produced by the simulation software Evi and
- trial data obtained from evacuation drills on-board two different passenger ships performed during the SAFEGUARD project.

This chapter is organised as follows:

- Discussion on the quality of the data
- Presentation and description of the evacuation simulation data
- Analysis of the simulated data
- Presentation and description of the real data
- Analysis of the real data.

Details are presented in the following sections.

6.2 Data quality

When using data to build a model, it should be kept in mind that the quality of the data will have an impact on the accuracy and prediction capability of the resulting model. So before proceeding with the description and analysis of both the simulated and real data, a brief discussion on the quality of the data is needed.

By definition simulation data is the result of an interpretation (model) of the reality. Thus, it will suffer from a number of shortcomings such as model simplifications, coding implantation, error propagation and (pseudo) random generation of numbers.

Real or trial data are not exempt from errors or weaknesses either. They can suffer from errors due to the data collection methods, might not be replicated as a number of parameters cannot be controlled or are limited in terms of the entities that can be measured.

For example, in the case of the real data that has been used in this work, in one of the trials an unknown number of people decided to take part in the drill at the last minute so they were not provided with tracking devices. Their arrival times at the muster stations could not be accounted for but they had an influence on the overall mustering process. This has introduced uncertainties which are hard to assess.

Uncertainty quantification of both the simulation and real data is outside the scope of this work and data quality and its impact on the resulting stochastic model have not been investigated further. Nevertheless, when interpreting the results of the model fitting and then the generation of the batches as well as the NHPP, this was taken into account to a certain degree.

6.3 Ship model

This section describes the ship model used to produce the simulated data.

The ship, the model of which was used in the evacuation simulation, is a 166m ROPAX vessel carrying up to 1800 passengers and 137 crew members. The ship characteristics are given in Table 6-1 below:

Length Overall (m)	166.1
Length between perpendiculars (m)	150
Moulded beam (m)	29
Maximum draught (m)	6.78
Displacement (tonnes)	16 939
Number of passenger	1 800
Number beds	1 601
Number of cars	510
Total crew	137

Table 6-1: ship particulars

For confidentiality reasons, the general arrangement of the ship cannot be shown. Instead a brief description of the different decks is given below.

- Deck 2 has crew cabins and crew recreation areas (sauna, swimming pool and gym).
- Deck 3 (upper and lower) is the car deck.
- Deck 4 is an accommodation deck and contains disable passengers cabins. The gang ways are also situated on this deck.
- Deck 5 and Deck 6 are also accommodations decks with very similar layout.
- On Deck 7 there are public spaces with shops, casino, bars, the galley and crew mess.
- The main restaurant is on Deck 8, with the 1st level of the auditorium, crew cabins and the crew recreation room.
- On Deck 9 there is the second level of the auditorium, cinema and projection rooms.
- Deck 10 has the sundeck, bar and lounge, crew cabins (officers) and some crew spaces (sauna, offices,...).
- On Deck 11, there is the bridge and the helicopter landing area.
- Deck 12 is the wheel house top.

In addition, there are three (03) muster stations on-board the ship:

- two (02) muster stations are located on deck 7: the “Gaming area” and the “Bar” muster stations and
- one (01) on deck 8 the “Restaurant” muster station.

Each space on-board is assigned a muster station. Passengers would then go to the muster station assigned to the space they would find themselves in.

Figure 6-1 below shows the Evi model of the ship (profile and deck layout). Areas in pink in Figure 6-2 show the muster stations in the Evi model of the ship.

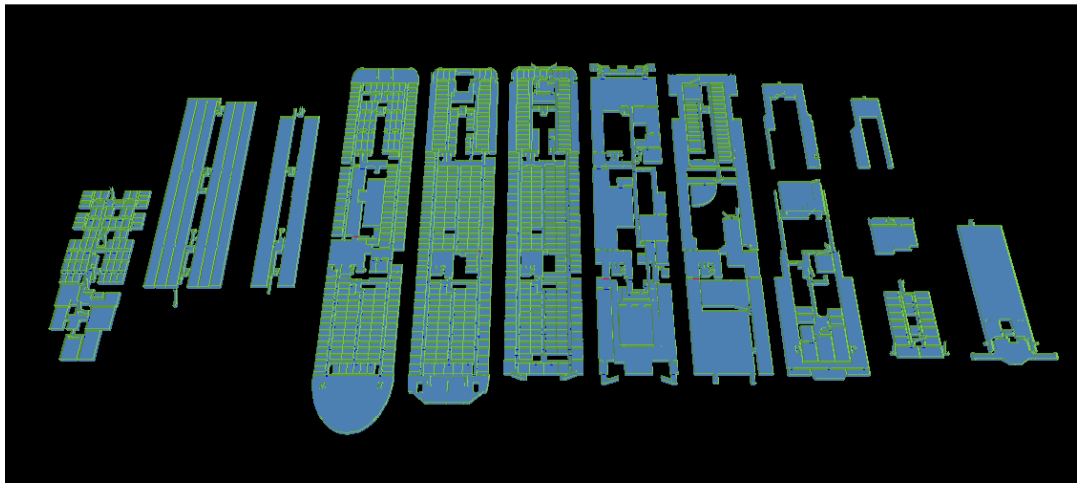
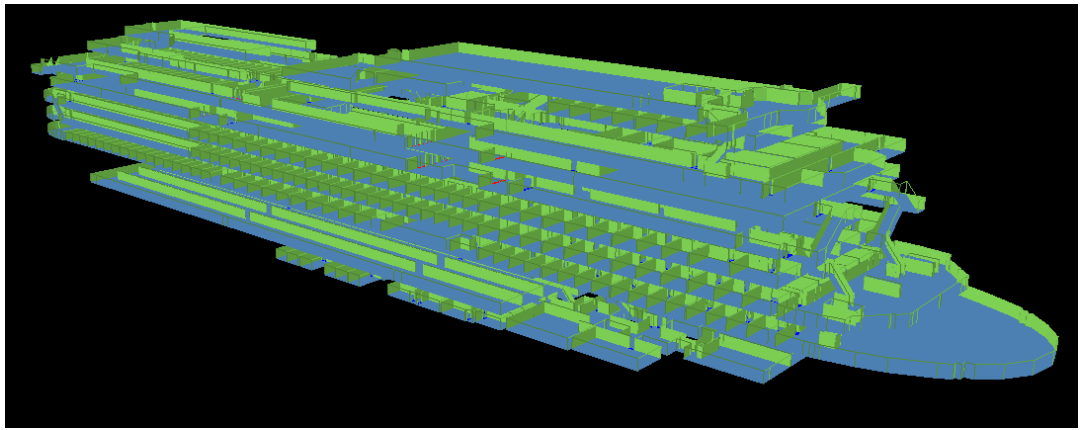


Figure 6-1: Evi model of the ROPAX ship used for the study

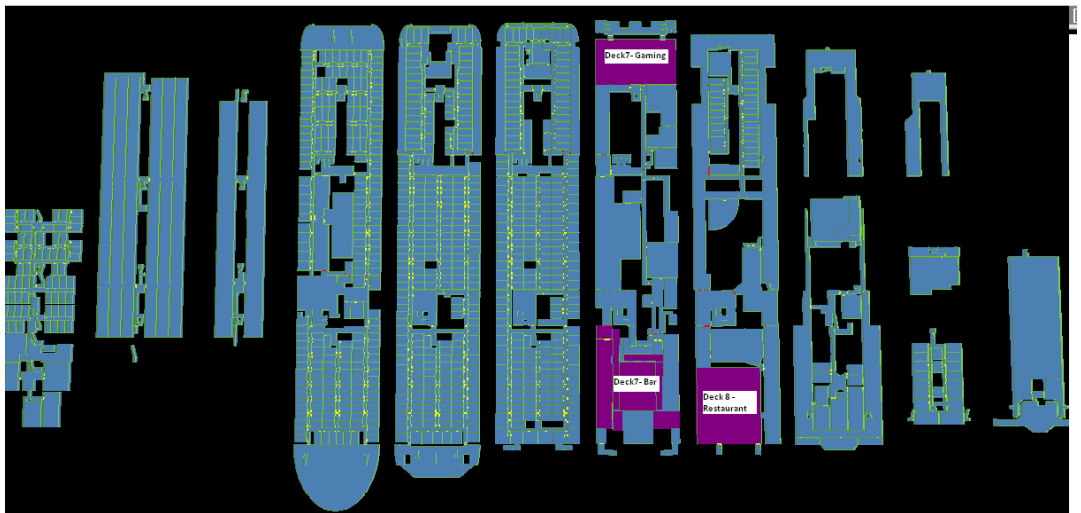


Figure 6-2: Location of the muster stations on-board the ship

6.4 Simulation setting

In order to derive a parametric model of the simulation process a number of simulations have been performed. The IMO [2] primary scenarios have been used in this study.

6.4.1 IMO Scenarios

The IMO night and day cases are summarised hereafter. A detailed description can be found in [2].

Case 1 (primary evacuation case, night)

- All passengers are in cabins with maximum berthing capacity fully occupied;
- Two thirds (2/3) of crew members in their cabins;
- Of the remaining 1/3 of crew members:
 - 50% should be initially located in service spaces and behave as passengers having walking speed and reaction time as defined in the IMO guidelines and presented in Chapter 4;
 - 25% should be located at their emergency stations and should not be explicitly modelled; and
 - 25% should be initially located at the assembly stations and should proceed towards to the most distant passenger cabin assigned to that assembly station in counterflow with evacuees;

Case 2 (primary evacuation case, day)

- Public spaces are occupied to 75% of maximum capacity of the spaces by passengers. Crew will be distributed as follows:
- 1/3 of the crew, initially distributed in their cabins, will behave as passengers with crew's walking speeds and reaction times;
- 1/3 of the crew, initially distributed in the public spaces, will behave as passengers with crew's walking speeds and reaction times;
- The remaining 1/3 should be distributed as follows:
 - 50% should be located in service spaces;

- 25% should be located at their emergency stations and should not be explicitly modelled; and
- 25% should be initially located at the assembly stations and should proceed towards to the most distant passenger cabin assigned to that assembly station in counterflow with evacuees;

Cases 3 and 4 (secondary evacuation case, night and day)

In these cases, only the main vertical zone, which generates the longest assembly time, is further investigated. These cases utilise the same population demographics as in case 1 (for case 3) and as in case 2 (for case 4).

The secondary cases were not simulated in the context of this thesis. There are mentioned here only for completeness.

6.4.2 Parameters of the simulated scenarios

In the different scenarios considered in this work, the following elements were varied:

- Time of day
- Passengers loads
- Reaction time
- Walking speed

The variations were considered as follows:

1. Day scenarios and Night scenarios for the 1st parameter
2. The second parameter, passenger load, varied from 10% to 100% with an increment of 10% of the total number of passengers who could be carried on-board. It was assumed that crew numbers would stay the same in all scenarios.
3. The reaction time was set to a fixed value (0s) for all agents and then to the reaction time as defined in the IMO guidelines (log normal distribution) for both night and day scenarios.
4. Walking speed was set to a fixed value then to the IMO defined values for walking speed.

The following are the numbers of scenarios considered for which simulations have been performed:

- For a fixed speed and varying reaction time, 10 passenger loads for the day case, and 10 passengers load for the night case,
- For a varying speed and a fixed reaction time, 10 passenger loads for the day case, and 10 passengers loads for the night case,
- For a varying speed and a varying reaction time, 10 passenger loads for the day case, and 10 passengers loads for the night case.
- For a fixed speed and fixed reaction time, 10 passenger loads for the day case, and 10 passengers load for the night case,

This gives a total number of 80 scenarios, where each of the scenarios has been simulated 100 times.

The simulation produces an evacuation curve where the arrival time of the passenger agents to the muster station is recorded. Here the arrivals are aggregated for all the muster stations. Arrival at individual muster stations was not studied for this part of the work as this information was not available. Arrival at individual muster stations was analysed for the trial data as will be detailed in the dedicated section later in this chapter.

6.5 Analysis of the simulated data

The data generated from the 8000 individual runs was analysed in terms of batch sizes (number of people arriving at the muster stations at the same time) and the number of arrivals as these two aspects characterise the arrival process to be modelled.

In the following subsections, analysis of the data for the simulated Day and Night cases is presented.

6.5.1 Analysis of the batch sizes and events count for the Day cases

The Day scenarios are defined as Random Day case (random speed and random reaction time), Fixed Reaction Day case (random speed), Fixed Speed Day case (random reaction) and Fixed Speed and Fixed Reaction Day case. The results of each case are presented below.

As the minimum value that a batch size can take is 1, the interested focuses in the max value of the batch sizes which are shown hereafter.

6.5.1.1 Day Random

For the **Day Random** the maximum and minimum values over a hundred runs per passengers load, of the Max batch size value are shown in the graph below.

As can be seen in Figure 6-3 there is quite a large variation in the size of the batches over the runs and per passengers load.

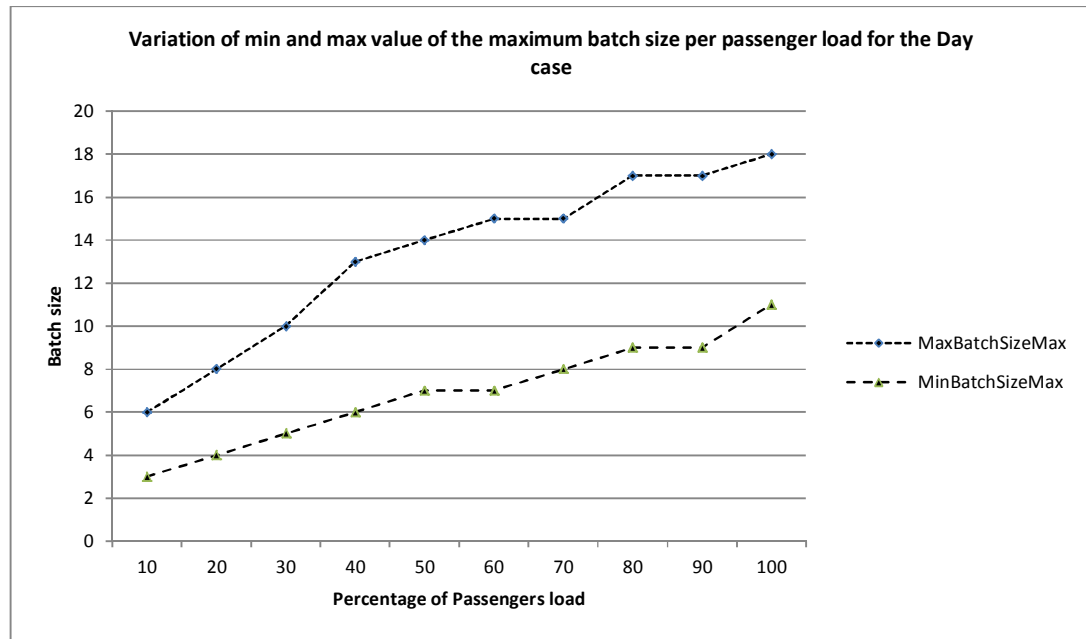


Figure 6-3: Variation of max and min values of the maximum batch size for the day case per passengers load.

The number of events over the simulation runs per passengers loads does not vary as much. The difference between the minimum and maximum number of events is quite small as can be seen in Figure 6-4 below.

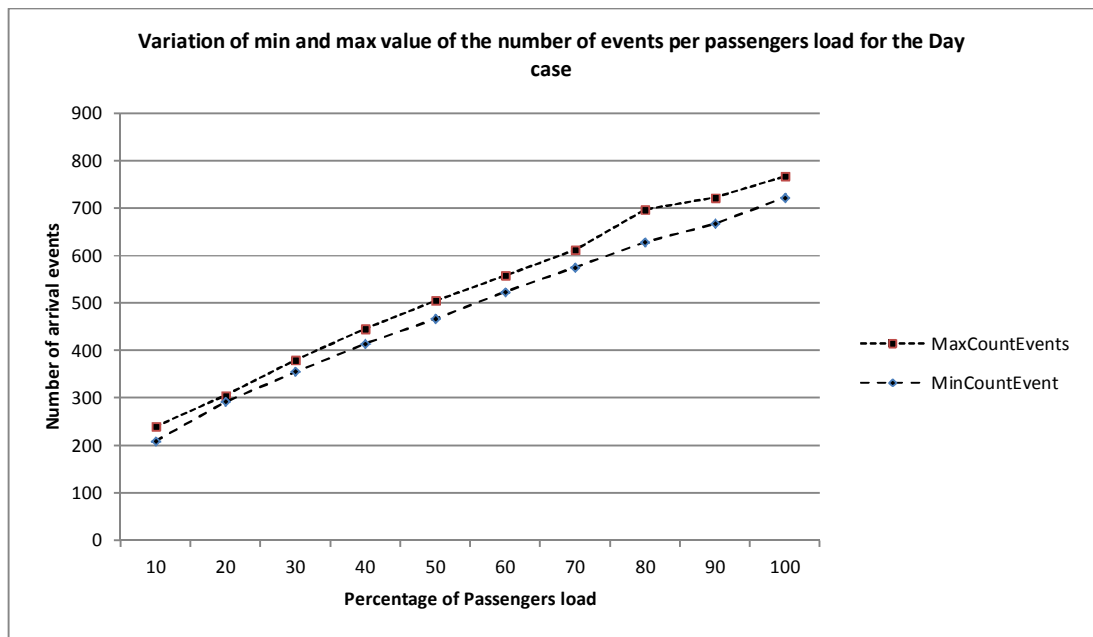


Figure 6-4: Variation of number of events in the simulation runs for the day case per passengers load.

6.5.1.2 Day Fixed Reaction

For the **Day Fixed Reaction** case, very similar results are obtained. There is quite a large variation between the min and max values of the maximum batch size and a small variation between the min and max values of the number of events as can be seen in Figure 6-5 and Figure 6-6.



Figure 6-5: Variation of max and min values of the maximum batch size for the day case with fixed reaction per passengers load.

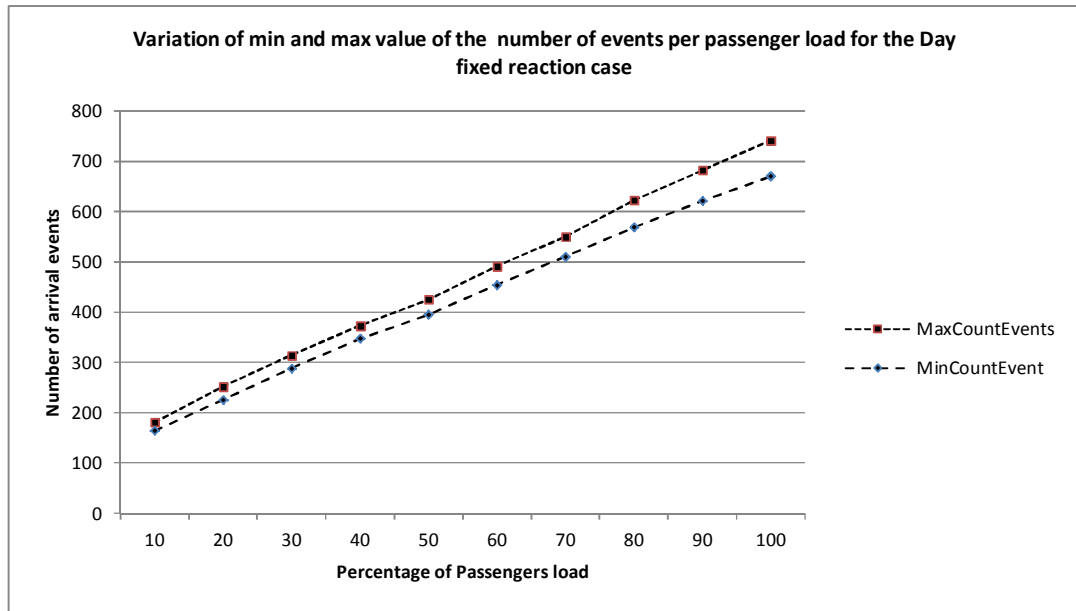


Figure 6-6: Variation of number of events in the simulation runs for the day with fixed reaction case per passengers load

6.5.1.3 Day Fixed Speed

Results for the **Day Fixed Speed** case are very similar to the previous cases as can be seen in Figure 6-7 and Figure 6-8 below.

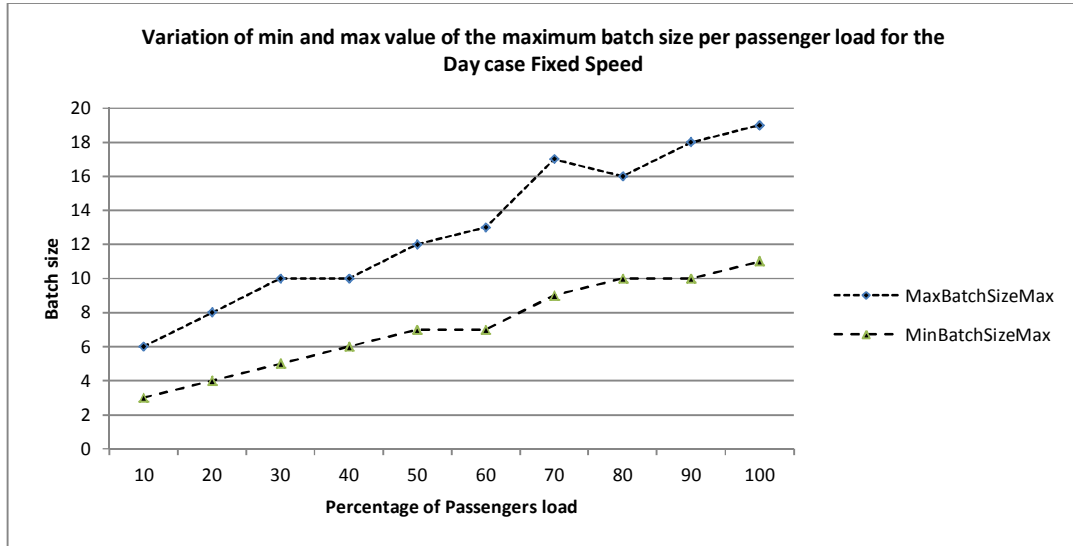


Figure 6-7: Variation of max and min values of the maximum batch size for the day case with fixed speed per passengers load.

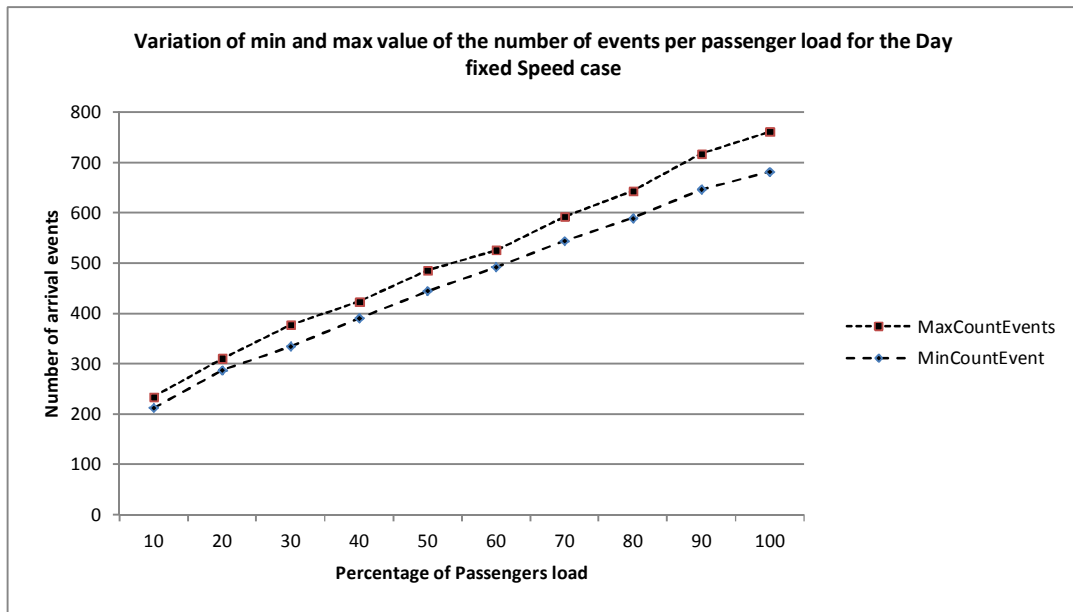


Figure 6-8: Variation of number of events in the simulation runs for the day with fixed speed case per passengers load

6.5.1.4 Day Fixed Speed and Fixed Reaction

Finally, for the **Day Fixed Speed and Fixed Reaction** case, the results are shown in Figure 6-9 and Figure 6-10.

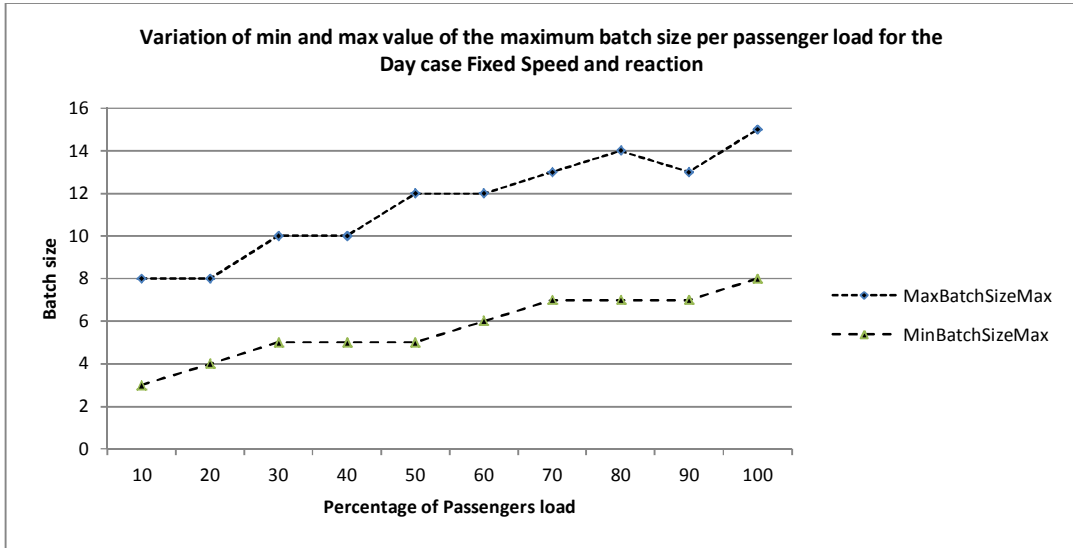


Figure 6-9: Variation of max and min values of the maximum batch size for the day case with fixed speed and reaction per passengers load.

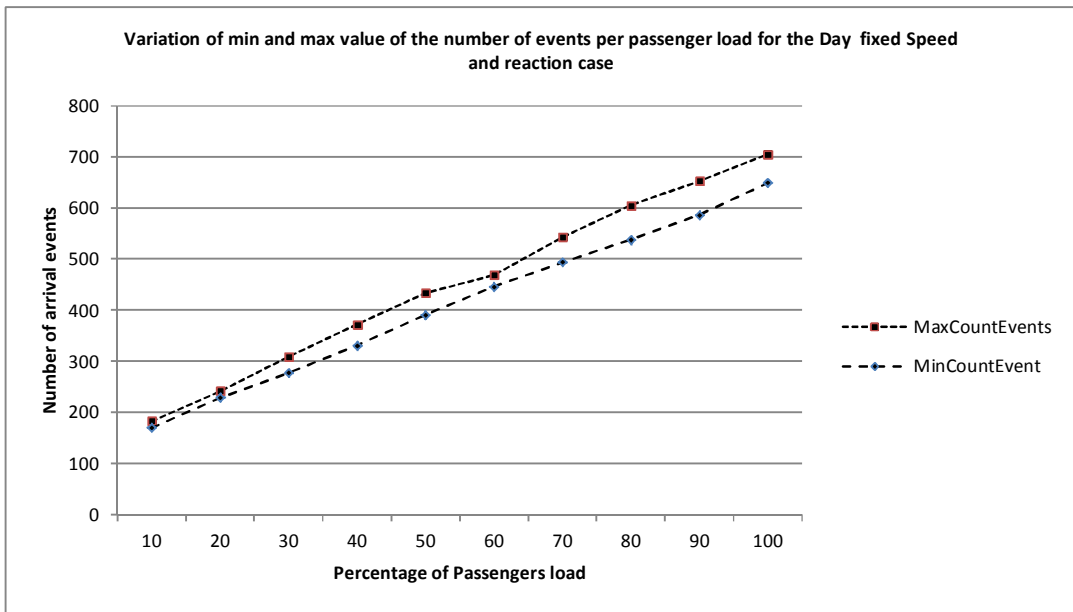


Figure 6-10: Variation of number of events in the simulation runs for the day with fixed speed and reaction case per passengers load

Here again results are very similar to the previous ones.

6.5.1.5 Summary

As expected, the number of events (arrivals at the muster stations) increases linearly with the passengers load and this is regardless of the speed or reaction time being random or fixed.

As can be seen in Table 6-2 below, for passengers load below 50%, the max number of events for both the “Fixed Speed and Reaction” and “Fixed Reaction” cases are very similar. The difference starts to be more significant for loads higher than 50%.

For the “Day Random” and the “Fixed Speed” cases, the max numbers of events are similar for loads below 30% and above 70%. In between the difference in the max number of events between these two cases is bigger.

For the minimum number of events, the trends are also very similar. The results for the “Day Random” case and the “Fixed Speed” case are close together and the ones for the “Fixed Speed and Reaction” and “Fixed Reaction” cases are close together.

% Pax Load	Max Number of Events				Min Number of Events			
	Day random	Fixed Reaction	Fixed speed	Fixed Speed + Reaction	Day random	Fixed Reaction	Fixed speed	Fixed Speed + Reaction
10	240	181	234	183	209	164	212	170
20	305	252	310	242	292	226	287	229
30	380	314	377	309	355	288	334	277
40	446	373	423	372	414	347	390	331
50	505	425	485	434	467	395	444	391
60	558	491	525	469	523	454	492	446
70	612	550	592	543	575	510	544	494
80	697	622	643	605	628	568	589	538
90	722	682	717	653	667	621	646	586
100	767	741	761	705	722	670	681	649

Table 6-2: Max and min number of events for different passengers loads and for the different day cases.

6.5.2 Analysis of the simulated data for the Night cases

The analysis of the batch size and the number of events per evacuation simulation as produced by the simulations for the night case are presented hereafter.

The Night scenarios are defined as Random Night case (random speed and random reaction time), Fixed Reaction Night case (random speed), Fixed Speed Night case (random reaction) and Fixed Speed and Fixed Reaction Night case. The results of each case are presented below.

Similarly to the day case, we are only interested in the maximum value of the batch sizes.

6.5.2.1 Night Random

The maximum and minimum values over a hundred runs per passengers load, of the Max batch size value are shown in the graph below, for the **Night Random** case.

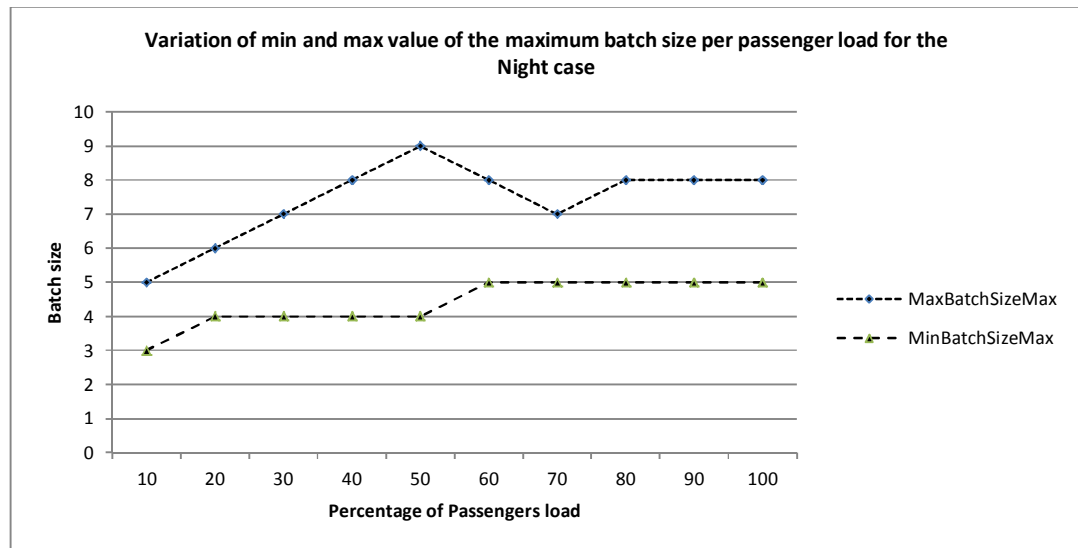


Figure 6-11: Variation of the min and max values of the maximum batch size per passengers load for the night case

As can be seen in Figure 6-11 above there is quite a large variation in the size of the batches over the runs and per passengers load. For loads greater than 60% the minimum value of the max batch size becomes constant. The maximum value of the batch sizes becomes

constant at a value of 8 for loads bigger than 80% but it is worth noting that at 70% passengers load if it was not for the drop in the batch size by one unit, the maximum value could have been constant from 60% passenger load.

The number of events over the simulation runs per passengers loads does not vary as much. The difference between the minimum and maximum number of events is quite small as can be seen in Figure 6-12 below with the exception of the 100% load where a “jump” can be observed for the maximum number of events.

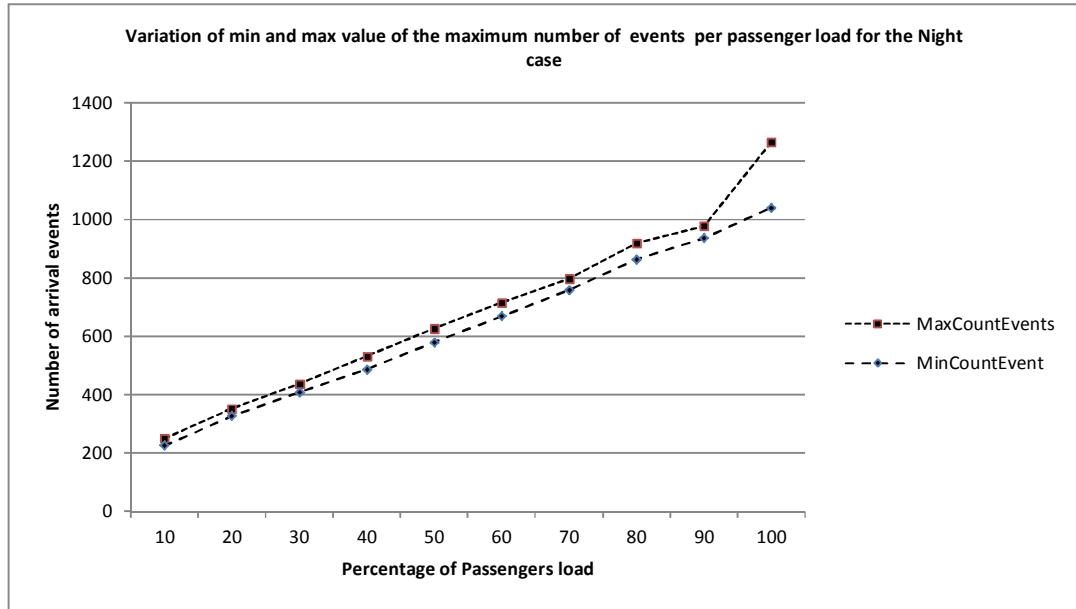


Figure 6-12: Variation of the min and max values of the number of events per passengers load for the Night case.

6.5.2.2 Night Fixed Reaction

For the **Night Fixed Reaction** case, the shape of the curves for the max and min of the maximum batch size is quite similar to the Random Night case. Here the minimum value of the max batch size becomes constant for loads greater than 40%. The maximum value is constant for loads bigger than 70% as in the previous case if it was not for an increase by one unit at 60% load, the maximum value of the max batch size could have been constant from a 50% load as can be seen in Figure 6-13.

As can be seen in Figure 6-14, there is not much difference between the min and max number of events.

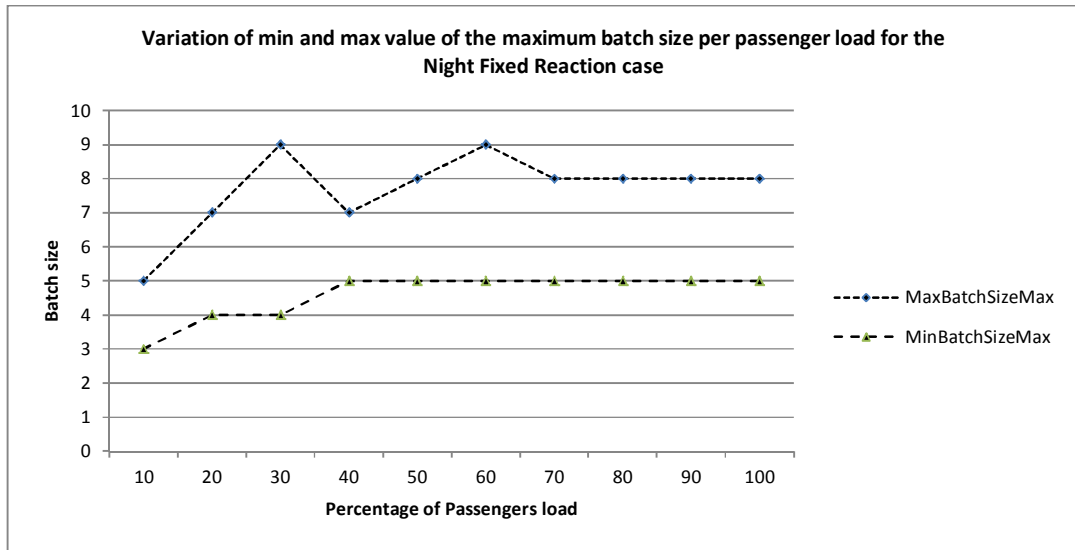


Figure 6-13 Variation of the min and max values of the maximum batch size per passengers load for the night fixed reaction case

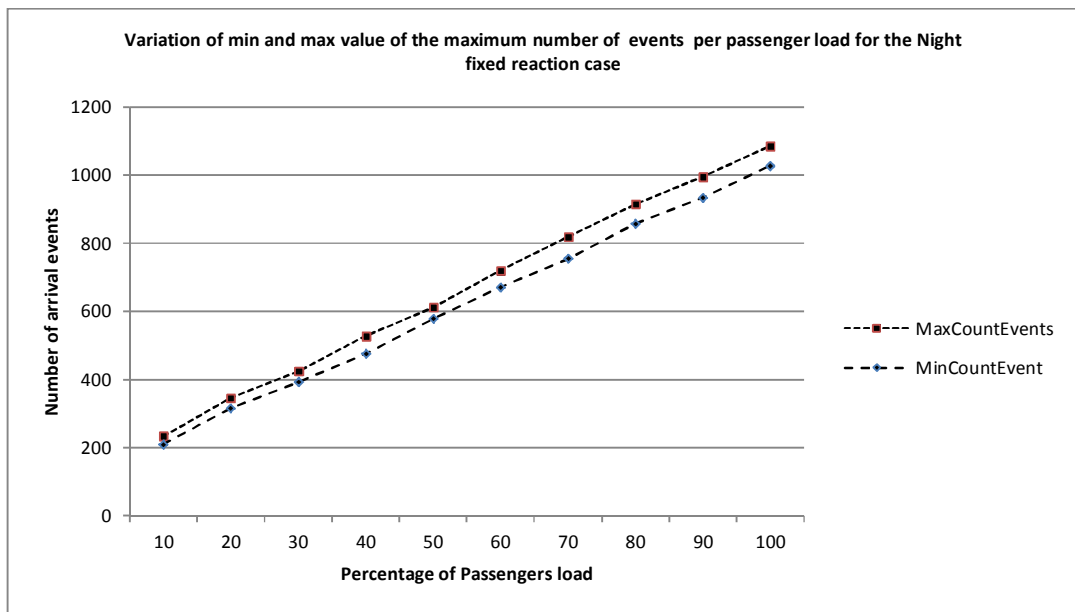


Figure 6-14: Variation of the min and max values of the number of events per passengers load for the Night fixed reaction case

6.5.2.3 Night Fixed Speed

For the **Night Fixed Speed** case, there is still a significant difference between the min and max values of the maximum batch size as can be seen in Figure 6-15. For this case the minimum value of the max batch size is constant starting from 50 % load. For the max value, it is constant for loads bigger than 60% with a slight “dip” at 90% loads.

The difference between the min and max values of the number of events is not very significant as can be seen in Figure 6-16.

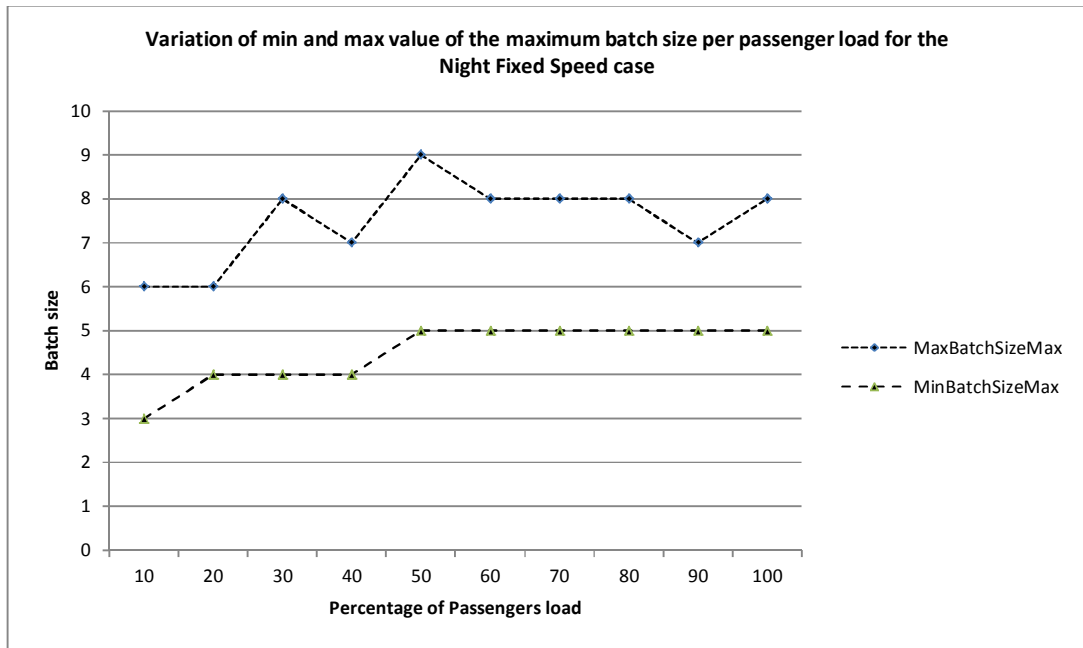


Figure 6-15: Variation of the min and max values of the maximum batch size per passengers load for the night fixed speed case

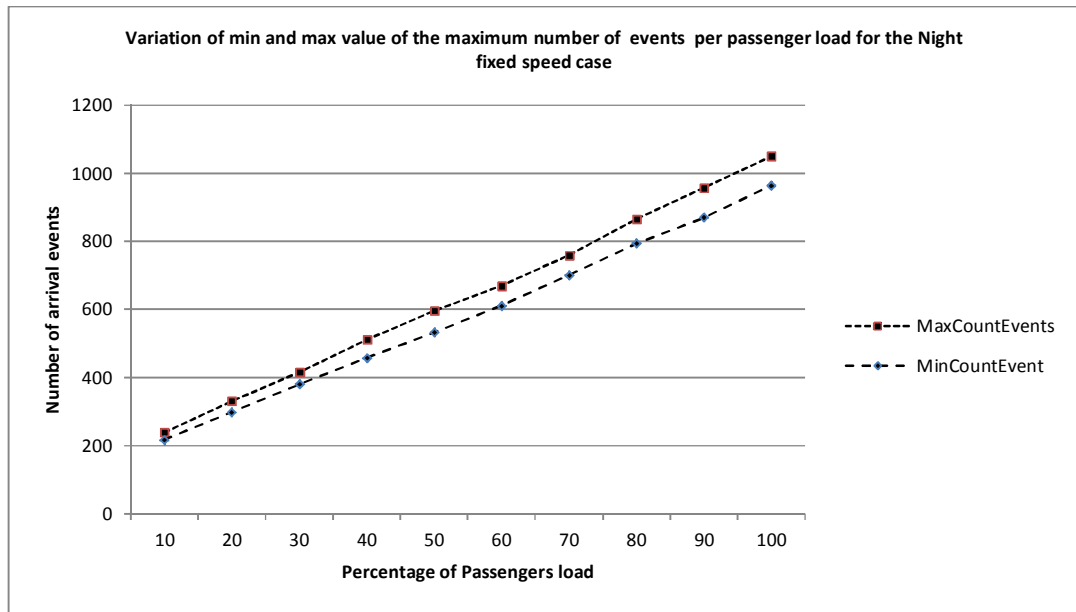


Figure 6-16: Variation of the min and max values of the number of events per passengers load for the Night fixed speed case

6.5.2.4 Night Fixed Speed and Fixed Reaction

For the **Night Fixed Speed and Fixed Reaction** case, the curve for the minimum number of max batch size is identical to the one for the Night Fixed Reaction case. There are still some differences between the max and min values (Figure 6-17). The curves for min and max values for the number of events are still close together (Figure 6-18) for this case.

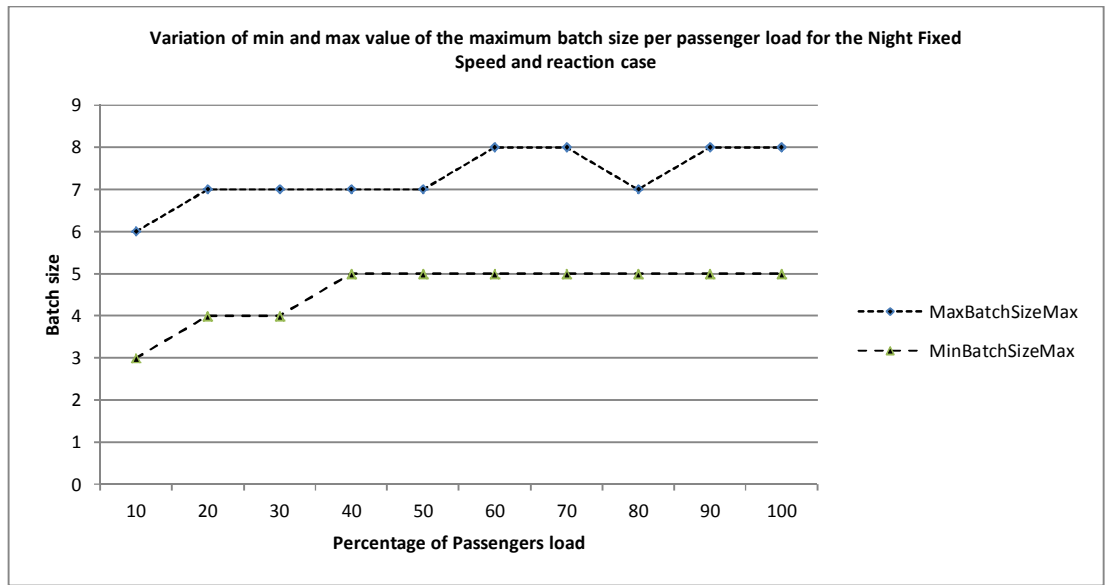


Figure 6-17: Variation of the min and max values of the maximum batch size per passengers load for the night fixed speed and reaction case

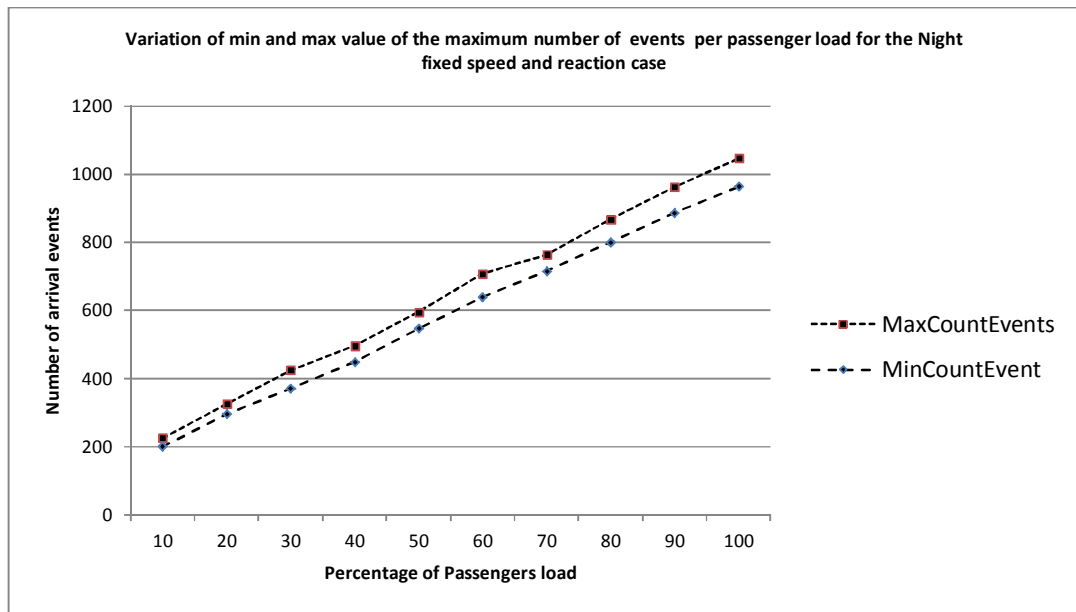


Figure 6-18: Variation of the min and max values of the number of events per passengers load for the Night fixed speed and reaction case

6.5.2.5 Summary

Similarly to the Day cases, the number of events (arrivals at muster stations) increases linearly with the passengers load and this is not affected by the speed or reaction time being random or fixed.

As can be seen in Table 6-3 below, the max numbers of events for all cases are quite similar. Notice that the results for the “Night Random” and “Fixed Reaction” cases could be grouped together as their ranges are comparable. The same can be said of the results for the “Fixed Speed” and “Fixed Speed and Reaction”.

For the minimum number of events, the trends are also very similar. The results for the “Night Random” case and the “Fixed Reaction” fall within similar ranges. The same is applicable to the results for the “Fixed Speed and Reaction” and “Fixed Speed” cases.

% Pax Load	Max Number of Events				Min Number of Events			
	Night random	Fixed Reaction	Fixed speed	Fixed Speed + Reaction	Night random	Fixed Reaction	Fixed speed	Fixed Speed + Reaction
10	250	234	239	225	225	210	217	200
20	352	346	331	326	326	316	298	296
30	437	425	416	425	408	393	380	371
40	531	528	511	496	486	476	457	448
50	626	612	596	595	579	578	532	546
60	715	720	669	708	668	671	611	639
70	797	819	759	764	758	755	701	715
80	919	916	865	867	863	858	794	800
90	978	996	957	962	936	934	870	886
100	1265	1086	1050	1046	1040	1028	964	963

Table 6-3: Max and min number of events for different passengers loads and for the different night cases

6.5.3 Discussion

The above results show that for the Max batch size, the Day cases show more randomness in the results than the Night cases. The maximum and minimum values of the Max Batch size are also bigger for the Day cases (up to 19 for Day cases and 8 for the Night cases for max values and up to 11 for the Day cases and 5 for the Night cases for minimum values).

This leads to less events happening but more people in each batch. For the Night case, the opposite happens, where more events are happening but at smaller batch sizes.

This could be explained by the fact that for the Night cases, all passengers start from the cabins and there is very little randomness in the starting location of the passengers from one simulation run to the other. In contrast for the Day cases, passengers are located in public spaces and can be spread out throughout the ship. In addition, some of those public spaces are muster stations meaning that some passengers might already be in their assigned muster station explaining bigger batch sizes.

6.6 Real data

The data presented and analysed in this section has been produced by the FP7, EU-funded project Safeguard (2009-2012), the aim of which was to propose new benchmark scenarios for the evacuation analysis of passenger ships. During the project a number of assembly drills on-board a large RO-PAX ferry and a Cruise Ship were carried out.

Passengers who took part wore Infrared (IR) tags so their starting and ending locations as well as their arrival times were recorded by means of a number of beacons located at different positions on-board. Video cameras were also used to record the drills and extract reaction times.

This has produced two data sets: The Safeguard Validation Data Sets (SGVDS), SGVDS1 and SGVDS2 for the large RO-PAX ferry and the Cruise Ship, respectively. These datasets were made public and can be accessed at this address:

http://fseg.gre.ac.uk/validation/ship_evacuation (last accessed on September 2016). They can be used to assess evacuation simulation tools [23-26].

In the context of this thesis, the data is analysed from the point of view of the arrival processes. In addition, the author (who participated in the project) contributed to the generation of Evi simulations corresponding to the actual drill and so had access to this data, which is also analysed in the context of this thesis and allows for a comparison with the real data.

The datasets are briefly described in the following subsections. More details can be found in [23-26].

6.6.1 SGDVS1

The information provided in this subsection is largely taken from [27].

The dataset was collected on-board a large RoPax Ferry which layout is shown in Figure 6-19 below. Only three decks were used in the drills.

The ship has four (04) muster stations A, B, C and D. They are shown below (Figure 6-20).

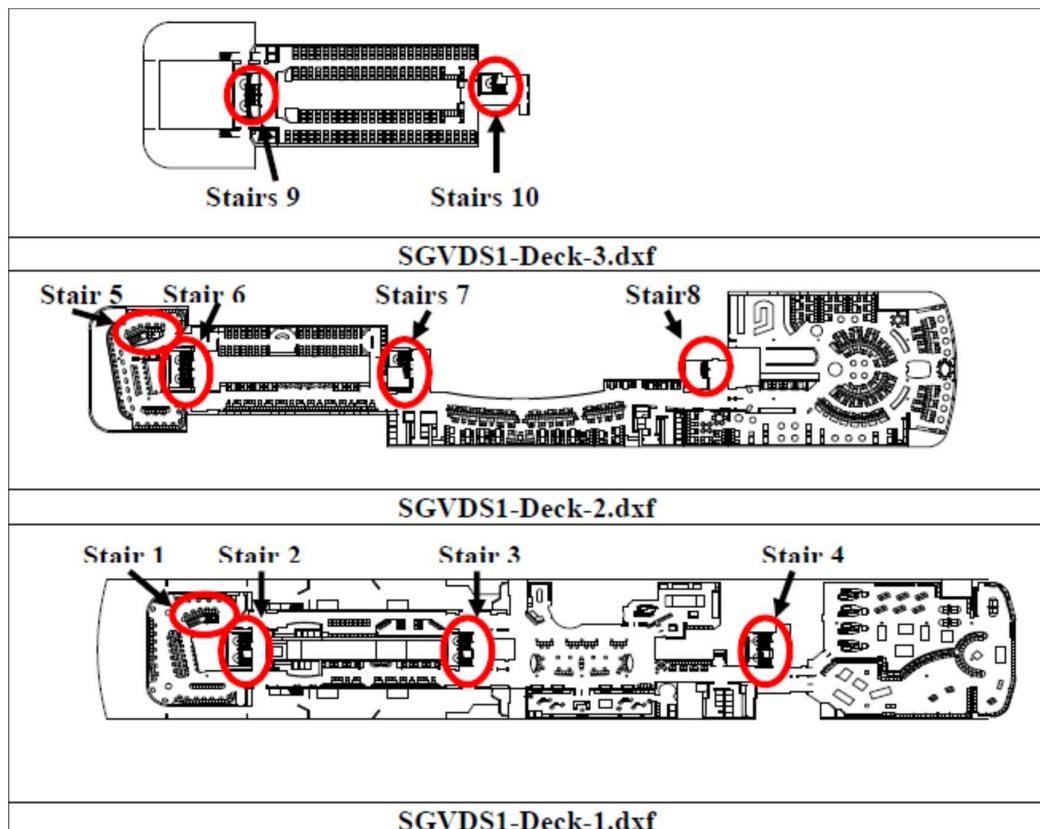


Figure 6-19: RoPax layout- taken from [27]

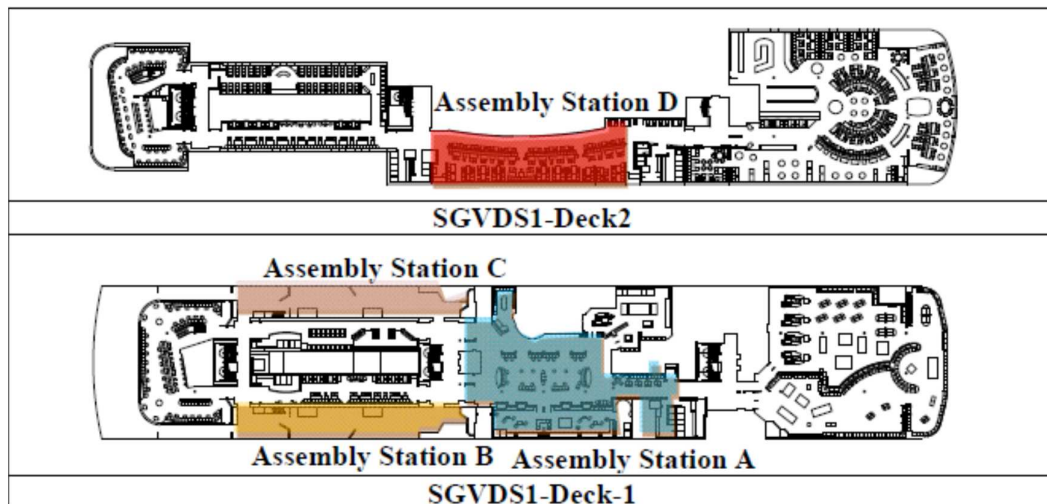


Figure 6-20: Location of RoPax Muster Stations - taken from [27]

During the drills 764 passengers took part and wore the IR tracking device. As taking part was not compulsory 569 decided not to participate and so were not given tags. Eventually a

large proportion of the 569 took part. It was not possible to determine how many of them did the drill so it was assumed that 250 additional passengers took part. When simulations were set for this dataset, the 250 additional passengers were added to the simulation as being part of the overall population but were not included in the analysis of the assembly station arrival curves and the total assembly times. The gender, age and walking speed distributions were defined according to the IMO Guidelines [2].

The starting locations of the passengers are shown in Figure 6-21.

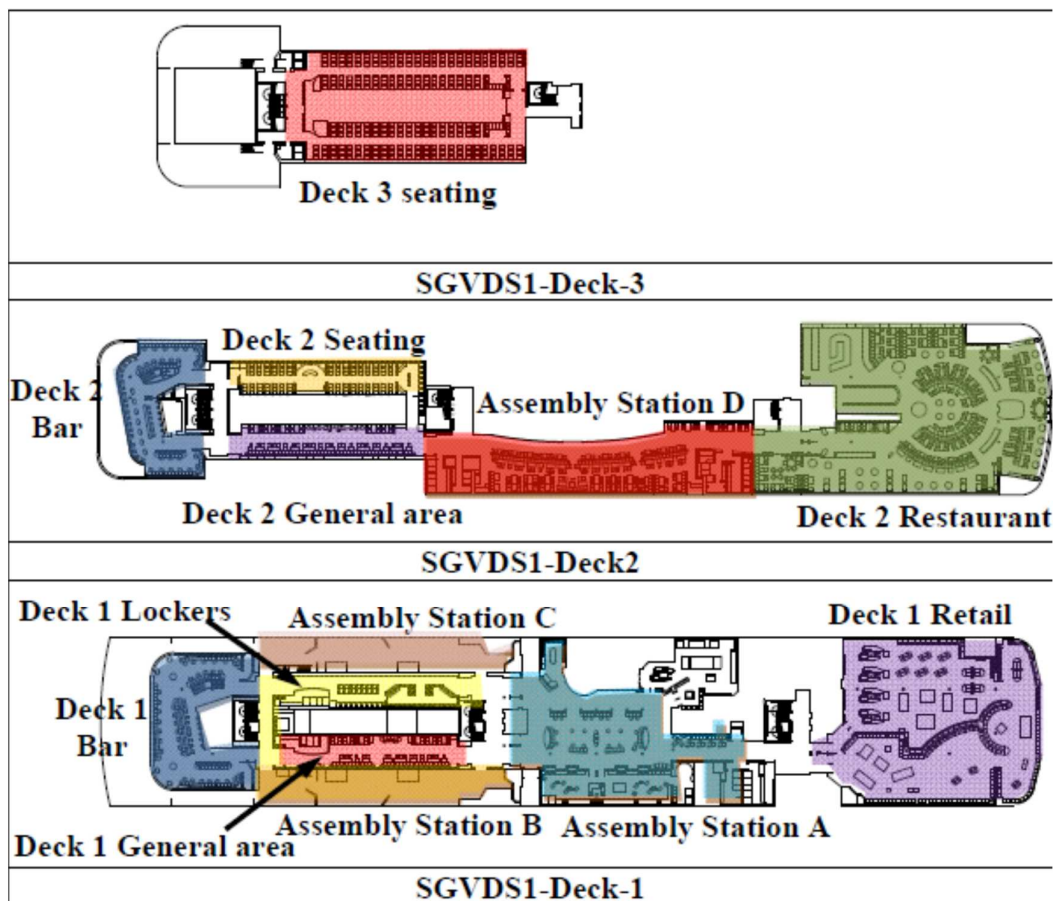


Figure 6-21: Stating locations of the passengers during the drill on-board the RoPax Ferry - taken from [27]

Passengers distribution per space and their final distribution is shown in Table 6-4 and Table 6-5 for the passengers who wore tracking devices and those who didn't respectively.

Starting Location of Population with IR Tags	Total number of agents starting in each area	End locations- Muster Stations			
		A	B	C	D
Deck 3- Seating	77	2	45	6	24
Deck 2 - Bar	39	0	9	30	0
Deck 2 - Seating	4	0	0	2	2
Deck 2 - General area	35	6	22	0	7
Muster Station D	145	5	1	0	139
Deck 2 - Restaurant	190	43	0	0	147
Deck 1 - Bar	30	3	19	19	0
Muster Station C	34	3	2	28	1
Deck 1- General area	35	2	28	5	0
Muster Station B	30	3	37	1	1
Muster Station A	99	80	13	1	5
Deck 1- Shop	7	7	0	0	0
Deck 1- Lockers	16	3	3	10	0
Total arriving at each Muster Station		157	179	102	326

Table 6-4: Number and starting location for the passengers wearing IR tags. RoPax Ferry- Adapted from [27]

Starting Location of Population without IR Tags	Total number of agents starting in each area	End locations- Muster Stations			
		A	B	C	D
Deck 3- Seating	30	6	14	2	8
Deck 2 - Bar	13	0	3	10	0
Deck 2 - Seating	1	0	0	0	1
Deck 2 - General area	11	2	7	0	2
Muster Station D	46	2	0	0	44
Deck 2 - Restaurant	61	14	0	0	47
Deck 1 - Bar	18	2	7	9	0
Muster Station C	11	1	1	9	0
Deck 1- General area	11	1	8	2	0
Muster Station B	13	1	12	0	0
Muster Station A	32	26	4	0	2
Deck 1- Shop	2	2	0	0	0
Deck 1- Lockers	1	0	1	0	0
Total arriving at each Muster Station		57	57	32	104

Table 6-5: Number and starting location for the passengers not wearing IR tags. RoPax Ferry- Adapted from [27]

Reaction times of the passengers were extracted from video footage. The probability distribution (log normal) is given by the following equation:

$$y = \frac{1}{\sqrt{2\pi} \sigma x} \exp \left[-\frac{(\ln(x) - \mu)^2}{2\sigma^2} \right]$$

Where: $min \leq x \leq max$

The values of the parameters were different per area and are defined as follows:

Location	Min	Max	μ	σ
Airline seating (A)	0	145.64	3.413	0.608
Bar Area (B)	0	402.4	3.432	0.924
General Ares (G)	0	311	4.019	1.032
Restaurant Area (R)	0	259.56	3.796	0.847
Retail/ Shopping area (S)	0	104.8	2.479	0.89

The different starting locations had the following reaction times allocated to them.

Starting Location	Reaction time distributions
Deck 3- Seating	A
Deck 2 - Bar	B
Deck 2 - Seating	A
Deck 2 - General area	G
Muster Station D	R
Deck 2 - Restaurant	R
Deck 1 - Bar	B
Muster Station C	G
Deck 1- General area	G
Muster Station B	G
Muster Station A	G
Deck 1- Shop	S
Deck 1- Lockers	G

Each muster station has an arrival curve associated to it. In addition, an overall arrival curve is also available.

6.6.2 SGDVS2

The information provided in this subsection is largely taken from [28].

The dataset was collected on-board a Cruise Vessel which layout is shown in Figure 6-22 below. Twelve (12) decks were used during the drills.

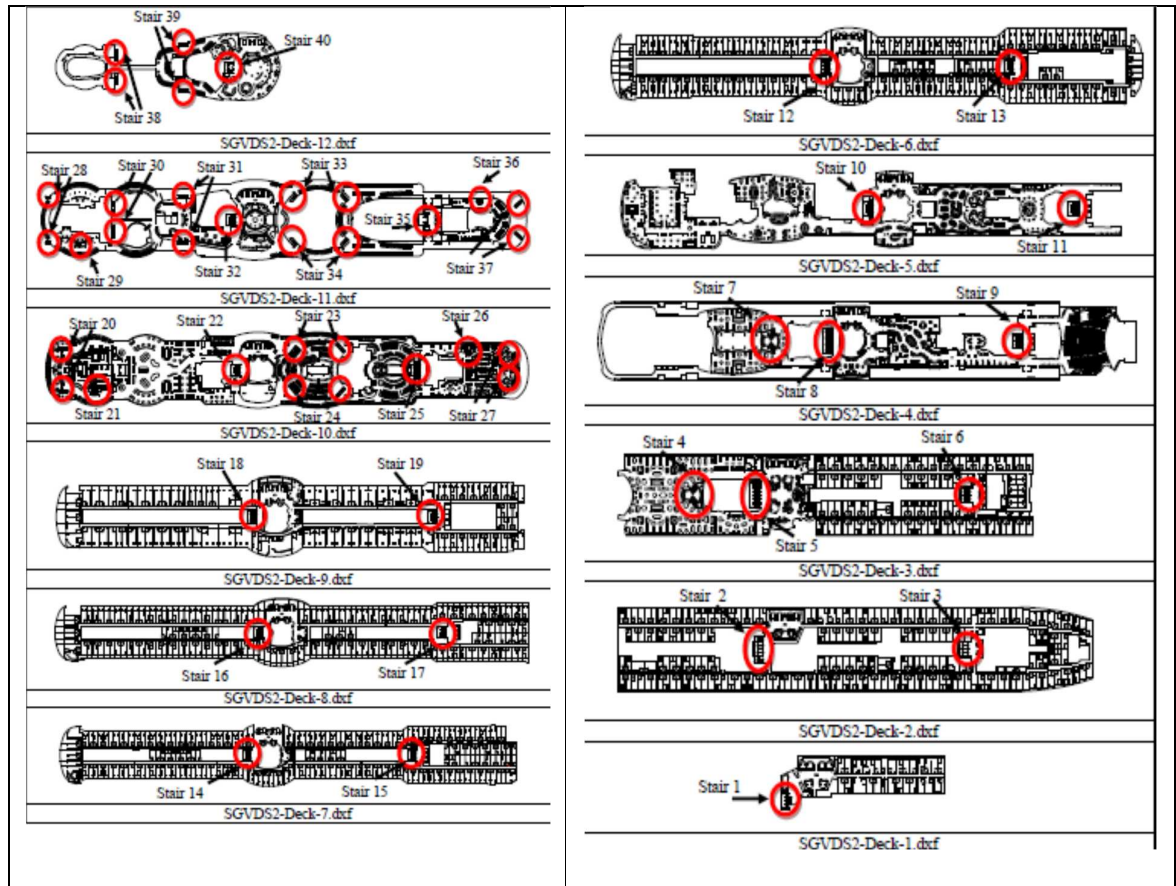


Figure 6-22: Cruise ship layout- taken from [28]

The vessel has four (04) Muster Stations: A, B, C and D. They are shown below (Figure 6-23).

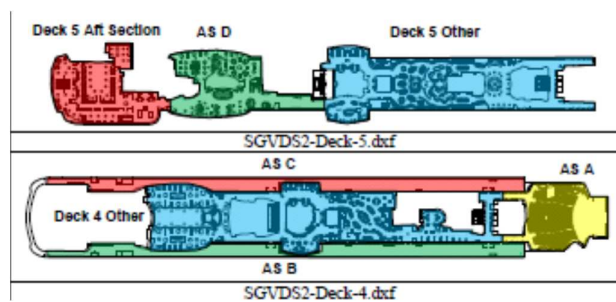


Figure 6-23: Location of Cruise ship Muster Stations - taken from [28]

During the drills 1779 passengers took part and wore the IR tracking device.

The gender, age and walking speed distributions were defined according to the IMO Guidelines [2] in the simulations corresponding to this dataset.

Passengers distribution per space and their final distribution are shown in Table 6-6

Starting Location	End locations- Muster Stations			
	A	B	C	D
Deck 12	0	6	2	0
Deck 11 Amidships	6	11	7	10
Deck 11 Other	16	14	14	12
Deck 10 Restaurant	129	126	103	65
Deck 10 Other	24	52	30	16
Deck 9 Aft Portside Cabins	1	5	12	13
Deck 9 Aft starboard side Cabins	0	10	2	14
Deck 9 Other	11	25	10	1
Deck 8 Aft Portside Cabins	0	4	14	35
Deck 8 Aft Starboard side Cabins	0	17	8	22
Deck 8 Other	25	21	7	0
Deck 7 Aft Portside Cabins	1	5	10	24
Deck 7 Aft Starboard side Cabins	0	22	3	6
Deck 7 Other	30	11	14	0
Deck 6 Aft Portside Cabins	0	4	11	22
Deck 6 Aft Starboard side Cabins	0	13	4	11
Deck 6 Other	33	19	20	2
AS D	4	3	6	14
Deck 5 Other	9	4	5	7
AS C	2	0	3	0
AS B	1	14	0	0
Deck 4 Other	18	31	28	25
AS A	5	0	0	0
Deck 3 Restaurant	46	43	56	52
Deck 3 Other	13	58	15	0
Deck 2 Aft Portside Cabins	0	0	18	7
Deck 2 Aft Starboard side Cabins	1	11	8	1
Deck 2 Other	25	45	15	2
Deck 1	2	1	12	4
Total	402	575	437	365

Table 6-6: Number and starting location for the passengers on-board the Cruise ship- Adapted from [28]

Like for SGVDS1, passengers reaction times were extracted from video footage. A global probability distribution was derived given by the following equation:

$$y = \frac{1}{\sqrt{2\pi} 0.89x} \exp \left[-\frac{(\ln(x) - 5.012)^2}{2(0.89)^2} \right]$$

Where: $0 \leq x \leq 1379$

Each muster station has an arrival curve associated to it. In addition, an overall arrival curve is also available.

6.6.3 Analysis of the real data: SGVDS1 dataset

The analysis of the number and size of batches of the SGVDS1 data set showed the following results

	Events count	Max Batch Size
Muster A	66	2
Muster B	102	4
Muster C	55	3
Muster D	115	6
Overall	223	8

Table 6-7: Event counts and max batch size for SGVDS1 dataset

6.6.3.1 Corresponding evacuation simulation runs.

When simulating evacuation of passengers corresponding to this dataset, to account for the passengers who took part in the drill and did not wear tracking devices as explained in the subsection describing SGVDS1, three scenarios were considered as follows;

- Scenario A: Passengers are sent to their assigned muster stations using regional response time.
- Scenario B: As scenario A, but with global reaction time distribution
- Scenario C: Passengers assemble in the nearest muster stations using regional reaction time distributions.

Passengers distribution over the ship is as described earlier.

Each scenario was runs 50 times. The analysis of the simulation runs is presented hereafter.

The events count “**N**” and the maximum value of the batch sizes “**Max BatchSize**” for each scenario are shown in Table 6-8 to Table 6-10 below.

Scenario A	N			Max BatchSize		
	Mean	Min	Max	Mean	Min	Max
Muster A	72.1	66	75	2.18	2	3
Muster B	126.42	118	128	2.52	2	4
Muster C	69.44	64	72	2.16	2	3
Muster D	158.24	148	167	2.94	2	4
Overall	308.02	289	316	5.12	4	8

Table 6-8: Statistics of the events count and max batch size for the Scenario A simulations for SGVDS1

Scenario B	N			Max BatchSize		
	Mean	Min	Max	Mean	Min	Max
Muster A	72.32	68	77	2.14	1	3
Muster B	126.82	120	130	2.52	2	3
Muster C	69.54	63	71	2.1	2	4
Muster D	158.58	146	162	3	2	4
Overall	310.5	292	330	5.1	4	6

Table 6-9: Statistics of the events count and max batch size for the Scenario B simulations for SGVDS1

Scenario C	N			Max BatchSize		
	Mean	Min	Max	Mean	Min	Max
Muster A	6.88	5	7	1.1	1	2
Muster B	83.58	79	85	2.14	2	3
Muster C	76.86	74	78	2.18	2	3
Muster D	206.72	192	215	3.46	3	5
Overall	287.38	271	295	4.82	4	6

Table 6-10: Statistics of the events count and max batch size for the Scenario C simulations for SGVDS1

When compared to the trial data, the events count obtained through simulations are overestimating those of the trial data for all scenarios as can be seen in Figure 6-24 to Figure 6-26 below.

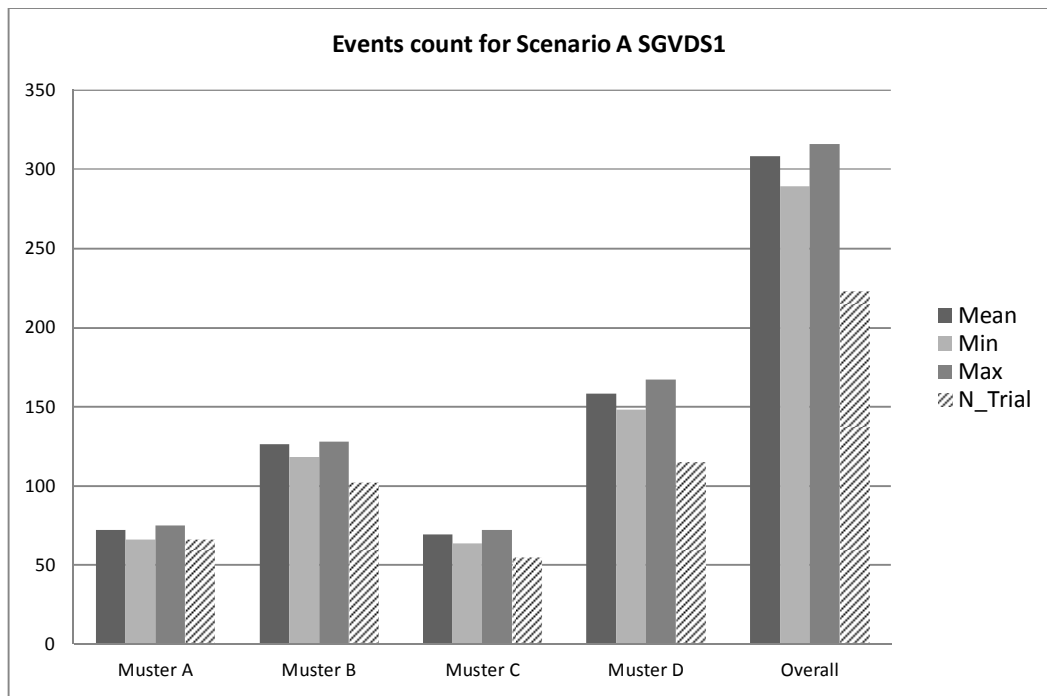


Figure 6-24: Comparison of the events count from simulation results with the trial data per muster station for scenario A

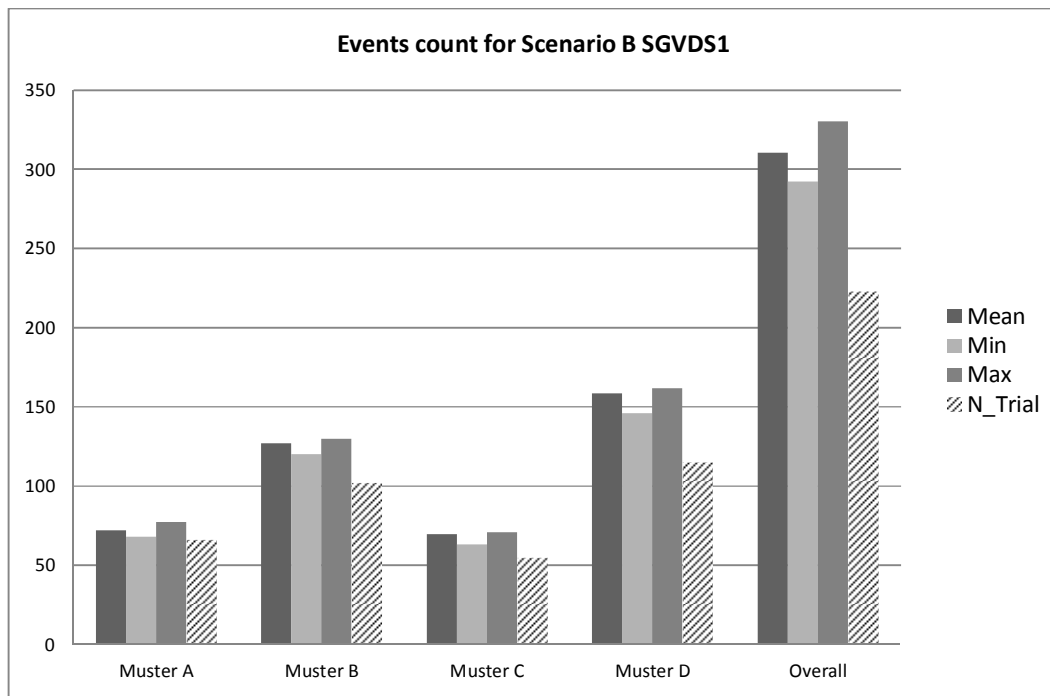


Figure 6-25: Comparison of the events count from simulation results with the trial data per muster station for scenario B

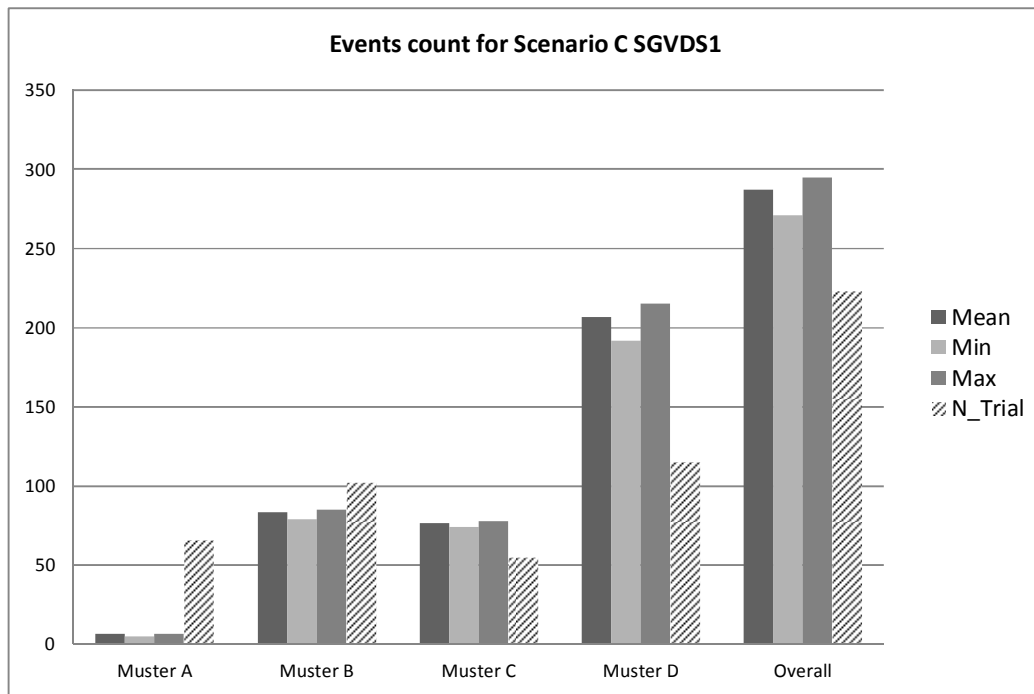


Figure 6-26: Comparison of the events count from simulation results with the trial data per muster station for scenario C

For the max batch size, the simulation results tend to underestimate the max batch size when compared to the trial data as can be seen in Figure 6-27 to Figure 6-29 below.

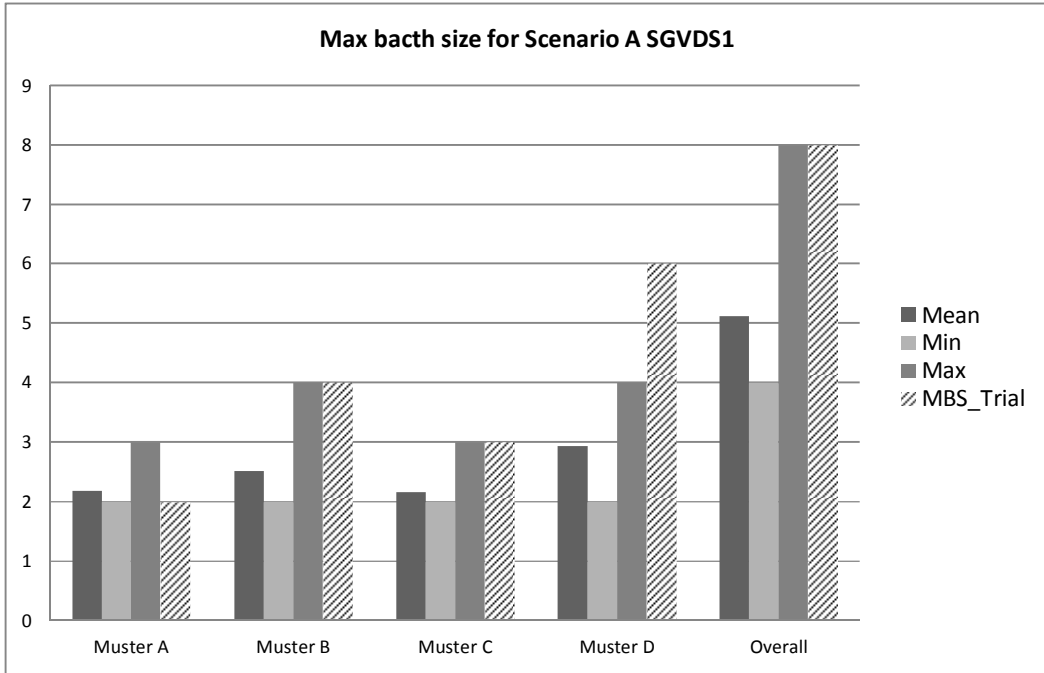


Figure 6-27: Comparison of the max batch size values from simulation results with the trial data per muster station for scenario A

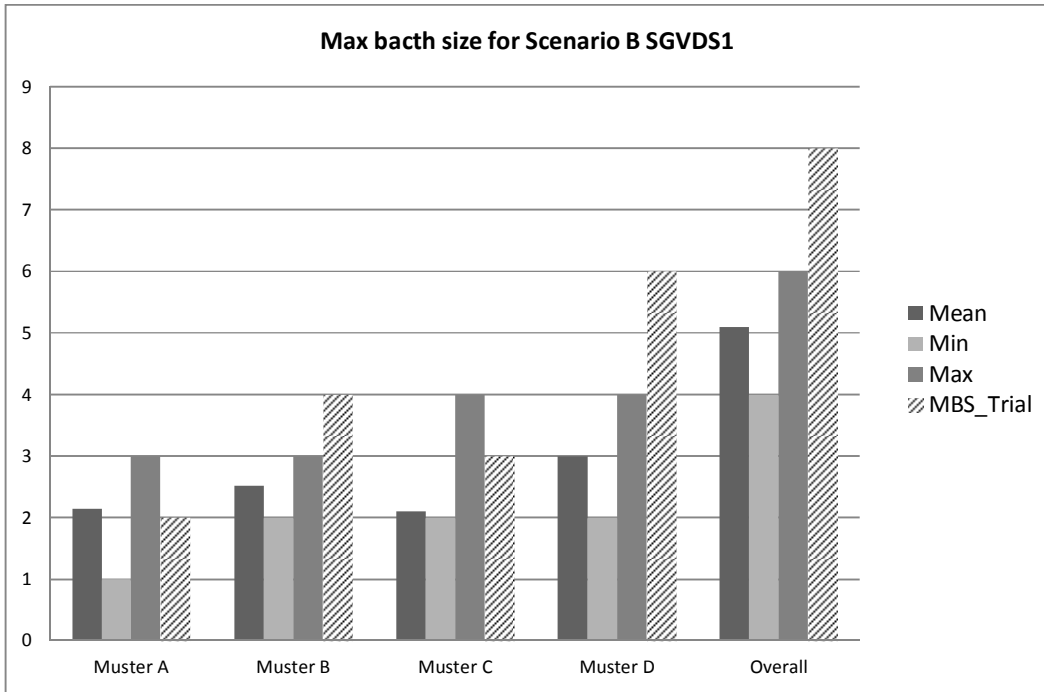


Figure 6-28: Comparison of the max batch size values from simulation results with the trial data per muster station for scenario B

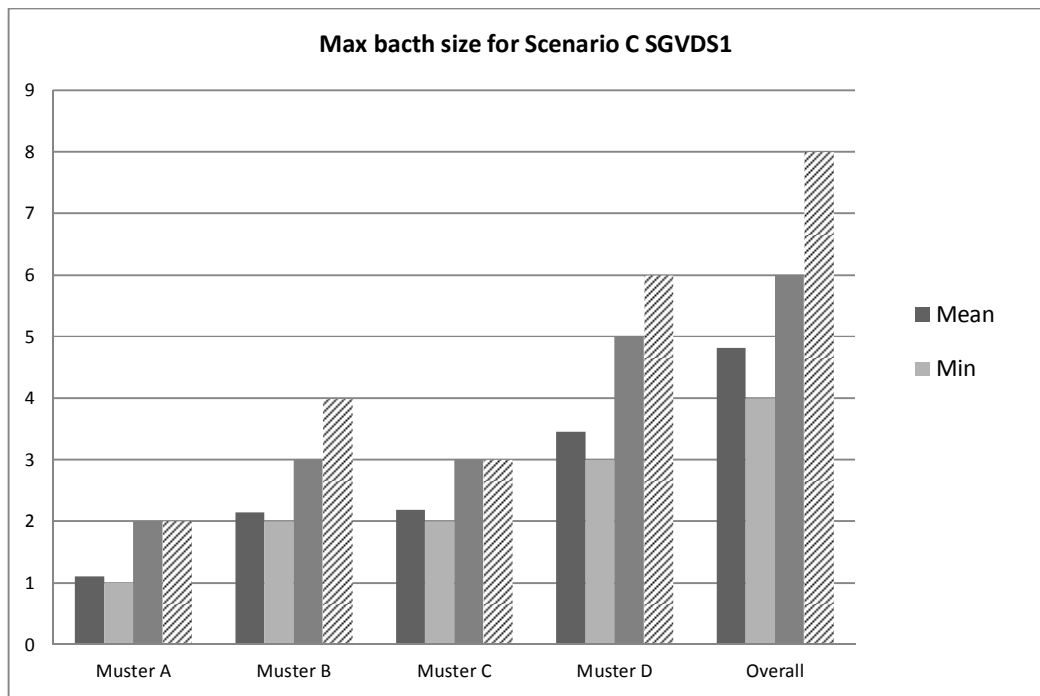


Figure 6-29: Comparison of the max batch size values from simulation results with the trial data per muster station for scenario C

Results for scenarios A and B are almost identical. The only difference between the two scenarios is the response time. In scenario A, regional response times are used whereas in scenario B global response times are used.

This could mean in this case that the impact of the response time on the arrival process (events count and batch size) is negligible.

As expected scenario C produces the results with the most significant differences when compared to the real data and this is because, agents would go to the nearest muster station instead of their designated muster station upsetting the events counts at the individual muster stations. Observing the overall arrival process only, then scenario C would provide the closest estimate in terms of event counts.

6.6.4 Analysis of the real data: SGVDS2 dataset

The analysis of the number and size of batches of the SGVDS2 data set showed the following results.

	Events count	Max Batch Size
Muster A	320	4
Muster B	398	5
Muster C	345	4
Muster D	273	3
Overall	790	8

Table 6-11: Event counts and max batch size for SGVDS2 dataset

6.6.4.1 Corresponding evacuation simulation runs.

For this dataset, the simulation scenario was run 50 times. Passengers distribution over the ship and their reaction time is as described in the subsection describing SGVDS2 dataset.

The events count and the batch sizes statistics over the 50 runs are shown in Table 6-12 below.

	N			Max BatchSize		
	Mean	Min	Max	Mean	Min	Max
Muster A	366.86	354	374	2.88	2	4
Muster B	505.04	488	519	3.06	2	4
Muster C	396.72	385	403	2.86	2	4
Muster D	331.9	319	337	2.18	2	3
Overall	1181.12	1145	1198	5.56	5	7

Table 6-12: Statistics of the events count and max batch size for simulation for SGVDS2

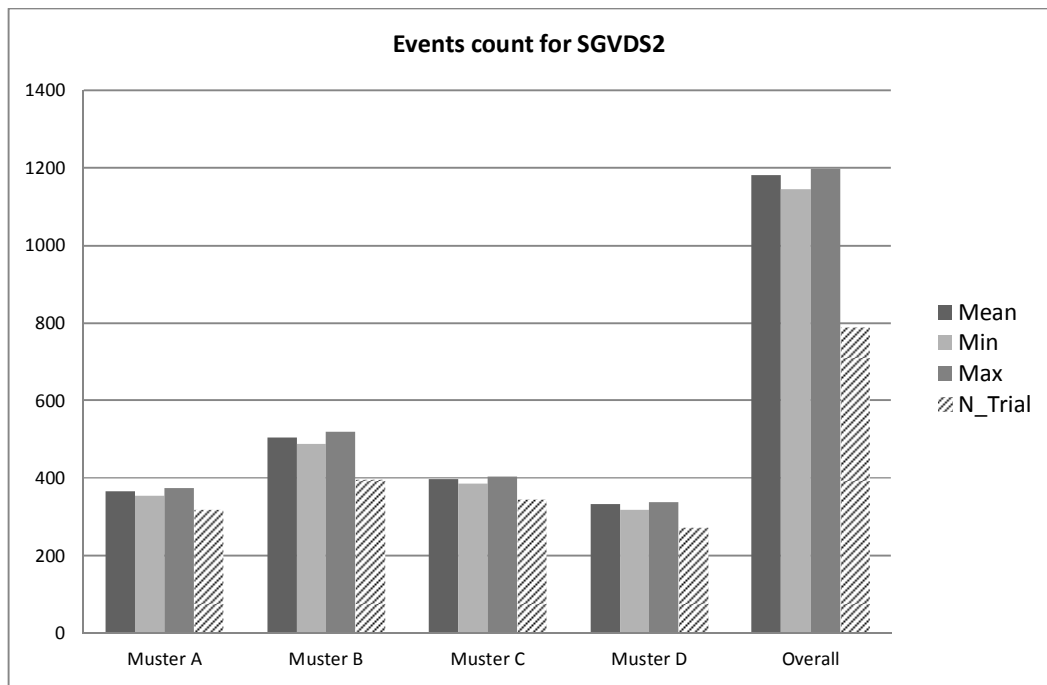


Figure 6-30: Comparison of the events count from simulation results with the trial data per muster station for SGVDS2

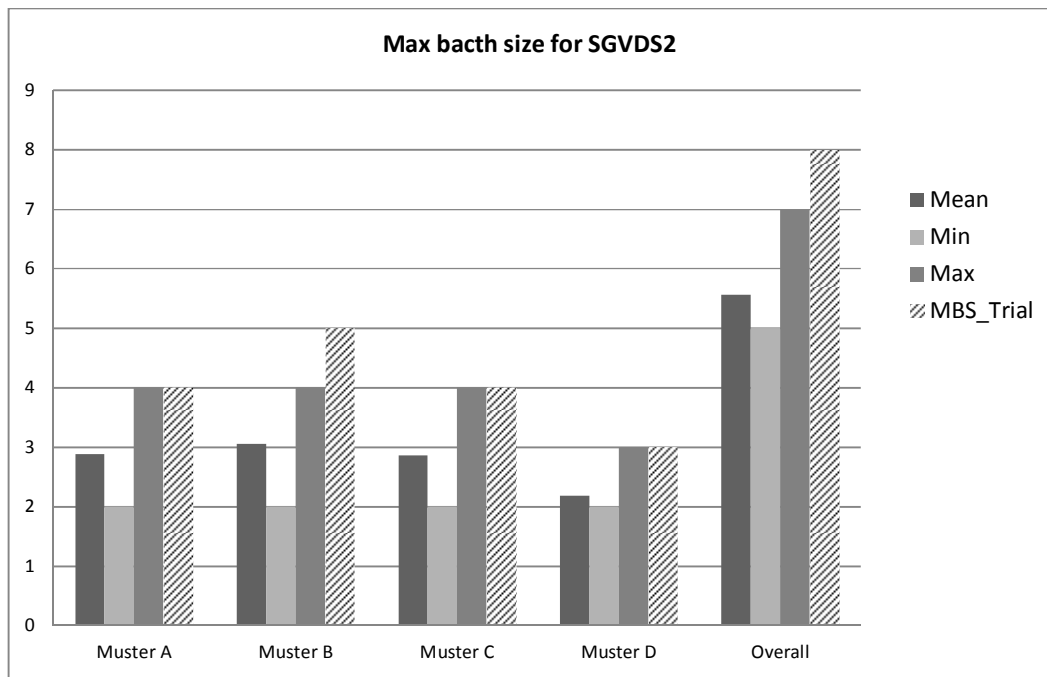


Figure 6-31: Comparison of the max batch size values from simulation results with the trial data per muster station for SGVDS2

Similarly to SGDVS1 results, the event counts from the simulation runs tend to overestimate the ones obtained from the trial dataset whereas the max batch size value is under estimated in the simulation runs.

6.6.5 Discussion

It was not expected that the simulations would provide an exact replication of the arrival processes. Differences in arrival times at muster stations are hence expected.

In the present case, Evi simulations predicted more arrivals with smaller batch sizes than the actual data and this is consistent for both datasets and all the muster stations.

At this stage it is not possible to say whether the simulations would have been able to reproduce the real arrival processes as too many parameters are unknown. Only the reaction times and initial locations of the people were known and like in the case of SGDVS1 even those elements were uncertain. In addition, only one trial per set was done. This is not enough to capture the variability of the different parameters influencing the evacuation process.

Based on the previous results, it seems that the maximum value of the batch size produced by the simulations provides a fairly good estimate of the real data.

Regarding the event counts, the minimum value produced by the simulations would be the closest to the actual values.

6.7 Concluding remarks

This chapter has presented the results of the analysis of the datasets used in this study to derive the simplified model for the evacuation process.

The following parameters were considered to build the evacuation simulation dataset, the first to be analysed:

- Time (day/night)
- Passenger's loads

- Speed
- Reaction time

The results showed that passenger's loads, as expected, are proportional to the number of event counts (arrivals at the muster stations) regardless of the time (day or night), speed or reaction time.

The impact of the time could be seen in the number of arrivals and the batch sizes. For the day case scenarios regardless of speed or reaction time, bigger batch sizes with fewer arrivals are observed while the opposite is true for the night cases. Smaller batch sizes with more frequent arrivals were observed.

For the day cases, the reaction time when random produced slightly higher number of arrivals (smaller batch sizes) regardless of passenger's loads or speed. This is to be expected as passengers starting at different times will tend to arrive at different times hence more arrivals.

For the night cases, no clear impact of the reaction time or speed can be seen as results in all cases are quite similar.

The second set analysed was the data obtained from drills on-board a large RO-PAX ferry and a cruise ship as part of the SAFEGUARD project.

The data corresponding to the actual drills on-board both vessels (SGVDS1 for the ferry and SGVDS2 for the cruise ship) were analysed and compared to their corresponding simulations obtained using Evi.

In the context in which the trial data was collected (quantity and type), it would have been extremely difficult to reproduce the results via simulation with the available information. Also having only one dataset per ship does not allow for any statistical analysis.

The results of the comparison between the real data and their corresponding simulations showed that the simulations tended to predict more arrivals with smaller batch sizes than what was observed in the trial data.

7 BATCH FITTING

7.1 General Remarks

As introduced in Chapter 5, the arrival process at the muster stations is characterised by the size of the batches and the actual arrivals.

In this chapter, the data produced by the simulations as well as the real data will be used to produce the fitted model of the batch sizes.

The results of the fitting will be presented.

Simulation of the batch sizes using the fitted parametric model will then be explained and compared to the original data.

7.2 Batch fitting

The batch arrivals of agents to the muster station, has been fitted to a geometric distribution with the probability mass function given by:

$$P(Bnum = k) = p(1 - p)^{k-1}, k \geq 1 \quad \text{Eq. 7-1}$$

Both the simulated data and the SAFEGUARD datasets (trial data and corresponding simulations) were analysed.

7.2.1 Batch fitting: Simulated data

For each simulation of the 8 000 runs produced, the arrivals data was used to derive the value of the parameter p of the geometric distribution. In each case, the fitting showed a good agreement with the initial data ($R^2 = 0.99$). The value of p was averaged over the 100 runs per passengers loads and the coefficient of variation $cov = \frac{\sigma}{\mu}$ which represents a

measure of data spread was very low meaning that there was very little dispersion of the data.

The results are presented for the Day and Night cases separately in the following subsections.

7.2.1.1 Day cases results

The results of the day cases fitting of p are summarised in Table 7-1 below. For each case the average value of p and the COV are provided.

It has been noticed that for the smallest population load the parameter p does not vary too much between its min and max values (2.39% change only). The percentage change starts to be significant for population loads of 30% and more as can be seen in Figure 7-1 below.

% population	Day random		Fixed Reaction		Fixed speed		Fixed Speed +Reaction	
	Average p	COV	Average p	COV	Average p	COV	Average p	COV
10	0.6892	4.22%	0.6853	4.20%	0.6890	3.75%	0.7016	3.68%
20	0.5835	3.86%	0.6270	5.05%	0.5620	3.49%	0.6025	4.40%
30	0.5164	4.12%	0.5837	3.86%	0.4800	3.80%	0.5519	4.49%
40	0.4754	3.45%	0.5648	4.02%	0.4367	4.06%	0.5277	4.51%
50	0.4501	3.96%	0.5428	3.80%	0.4153	5.26%	0.5189	4.72%
60	0.4356	4.46%	0.5312	4.44%	0.4079	6.16%	0.5090	4.73%
70	0.4302	4.78%	0.5235	4.19%	0.3976	6.40%	0.5011	4.40%
80	0.4293	5.51%	0.5158	3.82%	0.4010	6.14%	0.4965	4.81%
90	0.4195	5.14%	0.5148	4.28%	0.4017	6.26%	0.4909	5.17%
100	0.4172	4.58%	0.5029	3.50%	0.4042	6.49%	0.4929	4.81%

Table 7-1: Fitting of geometric distribution parameter. Results for day case

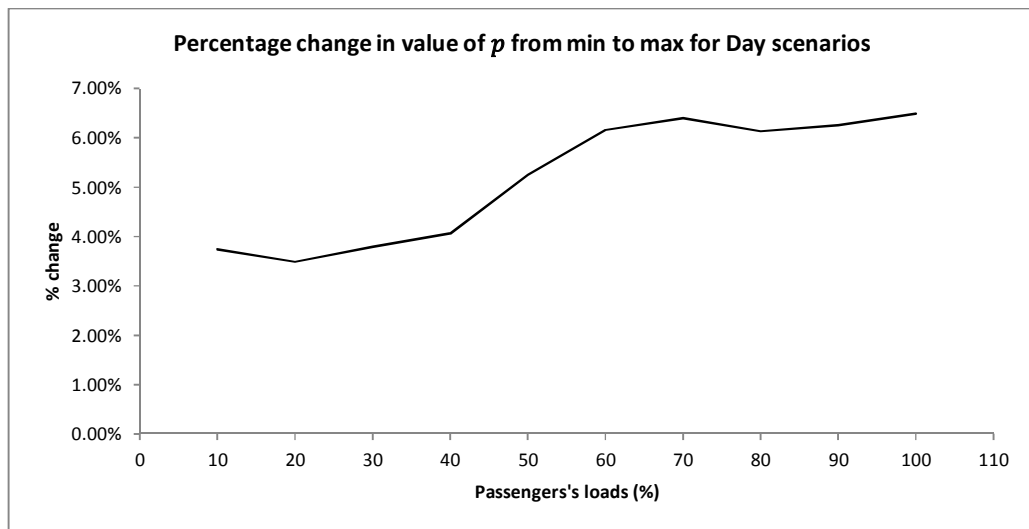


Figure 7-1: Percentage change (from min to max) in the value of the geometric distribution parameters with varying population loads for the day scenarios.

For all loads greater than 10%, the lowest value of p is achieved for the scenario with fixed speed. The highest value is obtained for scenarios when the reaction time is fixed. In addition, the probability of having bigger batch sizes decreases more rapidly when the speed is fixed. The slowest decrease in the probability of having big batch sizes is achieved in scenarios with fixed reaction time (see Figure 7-2 below for example of probability changes with batch sizes for a 20% passengers load).

This could be explained by the fact that in scenarios where the reaction time is fixed, all agents start at the same time creating more opportunities for a number of agents to arrive at the muster station at the same time. In the scenario where the speed is fixed, the reaction time is random so agents start their movements at different times allowing for more spread in the arrivals at the muster station and thus more frequent batches of smaller sizes.

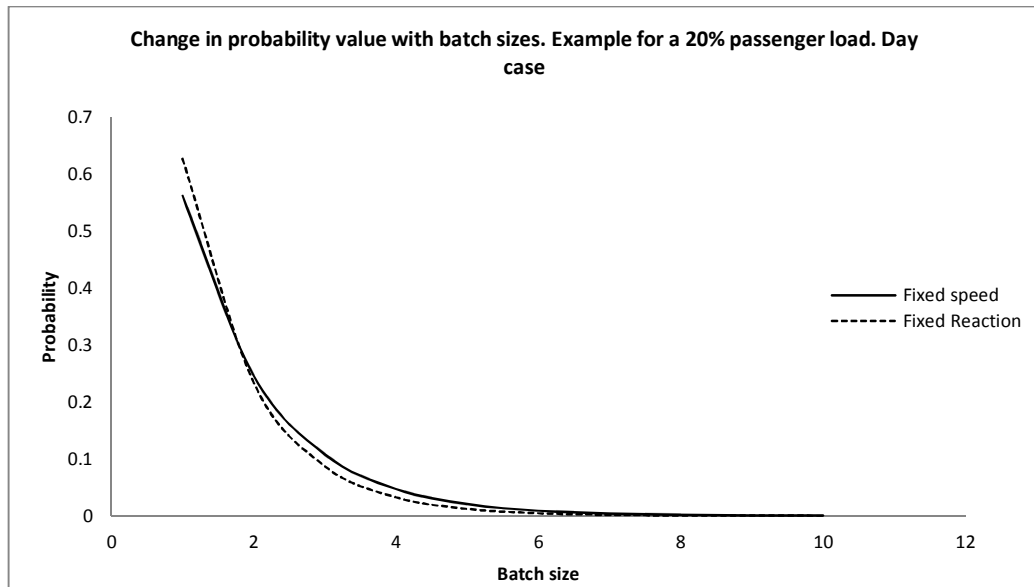


Figure 7-2: Changes of probability values for batch sizes for a day scenario for a 20% passengers load.

For the lowest load of passengers i.e. 10% the lowest value of p is obtained in the scenario with fixed reaction times whereas the highest value is obtained for the fixed speed and fixed reaction time scenarios although the difference is quite small. For this low load of passengers all scenarios have very similar results in term of probabilities of batch sizes. This could be explained by the fact that the number of agents in the simulation is very small (180 passengers).

7.2.1.2 Night cases results:

The results for the Night cases fitting of p are summarised in Table 7-2 below. For each case the average value of p and the *cov* are provided.

The percentage change in the value of the parameter p , presents a different profile for the Night scenarios as can be seen in Figure 7-3 below. The smallest percentage change (8.5%) is achieved for a population load of 30% whereas the highest percentage change (16.2%) occurs for a passenger load of 60%. Compared to the results of the Day cases, the range of percentage change for the Night cases is roughly half that of the Day cases scenarios.

% population	Night random		Fixed Reaction		Fixed speed		Fixed Speed +Reaction	
	Average p	cov	Average p	cov	Average p	cov	Average p	cov
10	0.7392	3.72%	0.6895	4.16%	0.7085	3.80%	0.6541	5.09%
20	0.6672	3.55%	0.6349	4.24%	0.5933	3.96%	0.6030	3.77%
30	0.5861	3.05%	0.5677	3.66%	0.5404	4.15%	0.5412	4.39%
40	0.5469	3.68%	0.5323	3.60%	0.5047	4.23%	0.4996	4.32%
50	0.5305	3.68%	0.5252	3.03%	0.4836	4.08%	0.4960	3.76%
60	0.5220	3.34%	0.5175	2.81%	0.4493	3.56%	0.4825	3.74%
70	0.5081	3.09%	0.5034	3.06%	0.4549	4.75%	0.4673	3.49%
80	0.5092	3.12%	0.5077	2.79%	0.4591	4.02%	0.4703	3.57%
90	0.4889	2.75%	0.4905	3.15%	0.4423	4.07%	0.4519	3.54%
100	0.4929	4.43%	0.4869	2.99%	0.4479	3.63%	0.4504	3.56%

Table 7-2: Fitting of geometric distribution parameter. Results for night case

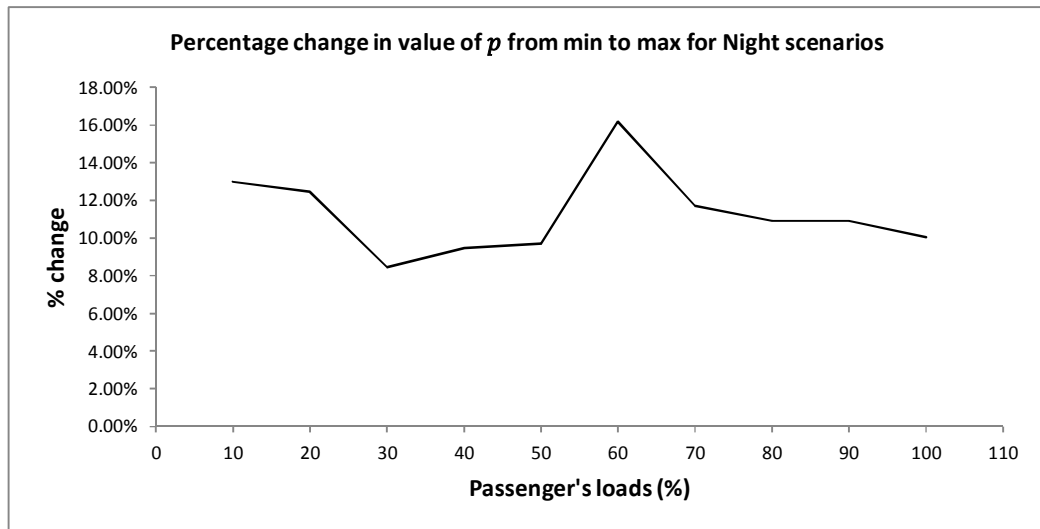


Figure 7-3: Percentage change (from min to max) in the value of the geometric distribution parameters with varying population loads for the night scenarios.

The highest value of p is achieved for the scenarios with random speed and reaction times for all passengers loads except for 90% load, where the highest value of p is achieved for the fixed reaction scenario, although the value of p for the 90% load varies only by 0.33% when the random speed and reaction times scenario and the fixed reaction scenario are

compared ($p = 0.4889$ for the random speed and reaction time scenario and $p = 0.4905$ for the fixed reaction scenario).

The lowest values of p are mostly achieved for the fixed speed scenario. Only for passengers loads of 10% and 40%, the lowest values of p are achieved for the fixed speed and fixed reaction scenarios. The difference is very small between the two scenarios for the 40% passengers load (1% difference).

The probability of having bigger batch sizes decreases more rapidly for the fixed speed scenarios. A slowest decrease is observed for scenarios with random speed and reaction times (see Figure 7-4 below). Like for the Day cases, a fixed speed and random reaction time could lead to a bigger spread in the arrivals because of different starting times.

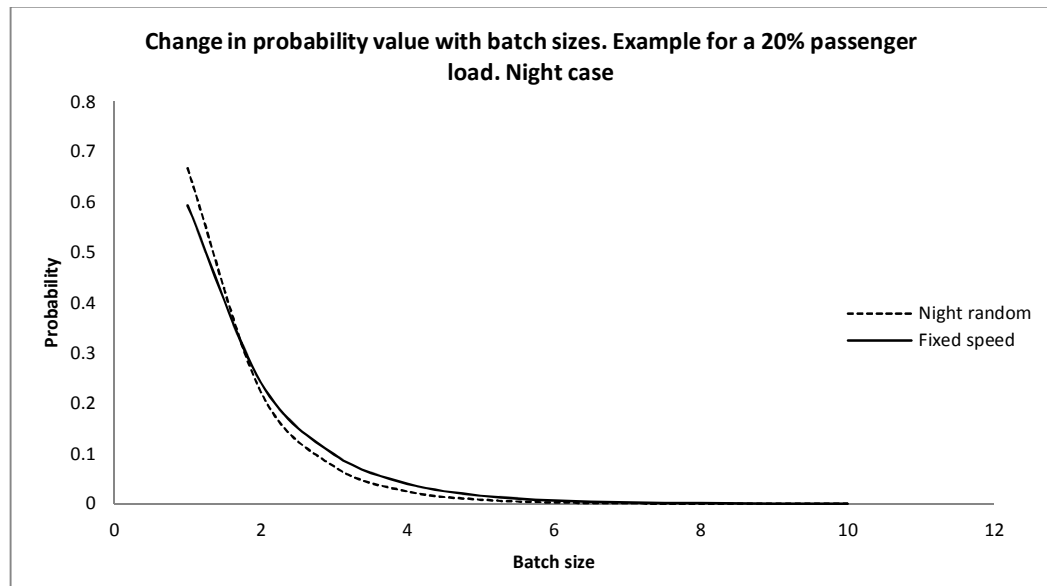


Figure 7-4: Changes of probability values for batch sizes for a night scenario for a 20% passengers load.

7.3 Simulating the batch sizes: simulated data

Having derived the parameter of the geometric distribution from the simulated data, the generation of batches using the fitted model uses the inverse of the geometric distribution given by the following equation:

$$Batch_i = \left\lceil \frac{\ln u_i}{\ln(1-p)} \right\rceil \quad \text{Eq. 7-2}$$

where u_i is a realisation of the uniform distribution on $[0,1]$ and p the parameter of the geometric distribution.

The algorithm to generate the batches of the NHPP is as follows:

1.	For a value of nb_events
2.	For a value of P.
3.	For i=1 to nb_events
	$u_i = \text{random}(0,1)$
	$batch_i = \left\lceil \frac{\ln u_i}{\ln(1-p)} \right\rceil$
	End for

To help decide how best to choose the parameters “nb_events” and “P”, a closer look at the results presented in the previous section was taken.

The results showed that the parameter of the geometric distribution for the batch sizes varies with the passenger loads and the type of scenarios (day/night, random, fixed speed, fixed reaction and fixed speed and reaction).

A summary of the average value of the parameter p of the geometric distribution per passenger load and the associated maximum and minimum values of the events count and max batch size as derived from the simulation data, are summarised in Appendix I, in Table I-1 to Table I-4 for the Days cases (Day Random, Fixed Reaction, Fixed Speed and Fixed Speed and Reaction cases, respectively) and in Table I-5 to Table I-8 for the Night cases

(Night Random, Fixed Reaction, Fixed Speed and Fixed Speed and Reaction cases, respectively).

First it was decided to take both “*nb_events*” and “*P*” equal to the average value obtained from the data. This produced sometimes large percentage changes when compared to the original data. It was then decided to have one of the parameter follow a random distribution and the other one having a fixed value. This did not improve much the results. Finally, it was assumed that the parameter of the geometric distribution *p* follows a Normal distribution with parameters μ_p and σ_p and that the number of event counts *n* also follows a Normal distribution with parameters μ_n and σ_n .

The algorithm then becomes:

1.	$nb_events = \text{realisation of } n \sim N(\mu_n, \sigma_n)$
2.	$P = \text{realisation of } p \sim N(\mu_p, \sigma_p)$
3.	For $i=1$ to nb_events
	$u_i = \text{random}(0,1)$
	$batch_i = \left\lceil \frac{\ln u_i}{\ln(1-p)} \right\rceil$
	End for

Fifty, a hundred and a thousand simulations of the above algorithm were run for each of the ten (10) passengers load and each of the four (04) cases for the Day and Night scenarios for a total of 92000 simulation runs ($50 \times 10 \times 4 \times 2 + 100 \times 10 \times 4 \times 2 + 1000 \times 10 \times 4 \times 2$).

The event counts and the max batch size generated using the fitted model were analysed and compared to the original data.

For clarity, only the results for the 50 runs set are shown below. The results of the hundred and thousand runs set are in Appendix II.

7.3.1 Day cases results

This subsection presents the results of the day cases (random, fixed speed, fixed reaction and fixed speed and reaction). First the event counts results are presented then the max batch size ones.

The graphs below show the number of events count simulated versus original per passenger load for the Day case random, Day case Fixed Reaction time, Day case Fixed Speed and Day case Fixed Speed and Reaction cases (Figure 7-5 to Figure 7-8 respectively).

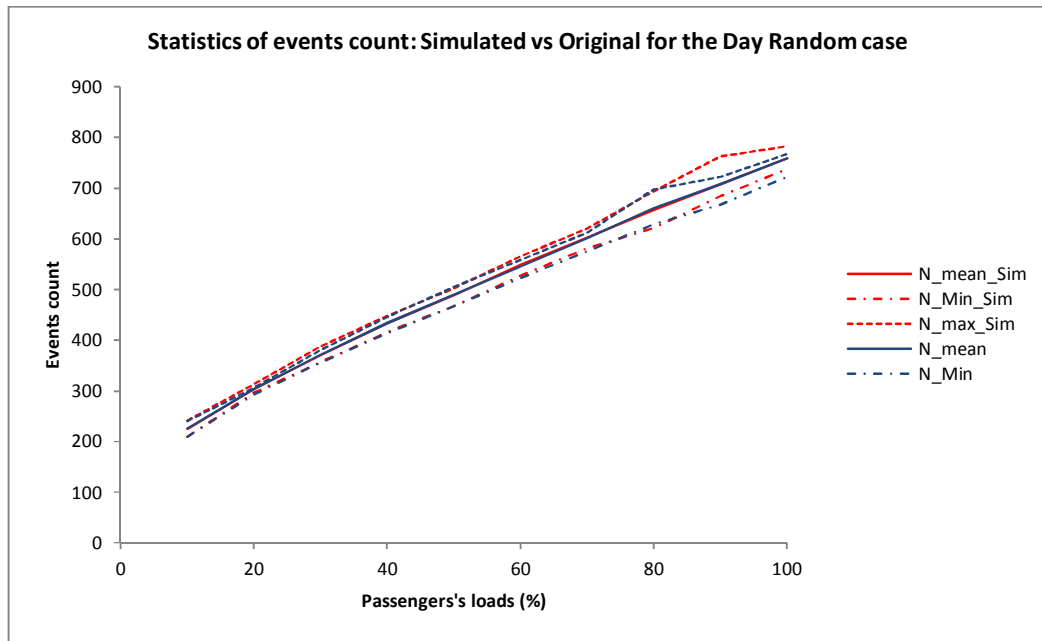


Figure 7-5: Events counts: simulated vs original for Day case Random

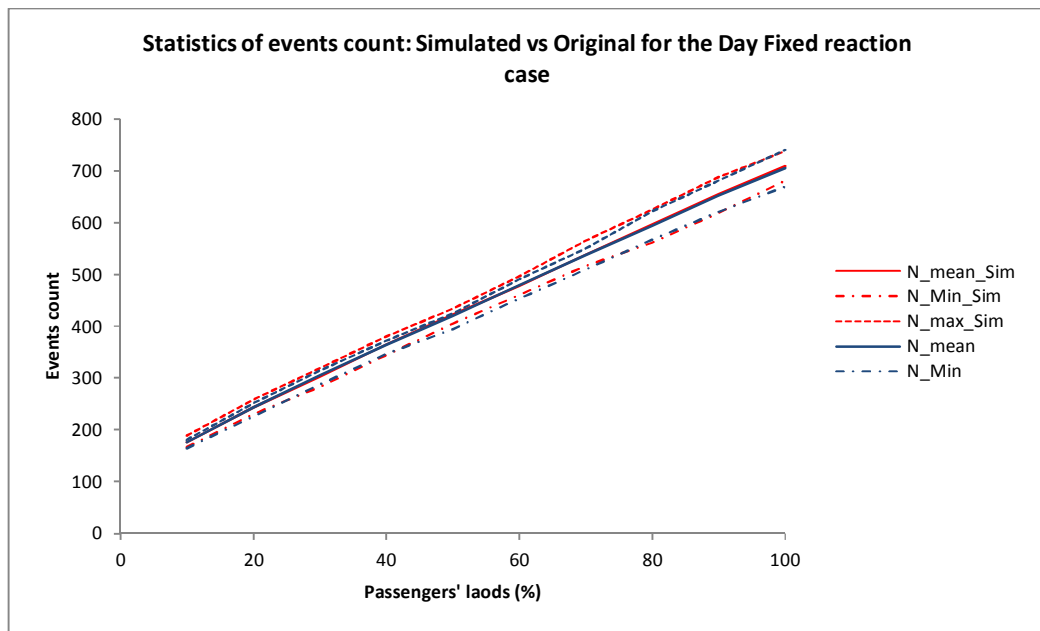


Figure 7-6: Events counts: simulated vs original for Day fixed reaction

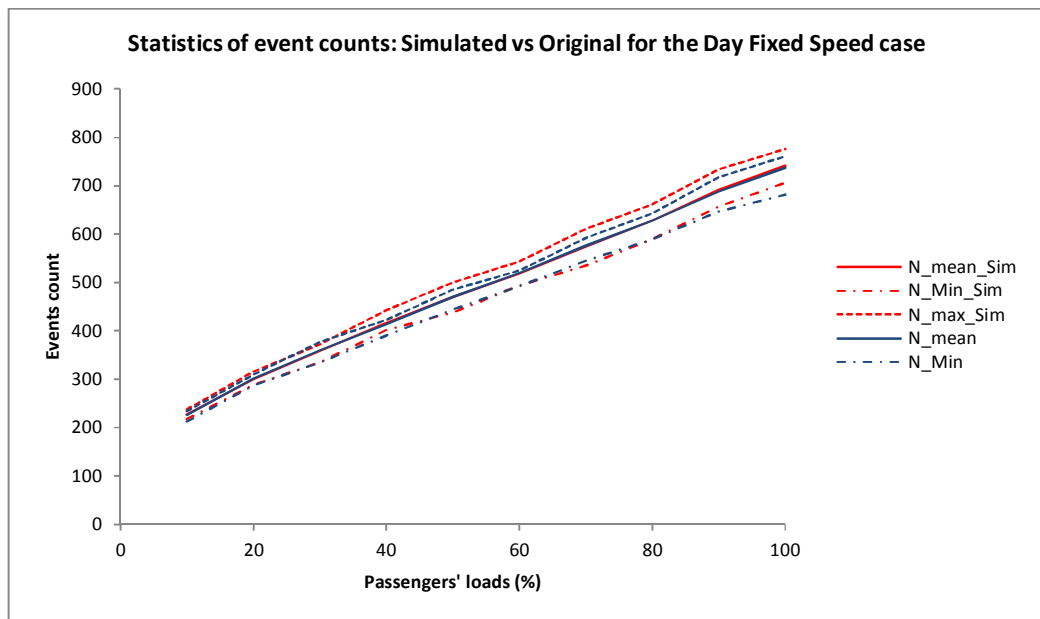


Figure 7-7: Events counts: simulated vs original for Day fixed speed

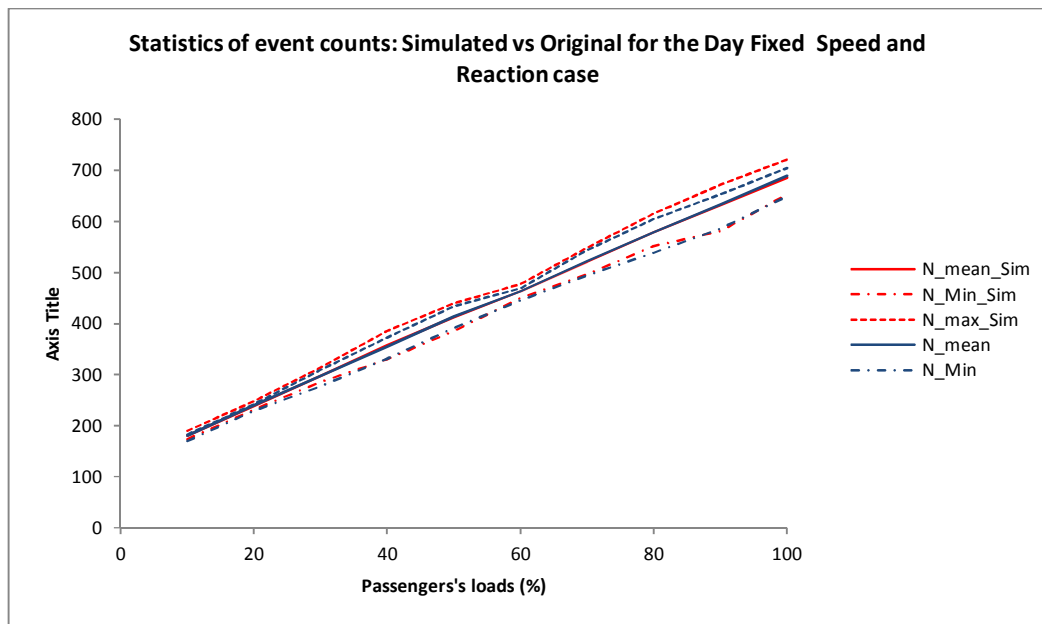


Figure 7-8: Events counts: simulated vs original for Day fixed speed and reaction case

Max batch size

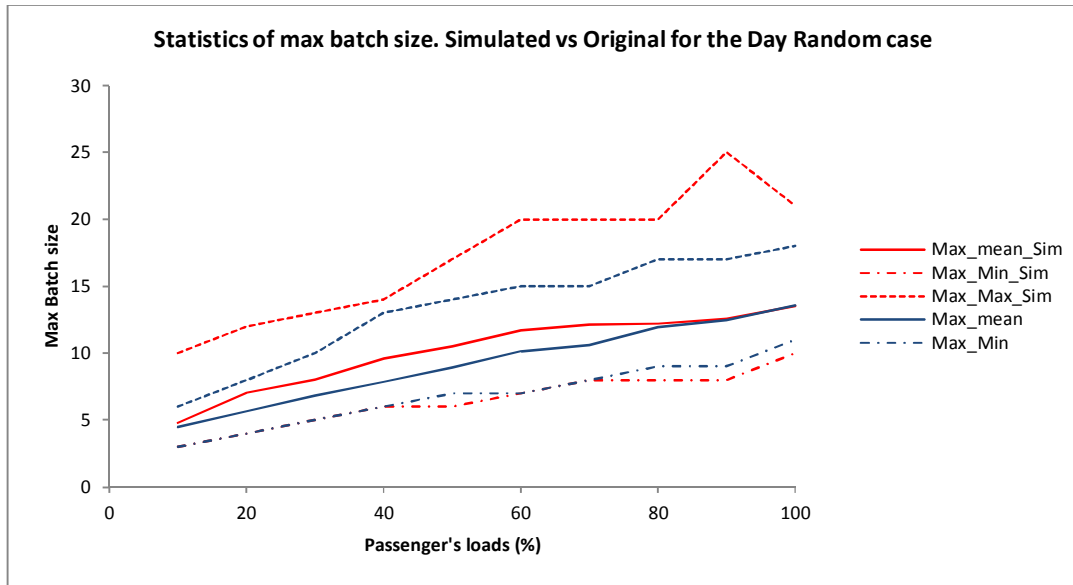


Figure 7-9: Max batch size statistics: simulated vs original for the Day random case

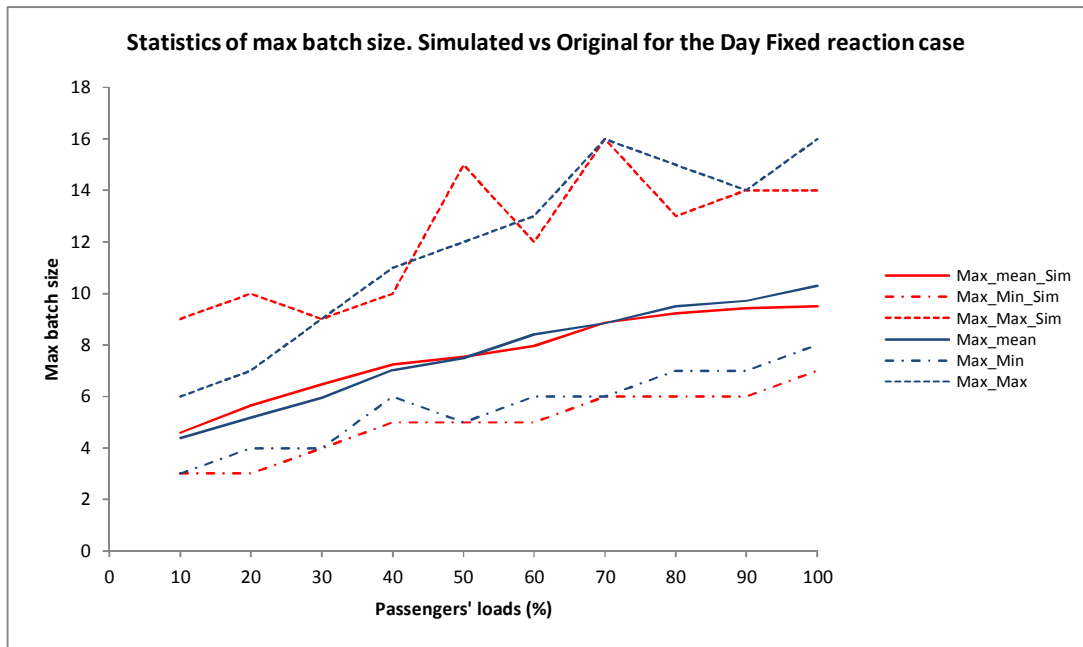


Figure 7-10: Max batch size statistics: simulated vs original for the Day fixed reaction case

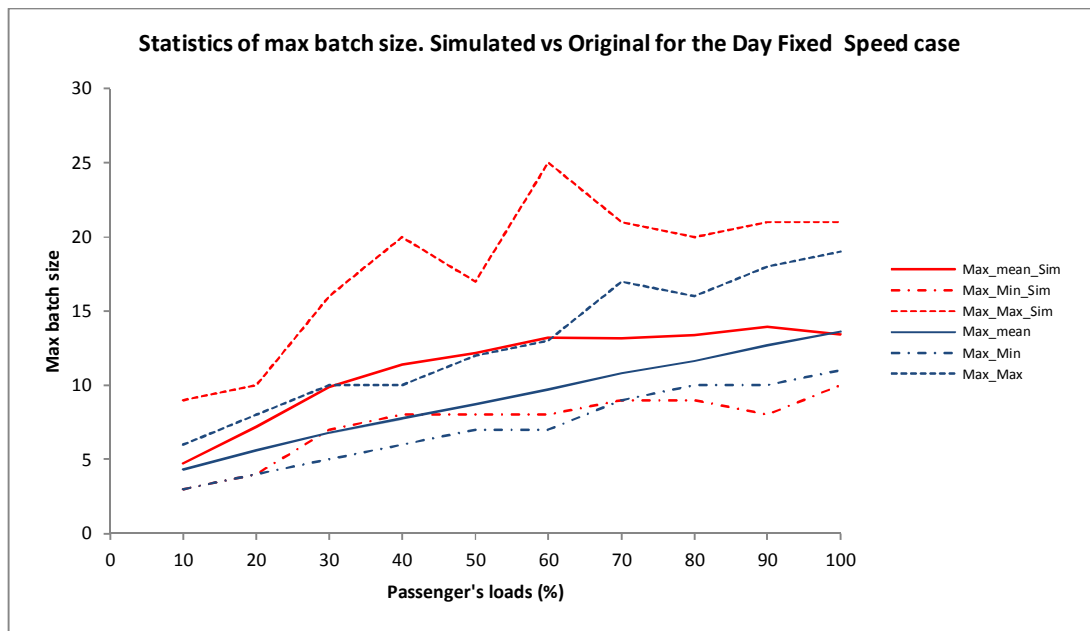


Figure 7-11: Max batch size statistics: simulated vs original for the Day fixed speed case

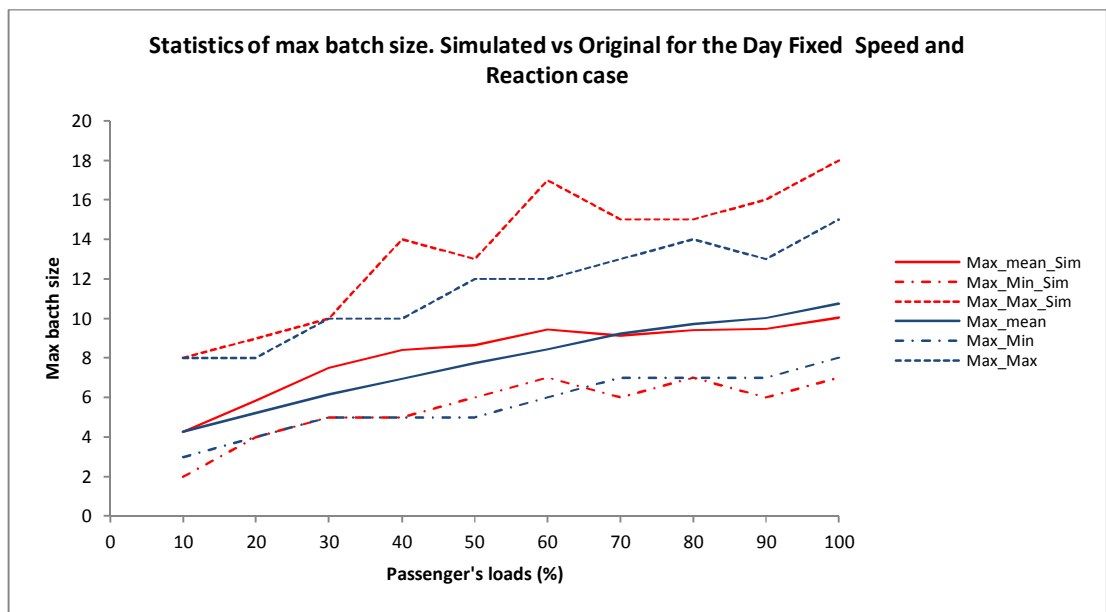


Figure 7-12: Max batch size statistics: simulated vs original for the Day fixed speed and reaction case

7.3.2 Night cases results

The results of the Night Cases are presented in this subsection. First the event counts then the max batch sizes.

The graphs below show the number of events count simulated versus original per passenger load for the Night case Random, Night case Fixed Reaction time, Night case Fixed Speed and Night case Fixed Speed and Reaction cases (Figure 7-13 to Figure 7-16 respectively).

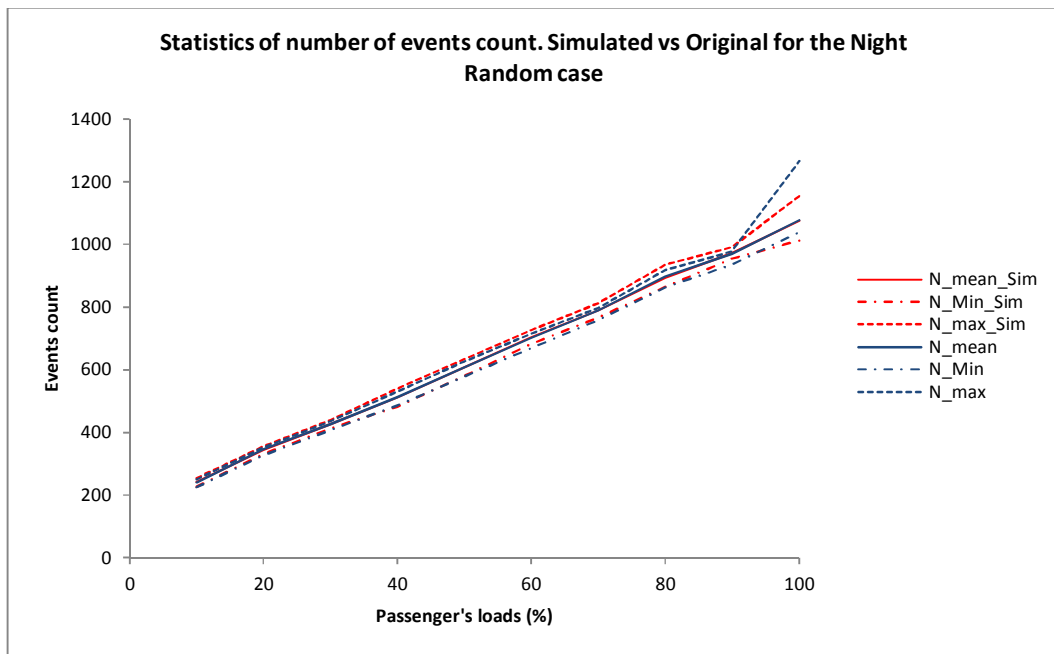


Figure 7-13: Events counts: simulated vs original for Night case

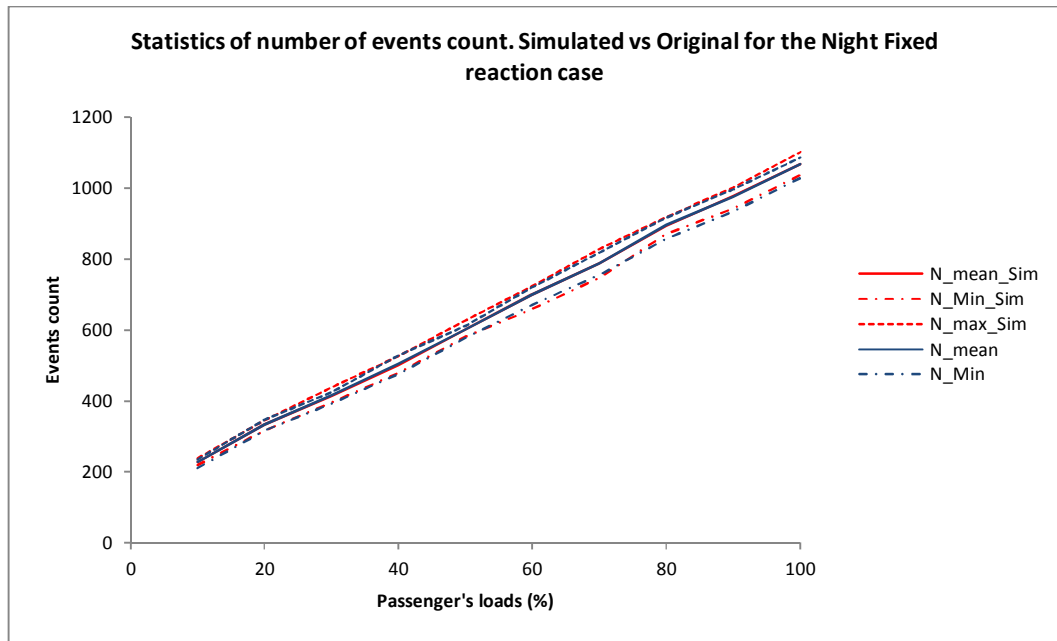


Figure 7-14: Events counts: simulated vs original for Night fixed reaction

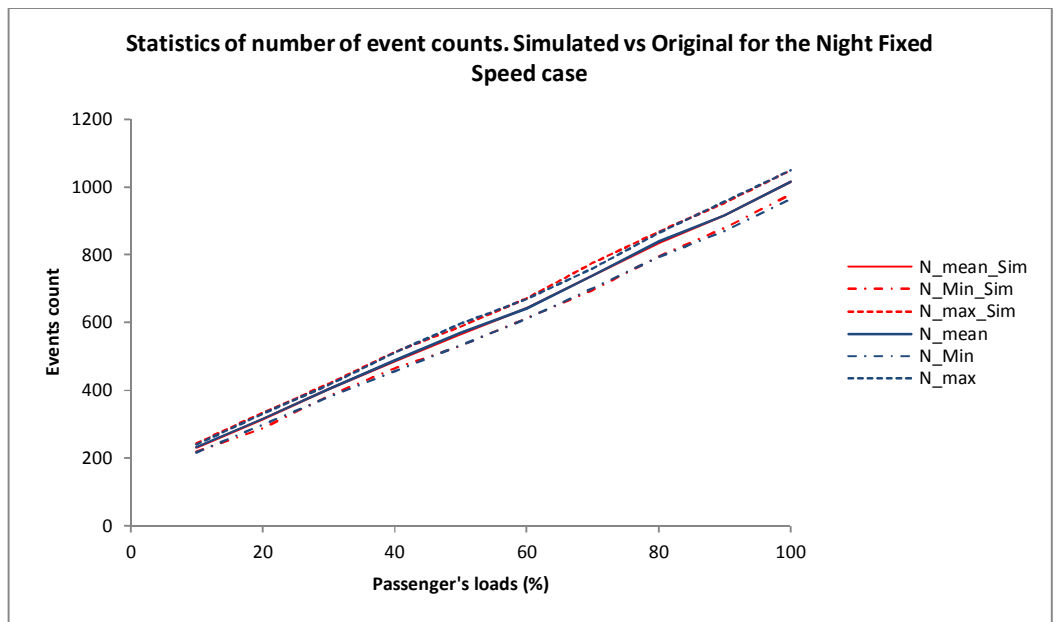


Figure 7-15: Events counts: simulated vs original for Night fixed speed

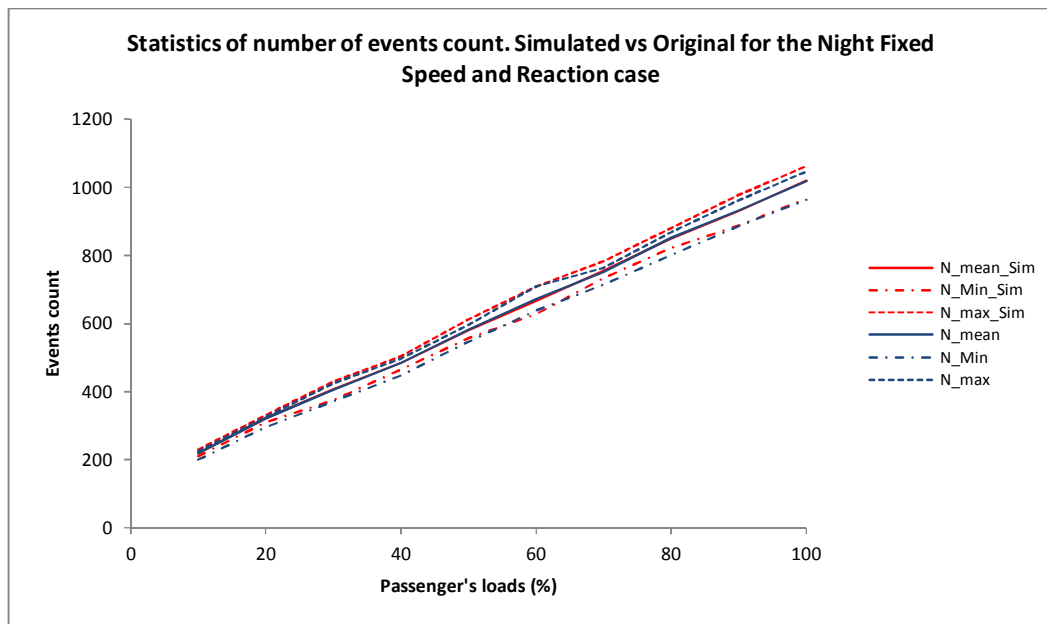


Figure 7-16: Events counts: simulated vs original for night fixed speed and reaction

Max batch size

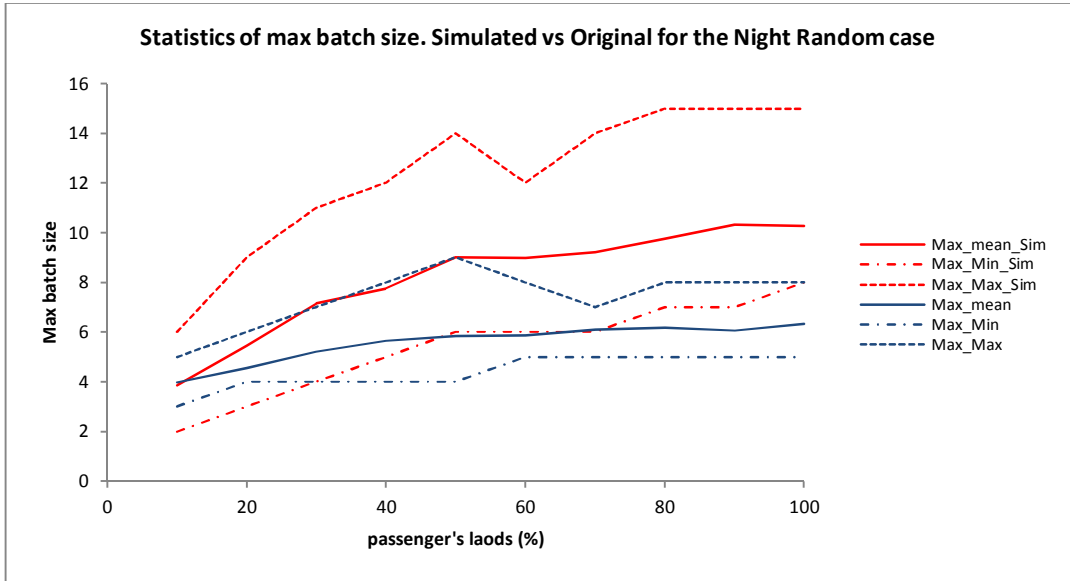


Figure 7-17: Max batch size statistics: simulated vs original for the Night random case

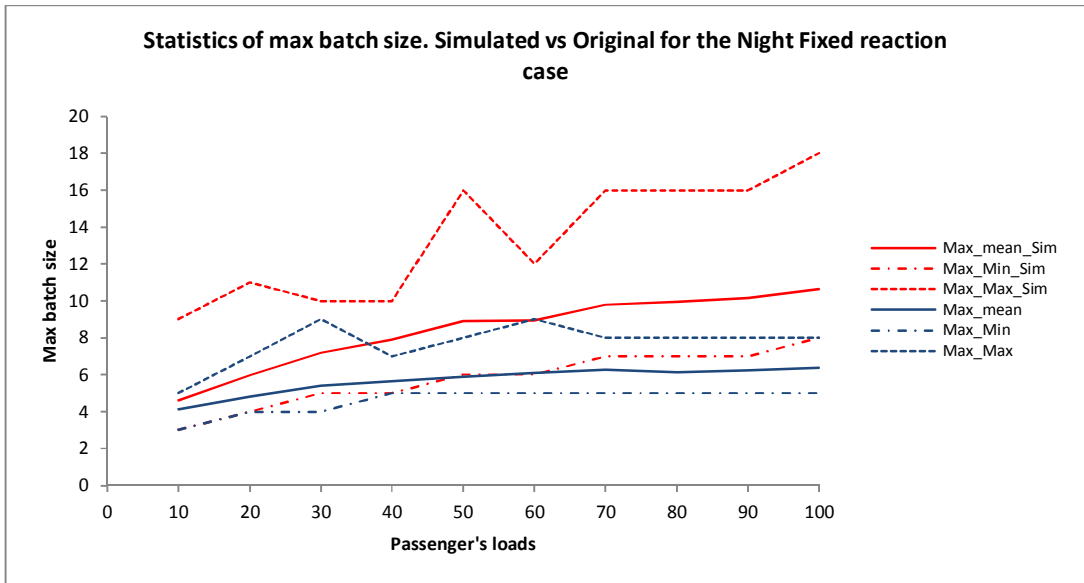


Figure 7-18: Max batch size statistics: simulated vs original for the Night fixed reaction case

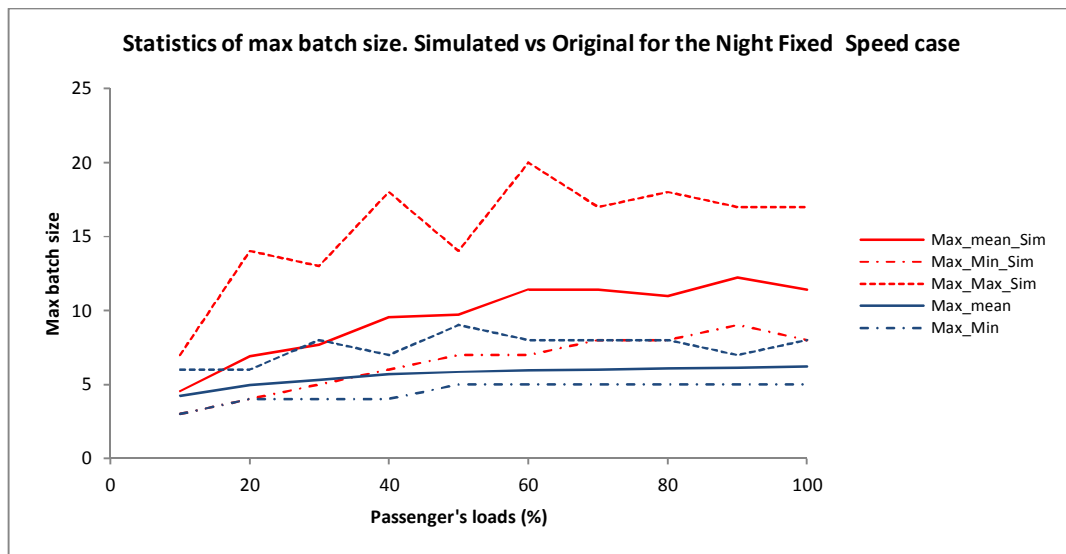


Figure 7-19: Max batch size statistics: simulated vs original for the Night fixed speed case

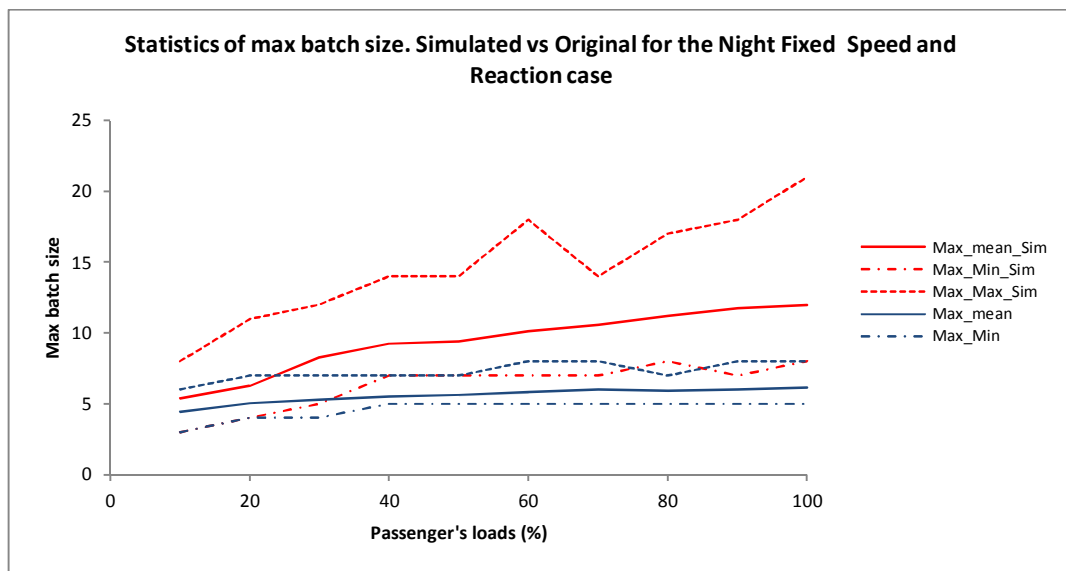


Figure 7-20: Max batch size statistics: simulated vs original for the Night fixed speed and reaction case

7.3.3 Discussion

The results presented above for both the Day and Night cases, exhibit some similarities. As can be expected a higher number of simulation produces results closer to the original set. This is particularly valid for the mean event counts and as can be seen in the previous

graphs where the solid blue and red line representing the mean original and simulated number, are very close to each other. The min and max values of the events counts for the simulated data also have very good agreement with the original min and max values across all cases.

A closer look at the results shows that on average the absolute percentage changes in the values of the min and max for the events count does not decrease when the number of simulations performed increases. For example for the night cases, the averages of the absolute percentage changes per case are shown in Table 7-3 below. Minimum values are highlighted.

	Number of runs	N_mean	N_Min	N_max
Night random	50 runs	0.21%	1.23%	2.16%
	100 runs	0.08%	1.26%	2.80%
	1000 runs	0.06%	1.74%	3.91%
Night fixed reaction	50 runs	0.21%	1.29%	1.20%
	100 runs	0.18%	0.78%	1.41%
	1000 runs	0.03%	1.39%	3.07%
Night fixed speed	50 runs	0.32%	1.14%	0.80%
	100 runs	0.18%	1.32%	1.97%
	1000 runs	0.05%	1.73%	3.16%
Night fixed speed and reaction	50 runs	0.23%	2.40%	1.69%
	100 runs	0.20%	1.45%	2.59%
	1000 runs	0.06%	1.43%	3.79%

Table 7-3: Average absolute percentage change for the different night cases for the events count

There does not seem to be a clear pattern for the minimum number of event counts but the average absolute percentage change for the max number seems to constantly be less for the 50 runs.

For the Day cases results are shown below.

	Number of runs	N_mean	N_Min	N_max
Day random	50 runs	0.24%	0.99%	1.64%
	100 runs	0.10%	0.78%	1.62%
	1000 runs	0.06%	1.38%	3.20%
Day fixed reaction	50 runs	0.30%	1.46%	1.81%
	100 runs	0.11%	1.25%	2.14%
	1000 runs	0.04%	1.90%	3.46%
Day fixed speed	50 runs	0.29%	1.46%	2.59%
	100 runs	0.15%	0.76%	1.91%
	1000 runs	0.05%	1.23%	3.64%
Day fixed speed and reaction	50 runs	0.23%	1.26%	2.17%
	100 runs	0.20%	0.61%	2.01%
	1000 runs	0.07%	1.24%	3.66%

Table 7-4: Average absolute percentage change for the different Day cases for the events count

In this case there is more consistency in the results as the 100 runs seems to produce the minimum absolute percentage change for both the min and max values of the events count across all the day cases.

It seems then reasonable to have the number of events count follow a normal distribution with parameters μ_p and σ_p obtained from the original data.

For the max batch size, there is much more randomness in the results (as Figure 7-9 to Figure 7-12 and Figure 7-17 to Figure 7-20 show) and the percentage changes are very high, especially for the night cases.

Table 7-5 and Table 7-6 below summarise the average absolute percentage changes in the statistics of the max batch sizes for the night and day cases respectively.

For the Night scenarios, almost all cases show the same pattern where the minimum percentage change in the mean and max value of the max batch size is achieved for the 50 runs simulations, whereas for the min value of the max batch size the minimum percentage change is achieved for the 100 runs simulations.

For the day scenarios, the pattern is not as clear as for the night scenarios but in most cases, the minimum percentage change of the max and min value of the max batch size is achieved for the 50 runs simulations.

	Number of runs	MaxBatch mean	MaxBatch Min	MaxBatch Max
Night random	50 runs	44.65%	31.33%	64.52%
	100 runs	46.61%	27.33%	95.11%
	1000 runs	46.60%	16.33%	121.16%
Night fixed reaction	50 runs	45.51%	24.50%	74.94%
	100 runs	50.49%	24.50%	102.87%
	1000 runs	47.79%	17.83%	117.46%
Night fixed speed	50 runs	67.43%	41.50%	106.81%
	100 runs	68.91%	44.83%	118.04%
	1000 runs	68.55%	34.33%	171.96%
Night fixed speed and reaction	50 runs	66.51%	34.50%	99.23%
	100 runs	65.42%	28.50%	105.12%
	1000 runs	67.07%	25.00%	171.19%

Table 7-5: Average absolute percentage change for the different Night cases for the max batch size

	Number of runs	MaxBatch mean	MaxBatch Min	MaxBatch Max
Day random	<i>50 runs</i>	12.29%	4.56%	32.38%
	<i>100 runs</i>	11.64%	10.72%	24.10%
	<i>1000 runs</i>	12.55%	13.74%	57.57%
Day fixed reaction	<i>50 runs</i>	4.46%	9.94%	16.05%
	<i>100 runs</i>	5.34%	12.86%	25.94%
	<i>1000 runs</i>	4.96%	19.29%	51.59%
Day fixed speed	<i>50 runs</i>	25.31%	14.10%	44.47%
	<i>100 runs</i>	22.50%	11.52%	60.27%
	<i>1000 runs</i>	22.57%	15.71%	92.83%
Day fixed speed and reaction	<i>50 runs</i>	9.41%	11.11%	16.81%
	<i>100 runs</i>	9.24%	17.37%	32.77%
	<i>1000 runs</i>	7.95%	21.14%	60.82%

Table 7-6: Average absolute percentage change for the different Day cases for the max batch size

7.3.4 Conclusion

In order to simulate batch sizes for an arrival process, both the number of events and the parameter of the geometric distribution need to be known in advance. The results presented in the previous subsection seem to suggest that the choice of the number of events following a normal distribution with parameters derived from the original dataset is a reasonable one. It also seems that a relatively low number of runs (50 to 100) are needed to generate a good approximation of the events count.

Regarding the size of the batches, the generated sizes are much bigger than the actual data. This can be due to a number of factors. One element that can introduce large uncertainties is the fact that a discrete distribution is reproduced by a continuous variable.

7.4 Batch fitting: Real data

The same process was applied to both SGVDS1 and SGVDS2 datasets and their corresponding Evi simulations as introduced in the previous chapter. The results of the model fitting and the generation of the batches for the real data are presented in this section.

The results of the fitted parameter of the geometric distribution are shown below in Table 7-7 and Table 7-8 for SGVDS1 and SGVDS2 respectively.

Muster station	P
Muster C	0.738086
Muster A	0.854883
Muster B	0.758008
Muster D	0.622852
Overall	0.483301

Table 7-7: Values of the fitted parameter for the geometric distribution for SGVDS1 dataset

Muster station	P
Muster C	0.7609
Muster A	0.8016
Muster B	0.7754
Muster D	0.6875
Overall	0.4090

Table 7-8: Values of the fitted parameter for the geometric distribution for SGVDS2 dataset

For the corresponding simulation runs, the values of the fitted parameters are shown in Table 7-8 and Table 7-10 for Evi simulations corresponding to SGVDS1 and SGVDS2 respectively. The values have been derived by fitting the individual runs and taking the average over the 50 runs. The tables also show the standard deviation as well as the coefficient of variation of each set of simulation.

	Scenario A			Scenario B			Scenario C		
	Average	Stand. Dev.	CV	Average	Stand. Dev.	CV	Average	Stand. Dev.	CV
Muster A	0.9323	0.0309	3%	0.9357	0.0316	3%	0.9772	0.0759	8%
Muster B	0.8916	0.0336	4%	0.8861	0.0307	3%	0.9153	0.0300	3%
Muster C	0.9349	0.0331	4%	0.9389	0.0266	3%	0.9388	0.0223	2%
Muster D	0.8262	0.0296	4%	0.8378	0.0307	4%	0.7549	0.0293	4%
Overall	0.6007	0.0271	5%	0.6067	0.0225	4%	0.6065	0.0253	4%

Table 7-9: Values of the fitted parameter for the geometric distribution for Evi simulations corresponding to SGVDS1 dataset

	Average	Stand. Dev.	CV
Muster A	0.9212	0.0115	1%
Muster B	0.8937	0.0149	2%
Muster C	0.9106	0.0146	2%
Muster D	0.9437	0.0127	1%
Overall	0.6484	0.0119	2%

Table 7-10: Values of the fitted parameter for the geometric distribution for Evi simulations corresponding to SGVDS2 dataset

7.4.1 Discussion

The percentage difference in the value of the parameter of the geometric distribution obtained from the simulation runs when compared to the values fitted from real data is shown in the following figures.

When comparing Evi simulation of the drill data to the actual data, the simulated data tend to overestimate the parameter of the geometric distribution derived from the real data and that is for both SGVDS1 and SGVDS2.

For SGVDS1, for the overall arrival process, all scenarios overestimate the parameter by about 25%. There are more variations when arrivals to individual muster stations are considered.

Scenarios A and B have roughly the same pattern of overestimation. These two scenarios differ only in the reaction time of the passengers, whereas scenario C has different

usage of the muster stations and this is quite visible from the graph below for muster stations A, B and D.

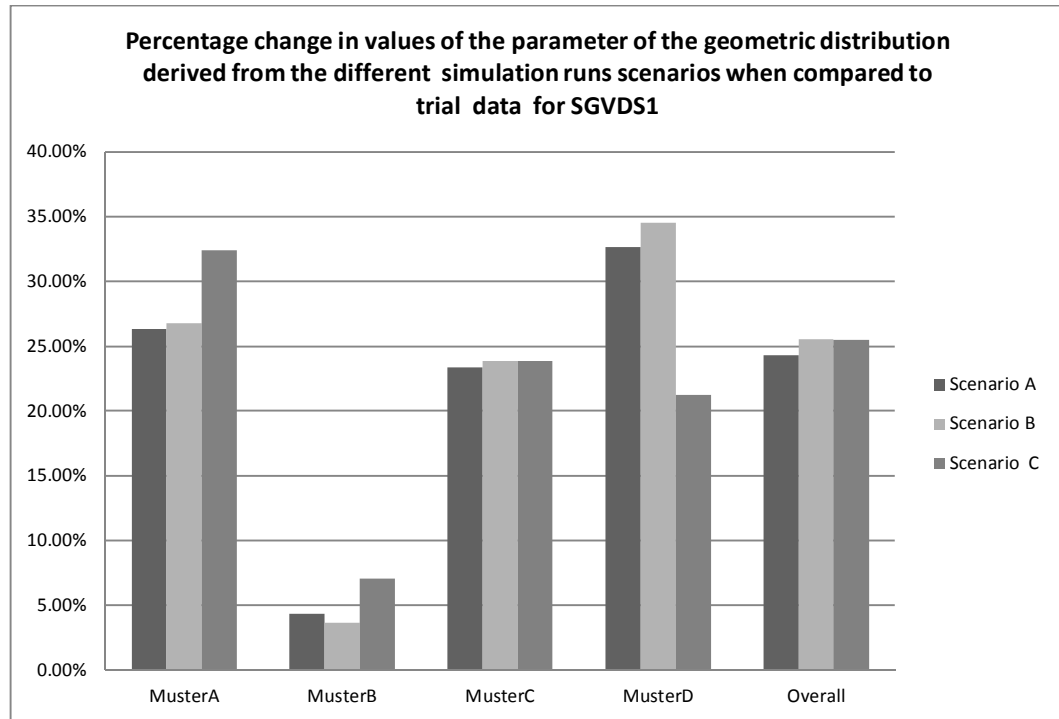


Figure 7-21: Percentage change in values of the parameter of the geometric distribution derived from the different simulation runs scenarios when compared to trial data for SGVDS1

For SGDVS2, the simulation runs have a much higher overestimation than the previous set as for example for the overall arrival process, the parameter of the geometric distribution is overestimated by almost 60%.

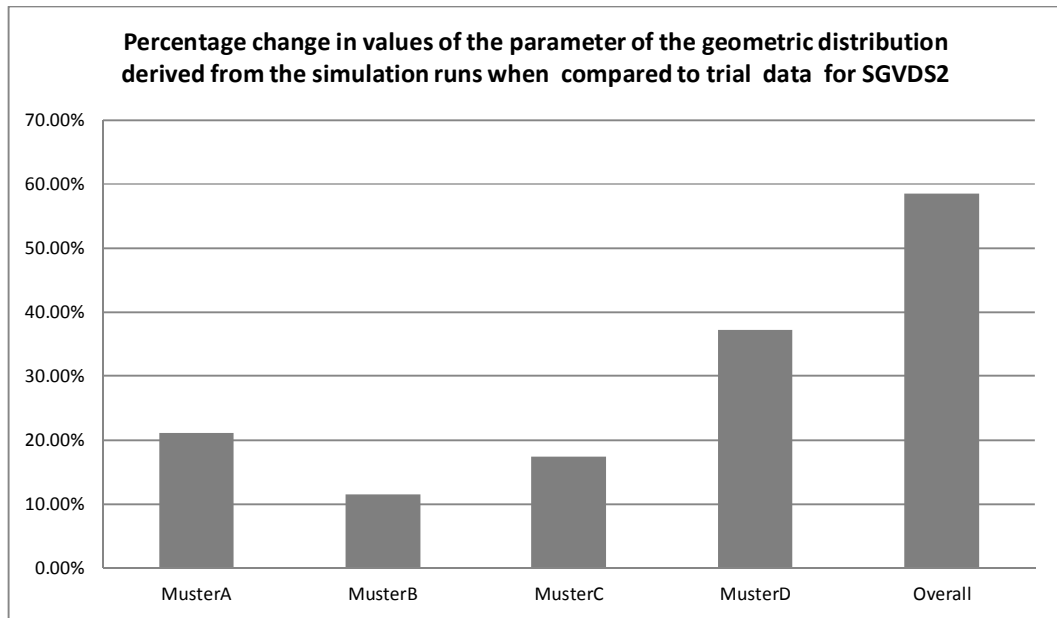


Figure 7-22: Percentage change in values of the parameter of the geometric distribution derived from the simulation runs when compared to trial data for SGVDS2.

7.4.2 Simulating the batch sizes: Real data

The Simulation of the batch sizes is done using the algorithm presented in the previous section 3.

The choice of the number of events “*nb-events*” and the parameter “*P*” is done as follows.

1. For the real data, there is only one arrival process with a fixed number of events count and a fixed value for the parameter of the geometric distribution.
2. For the corresponding Evi simulations, the parameters “*nb-events*” and “*P*” were assumed to follow a normal distribution with parameters derived from the Evi simulation data corresponding to the trial data.

Similarly to the previous analysis, 50, 100 and 1000 simulations were generated.

7.4.2.1 Trial data results

Figure 7-23 and Figure 7-24 show the results corresponding to SGDVS1 and SGVDS2 respectively. The graphs show the max batch size of the trial data compared to the average max batch size generated through the 50, 100 and 1000 runs.

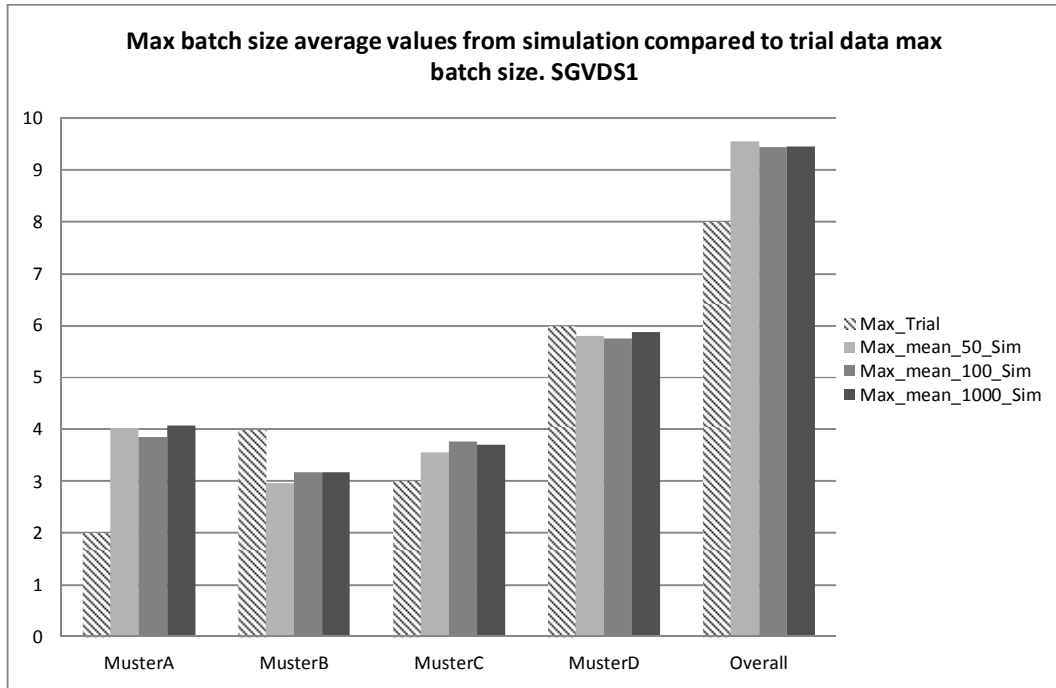


Figure 7-23: Max batch size average values from simulation compared to trial data max batch size. SGVDS1

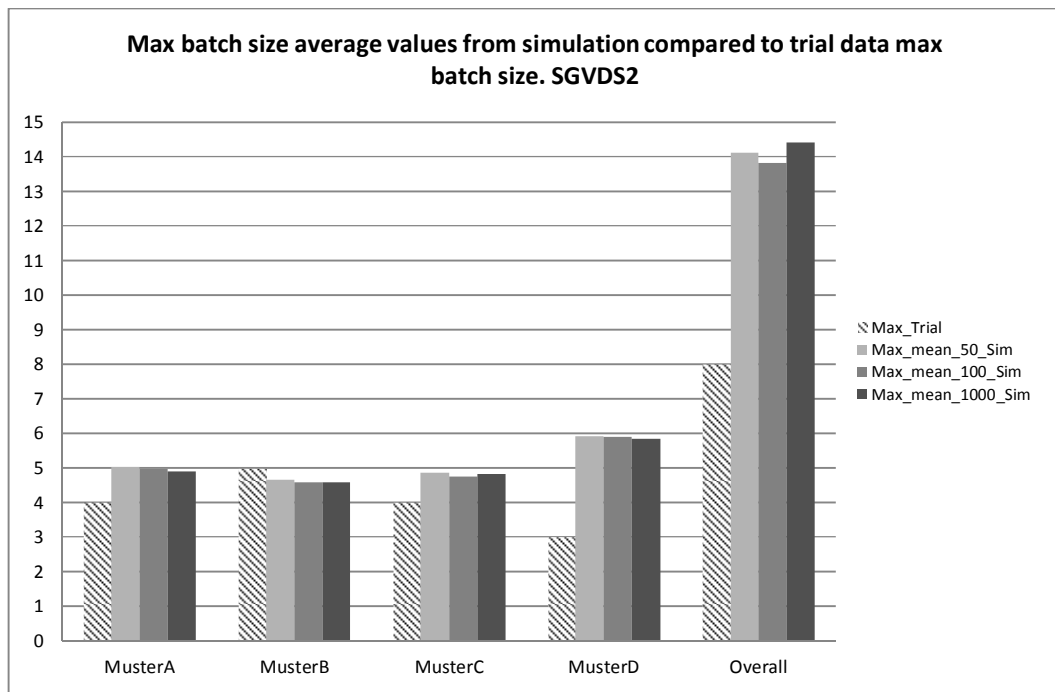


Figure 7-24: Max batch size average values from simulation compared to trial data max batch size. SGVDS2

7.4.2.2 Discussion

For SGVDS1 the simulations tend to overestimate the max batch size for Muster A, C and the Overall arrival process. For the other individual muster stations (B and D), the simulations tend to underestimate the max batch size.

For SGVDS2, apart for Muster B, the simulations overestimate the average max batch size.

The above results tend to confirm that generating discrete batch sizes following a geometric distribution using the inverse function expressed as a continuous variable introduces a high level of error.

7.4.2.3 Corresponding Evi simulated data results

Figure 7-25 to Figure 7-27 show the average value of the max batch sizes as fitted from the simulated data and the average max batch size as generated through the 50, 100 and 1000 runs for scenarios A, B and C respectively corresponding to SGVDS1 dataset.

Figure 7-28 shows the results for SGVDS2.

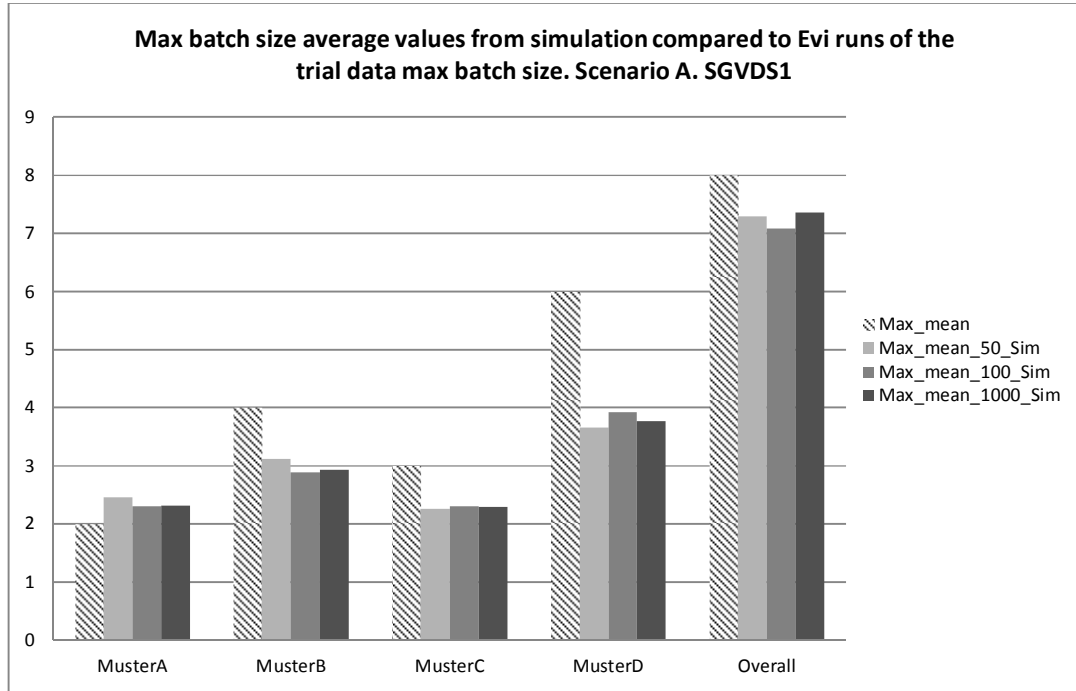


Figure 7-25: Max batch size average values from simulation compared to Evi runs of the trial data max batch size. SGVDS1- Scenario A.

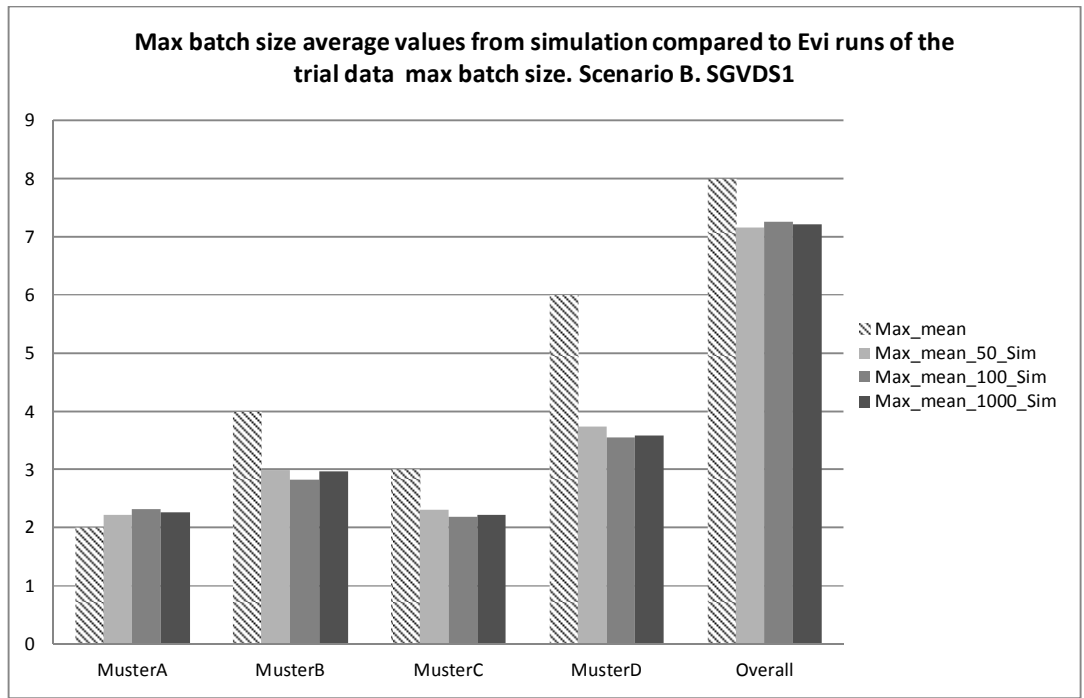


Figure 7-26: Max batch size average values from simulation compared to Evi runs of the trial data max batch size. SGVDS1- Scenario B.

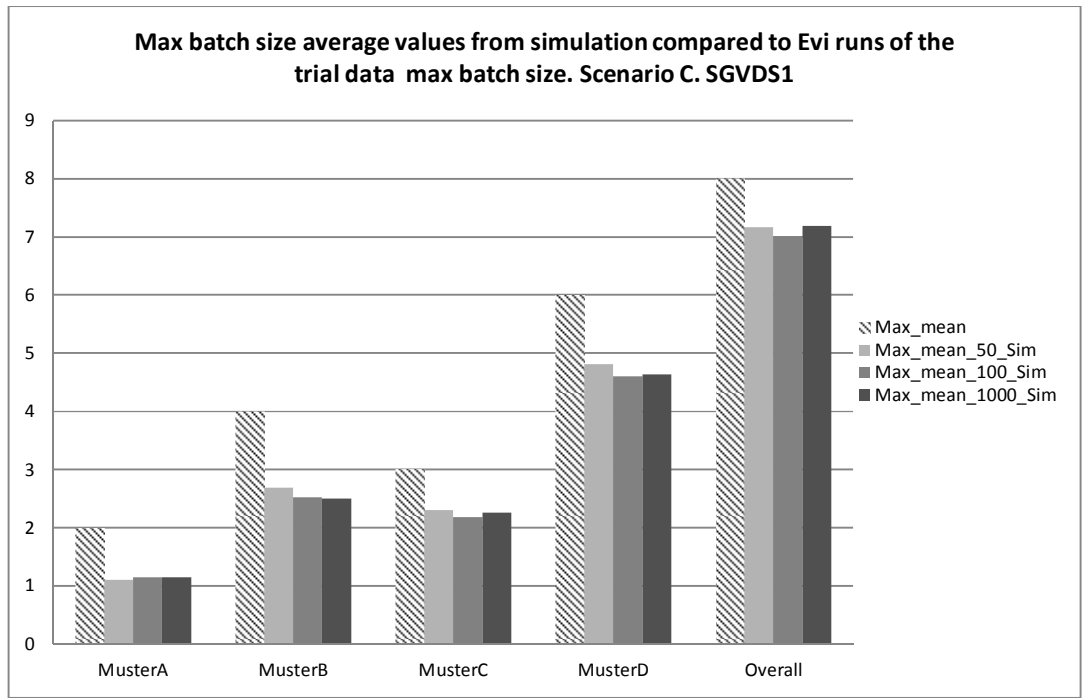


Figure 7-27: Max batch size average values from simulation compared to Evi runs of the trial data max batch size. SGVDS1- Scenario C

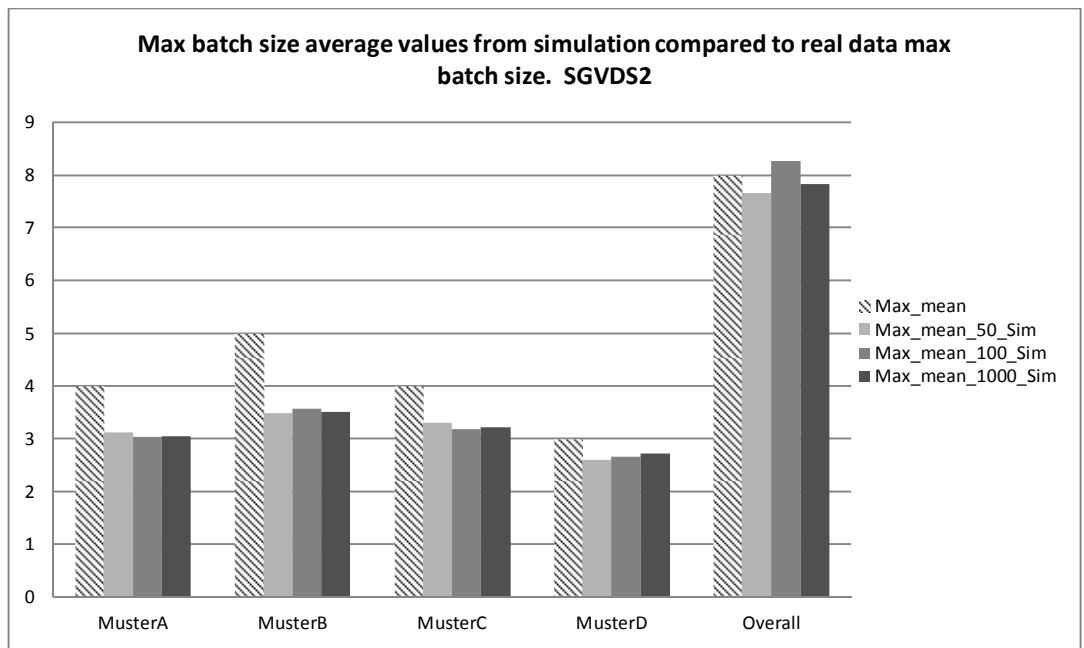


Figure 7-28: Max batch size average values from simulation compared to Evi runs of the trial data max batch size. SGVDS2.

7.4.2.4 Discussion

For SGVDS1 and in all cases the average simulated batch sizes are underestimated for all muster stations with the exception of Muster A.

For SGVDS2, the simulated average max batch size is also underestimated in all cases except for the 100 runs generated data, where the generated average is slightly overestimating the original one for the Overall arrival process.

Further analysis of the results presented above, showed that when the percentage change in the average value of the max batch size, when original data and generated data are compared, is smaller for simulated data then it is for the real data. To illustrate this, the results for SGVDS2 for 50 runs of generated batch sizes are presented in the figure below. The graph shows the percentage change of the average max batch size value when generated data are compared to the original one both in the case of trial data and the corresponding Evi data (results are similar for 100 and 1000 generation and are not shown here).

This could indicate that reproducing results of simulations is achieved with fewer errors when generating batch sizes.

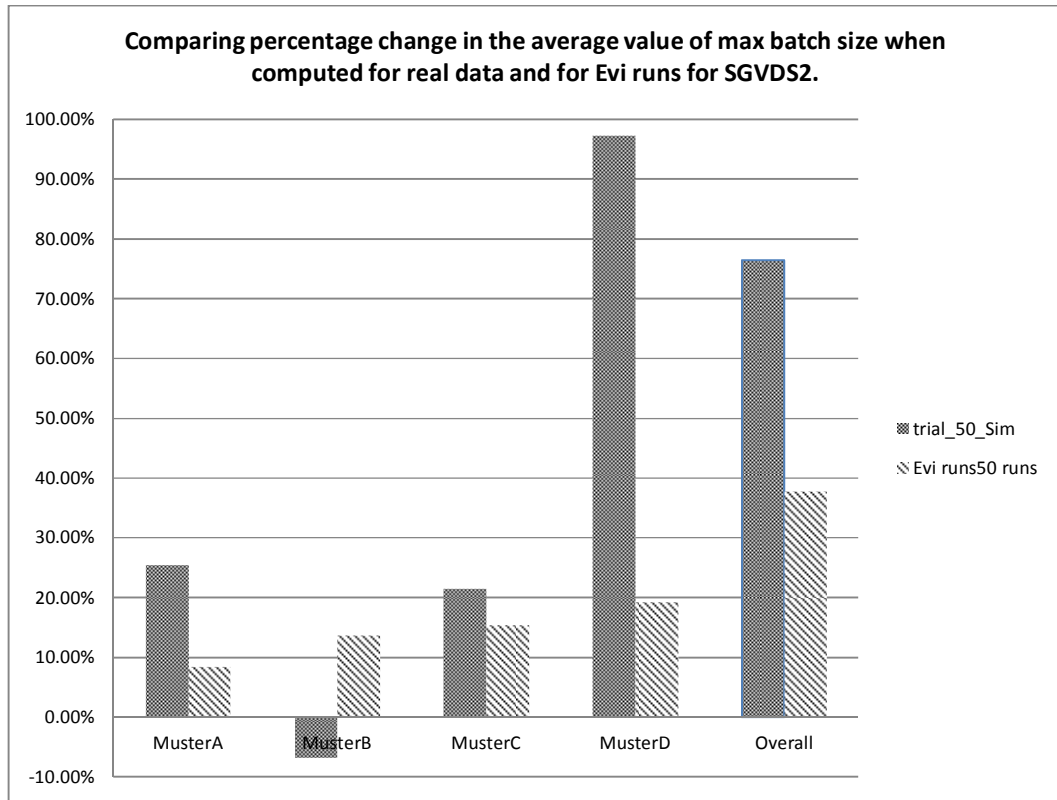


Figure 7-29: Percentage change in average value of max batch size for real and simulated data for SGVDS2

7.5 Concluding Remarks

This chapter concentrated on the fitting of a model for the batch sizes of the overall process of arrivals at the muster stations.

Using the derived fitted model, a generation of new data was performed and compared to the original data.

Both datasets of simulated data and the SAFEGUARD data (trial and corresponding simulations) were used.

The generation of new datasets from the fitted model was undertaken using the inverse method, where a random distribution (normal distribution) for choosing the number of events and the parameter of the Geometric distribution was used.

The generated data overestimated the original data in most cases for all the datasets considered in the analysis.

In addition, it was found that the fitted model derived from simulations produced less errors (smaller overestimation) when compared to its original data than what the fitted model derived from the real data produced when compared to its original data. This could be due to lack of statistical significance of the real data (only one dataset per ship).

8 NON-HOMOGENEOUS POISSON PROCESS (NHPP) FITTING

8.1 General Remarks

This chapter discusses the fitting of the NHPP model presented in Chapter 5 using the Kuhl and Wilson method for the simulation data and the real data.

The method through a variance stabilising transformation, derives the degree of the polynomial rate function of the NHPP.

Both the real data and the simulation data were fitted with this method which was programmed using R which a language and environment for statistical computing and graphics [30].

For the simulated data, a run at random was chosen from the 100 runs of each of the 80 scenarios defined in Chapter 6:

- fixed speed and varying reaction time, 10 passenger loads for the day case, and 10 passengers load for the night case,
- varying speed and a fixed reaction time, 10 passengers loads for the day case, and 10 passengers loads for the night case,
- varying speed and a varying reaction time, 10 passengers loads for the day case, and 10 passengers loads for the night case.
- fixed speed and fixed reaction time, 10 passengers loads for the day case, and 10 passengers load for the night case,

For the real data, both SGVDS1 and SGVDS2 arrival times were fitted as well as the corresponding Evi simulation runs. A run from each simulated scenario was chosen at random for the fitting.

8.2 NHPP model fitting: Simulation data

Overall the fitting of the data gave very good agreements between the fitted and the original data. In most cases high order polynomial for the rate function is obtained.

In the next subsection the results for the Day cases are presented followed by the Night case results.

8.2.1 Day cases

The number of coefficients of the polynomial rate function is shown in Table 8-1 below. Values of the coefficients are provided in Appendix III.

Load	10	20	30	40	50	60	70	80	90	100
Day	7	7	6	7	7	7	7	7	7	7
Day_Fixed Reaction	7	7	7	6	1	7	7	7	1	7
Day_Fixed Speed	7	7	7	6	6	7	7	7	1	7
Day_Fixed Speed & Reaction	6	7	6	7	7	7	7	1	1	7

Table 8-1: Number of coefficient of the rate function of the NHPP for the day case scenarios

As can be seen from the table above and Figure 8-1 below, in most cases, the degree of the polynomial rate function is 6.

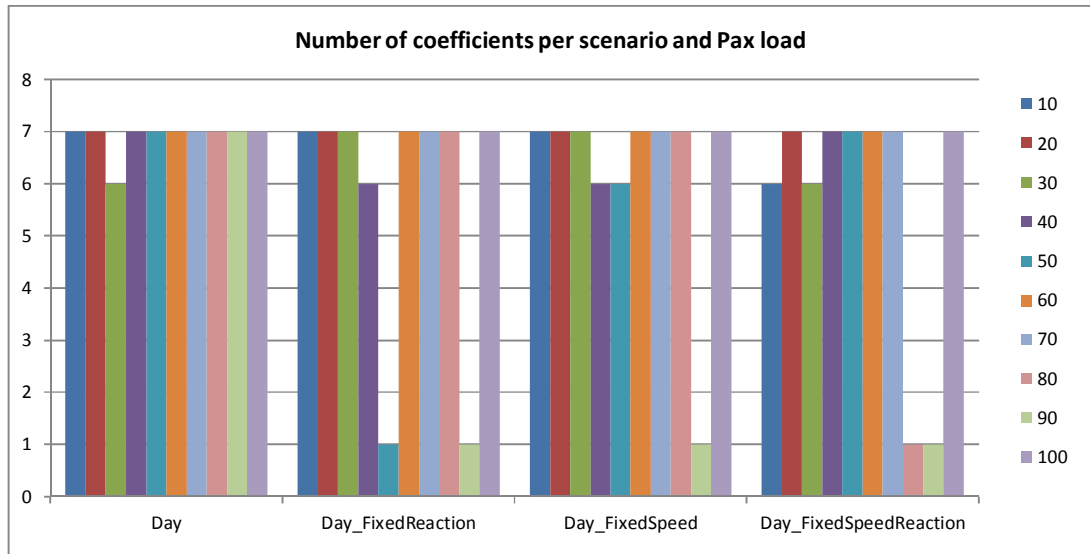
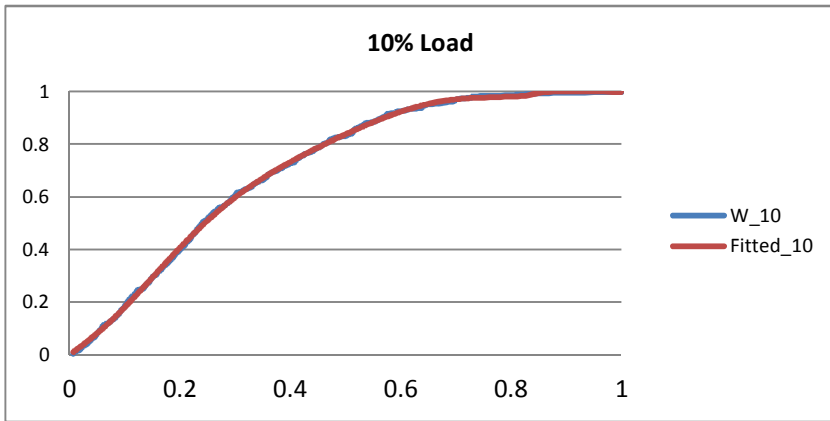
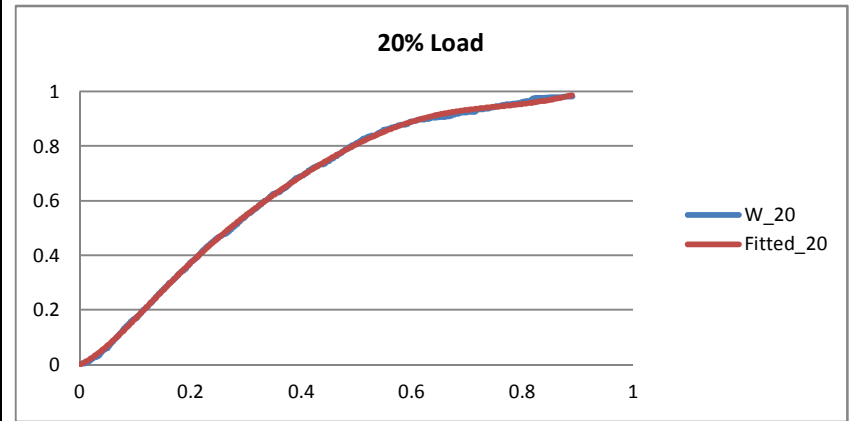


Figure 8-1: variation of number of coefficient of the rate function per scenario and passenger load for the day cases.

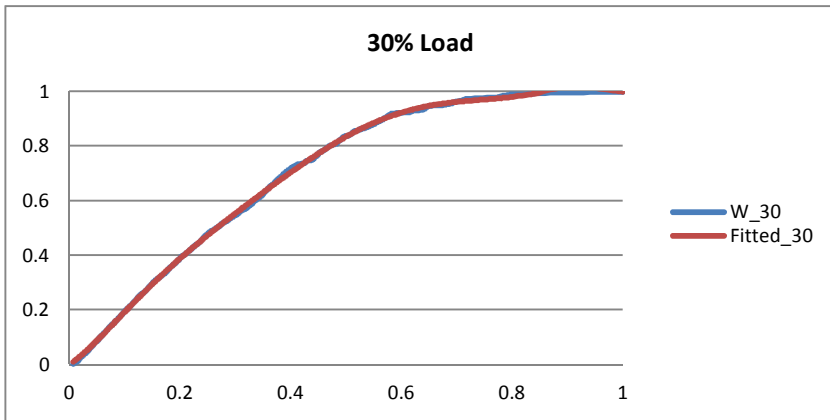
The scaled arrival curves obtained from the fitting were also in most case almost overlapping with the original data as can be seen below for the Day case scenarios (Figure 8-2). The results for the Day Fixed Speed, Fixed Reaction and Fixed Speed & Reaction are shown in Appendix III (Figure III-1, Figure III-2 and Figure III-3 respectively).



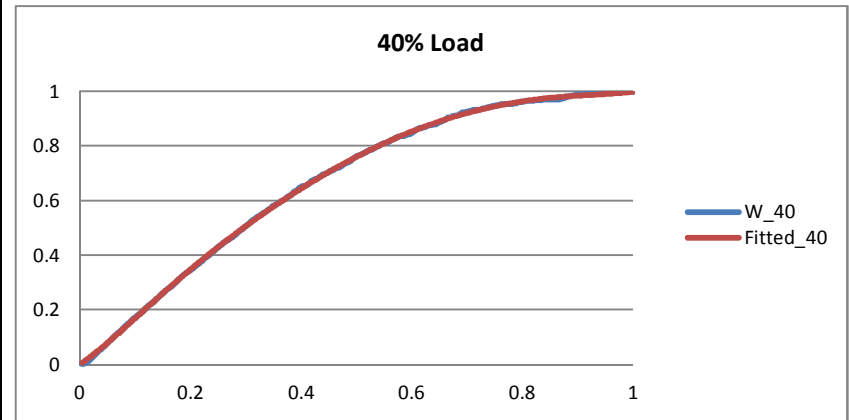
(a)



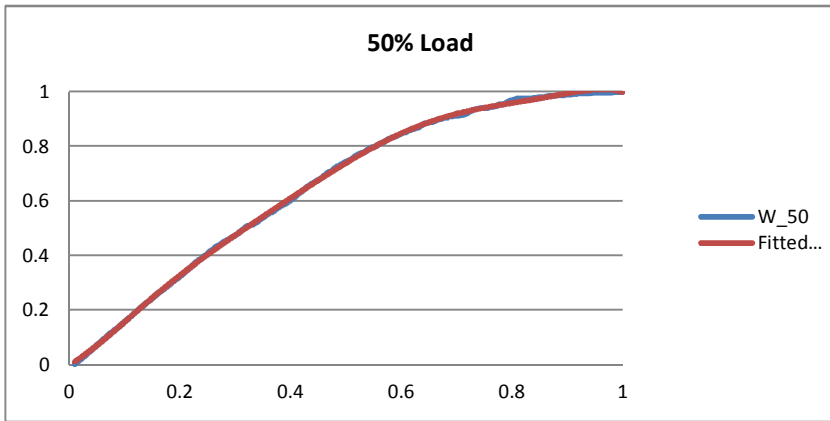
(b)



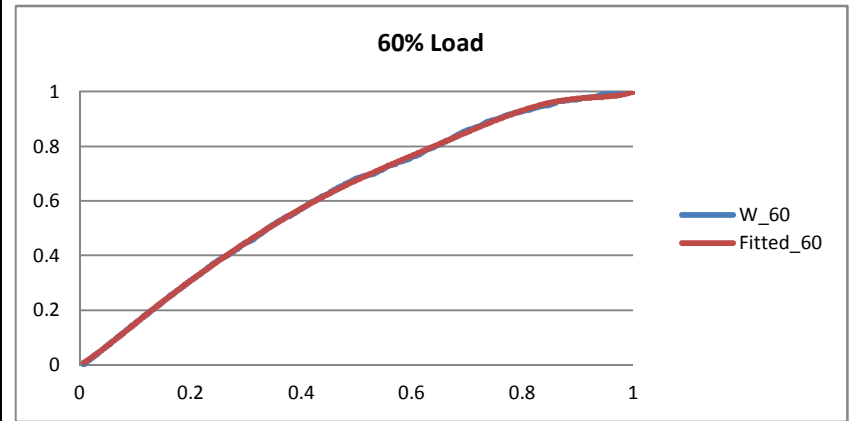
(c)



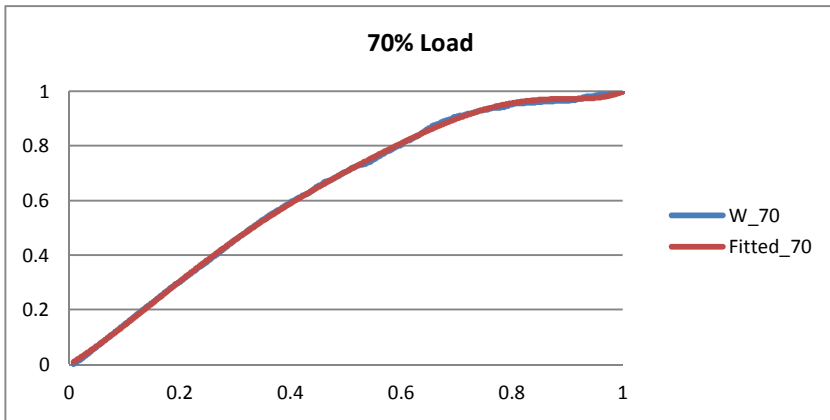
(d)



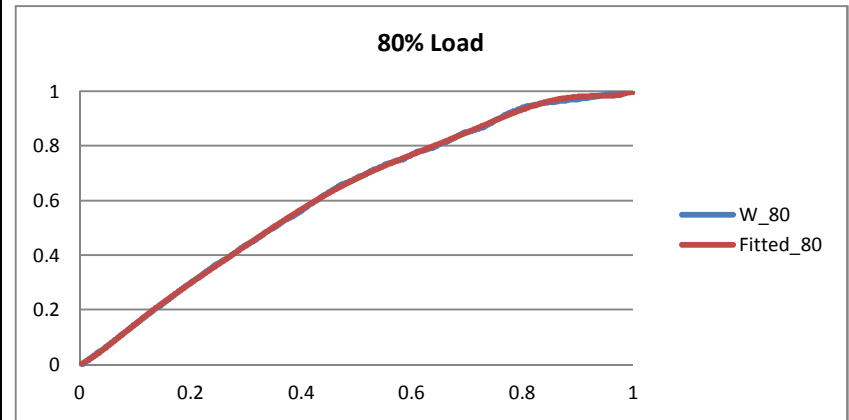
(e)



(f)



(g)



(h)

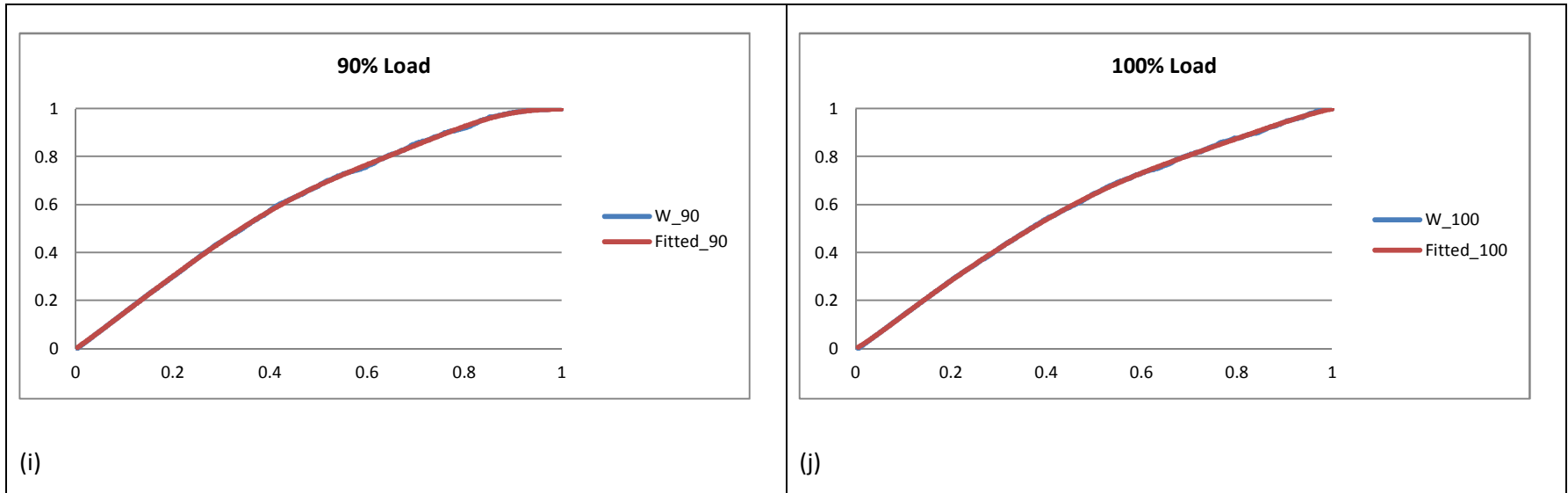


Figure 8-2: Fitted and original arrival process for the day cases for (a) 10% passenger load, (b) 20% passenger load, (c) 30% passenger load, (d) 40% passenger load, (e) 50% passenger load, (f) 60% passenger load, (g) 70% passenger load, (h) 80% passenger load, (i) 90% passenger load, (j) 100% passenger load

8.2.2 Night cases

At first the choice of the runs for the night cases produced the number of coefficients of the polynomial rate function as shown in Figure 8-3 below.

As can be seen from the figure, there is quite a lot of variation in the degree of the polynomial rate function. No clear pattern can be seen.

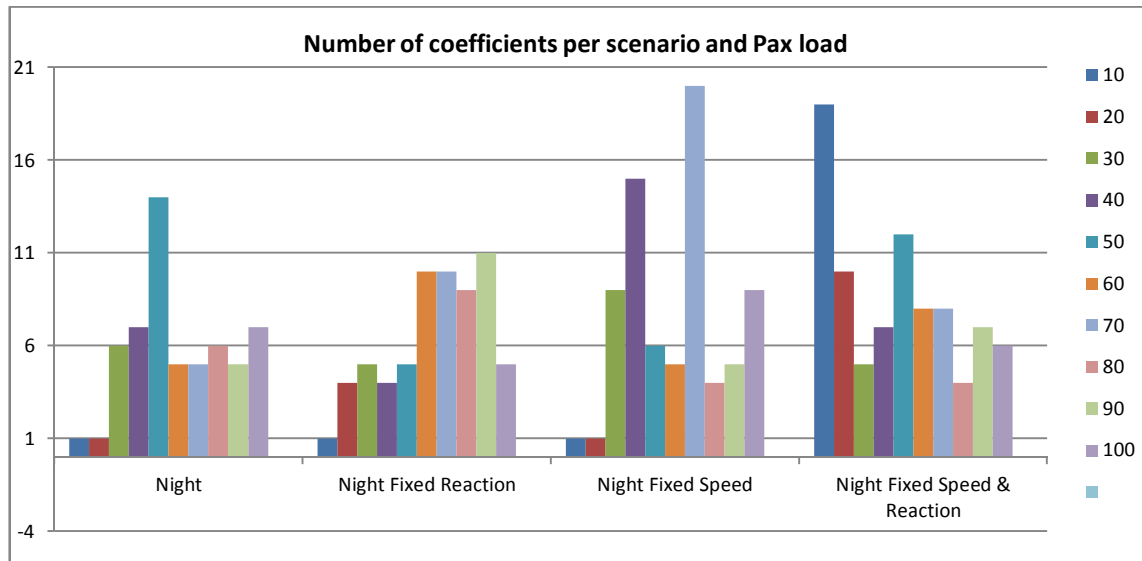


Figure 8-3: variation of number of coefficient of the rate function per scenario and passenger load for the night cases.

It was then decided to choose different input data to the fitting for the scenarios which produced a high number of coefficients of the polynomial rate function. The number of coefficients of the polynomial rate function corresponding to the new fitting is shown in Table 8-2 and in Figure 8-4 below. Values of the coefficients are provided in Appendix III.

Load	10	20	30	40	50	60	70	80	90	100
Night	1	1	6	7	7	5	5	6	5	7
Night Fixed Reaction	1	4	5	4	5	6	6	8	6	5
Night Fixed Speed	1	1	6	5	6	5	2	4	5	7
Night Fixed Speed & Reaction	4	8	5	7	10	8	8	4	7	6

Table 8-2: Number of coefficient of the rate function of the NHPP for the night case scenarios

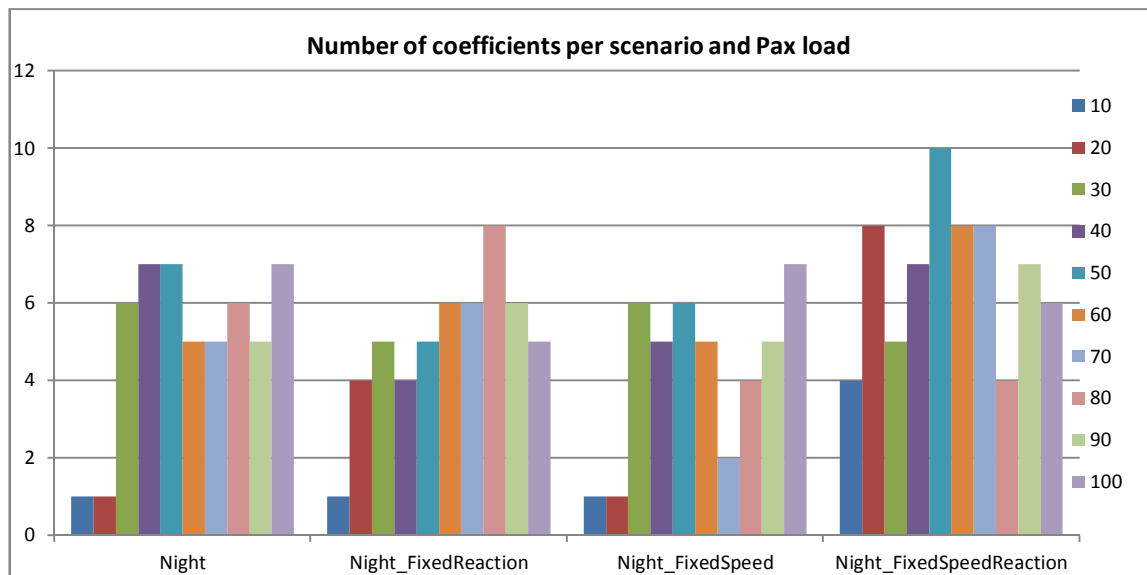
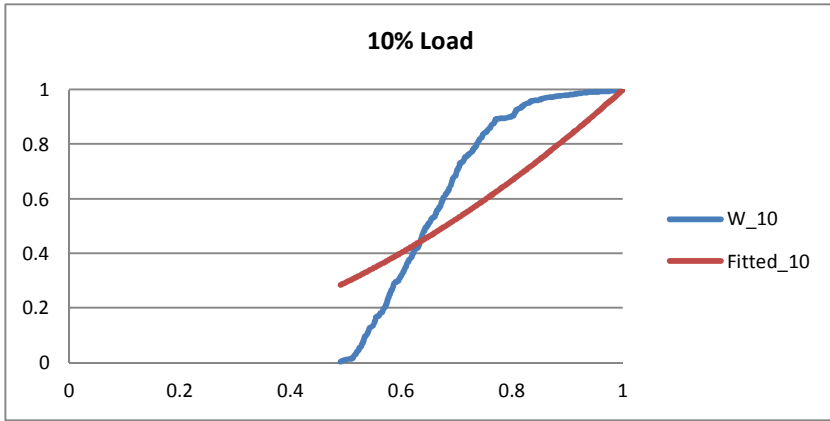
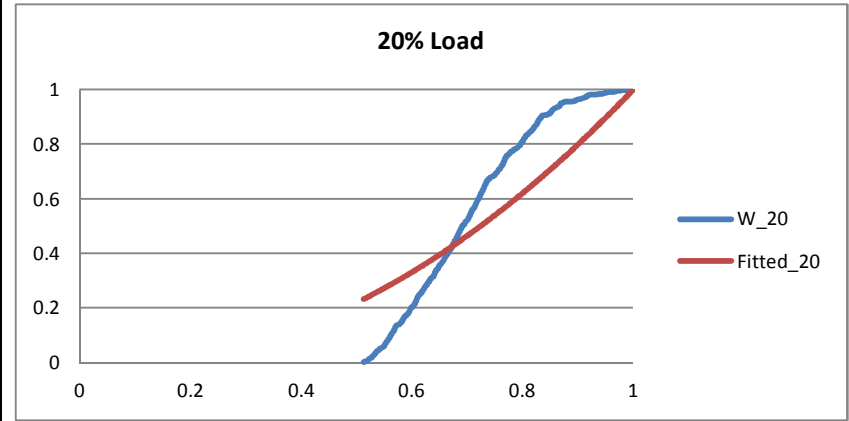


Figure 8-4: variation of number of coefficient of the rate function per scenario and passenger load for the night cases after selecting different runs.

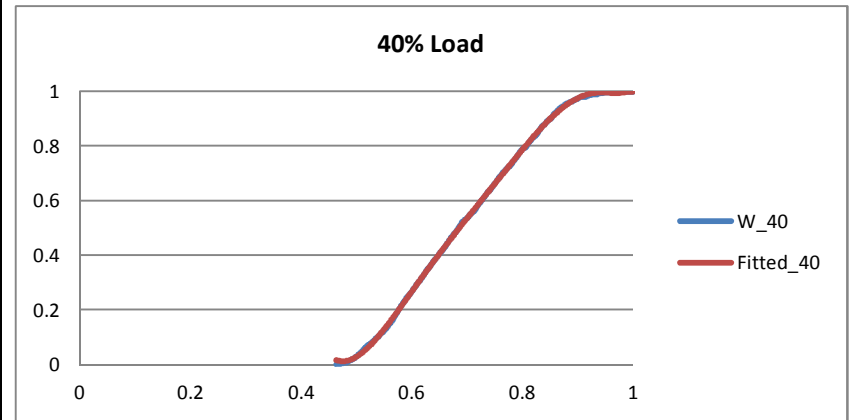
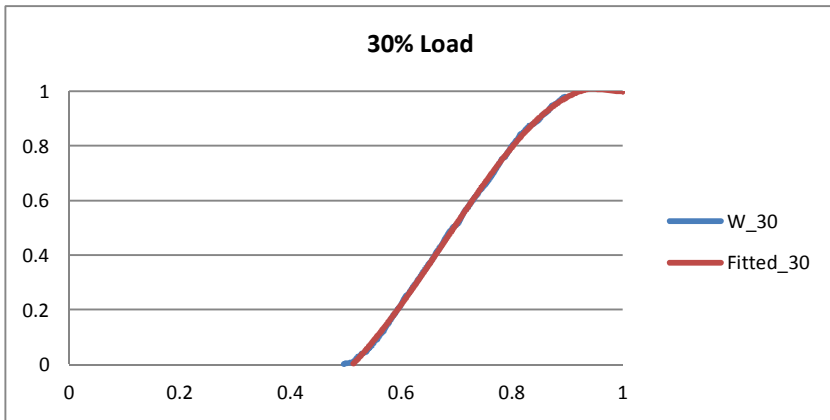
The scaled arrival curves obtained from the fitting showed very good agreements between the fitted data and the original apart from few exceptions. The result for the Night case can be seen in Figure 8-5 below. The results for the Night Fixed Reaction, Fixed Speed and Fixed Speed & Reaction are shown in Appendix III (Figure III-4, Figure III-5 and Figure III-6 respectively).



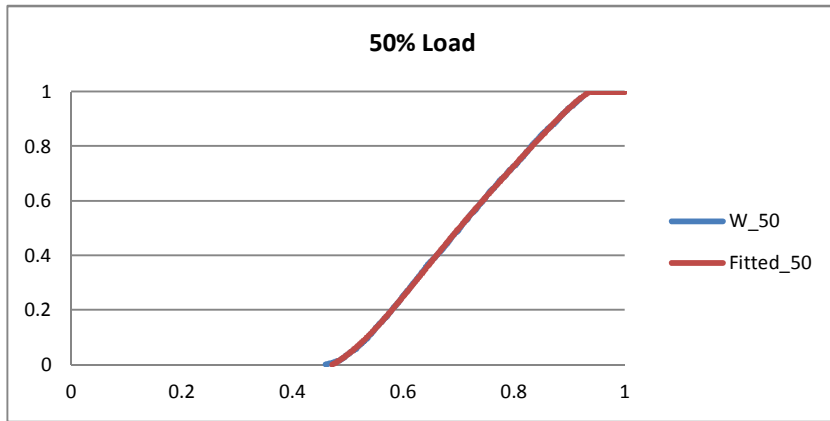
(a)



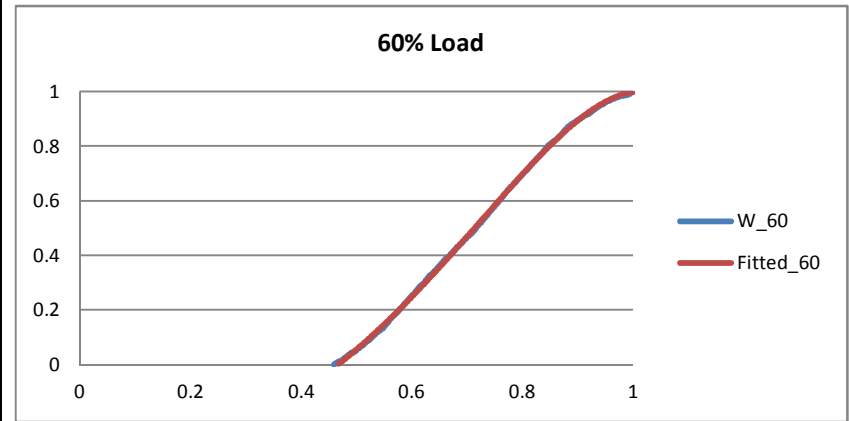
(b)



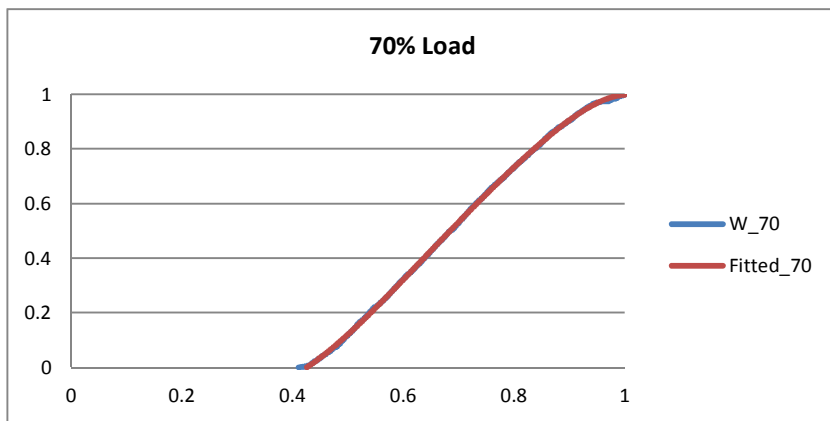
(c)



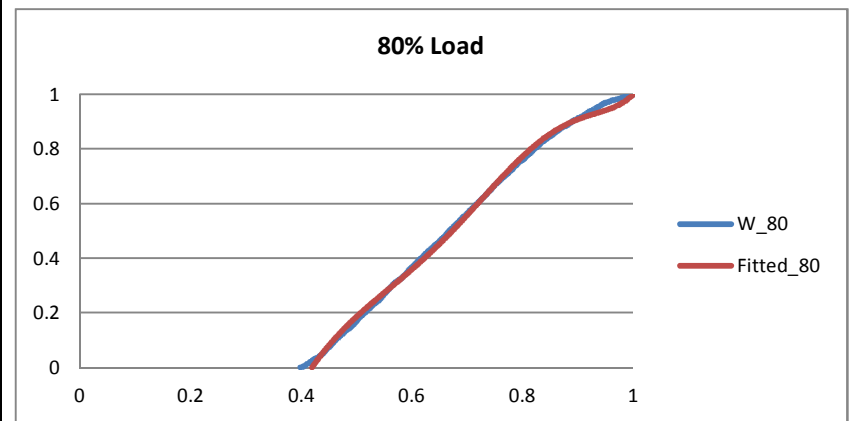
(d)



(e)



(f)



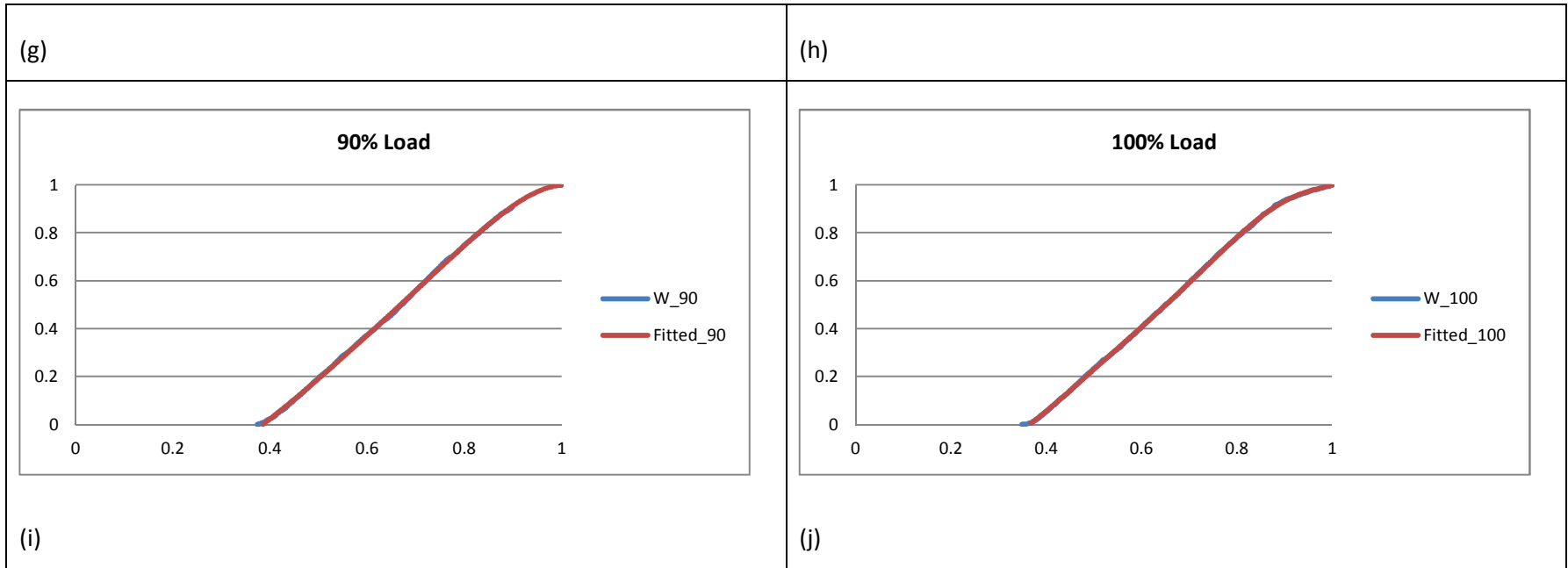


Figure 8-5: Fitted and original arrival process for the night cases for (a) 10% passenger load, (b) 20% passenger load, (c) 30% passenger load, (d) 40% passenger load, (e) 50% passenger load, (f) 60% passenger load, (g) 70% passenger load, (h) 80% passenger load, (i) 90% passenger load, (j) 100% passenger load

8.2.3 Sensitivity of the fitting to the chosen input data

The night results above showed that a change in the run chosen to be fitted can lead to very big variations in the degree of the polynomial rate function. For example, in the Night Fixed Speed scenario for a 70% passenger load the number of coefficients went from 20 to 02.

It was impractical to fit the 8000 runs produced by the simulations, but a small sample of 10 runs for the Day scenario for 10% passenger load was fitted. The results are shown below.

The number of coefficients of the polynomial function varies as shown in Table 8-3 below. The variation of the value of R^2 for then 10 fits is shown in Figure 8-6 below.

Run	1	3	3	4	5	6	7	8	9	10
Number of Coefficients	6	5	6	7	9	8	5	7	6	9

Table 8-3: Variation in number of coefficients for 10 different runs of Day scenario, 10% passenger load

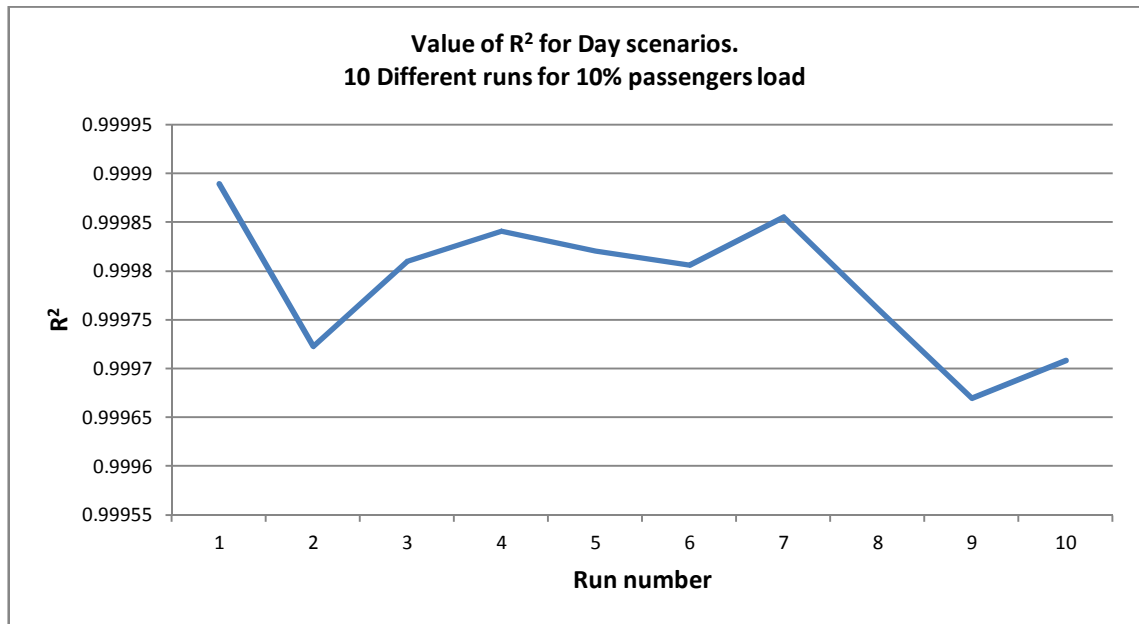


Figure 8-6: Variation of R^2 value over fitting of 10 different runs of Day scenario for 10% passenger load.

Overall when looking at the fitted curves (not shown here), there was a good agreement between the fitted and original data but some fits were better than others.

8.2.4 Discussion

The Day cases results seem to be overall consistent with a degree of the polynomial function being fixed across the different scenarios with some exceptions where the rate function is constant (Day Fixed Reaction, Day Fixed Speed and Day Fixed Speed and Reaction for a 90% passengers load).

For the Random Day case, the degree of the polynomial rate function is not affected by the load of passengers (with the exception of 20% load. The results for 30% load are deemed similar to the rest as there is only one degree difference in the polynomial rate function).

The fixed rate function could be the result of a particular configuration of agents' initial locations and their constant speed and /or reaction time. This could have led to a constant flow of arrival at the muster stations.

The Night cases offered a totally different picture. At first no clear pattern could be seen from the obtained data.

A choice of different runs to fit provided slightly more homogeneous results, lowering, in some instances, the degree of the polynomial function substantially. This led to smaller ranges.

For the Night cases results, the Random Night case and the Night Fixed Reaction case seem to exhibit some sort of consistency. Apart from the lower passenger's loads, the degree of the polynomial rate function seems to vary between 4 and 6 for the Night case and between 4 and 7 for the Night Fixed Reaction.

The fitting of the 10 different runs of the same scenario (Day 10% passenger load) shows that there are differences in terms of the number of coefficients of the polynomial rate function and the fitted curves, meaning sensitivity to the input data used in the fitting.

8.3 NHPP model fitting: Real data

The same procedure was applied to the real datasets and their corresponding Evi simulations.

First the fitting of the actual data, then the fitting of Evi simulation runs corresponding to both SGDVS1 and SGDVS2 datasets are presented.

8.3.1 Actual data

The coefficients of the fitted models are shown in Table 8-4 below.

SGVDS1					
Muster Station	A	B	C	D	Overall
Beta1	2.37	3.29	2.62	2.92	2.63
SGVDS2					
Muster Station	A	B	C	D	Overall
Beta1	0.88	2.18	1.77	2.35	1.83
Beta2	3.05	-0.43	0.07	-1.18	0.10

Table 8-4: Model Coefficients for both SGDVS1 and SGVDS2

The scaled fitted and original arrival curves are shown in Figure 8-7 and Figure 8-8 for SGDVS1 and SGVDS2 respectively.

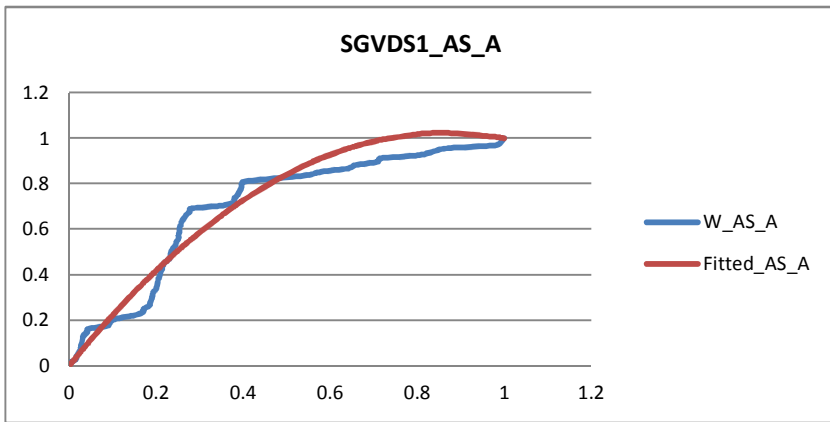
8.3.2 Discussion

For all muster stations of SGDVS1 data set, the rate function is a constant function. For SGVDS2, the rate function is a degree 1 polynomial function.

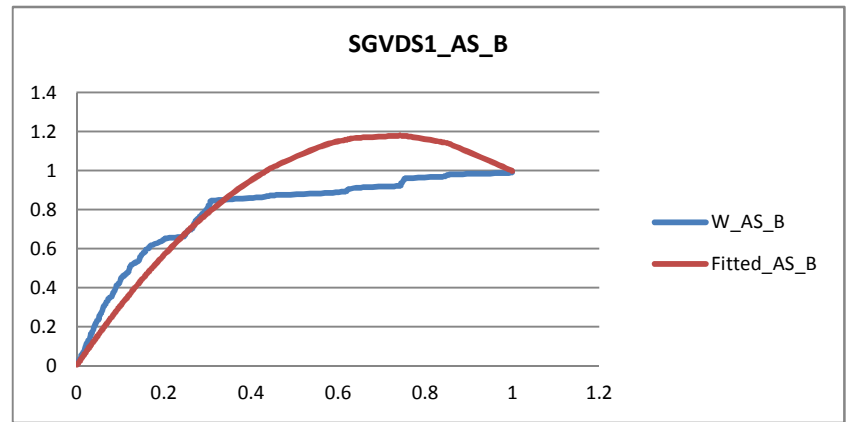
The R^2 of the fitting for SGVDS2 was overall better than for SGDVS1, even though for both data sets the smallest R^2 value was 0.9494.

As can be seen from the scaled fitted and original arrival curved in Figure 8-7 the curve for Muster station D and the overall arrival curve show the best fit for SGDVS1.

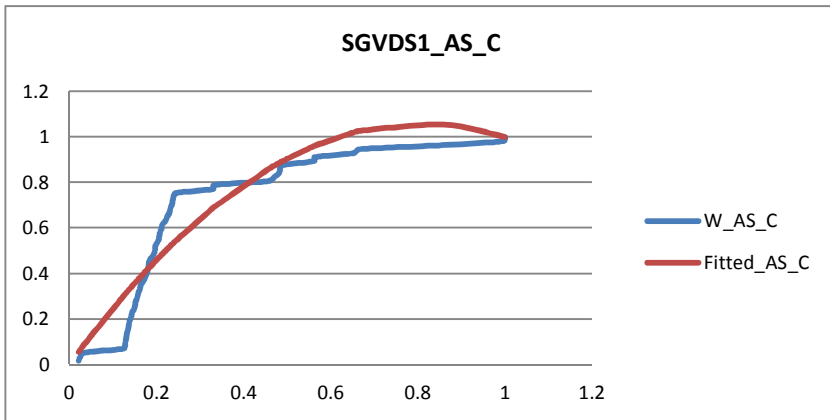
For SGDVS2 (Figure 8-8), the curves for Muster stations C and Overall show the best agreement followed by the curves for Muster D and B.



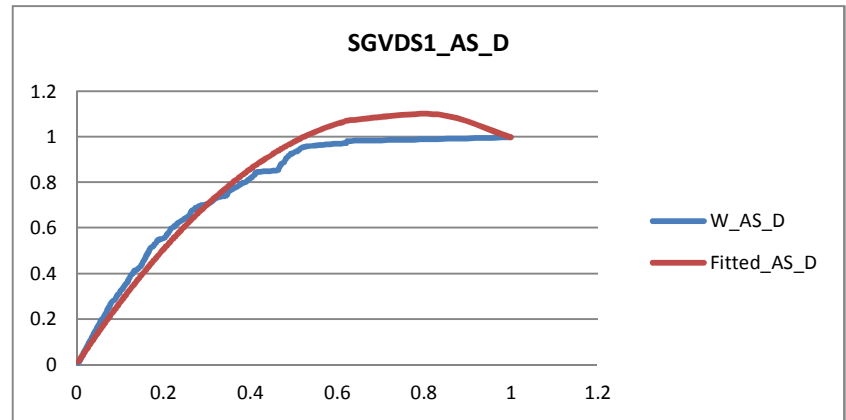
(a)



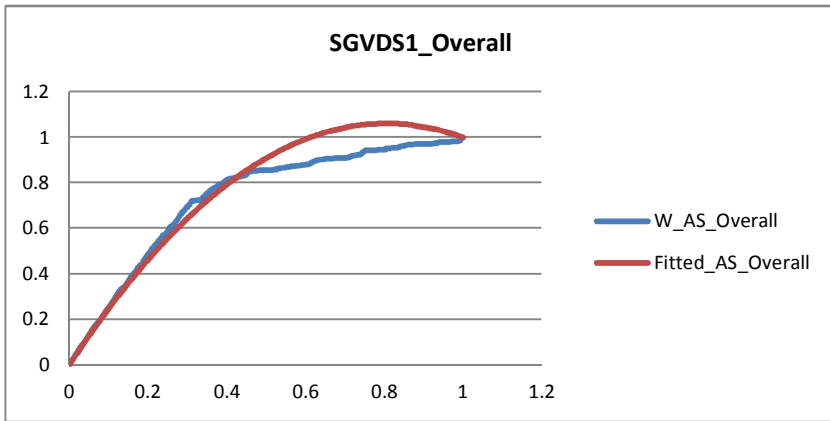
(b)



(c)

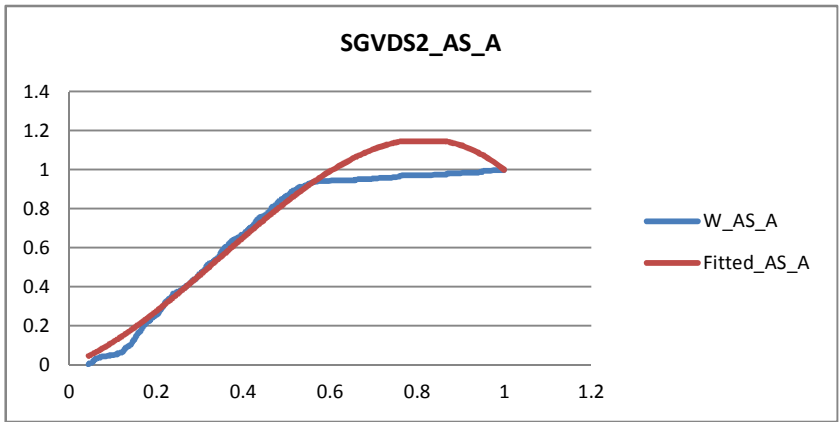


(d)

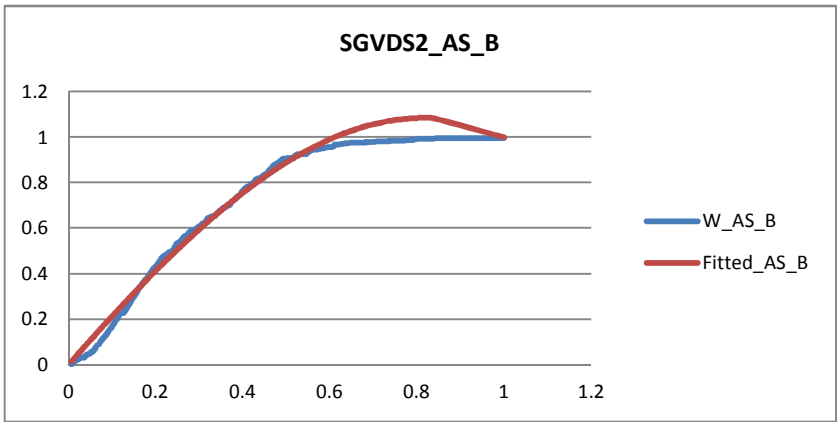


(e)

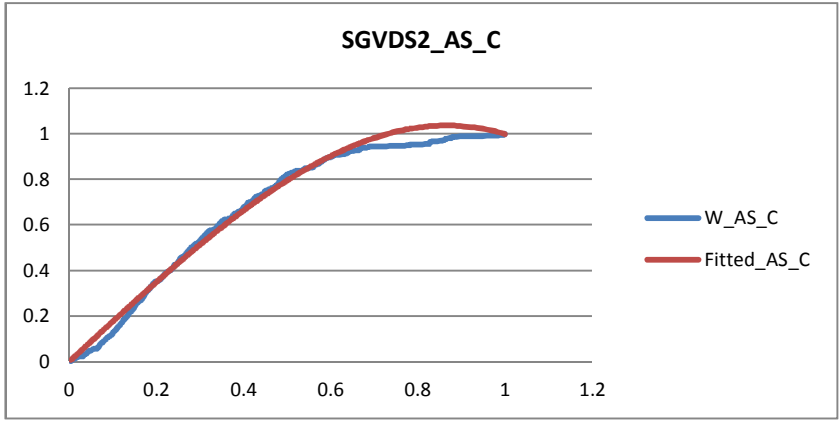
Figure 8-7: Fitted and original arrival process for SGVDS1 (a) Muster Station A, (b) Muster Station B, (c) Muster Station C, (d) Muster Station D, (e) Overall.



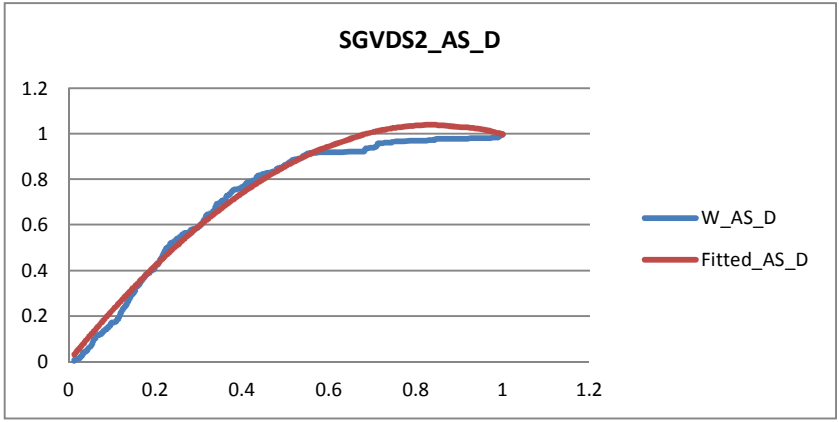
(a)



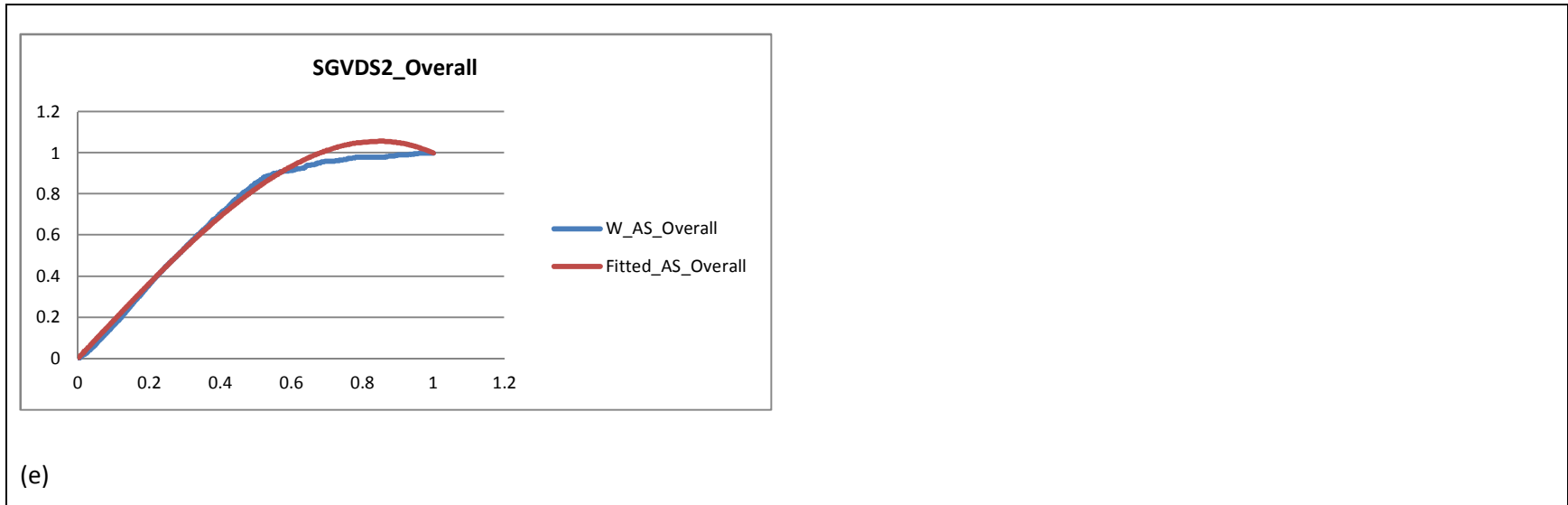
(b)



(c)



(d)



(e)

Figure 8-8: Fitted and original arrival process for SGVDS2 (a) Muster Station A, (b) Muster Station B , (c) Muster Station C, (d) Muster Station D, (e) Overall.

8.3.3 Corresponding simulated data

Similarly to the simulated data of section 3, one run has been chosen randomly from each set of the Evi simulated runs corresponding to each of the Muster stations of each data set.

Recall that for SGDVS1 three scenarios were run to simulate this data set, Scenarios A, B and C.

The coefficients of the fitted model per scenario are shown in Table 8-5 below.

SC A					
Muster Station	A	B	C	D	Overall
Beta1	0.29	0.22	-0.14	-0.04	-0.23
Beta2	2.73	4.46	4.23	0.52	10.44
Beta3				11.10	-17.04
Beta4				3.25	
Beta5				-90.29	
Beta6				152.95	
Beta7				-97.45	
SC B					
Muster Station	A	B	C	D	Overall
Beta1	0.59	0.62	-0.96	-0.73	-1.54
Beta2	2.63	-13.75	27.76	12.55	43.32
Beta3		138.61	-93.07	-21.14	-274.96
Beta4		-442.46	182.27	11.83	1028.24
Beta5		615.98	-231.82		-2246.27
Beta6		-309.36	103.79		2764.08
Beta7		-71.82	86.75		-1771.81
Beta8		81.59			

SC C					
Muster Station	A	B	C	D	Overall
Beta1	0.98	1.94	-0.80	-0.72	-0.29
Beta2		-30.60	16.76	8.45	7.23
Beta3		190.54	-50.37	-13.39	-10.74
Beta4		-421.18	80.71	8.75	34.23
Beta5		249.63	-65.91		-130.49
Beta6		261.16			217.81
Beta7		-160.80			-159.62
Beta8		-275.83			
Beta9		24.96			
Beta10		304.58			

Table 8-5: Model Coefficients for simulated runs of SGDVS1

For SGVDS2, the fitted coefficients are shown Table 8-6 below

SGVDS2					
Muster Station	A	B	C	D	Overall
Beta1	1.16	1.28	1.45	1.01	1.07
Beta2	0.89	0.85	0.88	2.09	1.57

Table 8-6: Model Coefficients for simulated runs of SGVDS2

The scaled fitted and actual arrival curve for SGDVS1 scenario A, B and C are shown in Figure 8-9, Figure 8-10 and Figure 8-11 respectively. For SGVDS2 they are shown in Figure 8-12.

8.3.4 Discussion

8.3.4.1 SGDVS1

Over the three scenarios for muster station A, the results of scenarios A and B are very similar. Both have a 1st degree polynomial rate function for the arrival process. The R² is also very high

(results not shown here). Graphically, the two curves (fitted and actual) for both scenarios have a good agreement. As expected the results for scenario C, show a weaker fit.

For muster station B fitted and actual arrival curves are almost overlapping for scenario B and C. In both case the rate function is a high order polynomial (degree 7 for scenario b and degree 9 for scenario C).

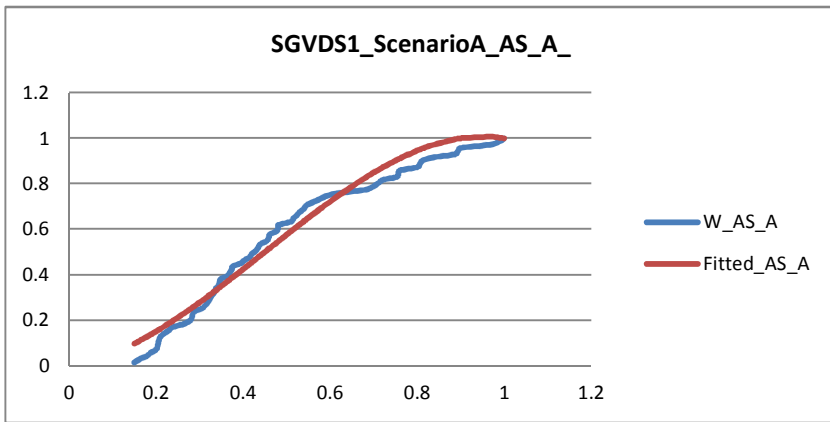
Muster station C shows similar results with scenario C having the best fit.

Muster station D, show overlapping curves in all scenarios.

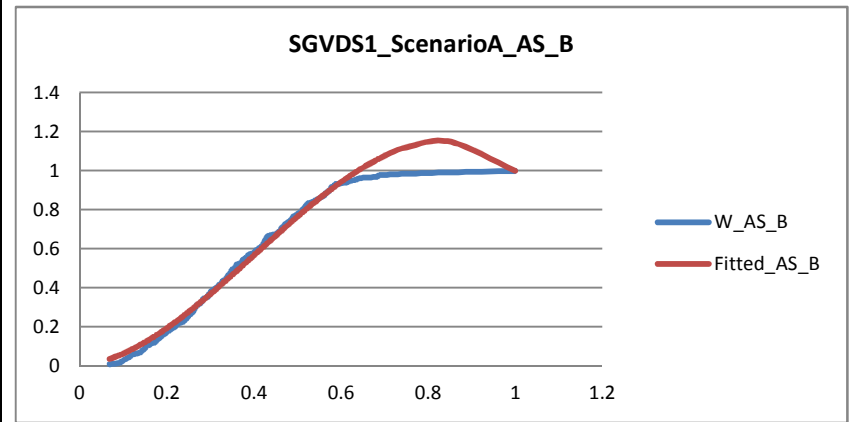
Finally, the Overall arrival curve is also overlapping with its fitted curve in all scenarios with scenarios A and B showing the best results.

8.3.4.2 SGDVS2

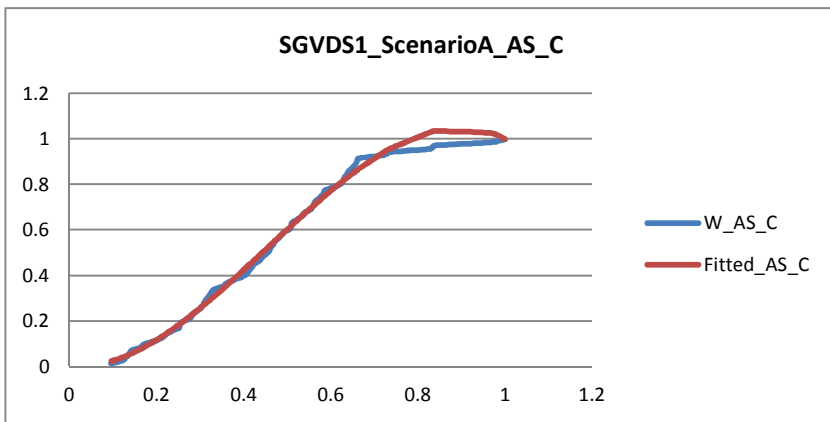
The results are more consistent over all the muster stations. All rate functions are a degree one polynomial and the fitted curves have a good agreement with the actual ones with the Overall arrival curve showing the best fit.



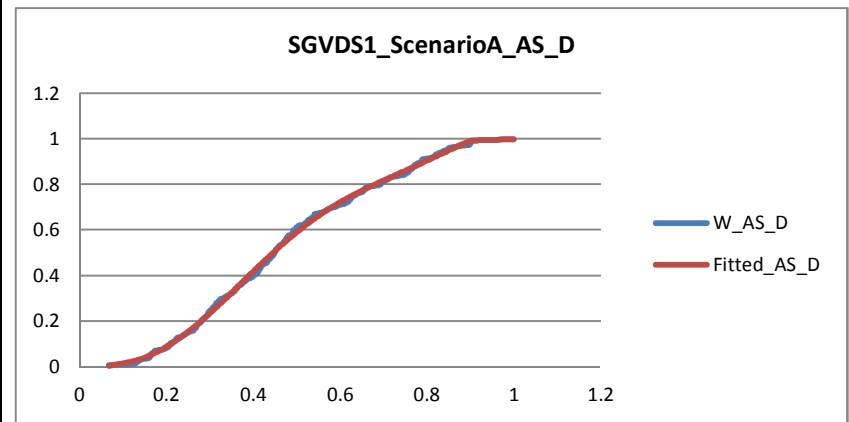
(a)



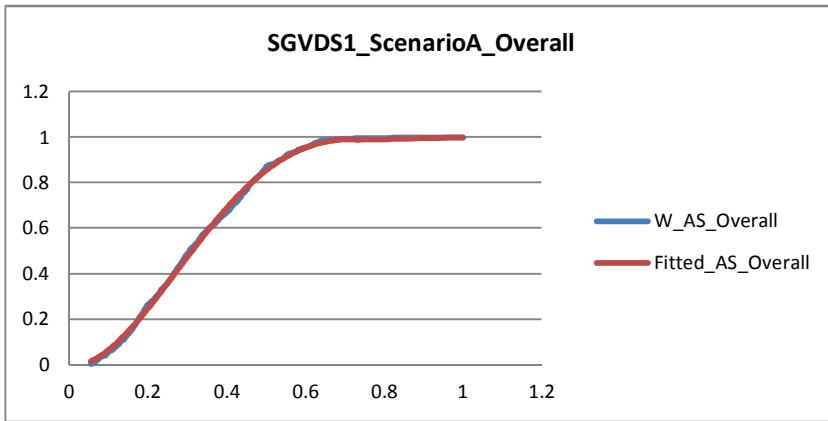
(b)



(c)

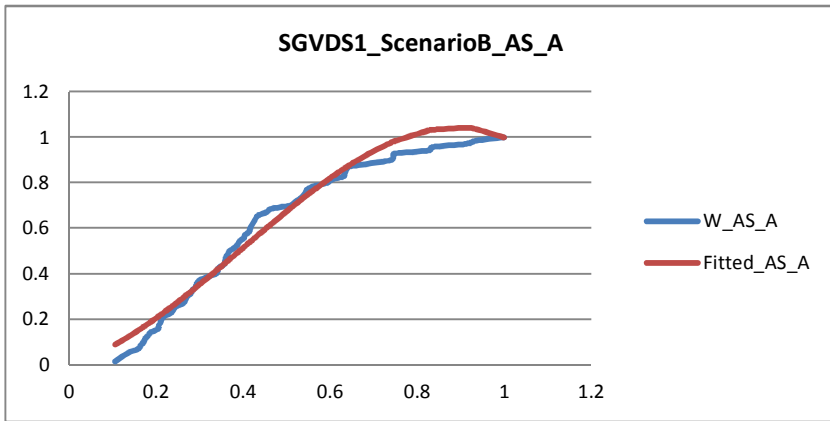


(d)

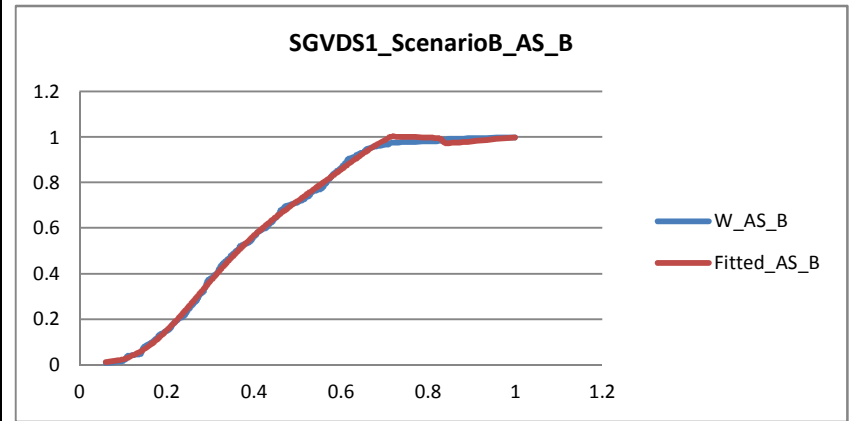


(e)

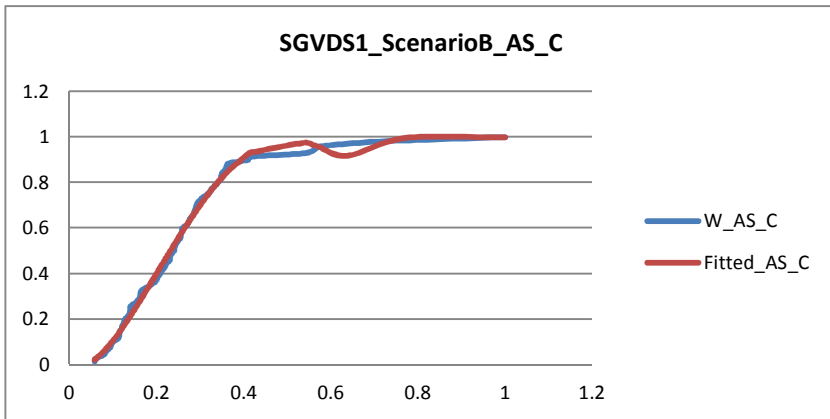
Figure 8-9: Fitted and original arrival process for SGVDS1 Scenario A (a) Muster Station A, (b) Muster Station B , (c) Muster Station C, (d) Muster Station D, (e) Overall.



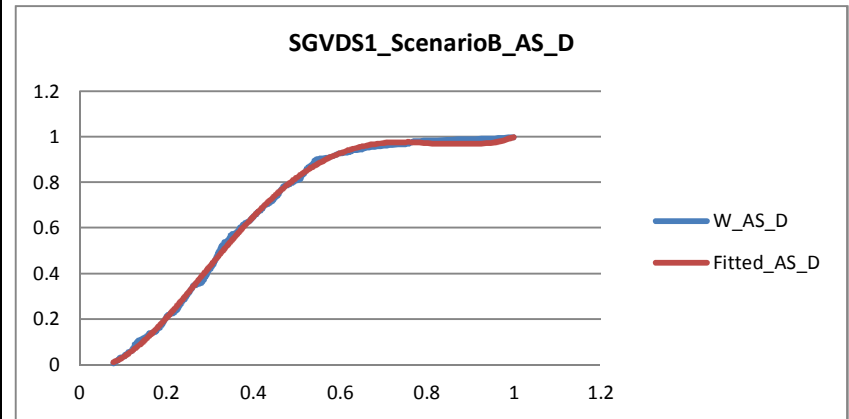
(a)



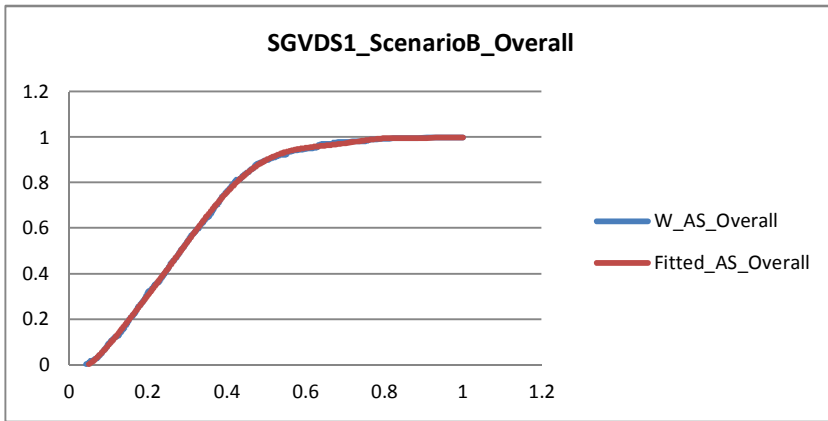
(b)



(c)

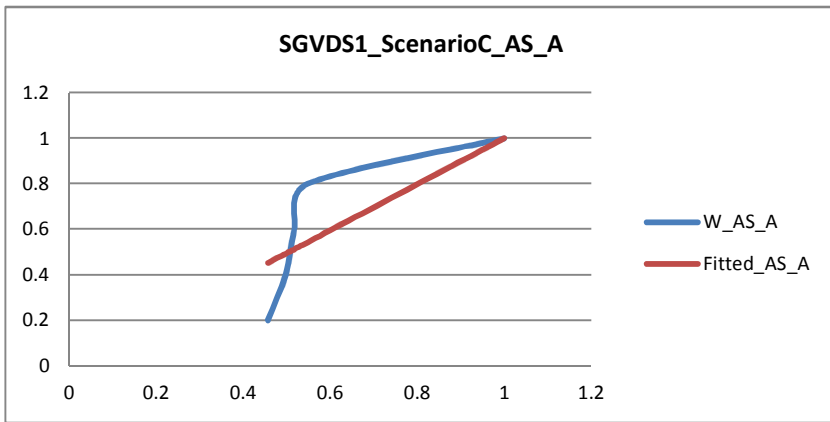


(d)

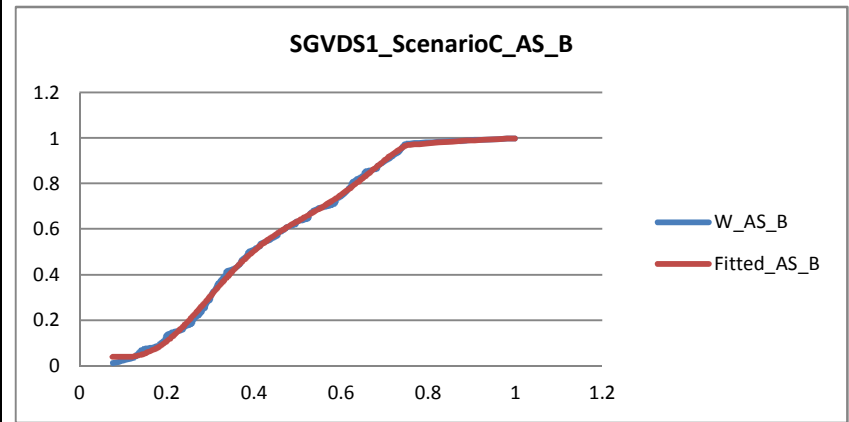


(e)

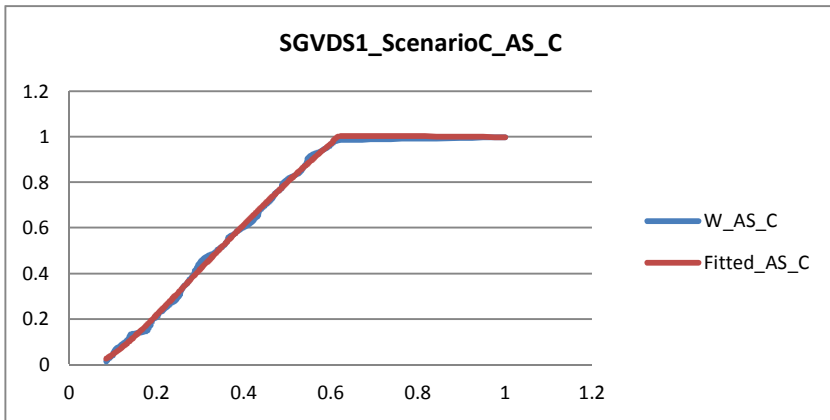
Figure 8-10: Fitted and original arrival process for SGVDS1 Scenario B (a) Muster Station A, (b) Muster Station B , (c) Muster Station C, (d) Muster Station D, (e) Overall.



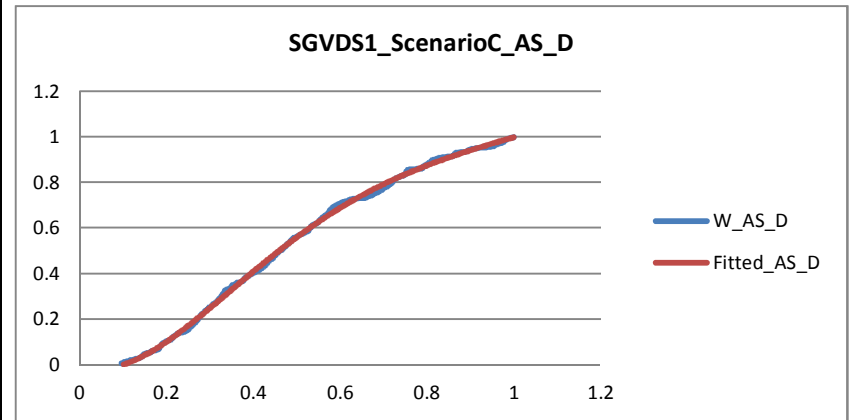
(a)



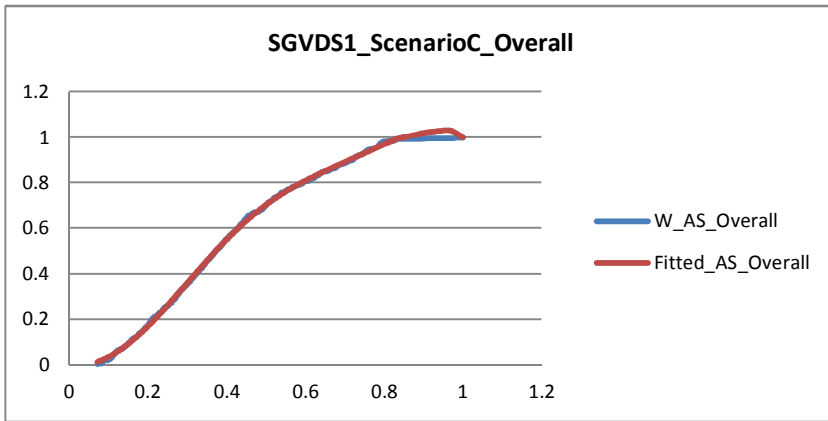
(b)



(c)

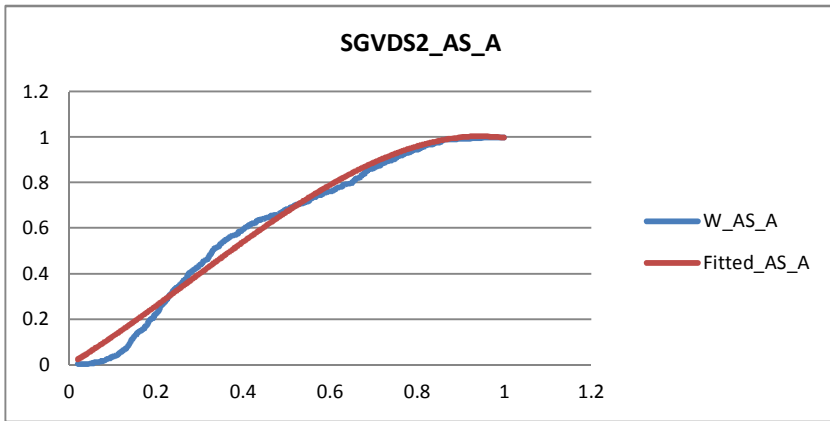


(d)

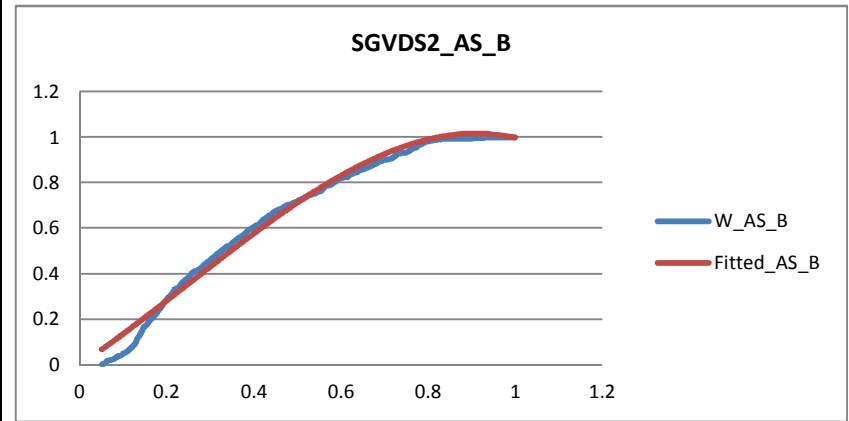


(e)

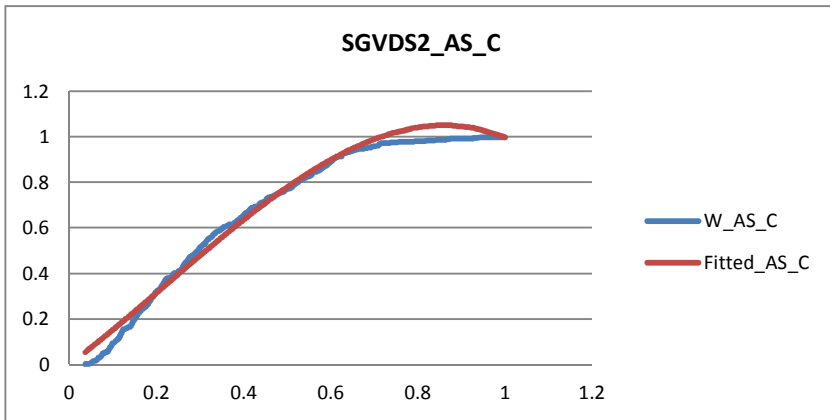
Figure 8-11: Fitted and original arrival process for SGVDS1 Scenario C (a) Muster Station A, (b) Muster Station B , (c) Muster Station C, (d) Muster Station D, (e) Overall.



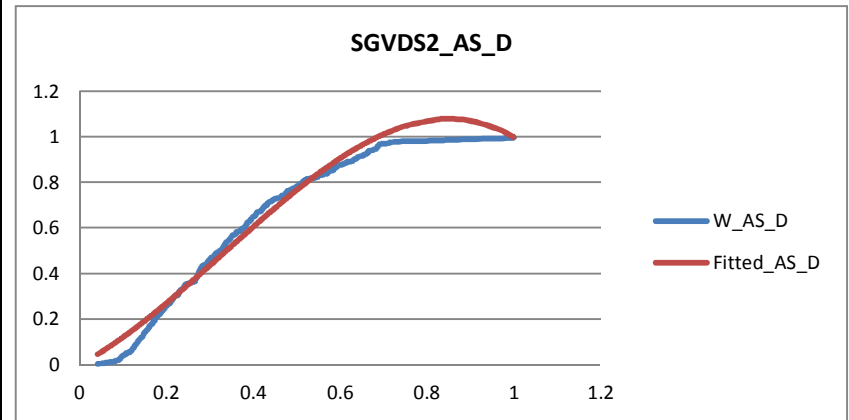
(a)



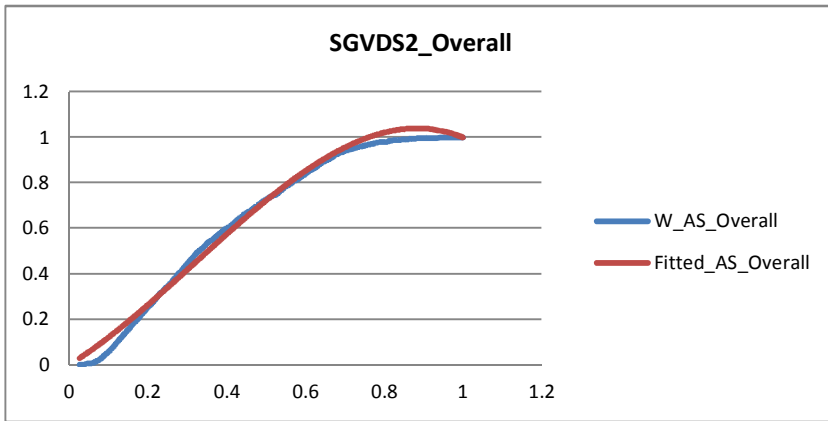
(b)



(c)



(d)



(e)

Figure 8-12: Fitted and original arrival process for SGVDS2 (a) Muster Station A, (b) Muster Station B, (c) Muster Station C, (d) Muster Station D, (e) Overall.

8.4 Simulating NHPP

Similarly to the fitting of the batches described in Chapter 7, a generation of NHPP through simulation was done using the results of the previous fitting.

Simulating NHPP is not a straightforward process. There exist a number of methods which can be grouped as follows: Inversion, rejection/acceptance and order statistics [29]. The method used here is a rejection method as developed by Kuhl and Wilson [12]. The method has been slightly adjusted as no trends or cyclic effects have been considered in this work.

Recall that the mean-value function of the NHPP over the interval $(0, S]$ is expressed as follows:

$$\mu(t) = \mu(S)R(t), \forall t \in (0, S] \quad \text{Eq. 8-1}$$

Where $R(t)$ is a non-decreasing function representing the cumulative proportion of arrivals up to time t .

A uniformly accurate approximation to the function $R(t)$ can be achieved using a polynomial of sufficiently high degree r with the special following form:

$$R(t) = \begin{cases} t/S, & r = 1 \\ \sum_{k=1}^{r-1} \beta_k (t/S)^k + \left(1 - \sum_{k=1}^{r-1} \beta_k\right) (t/S)^r, & r > 1 \end{cases} \quad \text{Eq. 8-2}$$

The estimator of the mean value function is thus,

$$\tilde{\mu}(t) = N(S)R(t, \tilde{r}, \tilde{\mathbf{B}}_{\tilde{r}}) \forall t \in (0, S] \quad \text{Eq. 8-3}$$

and the estimated rate function

$$\tilde{\lambda}(t) = \tilde{\mu}'(t) \forall t \in (0, S] \quad \text{Eq. 8-4}$$

To generate variates from an estimated NHPP, the estimates obtained in the fitting section are used.

For a rate function $\lambda(t), t \in [0, S]$, the cumulative distribution function of the next event time τ_i conditioned on the observed value of the last event time $\tau_{i-1} = t_{i-1}$ is given by:

$$F_{\tau/\tau_{i-1}}(t|t_{i-1}) \equiv Pr(\tau_i \leq t | \tau_{i-1} = t_{i-1}) \quad \text{Eq. 8-5}$$

$$F_{\tau_i|\tau_{i-1}}(t|t_{i-1}) = \begin{cases} 1 - \exp\left[-\int_{t_{i-1}}^t \lambda(z) dz\right] & \text{if } t \geq t_{i-1} \\ 0 & \text{otherwise} \end{cases} \quad \text{Eq. 8-6}$$

It amounts to solving the following equation for τ_i :

$$\int_{t_{i-1}}^t \lambda(z) dz = -\ln(1 - U_i) = \mu(\tau_i) - \mu(\tau_{i-1}) \quad \text{Eq. 8-7}$$

Where $U_i \sim \text{Uniform}(0,1)$, using the inverse method.

The expression of $\mu(t)$ is given by Eq. 8-1, and its estimator (which will be used for the generation of the NHPP) is given by Eq. 8-3 so solving equation Eq. 8-7 above leads to:

$$\tau_i = R^{-1}\left(\frac{\Delta}{N(S)} + R(\tau_{i-1})\right) \quad \text{Eq. 8-8}$$

Where $\Delta = -\ln(1 - U_i)$

As mentioned in the introduction to this section the method as proposed by Kuhl and Wilson [12] has been adapted.

It was found that dividing Δ by $N(S)$ makes the step increase very slow and a large number of data point is generated to reach the upper limit of the interval.

The method was then adapted following the inverse method detailed in [29]. The algorithm to generate a series of events on the interval $(0, S]$ is then as follows:

1.	Initialise $i \leftarrow 1, \tau_i = 0$
2.	Generate $U_i \sim \text{Uniform}(0,1)$
3.	Compute $\Delta = -\ln(1 - U_i)$
4.	$\tau_{i+1} = R^{-1}(\Delta + R(\tau_i))$
5.	If $\tau_i > S$, stop; otherwise $i \leftarrow i + 1$
6.	Go to step 2

Figure 8-13: Generation of NHPP Algorithm

The critical part of the algorithm is the inversion of the function $R(t)$ as this might not exist or be very complicated to compute.

To illustrate the algorithm above (Figure 8-13), a simple expression of the function $R(t)$ was used. The real data set SGVDS1 was chosen as its fitting produced a first degree polynomial function. The function $R(t)$ is then expressed as $R(t) = \beta t, t \in [0, S]$.

As described in section 8.3 above, the fitting of SGVDS1 produced the following results:

SGVDS1					
Muster Station	A	B	C	D	Overall
Beta	2.37	3.29	2.62	2.92	2.63

Using the values for β shown in the table above, for each muster station 10 sets of arrival times following a NHPP were generated and compared to the original and fitted data.

The first observation was that even if Δ was not divided by $N(S)$, as explained above, the incremental step was still small and a large number of data points were generated. Table 8-7 below summarises the number of events generated for each of the muster station above. For comparison, the number of events in the original data set is also given per muster station.

	MS A	MS B	MS C	MS D	Overall
Min	1349	1830	1376	1180	1444
Max	1424	1966	1502	1273	1671
Average	1380	1917.4	1456	1233.6	1547.5
Original	68	104	57	117	225

Table 8-7: number of events for the generated NHPP for SGVDS1.

As it can be seen the number of generated points is considerably bigger than the original dataset. For muster station C for example the number of generated points is 25 times the original number.

Looking at a plot of the generated data, compared to the original data and the fitted data, also show quite a difference in the curves as can be seen in Figure 8-14 below for muster station A. Arrivals have been scaled.

Similar results are observed for the other muster stations (results not shown here).



Figure 8-14: Generated NHPP curves (scaled)

If the generated events were to be combined with the batch arrivals, then the number of passengers on-board would be much bigger than the actual ship capacity.

In this case, the generation of the batches and the arrivals processes cannot be completely independent.

A possible explanation for the large number of arrivals might be that the rate function of the NHPP has jumps (there is a non-negative probability that no events will happen for a certain period of time). This is not something that is handled by the algorithm presented above. It is outside the scope of this work to look at rate functions with jumps.

It might also be possible that the steps at which the rate function increases during the generation process of the NHPP need adjustments.

Finally, another possible explanation would be that the parameters or indeed the fitted model, used to generate were not appropriate in the first place.

8.5 Concluding Remarks

This chapter showed the application of the fitting method presented in Chapter 5 as well as a generation of the NHPP based on the results of the fitting.

The Method by Kuhl et al [12] gave good results when the simulated data was fitted with fitted and original curves in most cases indistinguishable when plotted. The fitting also produced high degree polynomial rate functions. The fitting method showed a great sensitivity to the input data used. The degree of polynomial rate function was lowered in some cases when a different set of data (different run) was used as input.

The fitting of the real dataset also showed good agreement with the original data but with much lower degree of the polynomial rate function. The associated simulation data produced also high degree polynomial for the rate function for SGVDS1. SGVDS2 results were more consistent with the original data.

The generation of the NHPP proved to be more challenging than anticipated and was not a straight forward procedure.

The major concern with the inversion method to generate the NHPP was the inversion of the polynomial function. This was only demonstrated for the SGVDS1 dataset.

The generation of the NHPP highlighted a number of issues to be addressed:

- Possible jumps in the rate function
- Validity of the fitted model and its parameters
- Steps to increase the rate function in the algorithm for generating the NHPP
- Linking the batches and the arrivals for a complete model.

No other methods for generating the NHPP were investigated during the course of this work and no attempts have been made either to look at possible modifications of Kuhl's method (different ways to estimate the β coefficients or the polynomial rate function) as this was outside the scope of the research.

In conclusion, further analysis and attention is needed before the method could be used with confidence.

9 CONCLUSIONS AND FUTURE WORK

9.1 General Remarks

This Chapter will close the thesis by summarising the findings of this research and by discussing future work options.

9.2 Summary of the research

The aim of this research was to derive a parametric model to be used as a fast assessment of the evacuation time during emergency situations but with its applicability not limited to those situations.

To the best knowledge of the author no such parametric model has been proposed before.

The movement of people in particular on-board a vessel is a very complex problem to model and no simple method could capture all the different aspects of this problem.

Methods to simulate such phenomenon have been developed. Some simple, for example queuing systems, arrival processes and other more sophisticated such as agent-based simulation programs (microscopic, macroscopic and mesoscopic models).

The work undertaken during this research focused on investigating the possibility to derive a parametric model that could be simple enough to produce fast estimates of evacuation times but also capture the different elements of the evacuation process to satisfactory accuracy

At the beginning of the research, different parametric models were investigated. The nature of the problem led the author to investigate arrival processes, which were a good candidate for the underlying model explaining the evacuation of passengers. A close analysis of the data showed that a Non-Homogeneous Poisson Process was needed (NHPP) to model the problem at hand. In addition, arrivals at the muster stations were happening in groups, where the size of the group varies from 1 to a certain number N . Therefore, the whole evacuation could be modelled by a batch NHPP. The batch arrivals and the NHPP are independent of each other so they were modelled and studied separately.

Once the underlying model was identified, the fitting process could be done. Here again a number of methods were looked at and those (for batch fitting and NHPP) that were deemed to be the most appropriate were used for the fitting of the data.

The data used in this research came from a number of simulations (8 000 individual runs) performed with the Evacuation simulation software Evi [20] as well as from the validation dataset produced by the EU-funded project SAFEGUARD [23] and its associated Evi simulation runs (about 200 runs).

The work was split between the fitting of the batch sizes of the arrivals and the NHPP. The batch sizes were fitted using a Geometric distribution. A complete analysis of the data was performed.

For the NHPP a method developed by Kuhl et al [12] was used for the fitting of the data and a complete analysis also performed.

Using the fitted models, new data was generated and analysed. The results were compared to the original data for both the batch sizes and the NHPP.

9.3 Conclusions

The analysis of the simulated data which was the first step in this study allowed looking at the impact some parameters had on the arrival process.

When batch sizes were analysed, it was found that the Day cases showed more randomness in the results than the Night cases. In addition, larger batch sizes and fewer arrivals were observed for the Day case, while the opposite (smaller batch sizes and more frequent arrivals) was true for the Night cases.

For the day cases, the reaction time, when random, produced slightly higher number of arrivals (smaller batch sizes) regardless of passenger loads or speed. This was expected as passengers starting at different times will tend to arrive at different times hence more arrivals.

For the night cases, no clear impact of the reaction time or speed could be seen as results in all cases were quite similar.

The second set analysed was the data obtained from drills on-board a large RO-PAX ferry and a cruise ship as part of the SAFEGUARD project. The data corresponding to the actual drills on-board both vessels (SGVDS1 for the ferry and SGVDS2 for the cruise ship) were analysed and compared to their corresponding simulations obtained using Evi.

As only one dataset per ship was available for the trial data, no statistical analysis could be done. Only number of arrivals and batch sizes were derived for each dataset.

The corresponding simulations were also analysed and it was found that the simulations produced smaller batch size and more frequent arrivals than what was found in the real data.

The second stage of the study was to fit a model to the available data. The fitting of the batch sizes and the NHPP was done separately as previously explained.

It was found that the fitting of the batch sizes with a Geometric distribution produced very good results.

The fitting of the arrivals using a Non Homogeneous Poisson Process (NHPP) was also a good choice. The Method used for the fitting using a variance stabilising transformation and a polynomial rate function of a specific form produced very good results. When visually inspected, the curves obtained for the NHPP fitted model and the ones corresponding to the original data could not be distinguished.

It is worth noting that the fitting produced high degree polynomial rate functions and that the method showed a great sensitivity to the input data used. The degree of polynomial rate function was lowered in some cases when a different set of data (different run) was used as input.

The fitting of the real dataset also showed good agreement with the original data but with much lower degree of the polynomial rate function. The associated simulation data produced also high degree polynomial for the rate function for SGVDS1. For SGVDS2 results were more consistent with the original data.

The final stage was to generate new data using the fitted models obtained in the previous stage. The inverse method was used for both the batch sizes and the arrival process.

For the batch sizes, it was found that the generated data overestimated the original data in most cases for all the datasets considered in the analysis.

This could probably be explained by the fact that the Geometric distribution is a discrete distribution which is simulated using a continuous variable.

In addition, it was found that the fitted model derived from simulations produced less errors (smaller overestimation) when compared to its original data than what the fitted model derived from the real data produced when compared to its original data. This could be due to the lack of statistical significance of the real data (only one dataset per ship).

Regarding the NHPP generation, this proved to be more challenging and was not a straight forward process.

In most cases, the degree of the polynomial function was very high. Only the data corresponding to SGDVS1 was used to demonstrate the generation process as the inversion of the polynomial function was a major issue (either the inversion was not possible or would involve complex computation).

The model generated a large number of arrivals. There is a need for a deeper analysis of the fitted model in order to generate meaningful results.

9.4 Future work

The complex interactions between agents and their environment might not be accurately and totally captured by a simplified model. A deeper investigation of the arrivals at the muster stations would be needed before such a model could be used with confidence in an emergency situation.

The variability in the degree of the polynomial intensity function of the NHPP makes it computationally hard or sometimes not even possible to simulate data from the fitted model. More analysis is needed to understand the variability and to investigate the possibility to cap the degree of the polynomial function to a value that can be handled easily when generating data.

The possibility of having/allowing jumps in the rate function is another aspect of the NHPP that would benefit from a deeper analysis.

Investigating the best option for steps increase in the algorithm for generating the NHPP is another issue to consider.

The validity of the fitted model and its parameters could also represent an interesting research subject.

Data quality, error propagation and uncertainty analysis would be another investigation possibility.

Once the above are well understood, linking the batches and the arrivals process would need to be studied to produce a complete model.

From a more general perspective, other aspects such as the impact of different ship geometries would be an interesting point to investigate. In this research, as described in Chapter 6, simulated data was produced using a Ro-Pax model and real and simulated data from a Ferry and a Cruise ship. The scenarios producing the different data being different for the three geometries it was not possible to study the impact of the geometry on the model.

The impact of external factors such as crew actions, fire and flooding for example has not been considered in this research. This could constitute another avenue for research.

REFERENCES

1. Italian Ministry Of Infrastructures and Transports. Marine Casualties Investigation Body “Costa Concordia Marine Casualty on January 13, 2012. Report on the Safety technical investigation”. May 2013.
2. IMO, ‘Revised Guidelines On Evacuation Analysis for New and Existing Passenger Ships’. 06 June 2016. *IMO MSC/Circ 1533*.
3. <https://www.dnvgl.com/services/aeneas-the-standard-in-passenger-evacuation-analysis-48508> (last accessed: September 2016).
4. <http://www.principia.fr/expertise-fields-software-products-odigo-144.html> (last accessed: September 2016).
5. <http://fseg.gre.ac.uk/exodus/> (last accessed: September 2016)
6. <http://www.traffgo-ht.com/en/pedestrians/products/pedgo/index.html> (last accessed: September 2016)
7. L.M. Leemis. “Nonparametric Estimation Of The Cumulative Intensity Function For A Nonhomogeneous Poisson Process”.1991. *Management Science* 37:886-900.
8. A. M., Law, and W. D., Kelton, 2000. “Simulation modeling and analysis”. TheMcGraw-Hill Companies Inc.
9. W.A. Massey, G.A. Parker and W. Whitt. “Estimating the parameters of a nonhomogeneous Poisson process with linear rate”. *Telecommunication Systems* 5. 361-388. 1996.
10. E. P. C, Kao, S, Chang. “Modeling time-dependent arrivals to service systems: a case in using a piecewise-polynomial rate function in a NHPP”. 1988. *Management Science* 34. 1367-1379.
11. C. J. MacLean. “Estimation and Testing of an exponential polynomial rate function with the nonstationary Poisson process”. *Biometrika* 61. P.81. 1974.
12. M.E. Kuhl, J.R. Wilson .“Modeling and simulating Poisson processes having trends or nontrigonometric cyclic effects”.. *European Journal of Operational Research* 133. 566-582. 2001.
13. M.E. Kuhl, S.G. Sumant, J.R. Wilson. “An automated multiresolution procedure for modelling complex arrival processes”. *INFORMS Journal on Computing* 18 (1); 3-18. 2006.
14. M.E. Kuhl, S.C. Deo, J.R. Wilson. “Smooth flexible models for nonhomogenous Poisson processes using one or more process realizations”. *Proceedings of the 2008 Winter Simulation Conference*. S.J. Mason, R.R. Hill, L. Mönch, O. Rose, T. Jefferson, J.W. Fowler eds.

15. S. Harrod and W.D. Kelton. "Numerical Methods for Realizing Nonstationary Poisson Processes with Piecewise-Constant Instantaneous –Rate Functions". SIMULATION, Vol. 82, Issue 3. 147-157. 2006.
16. I. Gerhardt and B.L. Nelson. "Transforming renewal processes for simulation of nonstationary arrival processes." 2009. INFORMS Journal on Computing 21.4: 630-640.
17. L. Devroye. "Non- Uniform Random Variate Generation". 1986. Springer-Verlag, New York.
18. A. Pennycott, Y.Hifi. "Evacuability of a flooded passenger ship". 4th international Maritime Conference On Design for Safety. Italy. October 2010.
19. National Institute of Standards and technology (NIST) U.S Department of Commerce. Fire Dynamics Simulator. <https://www.nist.gov/services-resources/software/fds-and-smokeview>.
20. D., Vassalos, et al. "A mesoscopic model for passenger evacuation in a virtual ship-sea environment and performance-based evaluation." (2002): 369-391.
21. M, Ledvij. "Curve fitting made easy." Industrial Physicist 9.2 (2003): 24-27.
22. L, Wasserman. "All of statistics: a concise course in statistical inference". Springer Science & Business Media, 2013.
23. <http://www.safeguardproject.info/>
24. Galea, E.R., Deere, S., Brown, R.,Filippidis, L., "Two Evacuation Model Validation Data-sets for Large Passenger Ships", Submitted to SNAME (The Society of Naval Architects and Marine Engineers)Journal of Ship Research, Sept 2012.
25. Brown, R., Galea, E.R., Deere, S.J., Filippidis, L., "Passenger Response Time Data-sets for Large Passenger Ferries and Cruise Ships Derived from Sea Trials", Transactions of the Royal Institution of Naval Architects, International Journal of Maritime Engineering, Vol 155, Part A1, pp 33-48, 2013.
26. Deere, S.J., Galea, E.R., Filippidis, L., Brown, R., "Data Collection Methodologies Used in the Safeguard Project to Collect Human Factors Data", RINA SAFEGUARD Passenger Evacuation Seminar 30 November 2012, ISBN No: 978-1-909024-08-3.
27. Validation Data Set Manual - SGVDS1
28. Validation Data Set Manual – SGVDS2
29. R.,Pasupathy."Generating homogeneous Poisson processes." Wiley Encyclopedia of Operations Research and Management Science (2011).
30. <https://www.r-project.org/>

Appendix I - Summary values for the parameter of the geometric distribution, the event counts and the Max batch size.

Day random

% population	Average	Max Event count	Min Event count	Max Batch max size	Min Batch max size
10	0.6892	240	209	6	3
20	0.5835	305	292	8	4
30	0.5164	380	355	10	5
40	0.4754	446	414	13	6
50	0.4501	505	467	14	7
60	0.4356	558	523	15	7
70	0.4302	612	575	15	8
80	0.4293	697	628	17	9
90	0.4195	722	667	17	9
100	0.4172	767	722	18	11

Table I-1: Average value of the geometric parameter and min and max values of the event count and max batch size for the Day Random case.

Fixed Reaction

% population	Average	Max Event count	Min Even count	Max Batch max size	Min Batch max size
10	0.6853	181	164	6	3
20	0.6270	252	226	7	4
30	0.5837	314	288	9	4
40	0.5648	373	347	11	6
50	0.5428	425	395	12	5
60	0.5312	491	454	13	6
70	0.5235	550	510	16	6
80	0.5158	622	568	15	7
90	0.5148	682	621	14	7
100	0.5029	741	670	16	8

Table I-2: Average value of the geometric parameter and min and max values of the event count and max batch size for the Day Fixed Reaction case.

Fixed speed

% population	Average p	Max Event count	Min Even count	Max Batch max size	Min Batch max size
10	0.6890	234	212	6	3
20	0.5620	310	287	8	4
30	0.4800	377	334	10	5
40	0.4367	423	390	10	6
50	0.4153	485	444	12	7
60	0.4079	525	492	13	7
70	0.3976	592	544	17	9
80	0.4010	643	589	16	10
90	0.4017	717	646	18	10
100	0.4042	761	681	19	11

Table I-3: Average value of the geometric parameter and min and max values of the event count and max batch size for the Day Fixed Speed case.

Fixed Speed +Reaction

% population	Average p	Max Event count	Min Even count	Max Batch max size	Min Batch max size
10	0.7016	183	170	8	3
20	0.6025	242	229	8	4
30	0.5519	309	277	10	5
40	0.5277	372	331	10	5
50	0.5189	434	391	12	5
60	0.5090	469	446	12	6
70	0.5011	543	494	13	7
80	0.4965	605	538	14	7
90	0.4909	653	586	13	7
100	0.4929	705	649	15	8

Table I-4: Average value of the geometric parameter and min and max values of the event count and max batch size for the Day Fixed Speed and Reaction case.

Night random

% population	Average p	Max Event count	Min Event count	Max Batch max size	Min Batch max size
10	0.73919432	250	225	5	3
20	0.66716013	352	326	6	4
30	0.58608196	437	408	7	4
40	0.54694141	531	486	8	4
50	0.53048239	626	579	9	4
60	0.52198629	715	668	8	5
70	0.5081201	797	758	7	5
80	0.50918357	919	863	8	5
90	0.4889121	978	936	8	5
100	0.49289353	1265	1040	8	5

Table I-5: Average value of the geometric parameter and min and max values of the event count and max batch size for the Night Random case.

Night Fixed Reaction

% population	Average p	Max Event count	Min Even count	Max Batch max size	Min Batch max size
10	0.68953811	234	210	5	3
20	0.63492089	346	316	7	4
30	0.56766895	425	393	9	4
40	0.53233007	528	476	7	5
50	0.52516106	612	578	8	5
60	0.51749219	720	671	9	5
70	0.50336522	819	755	8	5
80	0.50772751	916	858	8	5
90	0.49050876	996	934	8	5
100	0.48686815	1086	1028	8	5

Table I-6: Average value of the geometric parameter and min and max values of the event count and max batch size for the Night Fixed Reaction case.

Night Fixed speed

% population	Average p	Max Event count	Min Even count	Max Batch max size	Min Batch max size
10	0.70845508	239	217	6	3
20	0.59332418	331	298	6	4
30	0.54042385	416	380	8	4
40	0.50471289	511	457	7	4
50	0.48362013	596	532	9	5
60	0.44926466	669	611	8	5
70	0.45490624	759	701	8	5
80	0.45914066	865	794	8	5
90	0.44226266	957	870	7	5
100	0.44789838	1050	964	8	5

Table I-7: Average value of the geometric parameter and min and max values of the event count and max batch size for the Night Fixed Speed case.

Fixed Speed +Reaction

% population	Average p	Max Event count	Min Even count	Max Batch max size	Min Batch max size
10	0.65411526	225	200	6	3
20	0.60298628	326	296	7	4
30	0.54124411	425	371	7	4
40	0.49959857	496	448	7	5
50	0.4960195	595	546	7	5
60	0.48249117	708	639	8	5
70	0.46731539	764	715	8	5
80	0.47033884	867	800	7	5
90	0.45186815	962	886	8	5
100	0.45043066	1046	963	8	5

Table I-8: Average value of the geometric parameter and min and max values of the event count and max batch size for the Night Fixed Speed and Reaction case.

Appendix II - Results of batch simulations for a hundred and a thousand runs: Percentage changes for Max batch size statistics.

Day Random

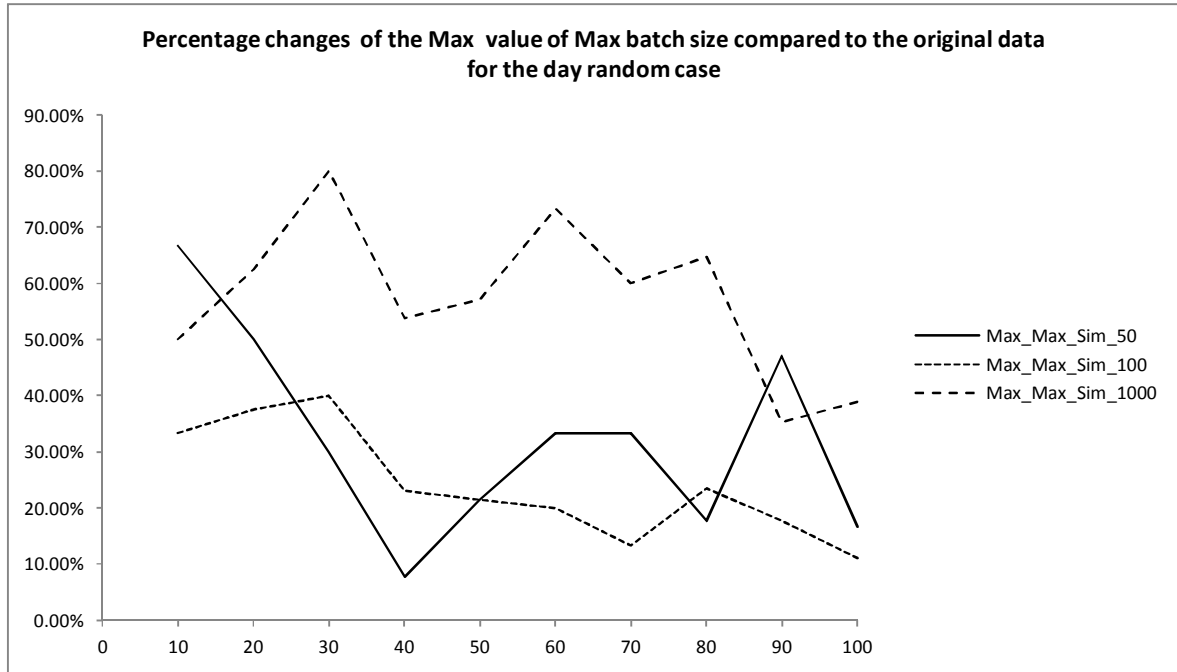


Figure II-1: Percentage change in Max value of max batch size when compared to original data. Day Random Case

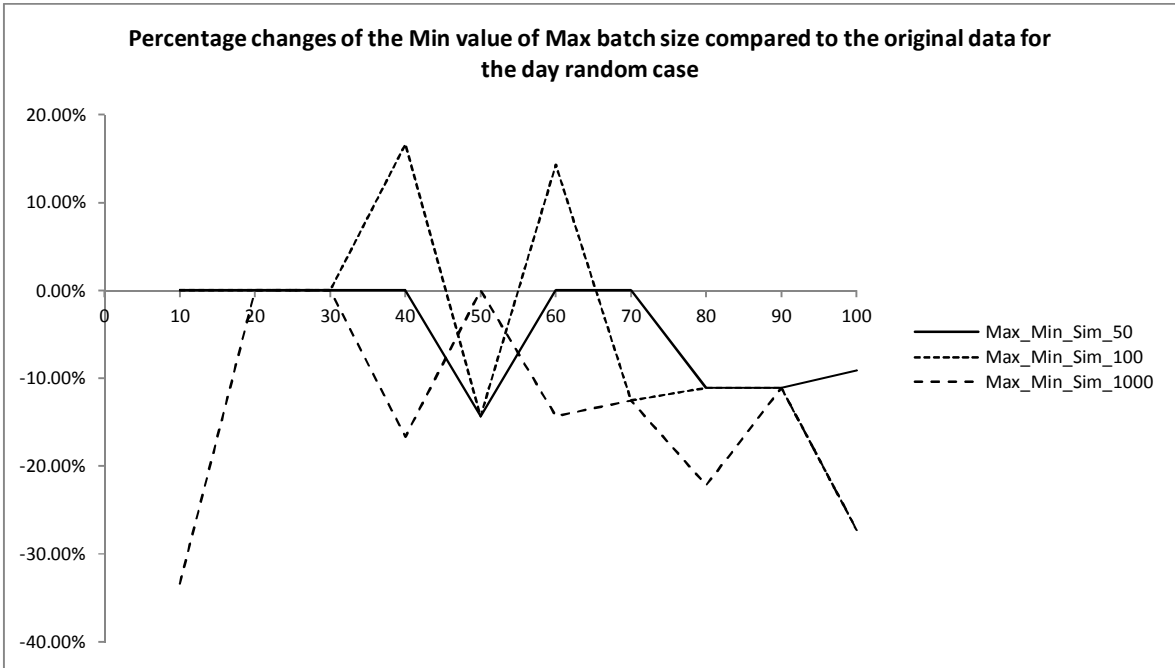


Figure II-2: Percentage change in Min value of max batch size when compared to original data. Day Random Case

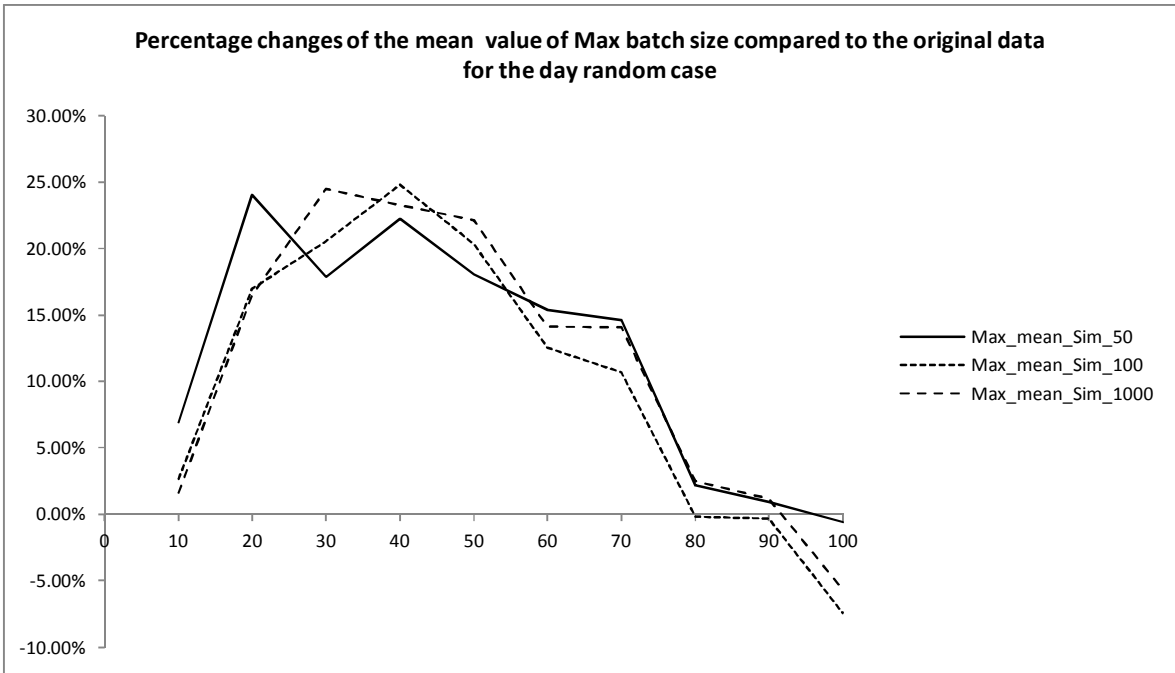


Figure II-3: Percentage change in average value of max batch size when compared to original data. Day Random Case

Day Fixed Reaction

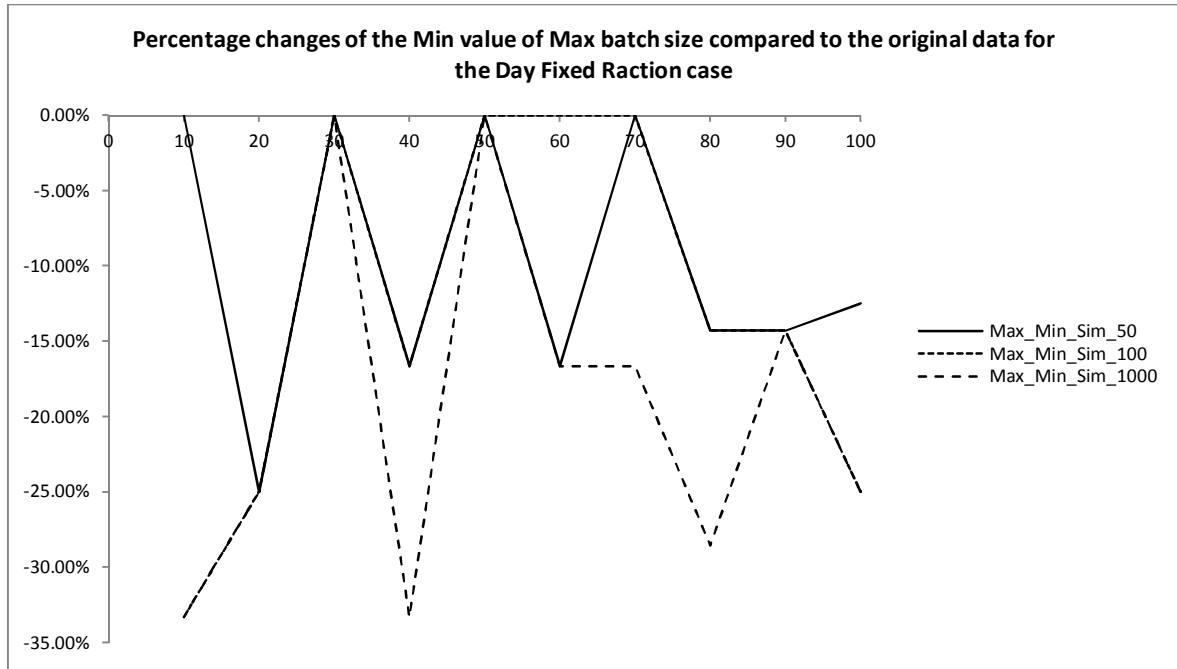


Figure II-4: Percentage change in Min value of max batch size when compared to original data. Day Fixed Reaction Case

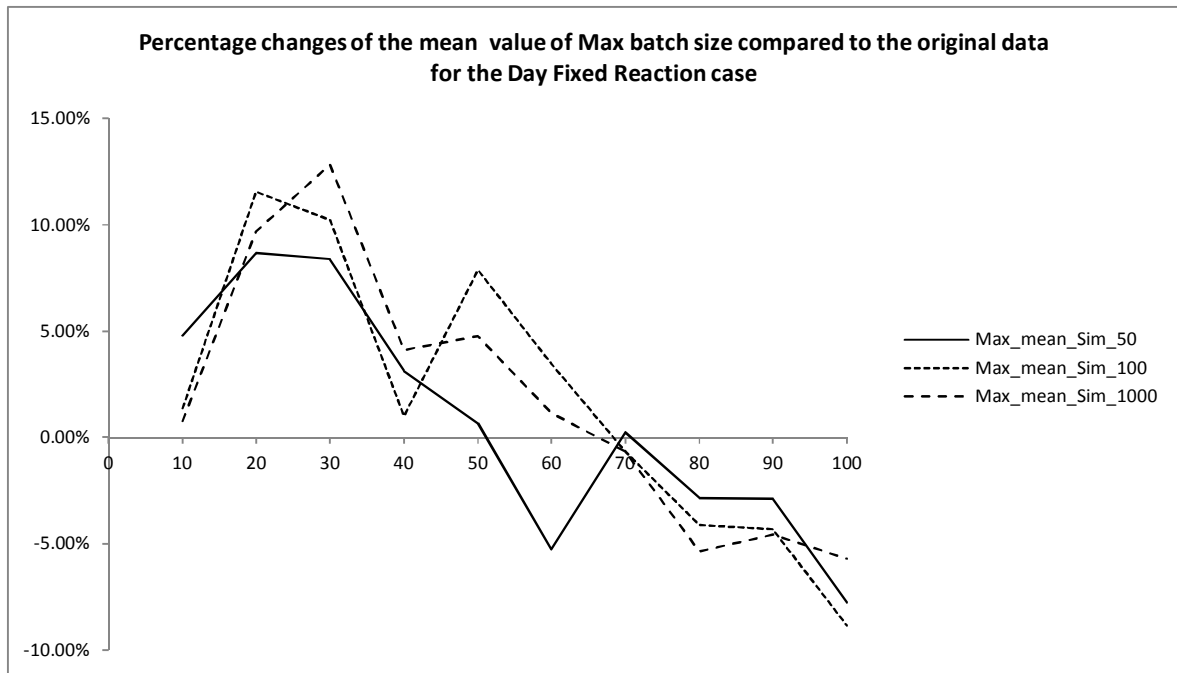


Figure II-5: Percentage change in Average value of max batch size when compared to original data. Day Fixed Reaction Case

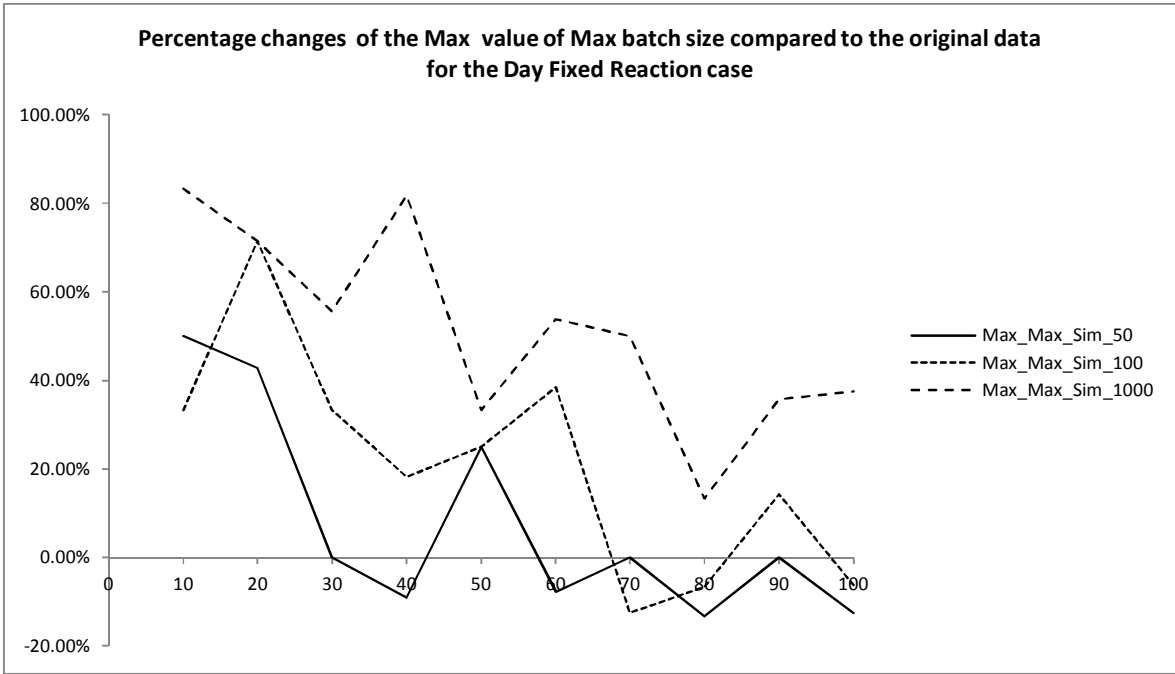


Figure II-6: Percentage change in Max value of max batch size when compared to original data. Day Fixed Reaction Case

Day Fixed Speed

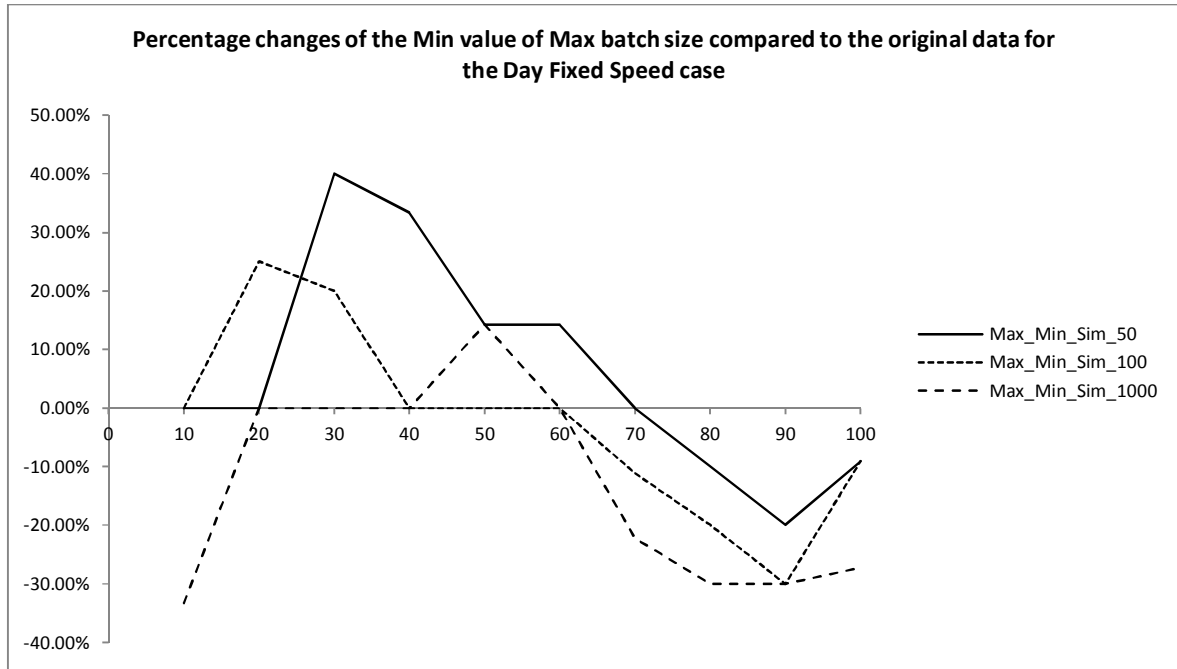


Figure II-7: Percentage change in Min value of max batch size when compared to original data. Day Fixed Speed Case

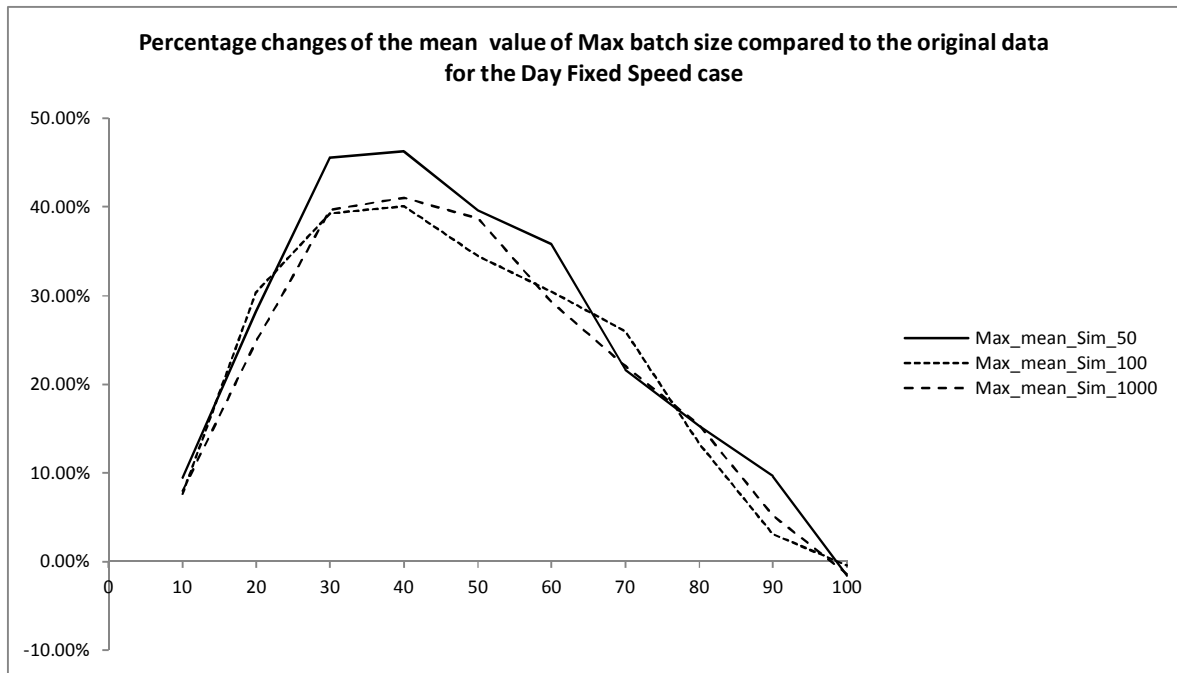


Figure II-8: Percentage change in Average value of max batch size when compared to original data. Day Fixed Speed Case

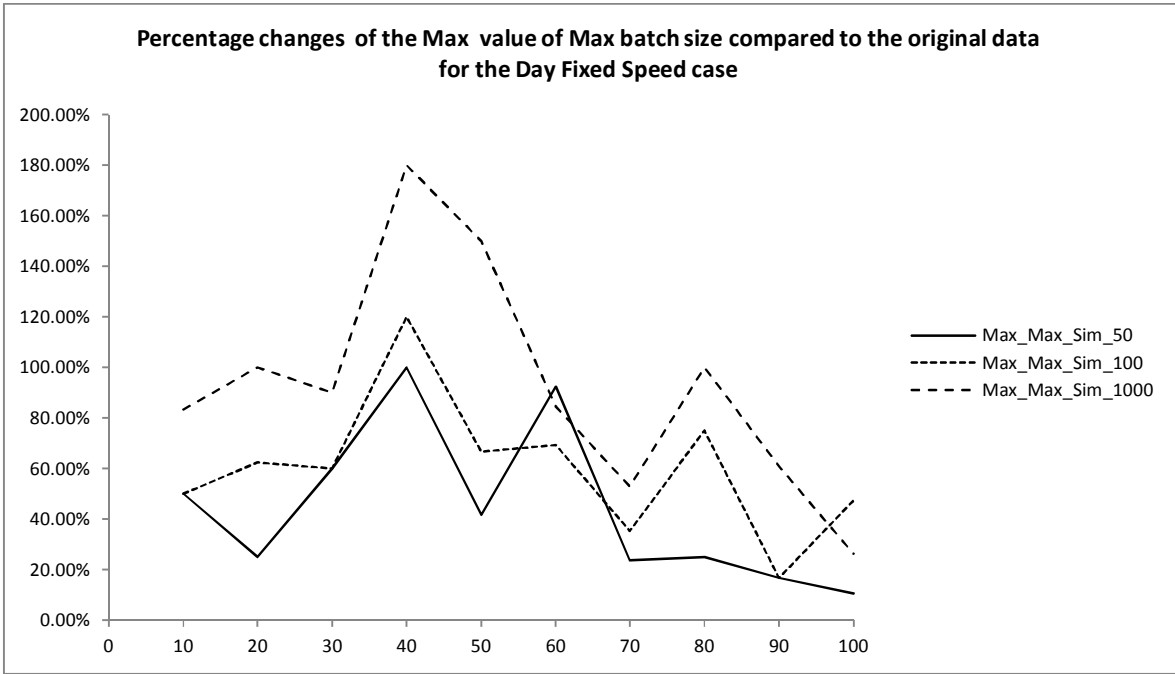


Figure II-9: Percentage change in Max value of max batch size when compared to original data. Day Fixed Speed Case

Day Fixed Speed and Reaction

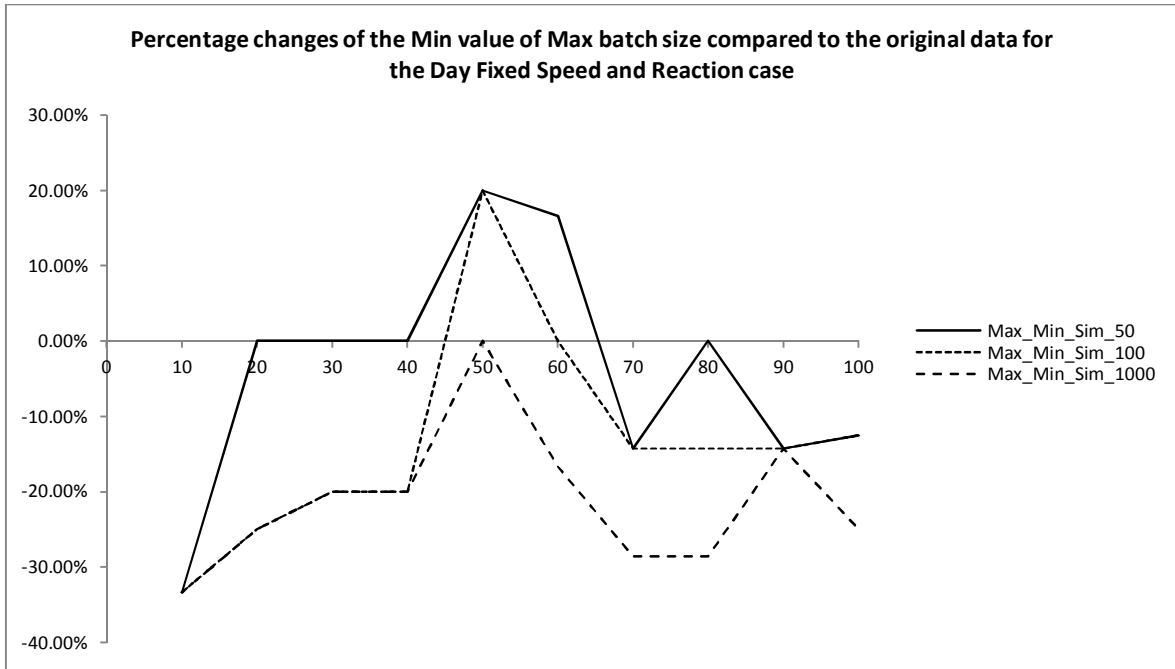


Figure II-10: Percentage change in Min value of max batch size when compared to original data. Day Fixed Speed and Reaction Case

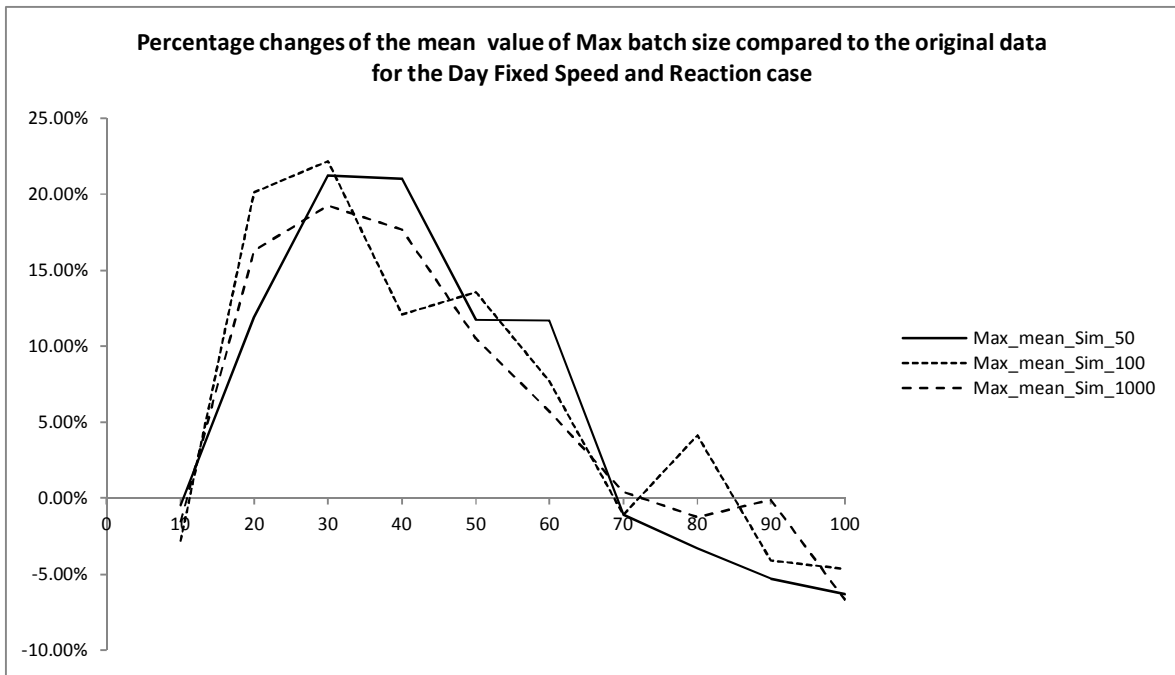


Figure II-11: Percentage change in Average value of max batch size when compared to original data. Day Fixed Speed and Reaction Case

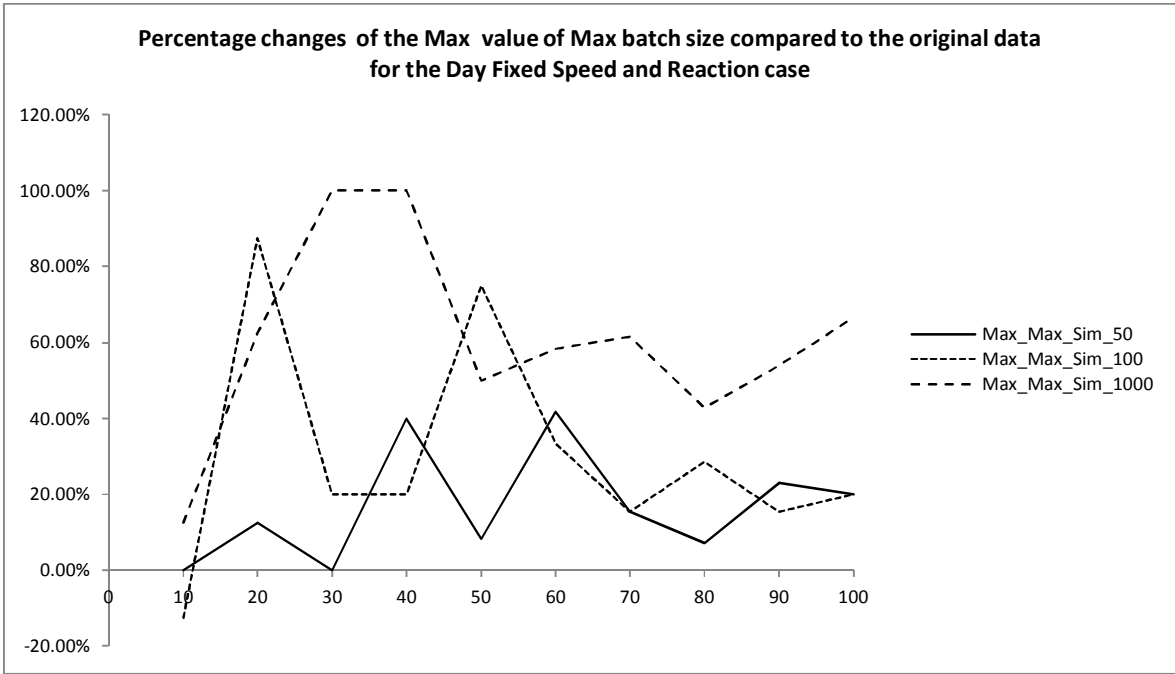


Figure II-12: Percentage change in Max value of max batch size when compared to original data. Day Fixed Speed and Reaction Case

Night Random

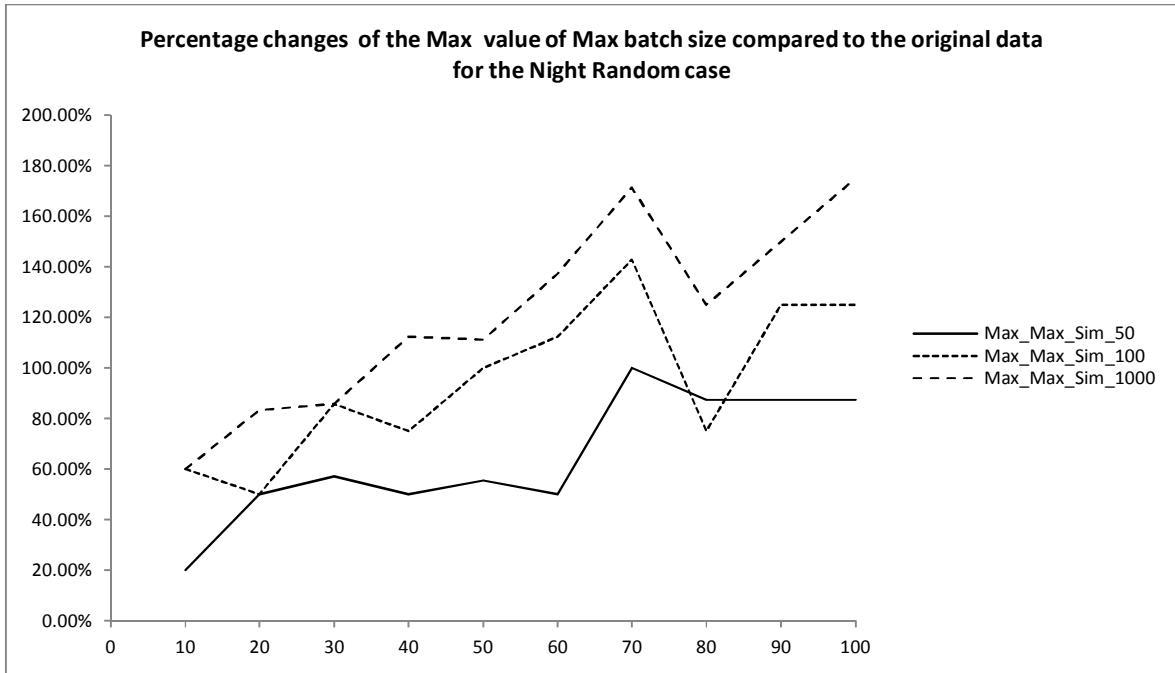


Figure II-13: Percentage change in Max value of max batch size when compared to original data. Night Random Case

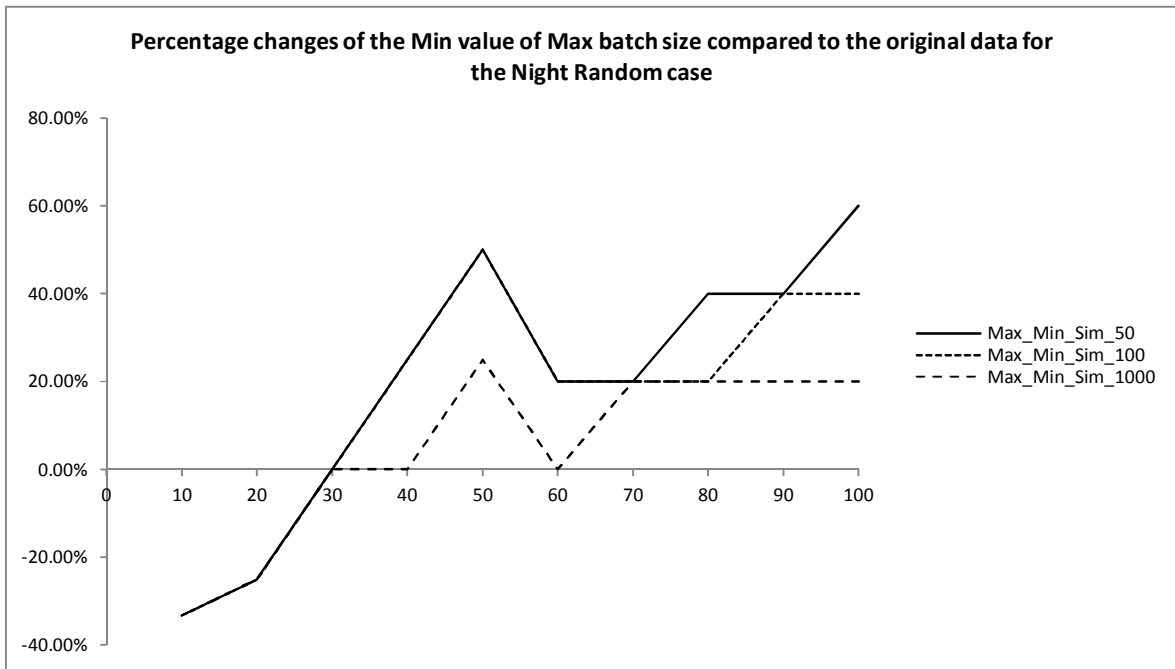


Figure II-14: Percentage change in Min value of max batch size when compared to original data. Night Random Case

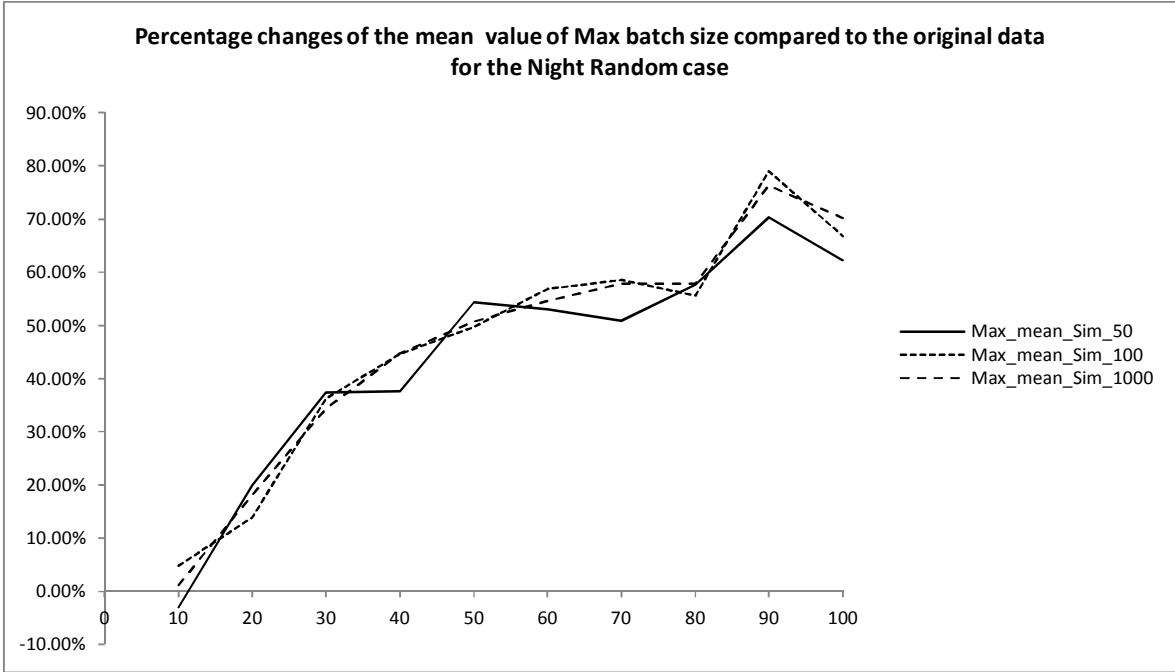


Figure II-15: Percentage change in Average value of max batch size when compared to original data. Night Random Case

Night Fixed Reaction

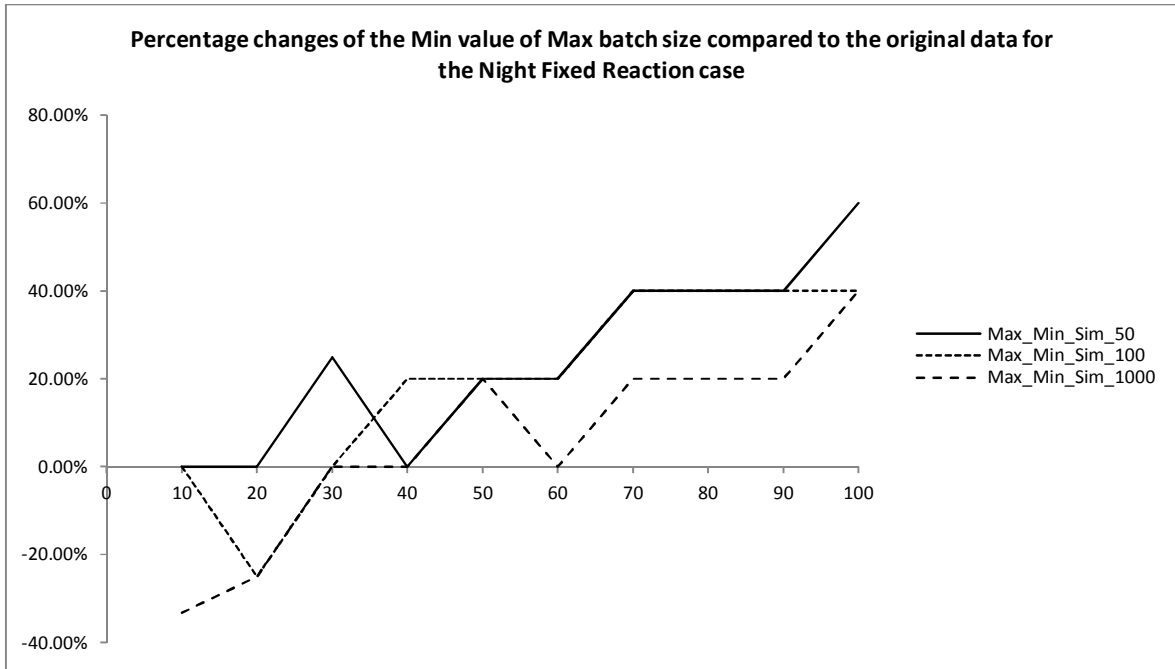


Figure II-16: Percentage change in Min value of max batch size when compared to original data. Night Fixed Reaction Case

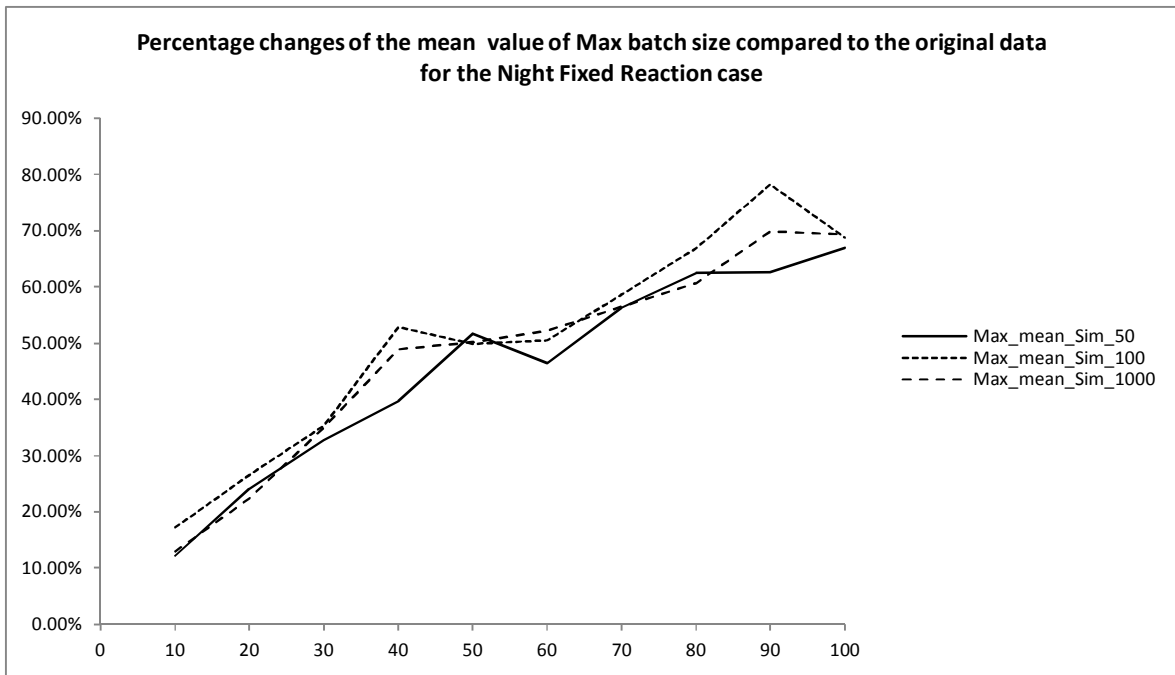


Figure II-17: Percentage change in Average value of max batch size when compared to original data. Night Fixed Reaction Case

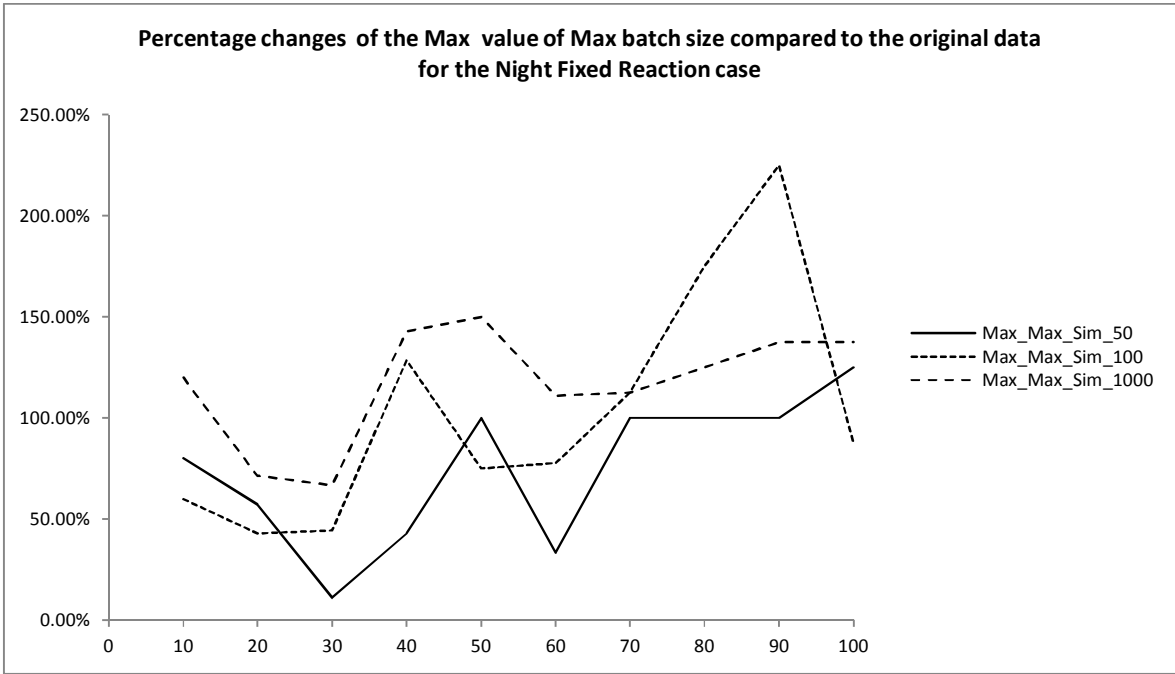


Figure II-18: Percentage change in Max value of max batch size when compared to original data. Night Fixed Reaction Case

Night Fixed Speed

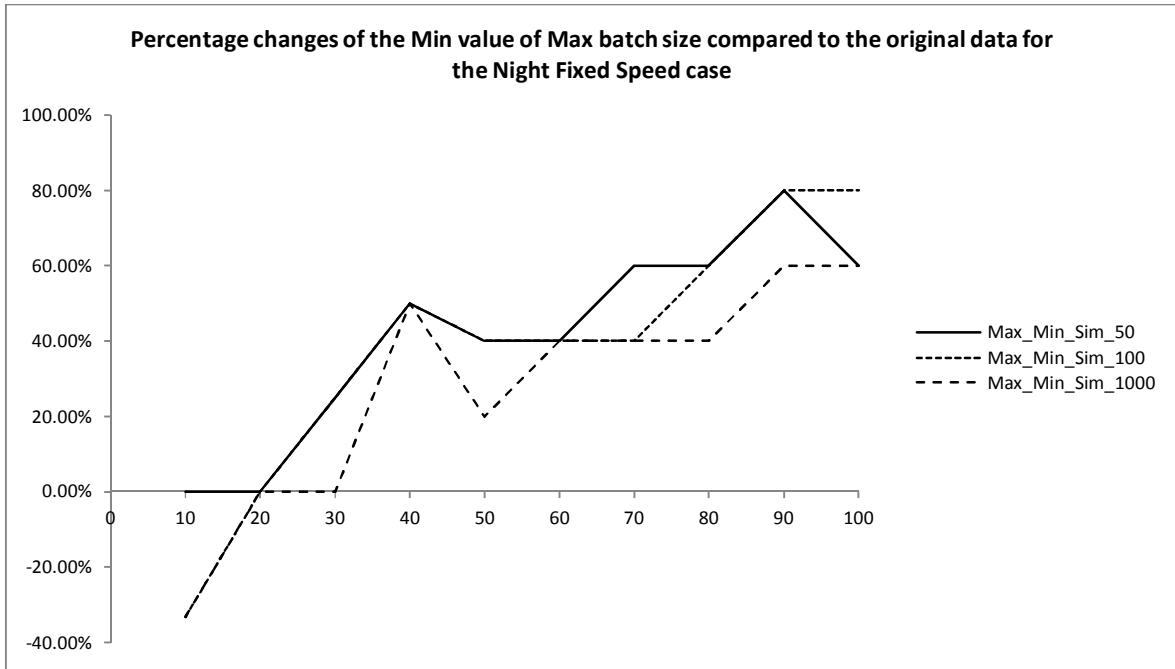


Figure II-19: Percentage change in Min value of max batch size when compared to original data. Night Fixed Speed Case

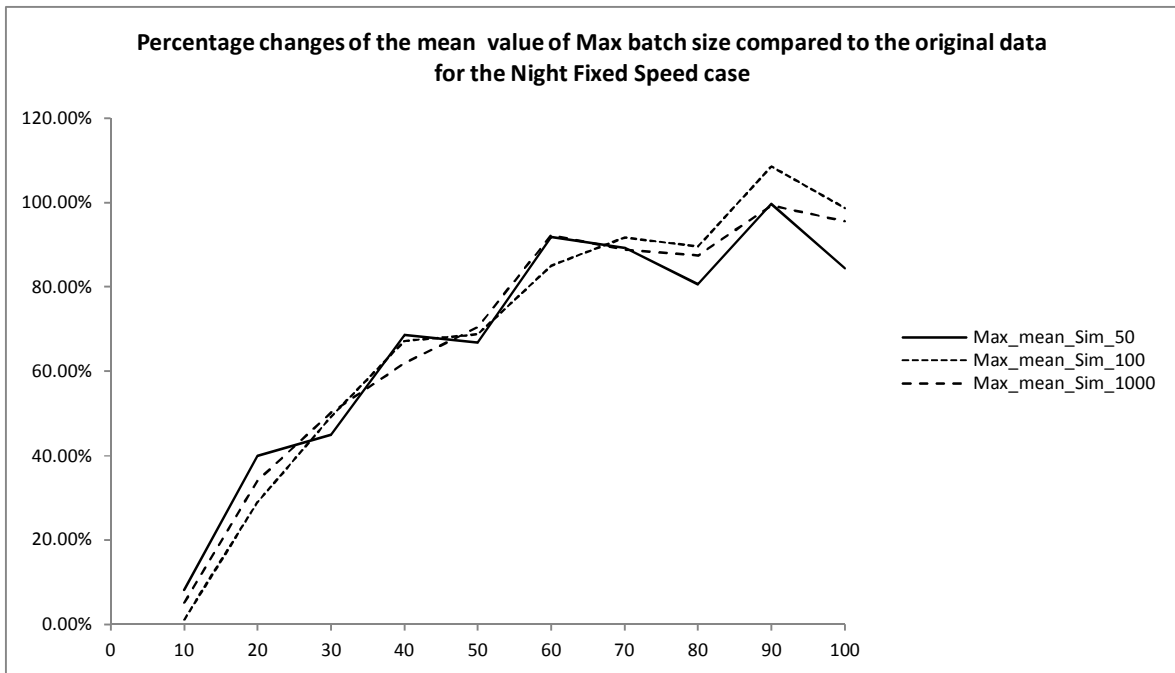


Figure II-20: Percentage change in Average value of max batch size when compared to original data. Night Fixed Speed Case

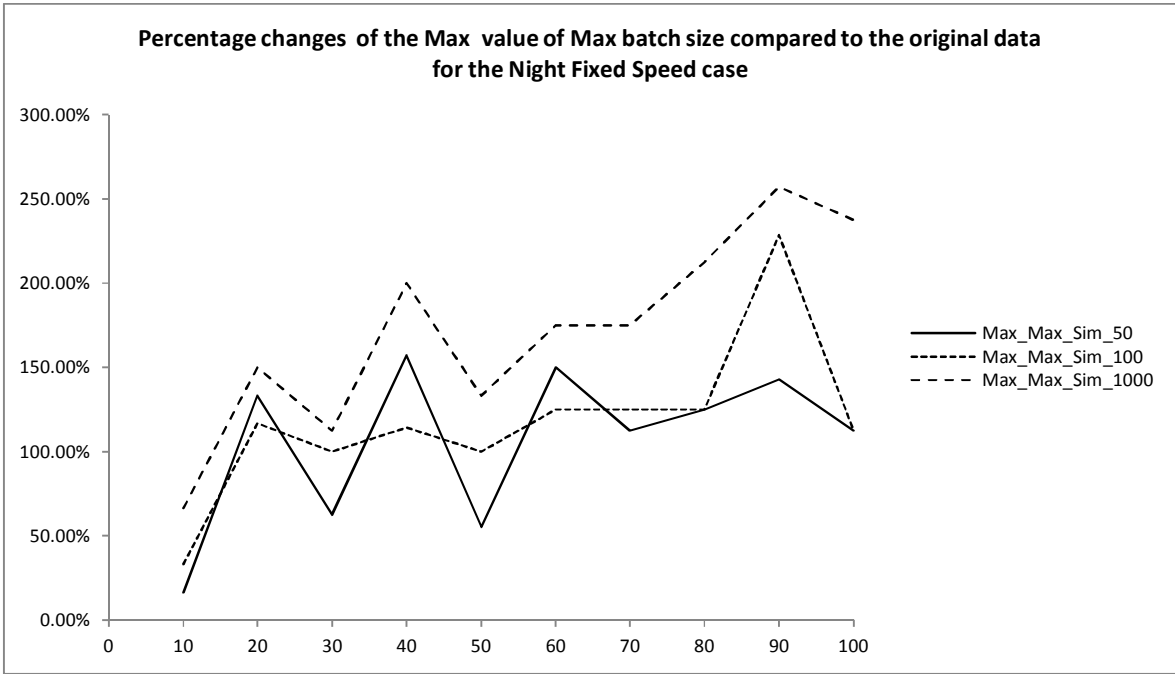


Figure II-21: Percentage change in Max value of max batch size when compared to original data. Night Fixed Speed Case

Night Fixed Speed and Reaction

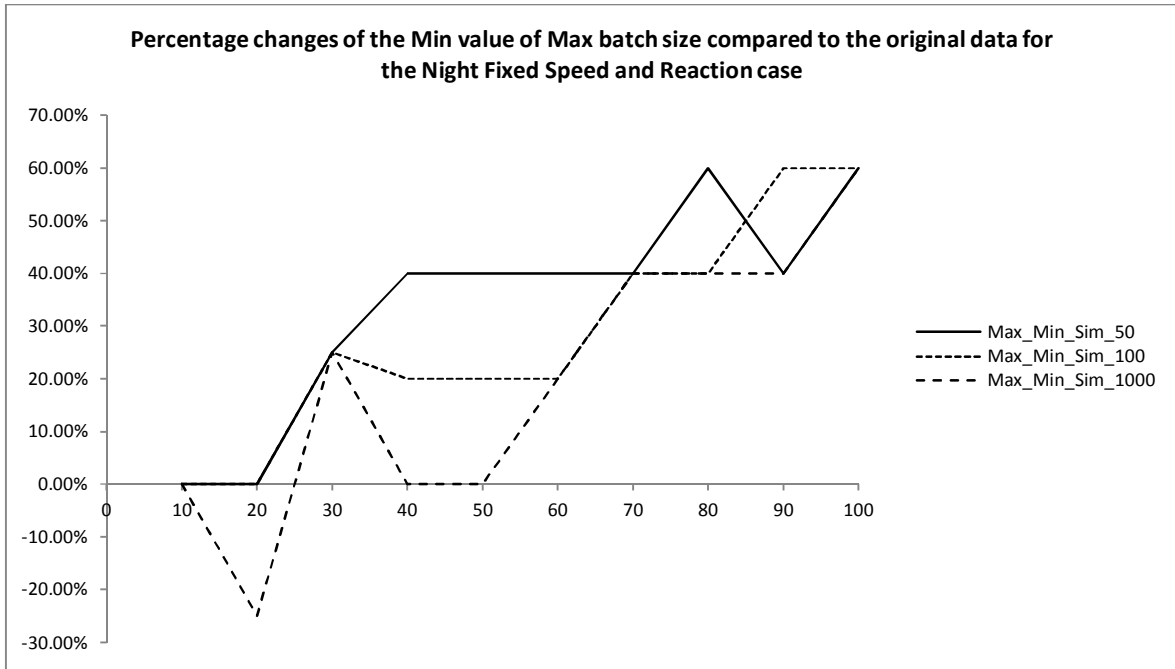


Figure II-22: Percentage change in Min value of max batch size when compared to original data. Night Fixed Speed and Reaction Case

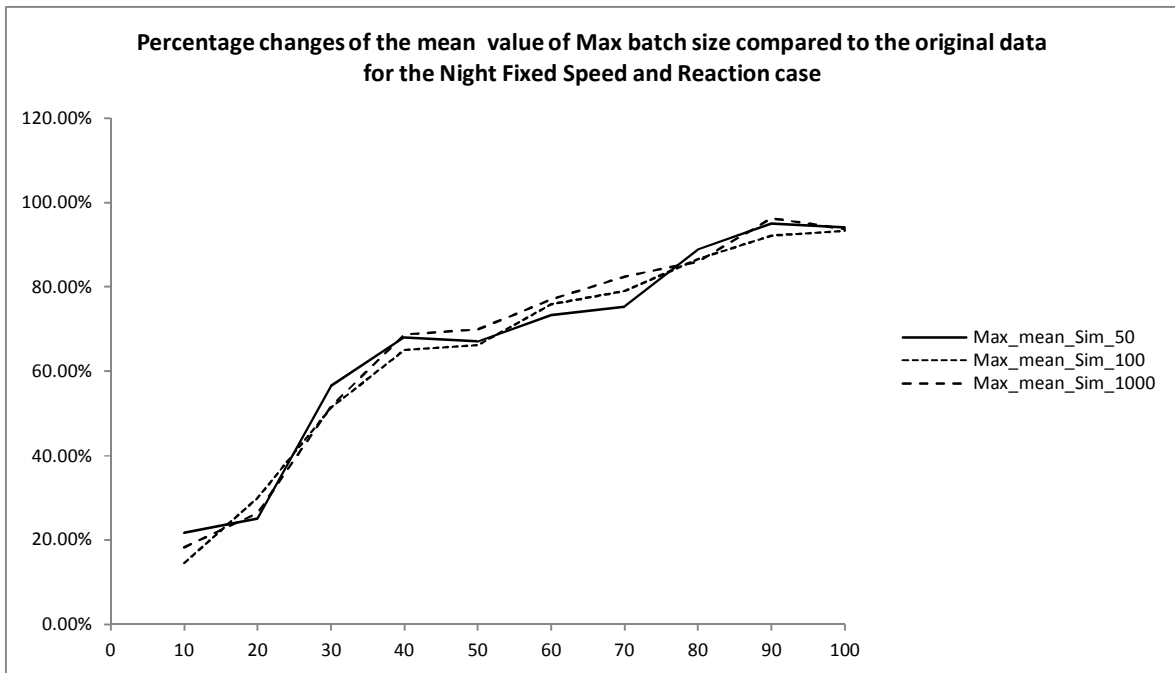


Figure II-23: Percentage change in Average value of max batch size when compared to original data. Night Fixed Speed and Reaction Case

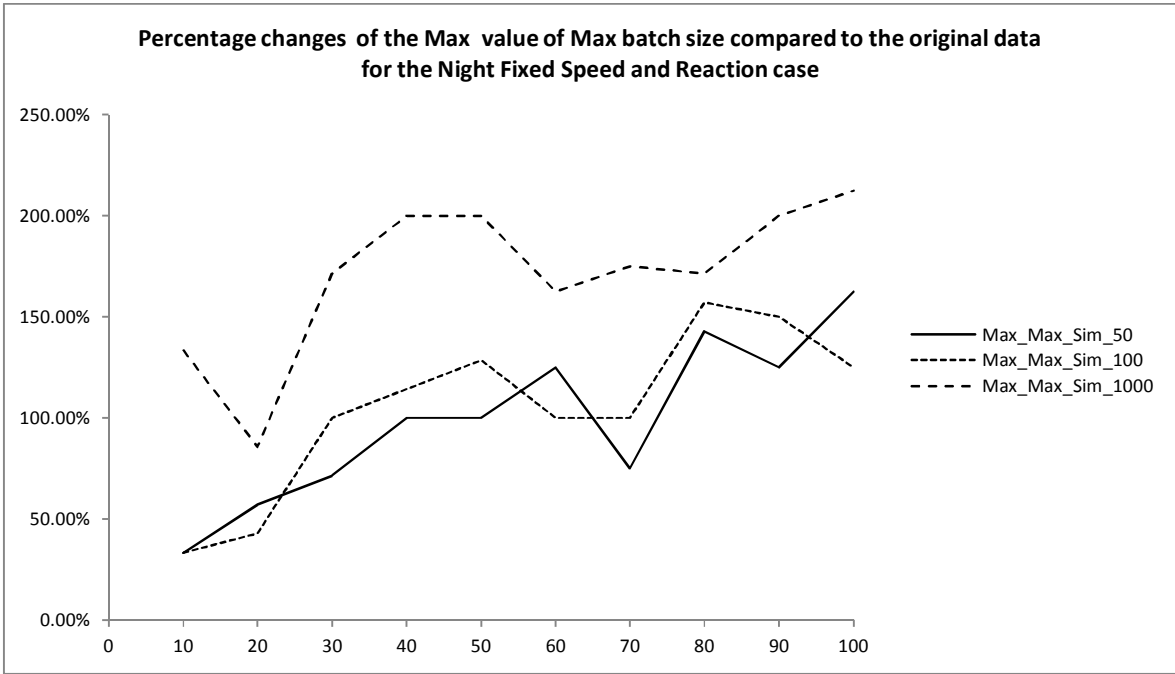


Figure II-24: Percentage change in Max value of max batch size when compared to original data. Night Fixed Speed and Reaction Case

Appendix III - Coefficient values of the polynomial rate function of the NHPP

Day case fitted coefficient

	10	20	30	40	50	60	70	80	90	100
Beta1	1.51	0.91	1.36	1.35	1.13	1.14	1.25	0.91	1.39	1.15
Beta2	0.17	12.16	11.06	6.07	7.60	7.63	2.52	12.57	2.08	4.52
Beta3	54.69	-55.59	-72.82	-34.76	-39.85	-55.40	-5.45	-101.56	-15.56	-28.99
Beta4	-360.98	110.19	219.19	98.29	86.24	207.48	-4.19	407.78	65.46	94.80
Beta5	970.23	-82.20	-343.12	-166.25	-64.64	-453.30	18.95	-903.69	-167.17	-180.67
Beta6	-1319.73	-43.42	264.89	165.81	-43.45	565.38	-8.51	1110.44	232.63	194.66
Beta7	897.51	100.12		-90.35	90.25	-370.20	-12.52	-707.73	-162.12	-109.15

Table III-1: Fitted coefficient of the rate function for the day case scenario per passenger loads

Day Fixed Reaction case fitted coefficient

	10	20	30	40	50	60	70	80	90	100
Beta1	2.03	2.84	1.97	2.19	1.68	2.41	1.79	1.89	1.59	1.96
Beta2	5.70	-4.98	-0.48	-4.10		-10.84	-3.93	-4.82		-8.66
Beta3	-88.11	-10.42	-2.49	12.84		82.37	21.37	24.88		63.56
Beta4	447.71	162.75	3.90	-18.42		-338.23	-54.03	-60.04		-233.58
Beta5	-1104.43	-537.34	12.20	4.21		744.57	51.26	52.40		460.86
Beta6	1422.93	794.78	-41.56	9.89		-894.87	7.22	14.00		-506.72
Beta7	-924.34	-559.40	40.22			553.54	-39.91	-45.35		293.56

Table III-2: Fitted coefficient of the rate function for the Day Fixed Reaction case scenario per passenger loads

Day Fixed Speed case fitted coefficient

	10	20	30	40	50	60	70	80	90	100
Beta1	1.62	1.20	1.52	0.99	1.17	0.98	1.26	1.10	1.37	0.93
Beta2	-3.75	5.04	5.77	12.71	1.94	8.97	2.38	4.04		10.45
Beta3	39.75	-22.07	-38.31	-77.82	-6.86	-67.04	-15.38	-26.68		-80.79
Beta4	-114.53	48.30	121.04	231.27	14.10	274.28	63.51	97.39		313.25
Beta5	100.65	-41.20	-190.12	-358.94	-21.12	-646.19	-160.72	-211.54		-670.98
Beta6	46.02	-26.15	124.01	273.93	18.33	848.07	220.23	258.57		793.24
Beta7	-116.26	62.75	-6.41			-573.32	-151.00	-163.15		-484.13

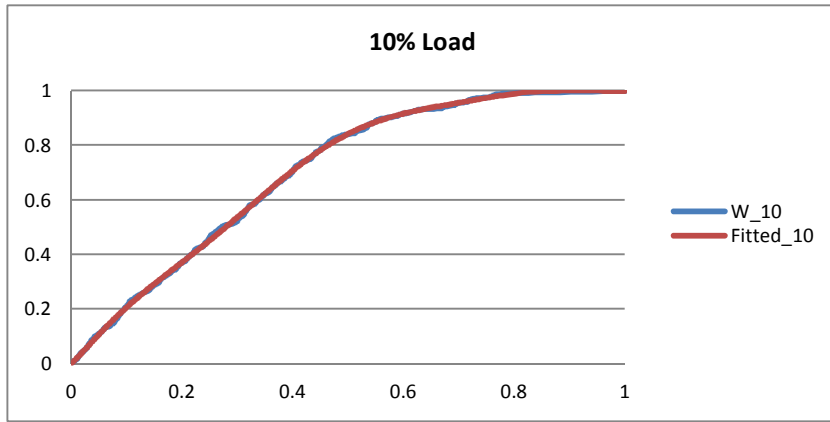
Table III-3: Fitted coefficient of the rate function for the Day Fixed Speed case scenario per passenger loads

Day Fixed Speed and Reaction case fitted coefficient

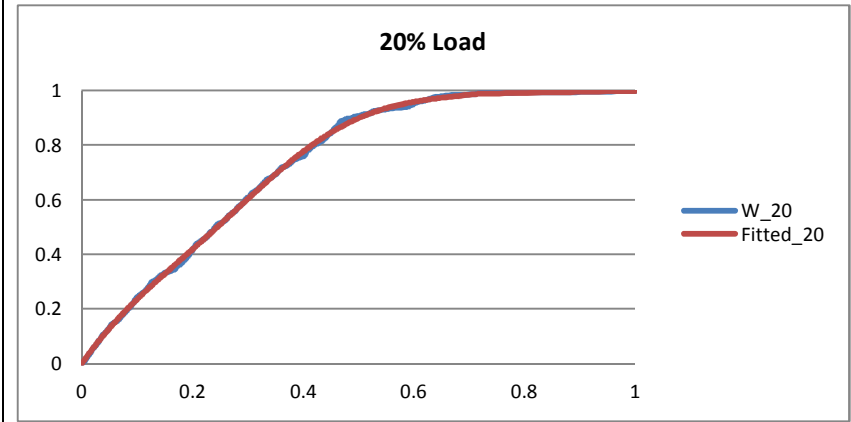
	10	20	30	40	50	60	70	80	90	100
Beta1	1.62	6.48	1.60	1.33	14.04	1.34	2.18	1.32	1.40	1.98
Beta2	8.47	-35.48	-1.86	-3.71	-164.73	-0.54	-5.59			-12.65
Beta3	-80.20	115.10	3.61	40.57	984.03	2.18	33.91			101.00
Beta4	281.75	-182.64	-2.76	-199.14	-3197.85	-4.20	-91.72			-386.62
Beta5	-471.48	101.23	2.50	487.26	5963.06	4.85	88.40			794.17
Beta6	375.32	72.66	-4.29	-627.31	-6371.47	-10.58	21.56			-905.79
Beta7		-116.26		407.48	3624.79	14.43	-85.95			540.37

Table III-4: Fitted coefficient of the rate function for the Day Fixed Speed and reaction case scenario per passenger loads

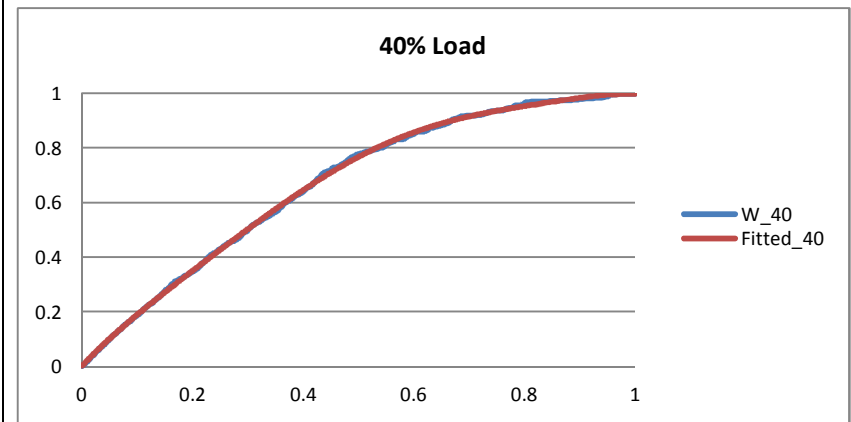
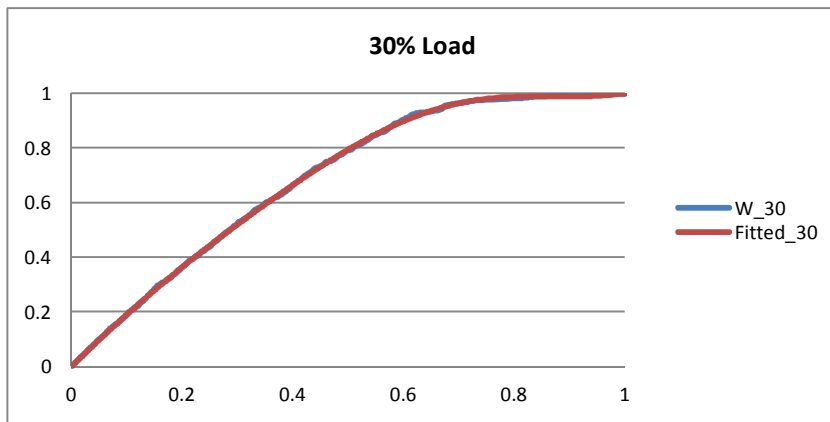
Fitted arrival curves for the Day Fixed Reaction



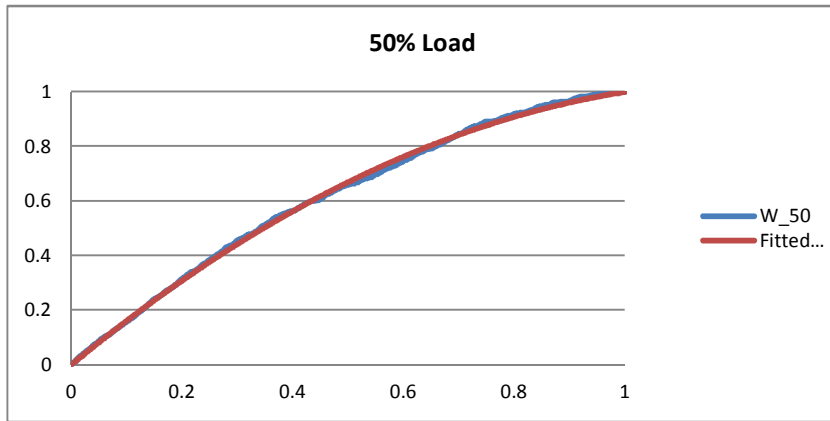
(a)



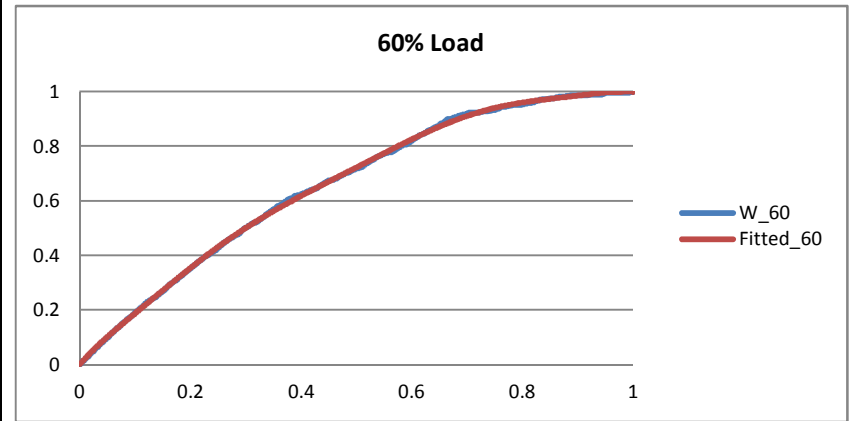
(b)



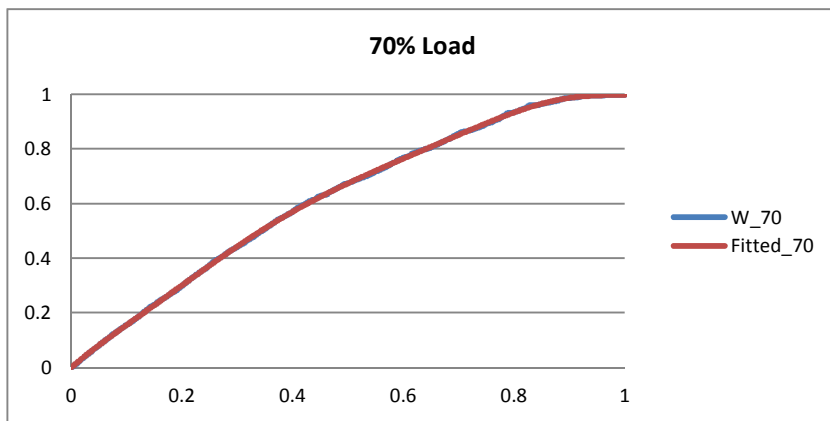
(c)



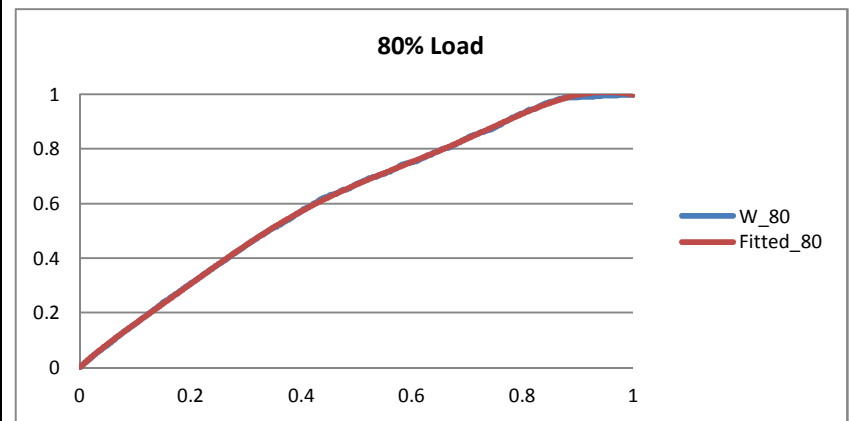
(d)



(e)



(f)



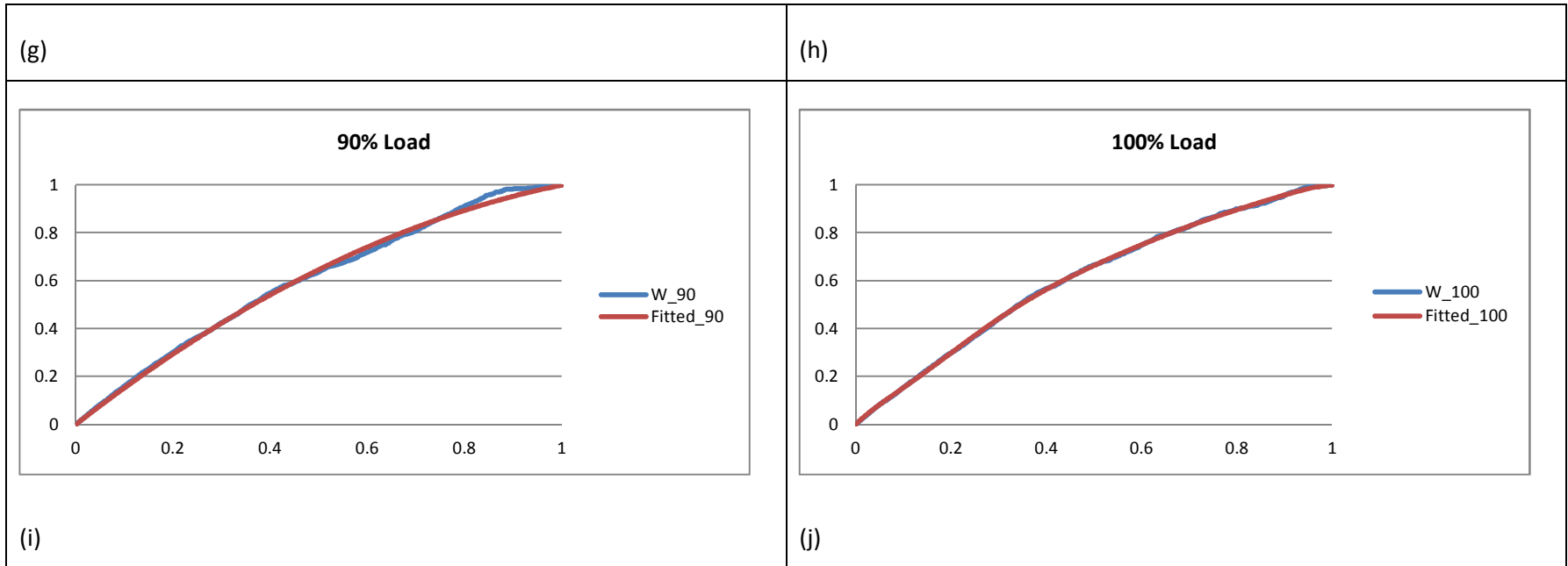
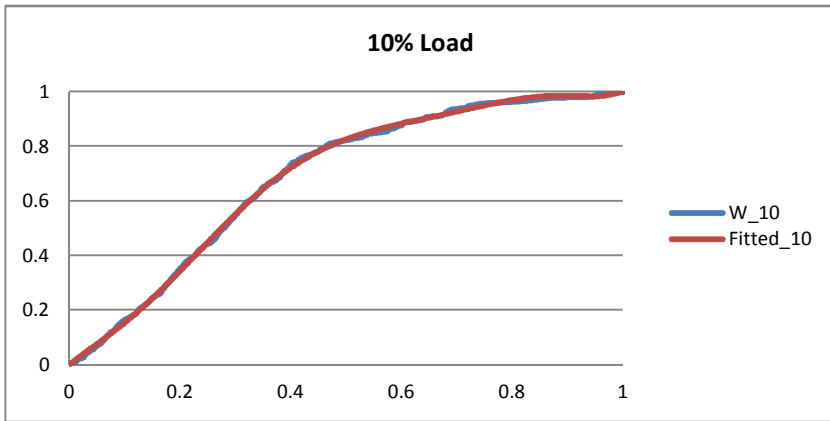
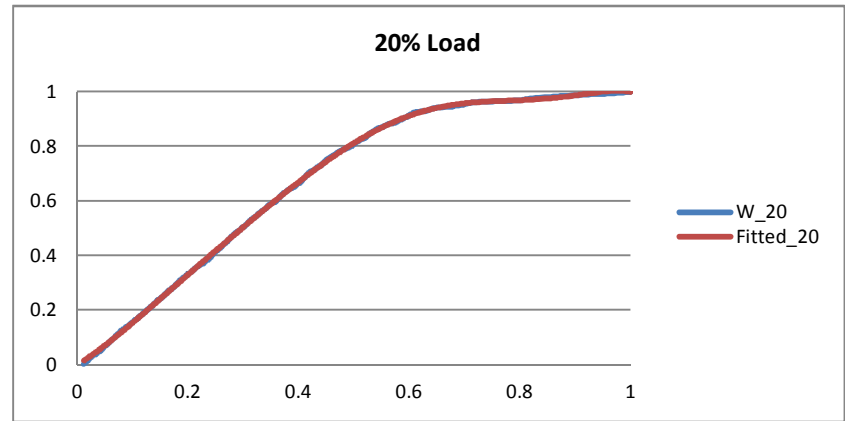


Figure III-1: Fitted and original arrival process for the Day Fixed Reaction cases for (a) 10% passenger load, (b) 20% passenger load, (c) 30% passenger load, (d) 40% passenger load, (e) 50% passenger load, (f) 60% passenger load, (g) 70% passenger load, (h) 80% passenger load, (i) 90% passenger load, (j) 100% passenger load

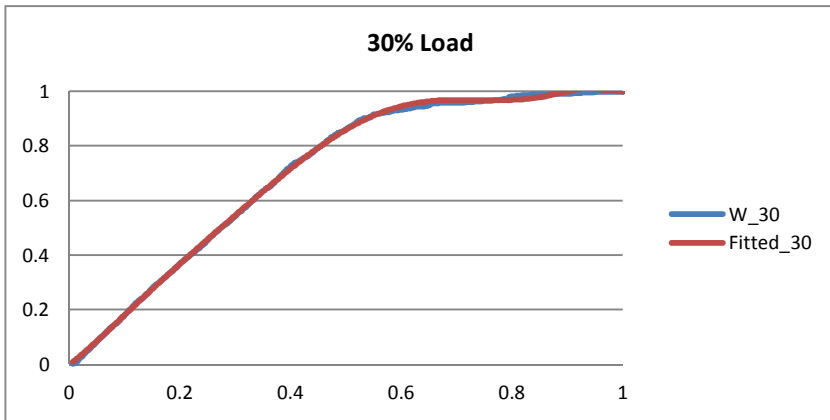
Fitted arrival curves for the Day Fixed Speed



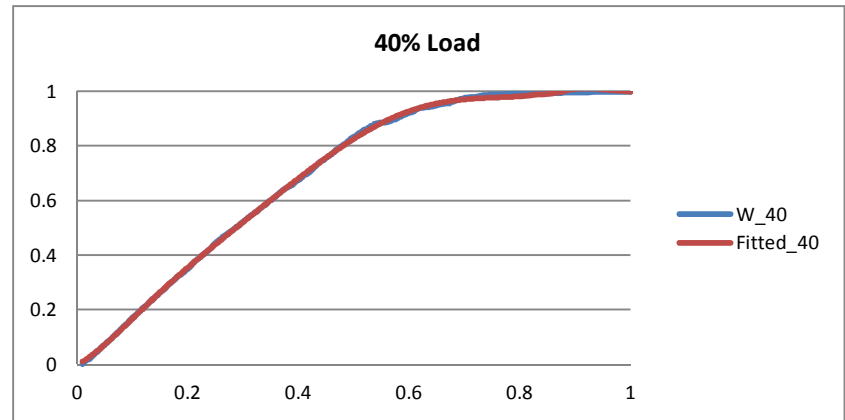
(a)



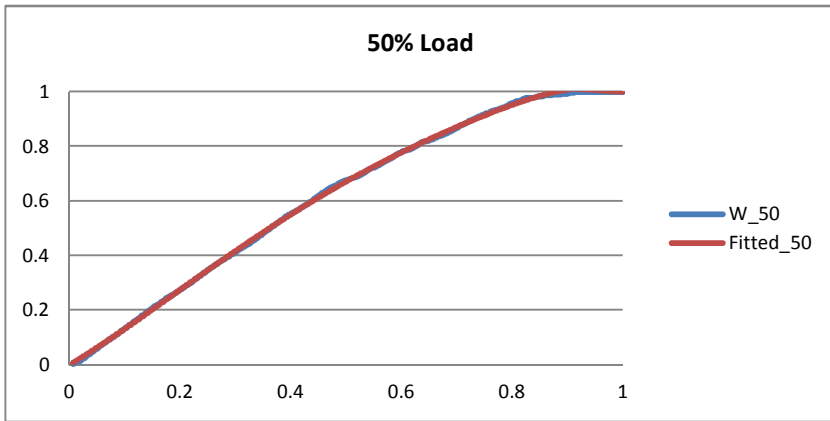
(b)



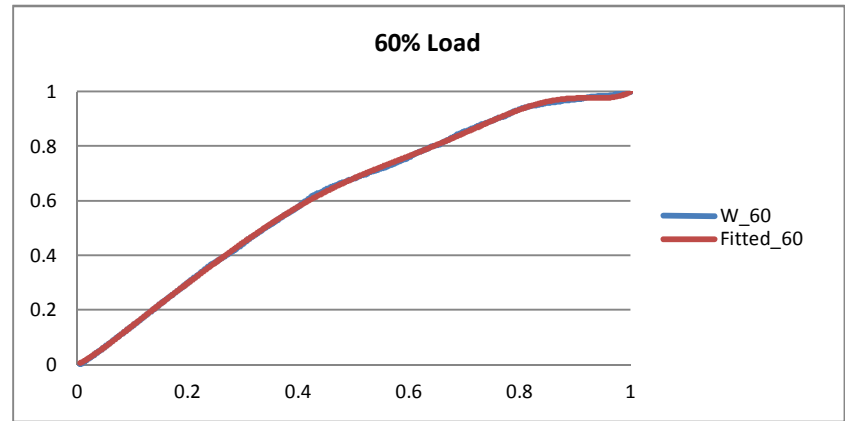
(c)



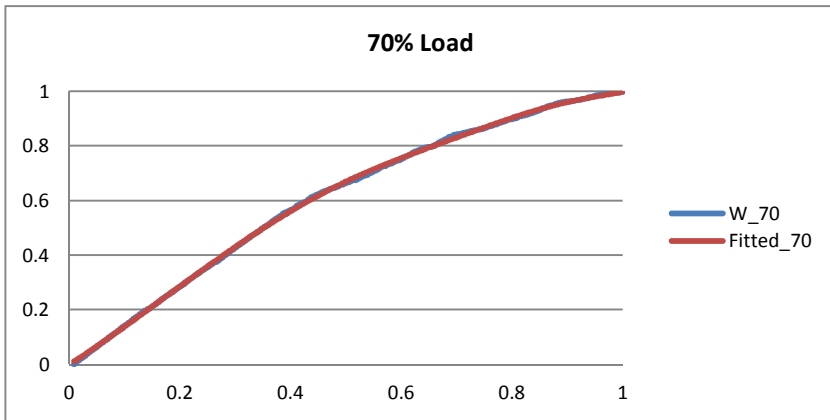
(d)



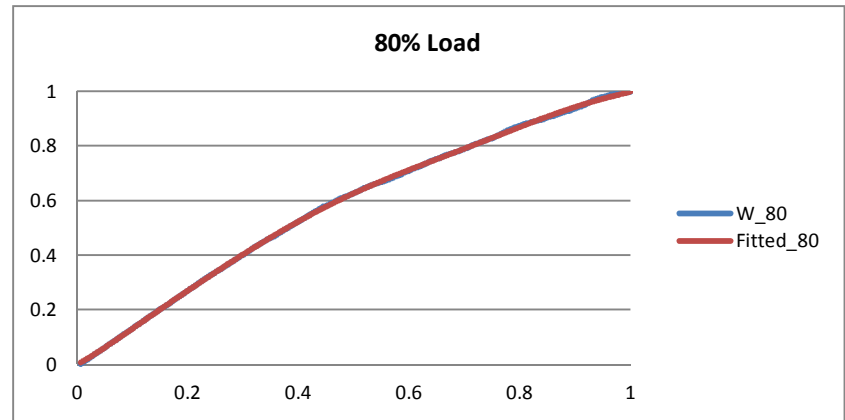
(e)



(f)



(g)



(h)

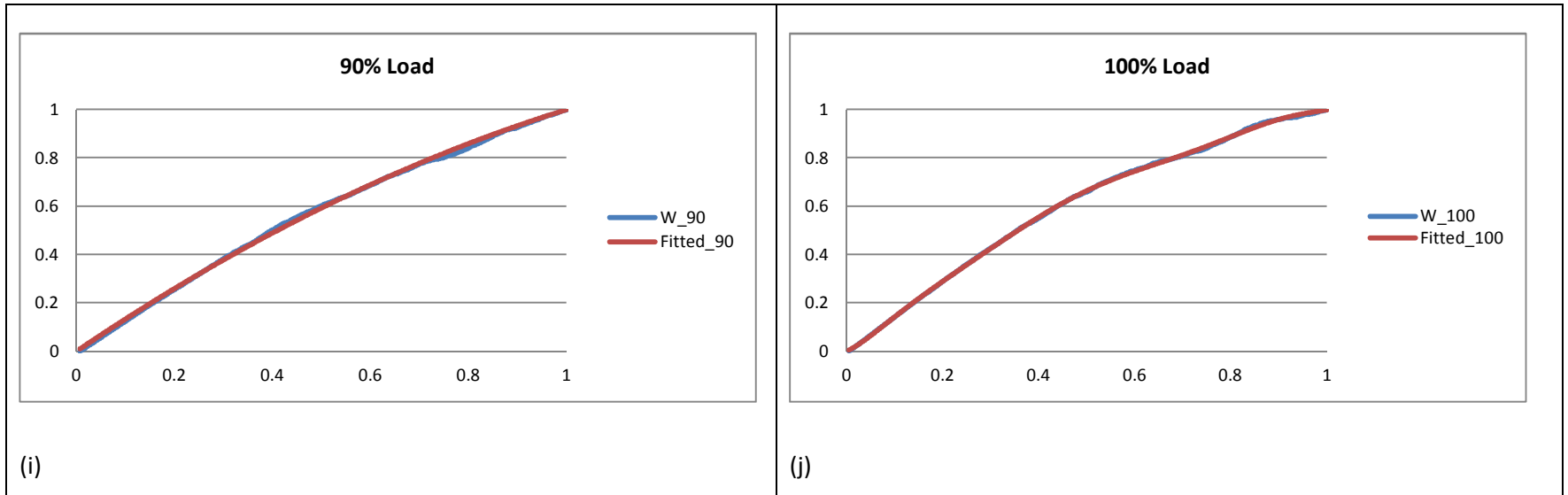
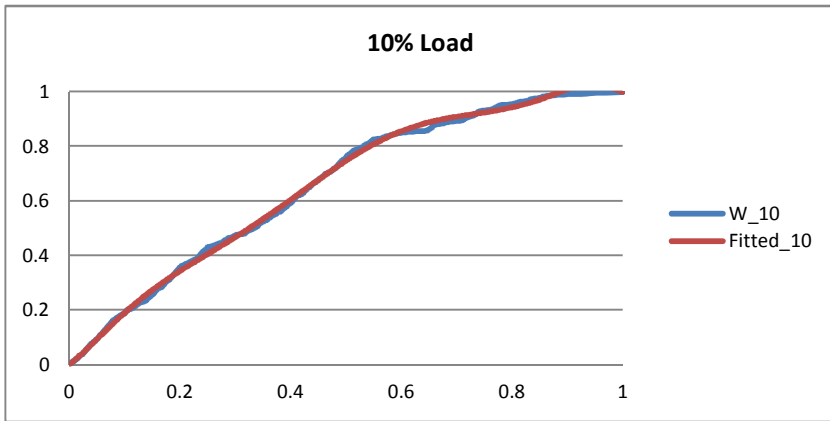
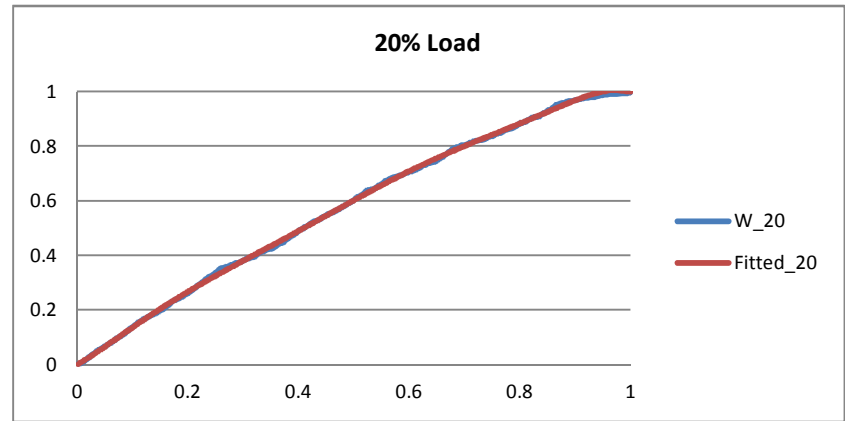


Figure III-2: Fitted and original arrival process for the Day Fixed Speed cases for (a) 10% passenger load, (b) 20% passenger load, (c) 30% passenger load, (d) 40% passenger load, (e) 50% passenger load, (f) 60% passenger load, (g) 70% passenger load, (h) 80% passenger load, (i) 90% passenger load, (j) 100% passenger load

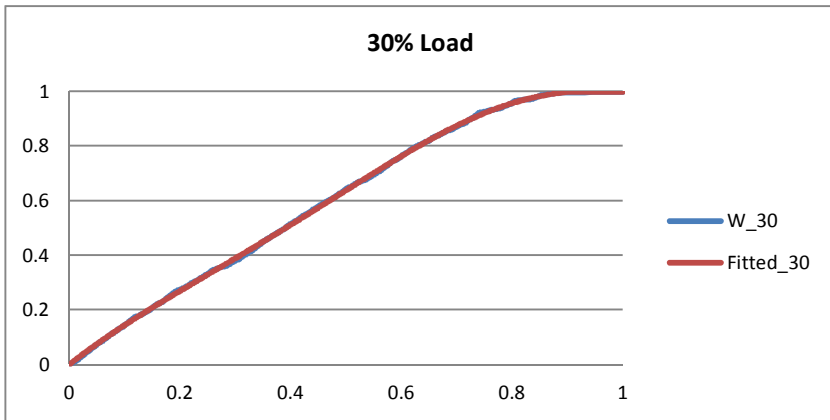
Fitted arrival curves for the day fixed speed and reaction



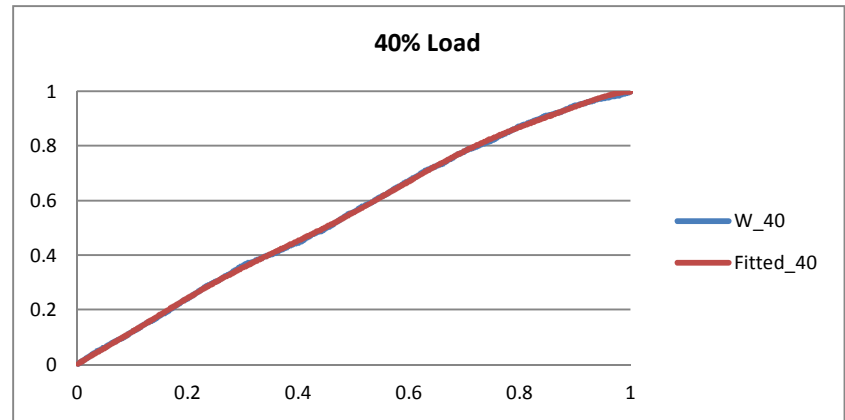
(a)



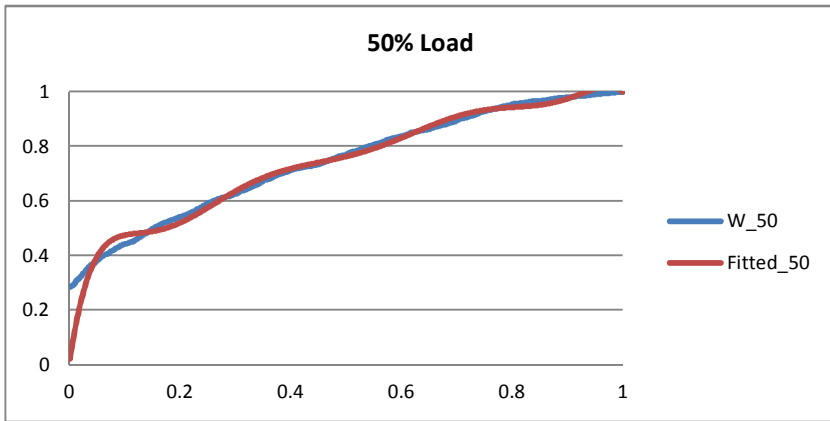
(b)



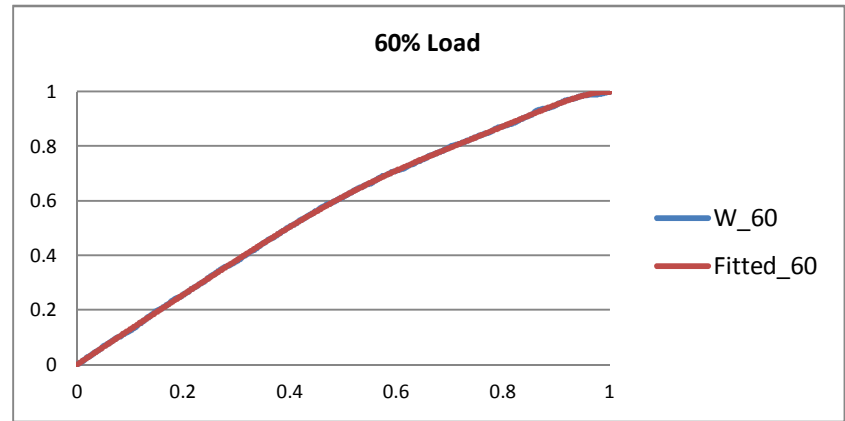
(c)



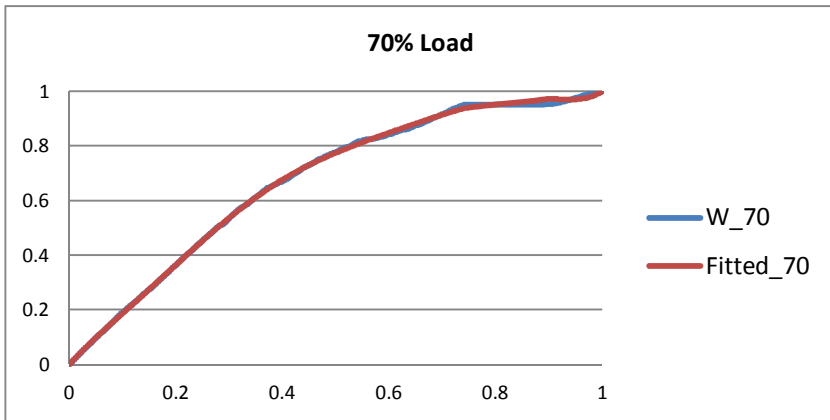
(d)



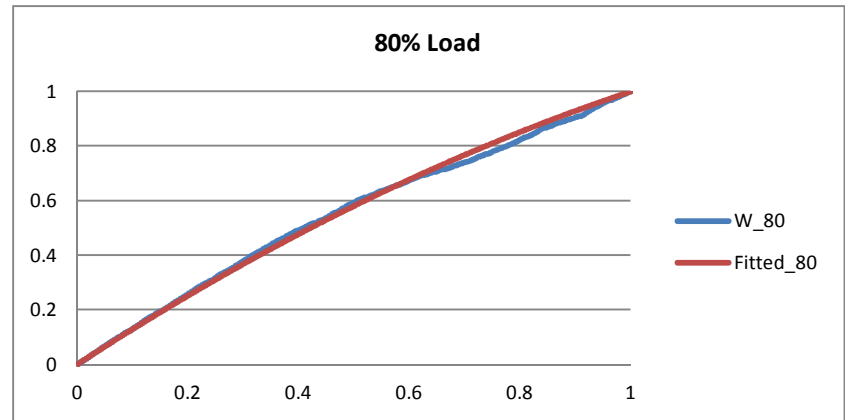
(e)



(f)



(g)



(h)

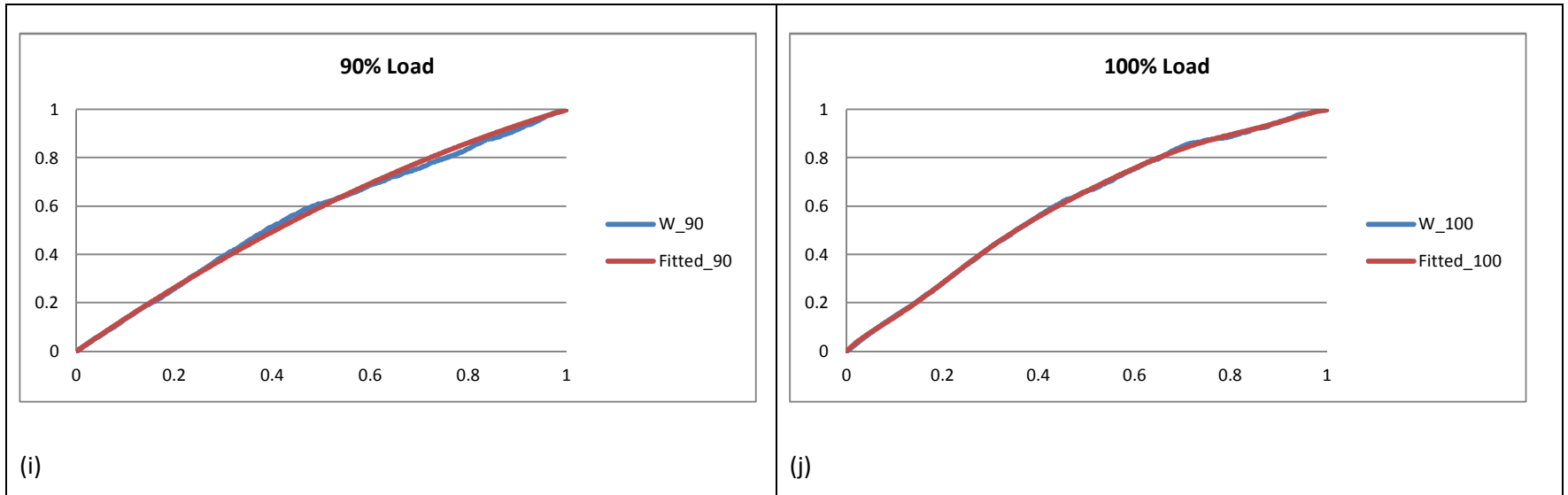


Figure III-3: Fitted and original arrival process for the Day Fixed Speed and Reaction cases for (a) 10% passenger load, (b) 20% passenger load, (c) 30% passenger load, (d) 40% passenger load, (e) 50% passenger load, (f) 60% passenger load, (g) 70% passenger load, (h) 80% passenger load, (i) 90% passenger load, (j) 100% passenger load

Night case fitted coefficient

	10	20	30	40	50	60	70	80	90	100
Beta1	0.18	-0.12	-0.46	139.27	12.07	-2.21	3.10	-22.88	-2.90	2.17
Beta2			-4.39	-1046.90	-75.97	6.51	-33.03	140.93	11.79	-35.65
Beta3			12.55	2958.00	148.86	-4.54	112.95	-302.28	-12.03	162.55
Beta4			-1.18	-3505.92	-61.07	1.00	-168.17	202.35	-0.82	-298.85
Beta5			-5.02	331.00	-81.88	2.36	119.96	173.38	10.89	199.08
Beta6			-4.19	3293.68	10.23			-307.01		86.99
Beta7				-3032.89	106.34					-182.40

Table III-5: Fitted coefficient of the rate function for the night case scenario per passenger loads

Night Fixed Reaction fitted coefficient

	10	20	30	40	50	60	70	80	90	100
Beta1	-0.28	9.58	3.54	-4.26	-3.80	6.28	-2.49	0.99	6.28	-2.78
Beta2		-62.56	-19.45	17.12	13.50	-54.82	7.75	-15.17	-54.82	12.05
Beta3		137.67	24.50	-28.57	-13.97	173.95	-3.18	50.34	173.95	-12.76
Beta4		-121.82	13.74	27.28	1.17	-264.35	-3.59	-39.12	-264.35	-0.80
Beta5			-35.30		10.32	219.15	1.53	-42.11	219.15	11.52
Beta6						-98.43	3.46	59.39	-98.43	
Beta7								31.99		
Beta8								-73.76		

Table III-6: Fitted coefficient of the rate function for the night Fixed Reaction case scenario per passenger loads

Night Fixed Speed fitted coefficient

	10	20	30	40	50	60	70	80	90	100
Beta1	0.38	-0.31	6.85	2.95	10.17	-3.37	-2.17	-2.24	4.89	-19.90
Beta2			-31.86	-19.11	-67.28	10.71	6.07	6.10	-46.03	154.96
Beta3			35.12	26.30	141.37	-9.58		-2.40	149.17	-491.67
Beta4			11.48	18.58	-77.87	1.20		-0.38	-217.38	781.17
Beta5			-12.25	-47.77	-83.82	6.03			152.32	-558.33
Beta6			-25.02		118.80					10.83
Beta7										204.54

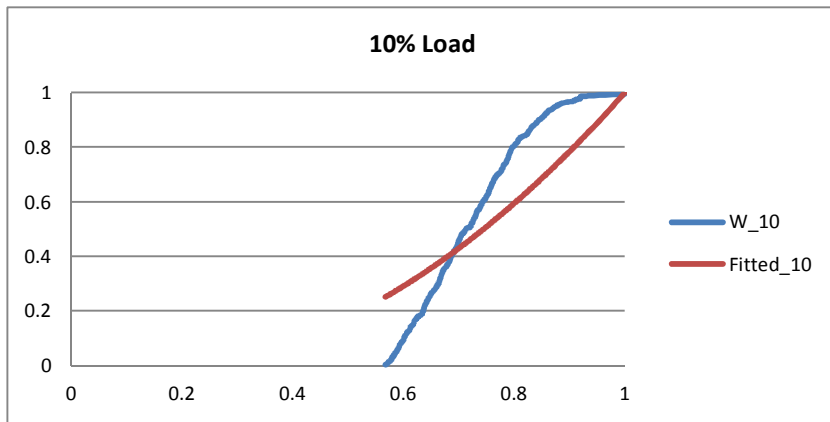
Table III-7: Fitted coefficient of the rate function for the night Fixed Speed case scenario per passenger loads

Night Fixed Speed & Reaction fitted coefficient

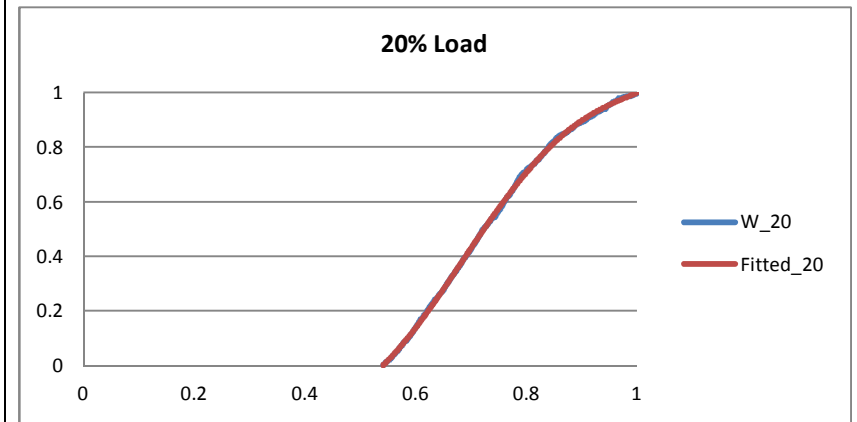
	10	20	30	40	50	60	70	80	90	100
Beta1	56.11	16.74	18.44	-3.43	0.37	0.44	-2.92	-1.11	11.56	0.48
Beta2	-297.31	-61.97	-131.95	6.98	-8.96	-6.68	17.17	-0.52	-109.71	-17.60
Beta3	569.47	38.10	352.99	3.90	26.03	12.86	-53.37	14.64	381.36	92.01
Beta4	-467.44	66.23	-451.44	-9.66	-20.96	3.28	93.98	-19.15	-603.16	-190.53
Beta5		-34.52	286.15	-2.99	3.86	-9.40	-61.87		387.95	200.55
Beta6		-52.33		5.37	-5.02	-8.42	-15.66		64.33	-105.78
Beta7		2.27		9.13	6.40	3.87	21.25		-201.82	
Beta8		38.01			7.38	12.85	13.62			
Beta9					-5.12					
Beta10					-10.37					

Table III-8: Fitted coefficient of the rate function for the night Fixed Speed & Reaction case scenario per passenger loads

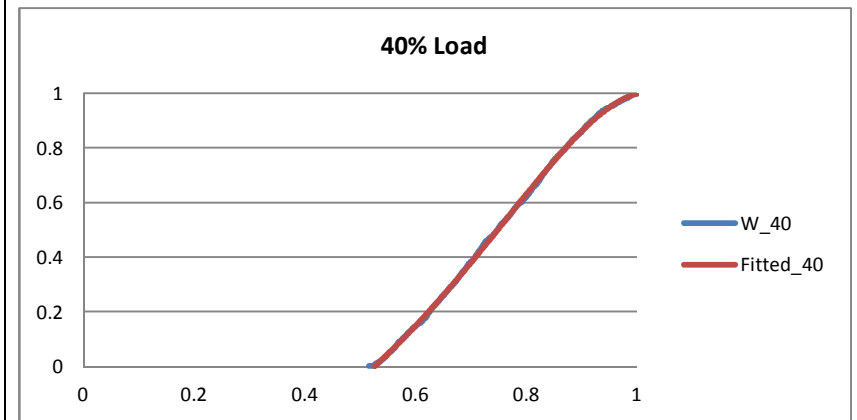
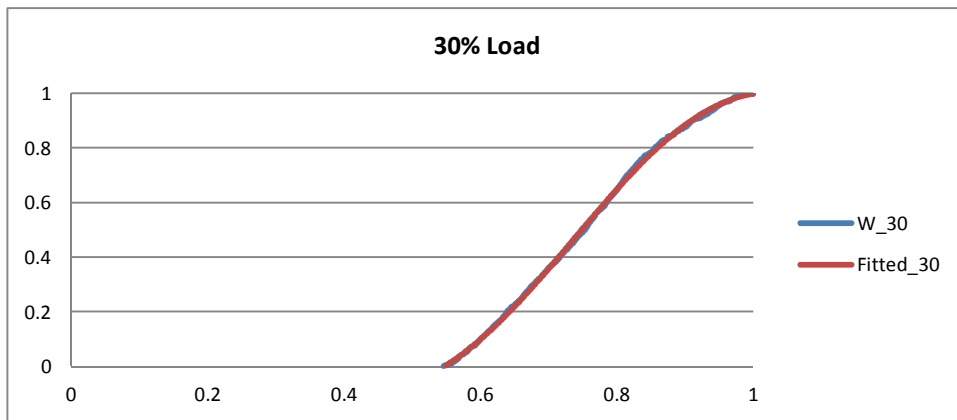
Fitted arrival curves for the Night Fixed Reaction



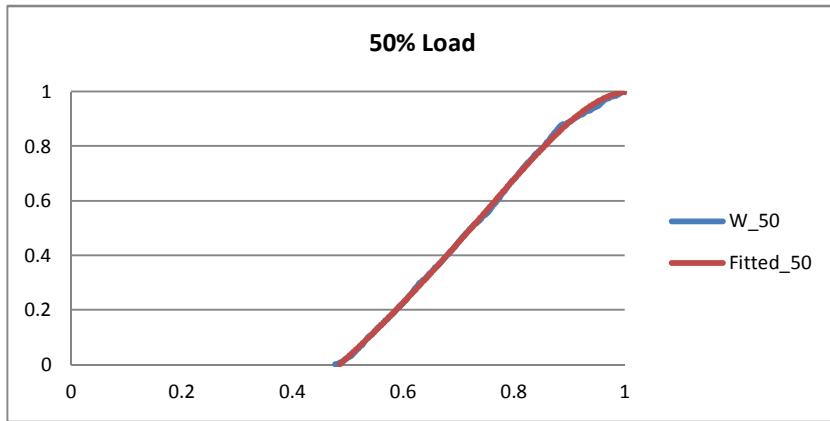
(a)



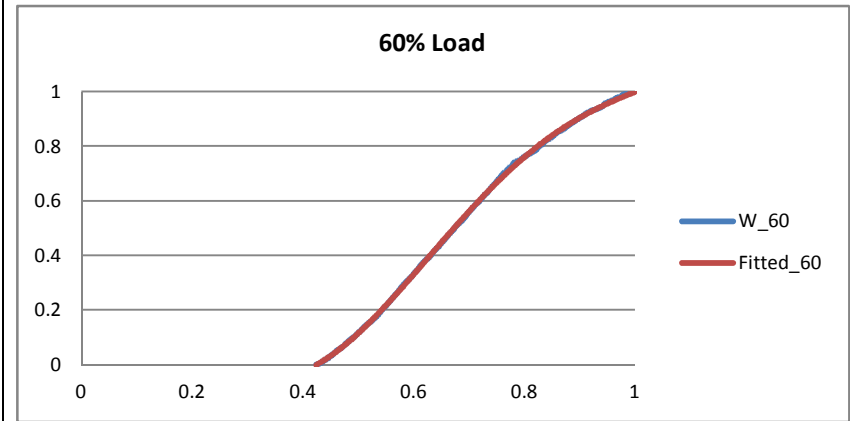
(b)



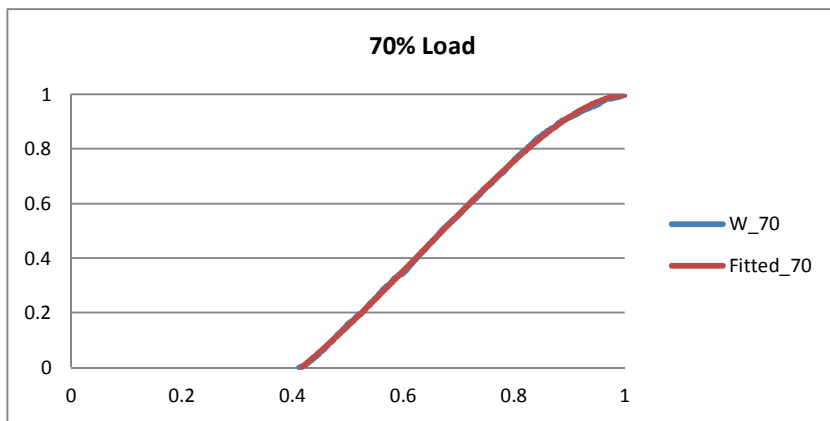
(c)



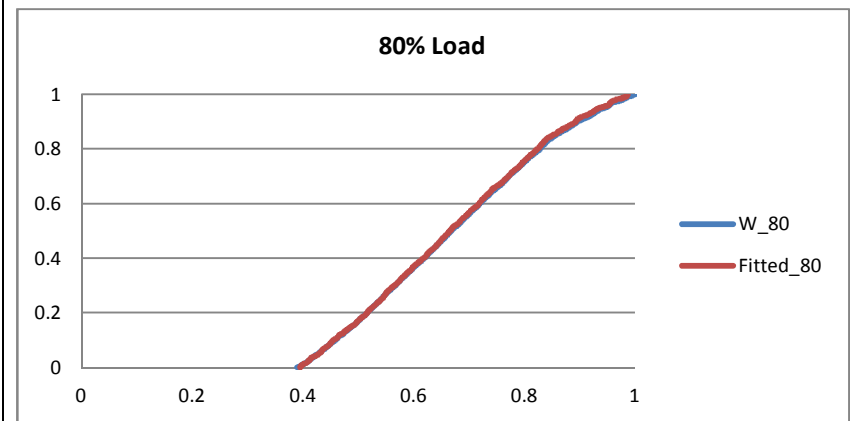
(d)



(e)



(f)



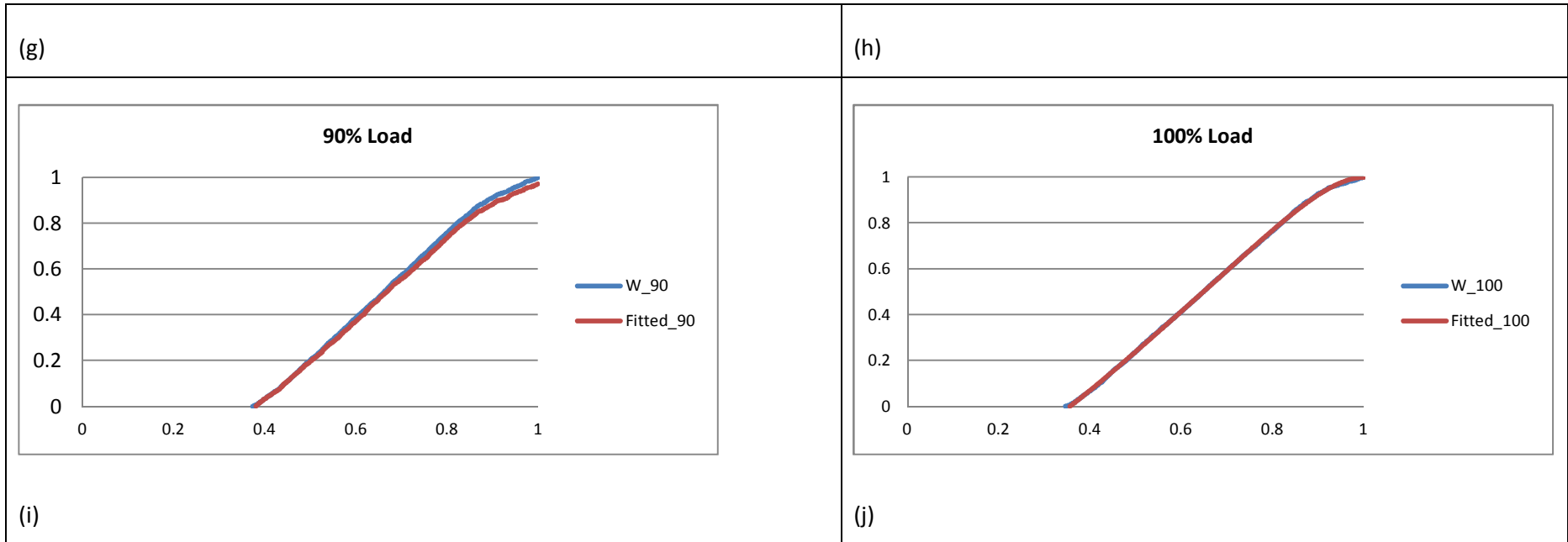
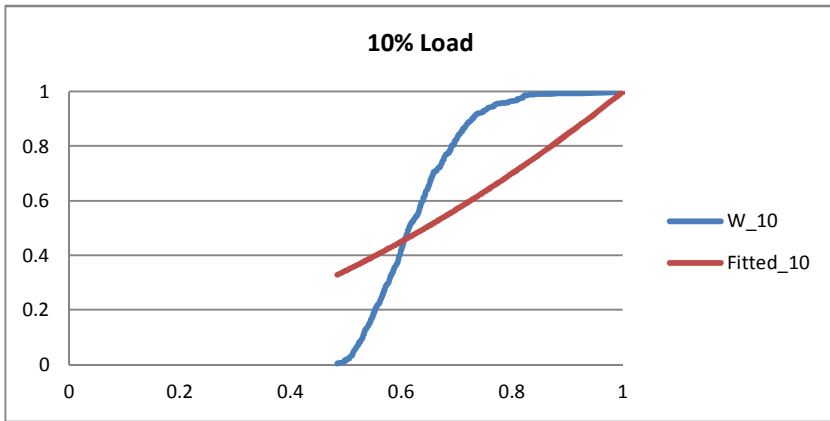
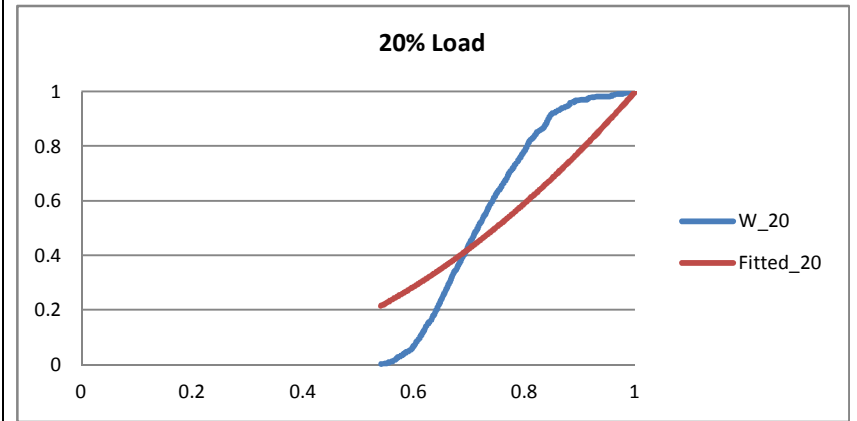


Figure III-4: Fitted and original arrival process for the Night Fixed Reaction cases for (a) 10% passenger load, (b) 20% passenger load, (c) 30% passenger load, (d) 40% passenger load, (e) 50% passenger load, (f) 60% passenger load, (g) 70% passenger load, (h) 80% passenger load, (i) 90% passenger load, (j) 100% passenger load

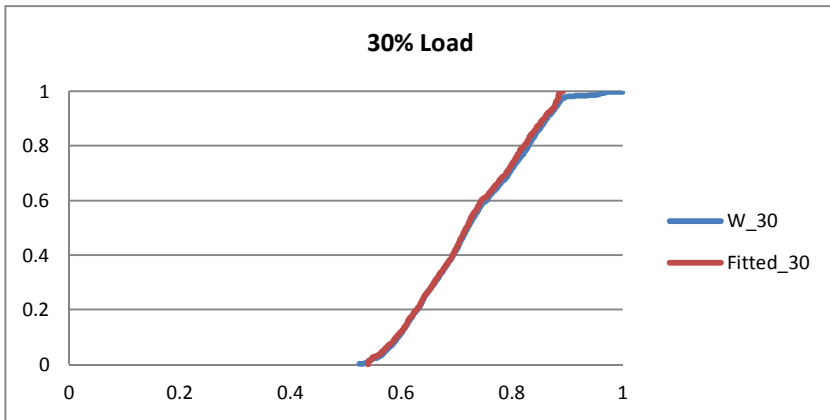
Fitted arrival curves for the Night Fixed Speed



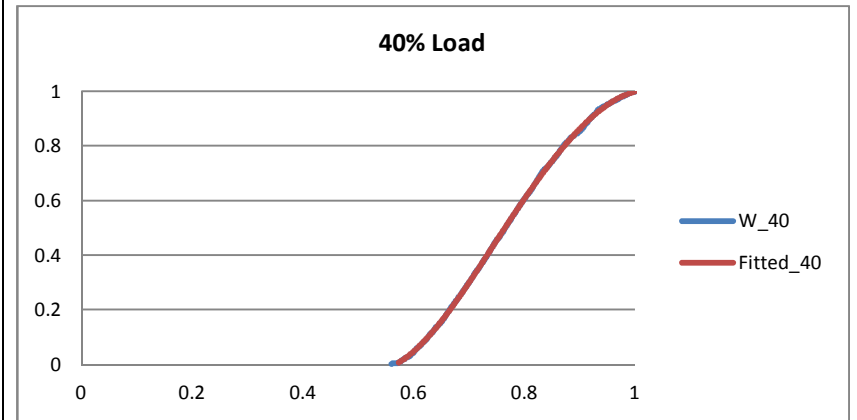
(a)



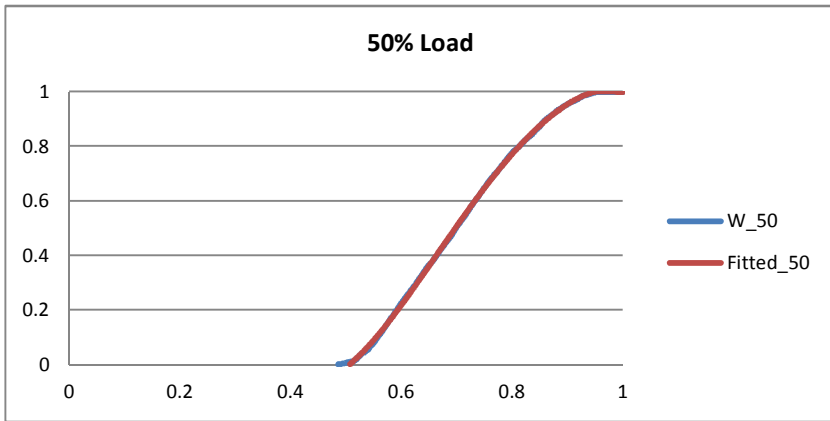
(b)



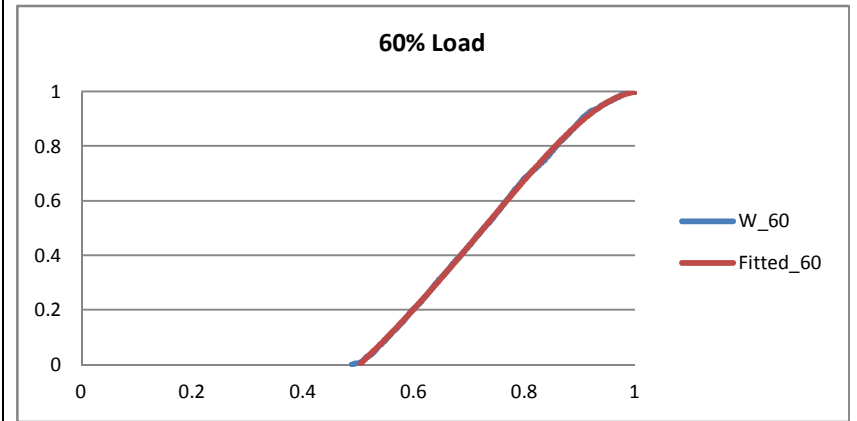
(c)



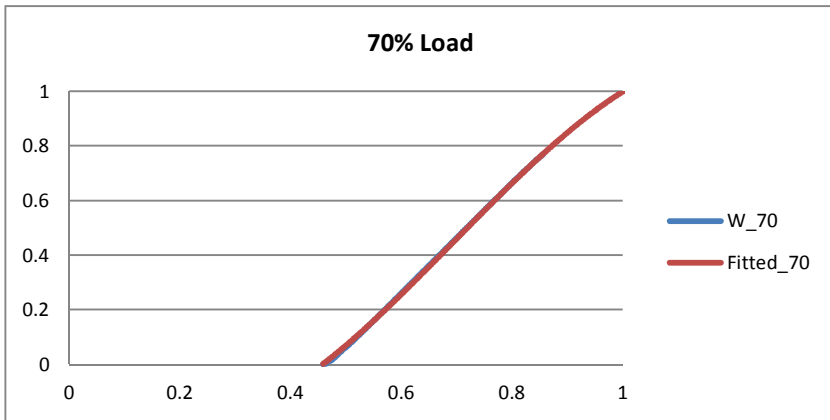
(d)



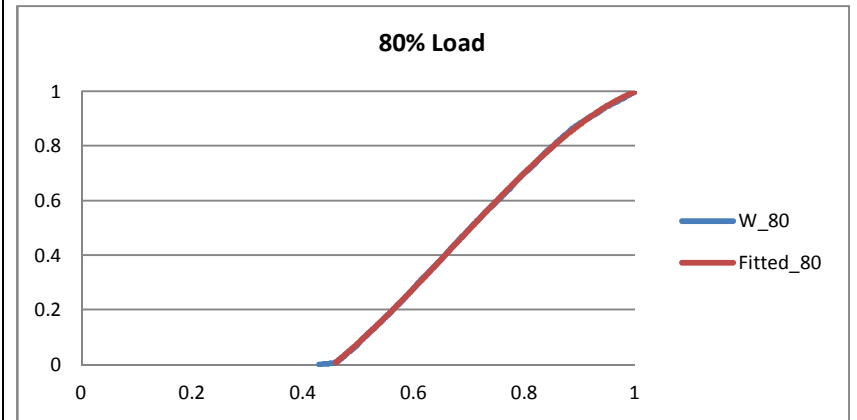
(e)



(f)



(g)



(h)

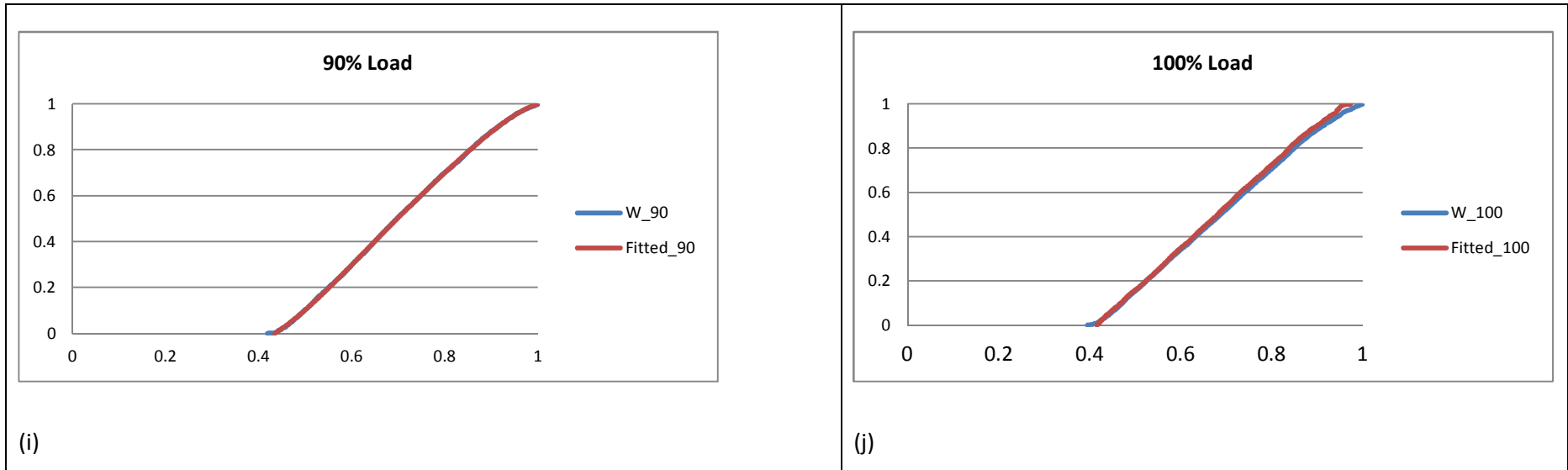
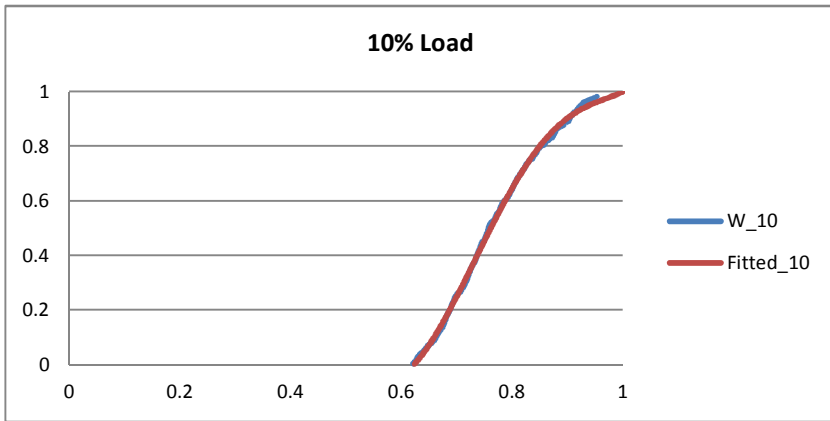
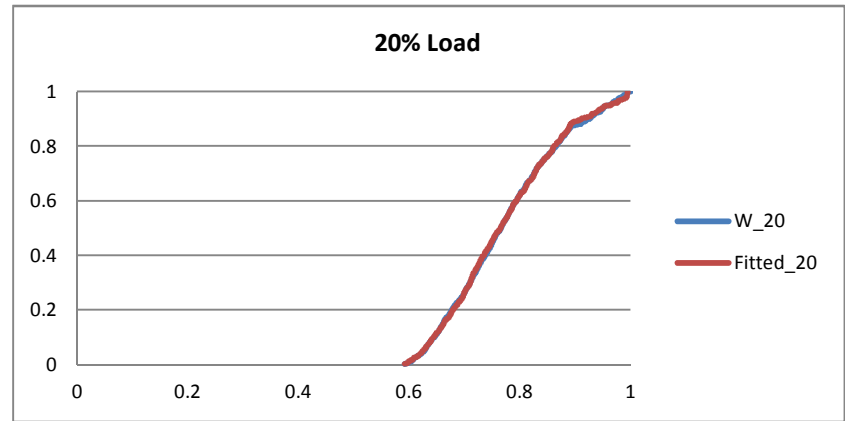


Figure III-5: Fitted and original arrival process for the Night Fixed Speed cases for (a) 10% passenger load, (b) 20% passenger load, (c) 30% passenger load, (d) 40% passenger load, (e) 50% passenger load, (f) 60% passenger load, (g) 70% passenger load, (h) 80% passenger load, (i) 90% passenger load, (j) 100% passenger load

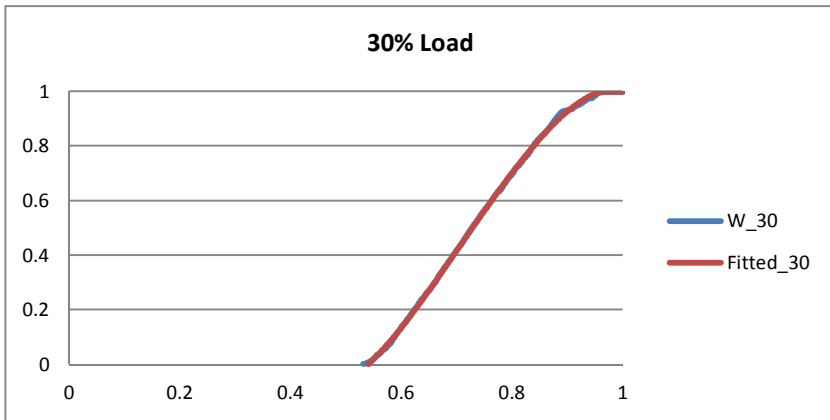
Fitted arrival curves for the Night Fixed Speed and Reaction



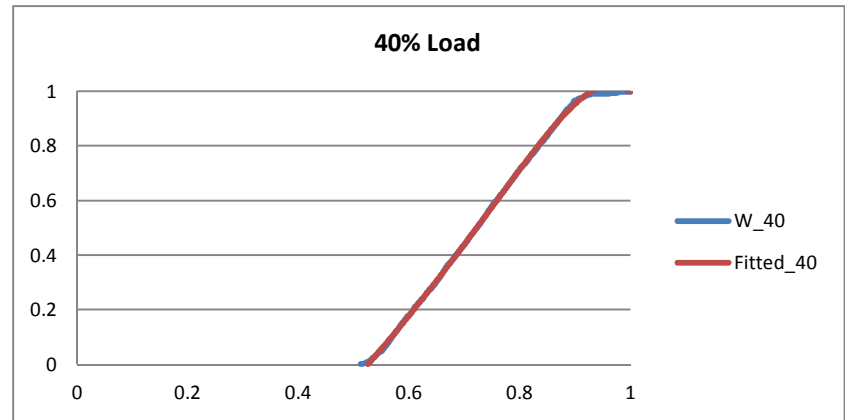
(a)



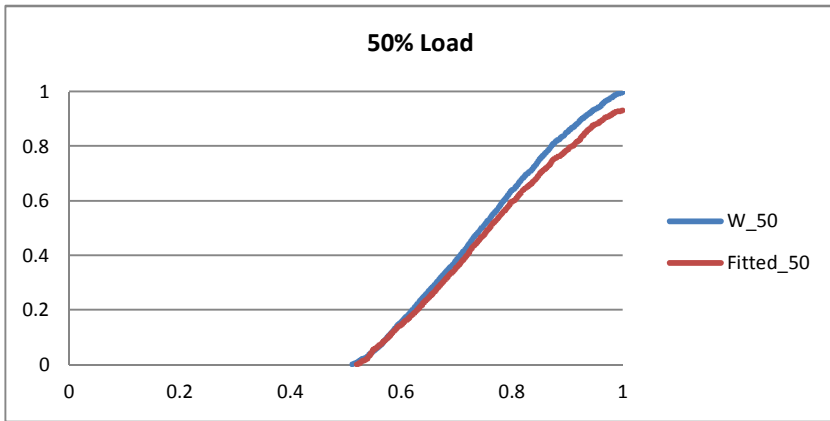
(b)



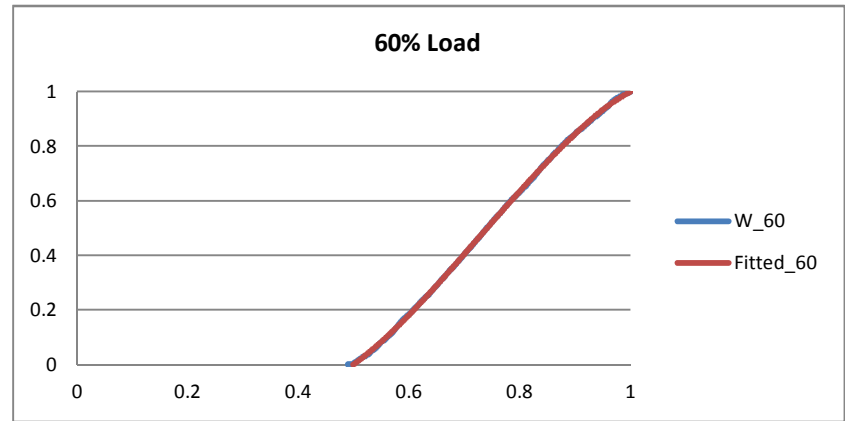
(c)



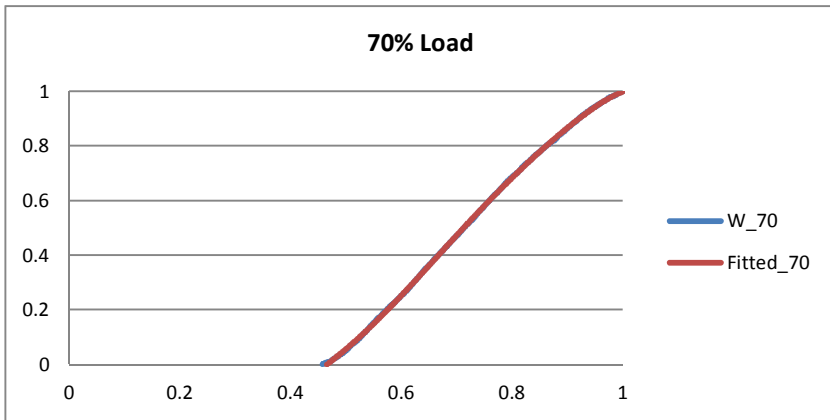
(d)



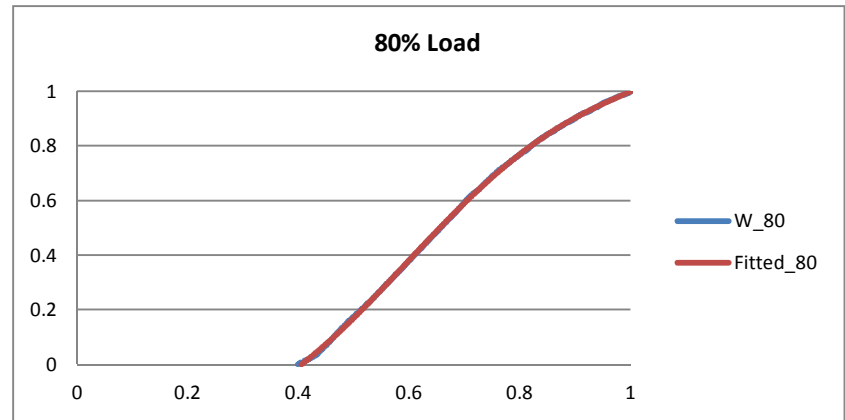
(e)



(f)



(g)



(h)

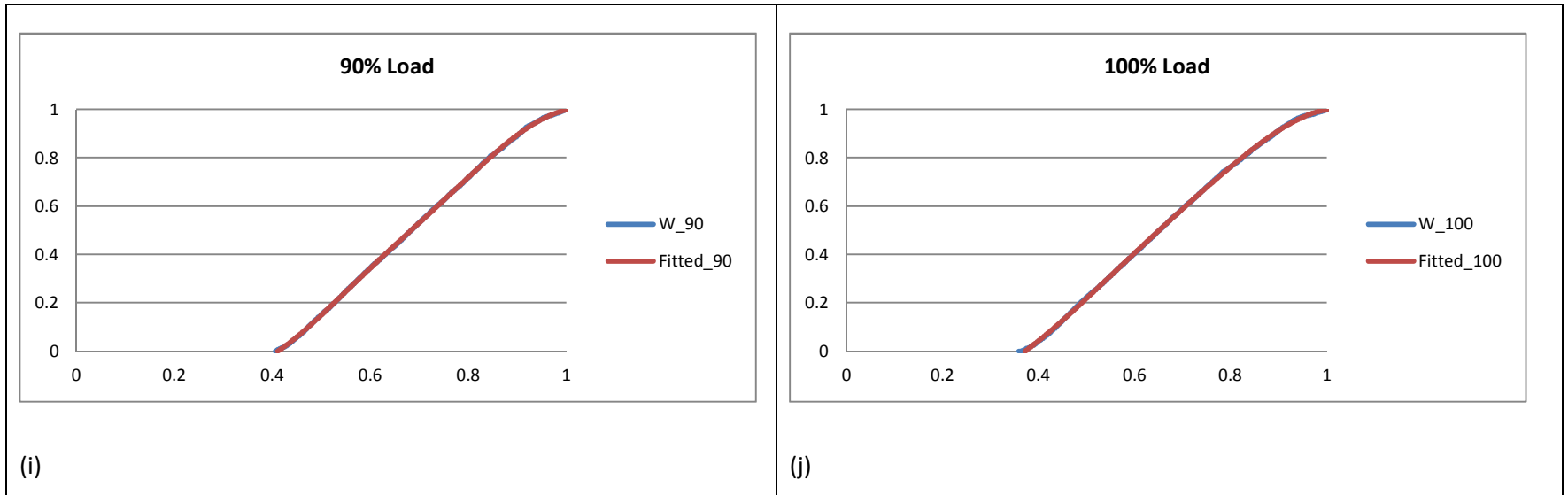


Figure III-6: Fitted and original arrival process for the Night Fixed Speed and Reaction cases for (a) 10% passenger load, (b) 20% passenger load, (c) 30% passenger load, (d) 40% passenger load, (e) 50% passenger load, (f) 60% passenger load, (g) 70% passenger load, (h) 80% passenger load, (i) 90% passenger load, (j) 100% passenger load

